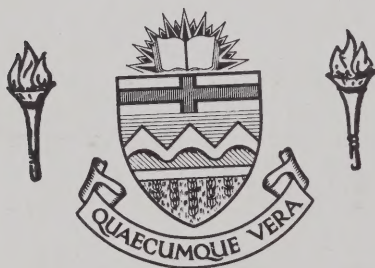


For Reference

NOT TO BE TAKEN FROM THIS ROOM

Ex LIBRIS
UNIVERSITATIS
ALBERTAENSIS



BRUCE PEEL SPECIAL COLLECTIONS LIBRARY
University of Alberta

REQUEST FOR DUPLICATION

I wish a photocopy of the thesis by _____
entitled _____

The copy is for the sole purpose of private scholarly or scientific study and research. I will not reproduce, sell or distribute the copy I request, and I will not copy any substantial part of it in my own work without the permission of the copyright owner. I understand that the Library performs the service of copying at my request, and I assume all copyright responsibility for the item requested.

Name Raj Dongre Turner-Fairbanks Highway Research Center

Address 6300 Georgetown Pike McLean, VA - 22101

List pages copied All - ILL

Date April 19/99 Signature D. Piche

Name _____

Address _____

List pages copied _____

Date _____ Signature _____

Name _____

Address _____

List pages copied _____

Date _____ Signature _____

Name _____

Address _____

List pages copied _____

Date _____ Signature _____

Name _____

Address _____

List pages copied _____

Date _____ Signature _____

THE UNIVERSITY OF ALBERTA

THE RESPONSE OF ASPHALTIC CONCRETE
PAVEMENTS TO LOW TEMPERATURES

by



John Thomas Christison


A THESIS

SUBMITTED TO THE FACULTY OF GRADUATE STUDIES AND RESEARCH
IN PARTIAL FULFILMENT OF THE REQUIREMENTS FOR THE DEGREE
OF DOCTOR OF PHILOSOPHY

DEPARTMENT OF CIVIL ENGINEERING

EDMONTON, ALBERTA

FALL, 1972



Digitized by the Internet Archive
in 2023 with funding from
University of Alberta Library

<https://archive.org/details/Christison1972>

ABSTRACT

Cracking of asphaltic concrete pavements due to thermal effects is recognized as a serious form of pavement distress in areas of low temperature climatic environment. In this study pavement temperature data obtained from field installations are summarized, an analytical model for predicting pavement temperatures is developed and using such temperature data together with appropriate materials definition the results of various thermal stress prediction methods are assessed in relation to observed low temperature behavior of pavement structures within two field test projects located in Western Canada.

The study firstly presents a review of various factors found from previous investigations to be related to the low temperature cracking problem. Following this review recorded temperatures in several pavement structures subjected to temperatures approaching -40 F are summarized. The summary includes specific information on daily air and pavement temperature variations, time rates of pavement temperature change and thermal regimes within subgrades of different pavement structures subjected to near identical climatic conditions. To extend this information to other climatic areas an analytical model for predicting pavement temperatures is developed and necessary input parameters for the model are described. Comparisons are given between predicted and recorded temperatures in various pavement structures. Such comparisons have shown excellent agreement which suggests that the model

can be used to obtain reliable predictions of pavement temperatures under actual climatic conditions.

Concepts used to characterize the time and temperature dependence of asphaltic concretes incorporated in the test projects are described and resulting stiffness values are presented. Tensile properties of pavement cores obtained from the projects and determined by means of the tensile splitting test are summarized. Using the stiffness values together with recorded and predicted temperature data thermally induced stresses within the pavements are computed by various stress predictive methods. Theoretical considerations for the formulation of the predictive methods are reviewed and numerical solutions of the stress equations are presented. Employing a postulated fracture criterion, computed stresses are compared with laboratory evaluated fracture strength-temperature relationships of the pavement cores to predict times and temperatures of fracture. These predicted fracture conditions are then compared with times and temperatures of observed cracking of the corresponding pavements. Based on these comparisons a simplified guideline for reducing the occurrence of transverse cracking is proposed.

The principal conclusion of this study is that stress prediction methods coupled with the use of recorded or predicted temperature data and appropriate materials characterization provide a means of reliably assessing the low temperature fracture susceptibility of asphaltic concrete mixes. For field data currently available such assessments can be made using thermal stresses computed by means of a suitable pseudo-elastic beam analysis.

ACKNOWLEDGEMENTS

This study was conducted under the direction of Professor K. O. Anderson, chairman of the supervisory committee. His continued interest and guidance throughout the course of the work and constructive criticisms during review of the manuscript have been invaluable and are gratefully acknowledged. Additional advice and assistance provided by other members of the committee are equally appreciated.

Primary financial support for the study was provided by the Alberta Cooperative Highway Research Program sponsored by the Research Council of Alberta, the Alberta Department of Highways and Transport and the Department of Civil Engineering, the University of Alberta, Edmonton. Additional assistance was derived from teaching assistantships from the Department of Civil Engineering, from the National Research Council of Canada under operating grant A2139, and through a Canadian Good Roads Scholarship provided by Allied Chemical Canada Limited of Montreal. This financial support received throughout the period of study is gratefully acknowledged.

Much of the field data presented has been made available by various agencies which include those within the Alberta Cooperative Highway Research Program, the Manitoba Department of Transportation and Shell Canada Limited. This data, together with technical assistance provided by employees of the Highway and River Engineering Division of the Research Council of Alberta during the course of experimental work

and in the preparation of the manuscript is gratefully acknowledged.

To my wife Sandra for her patience, encouragement and sacrifice the author wishes to express his sincere gratitude and appreciation.

TABLE OF CONTENTS

	<u>Page</u>
TITLE PAGE	i
APPROVAL SHEET	ii
ABSTRACT	iii
ACKNOWLEDGEMENTS	v
TABLE OF CONTENTS	vii
LIST OF TABLES	xiv
LIST OF FIGURES	xvi
 CHAPTER I. INTRODUCTION	 1
1.1. Introductory Remarks	1
1.2. Purpose and Scope	4
1.3. Outline of Contents	5
 CHAPTER II. A SELECTED REVIEW OF VARIOUS FACTORS RELATED TO LOW TEMPERATURE CRACKING OF FLEXIBLE PAVEMENTS	 10
2.1. Introduction	10
2.2. Description of Low Temperature Transverse Cracks	11
2.2.1. Crack Initiation	13
2.2.2. Crack Width Development	14
2.2.3. Crack Depth	15
2.2.4. Vertical Displacement	16
2.3. Performance and Economic Considerations	17
2.4. Factors Related to Transverse Crack Development	18
2.4.1. Asphalt Source	19
2.4.2. Asphalt Grade	20
2.4.3. Asphalt Stiffness	21

TABLE OF CONTENTS - (Cont'd.)

	<u>Page</u>
2.4.4. Asphaltic Concrete Fracture Characteristics	22
2.4.5. Asphaltic Concrete Age	25
2.4.6. Asphaltic Concrete Thickness	26
2.4.7. Subsurface Materials	27
2.5. Summary	28
CHAPTER III. TEMPERATURES IN ASPHALTIC CONCRETE PAVEMENT STRUCTURES SUBJECTED TO LOW TEMPERATURE CLIMATIC ENVIRONMENTS	
3.1. Introduction	33
3.2. Description of Test Sites	34
3.2.1. Alberta Test Project	34
3.2.2. Manitoba Test Project	36
3.2.3. Climatic Environment at Test Sites ...	37
3.3. Asphaltic Concrete Temperatures	39
3.3.1. Daily Temperature Variations	40
3.3.2. Temperature Gradients	41
3.3.3. Rates of Temperature Change	42
3.4. Subgrade Temperatures	44
3.5. Summary	46
CHAPTER IV. HEAT TRANSFER IN PAVEMENT STRUCTURES	
4.1. Introduction	65
4.2. Governing Heat Transfer Equation	65
4.3. Ambient and Pavement Surface Temperatures	67
4.4. Heat Transfer at an Air-Pavement Surface Boundary	69
4.4.1. Shortwave Radiation	70
4.4.2. Longwave Radiation	72
4.4.3. Conduction	74
4.4.4. Convection	75
4.5. The Energy Balance Approach	77

TABLE OF CONTENTS - (Cont'd.)

	<u>Page</u>
4.6. Thermal Properties of Component Layers	78
4.6.1. Thermal Conductivity of Asphaltic Concrete	79
4.6.2. Heat Capacity of Asphaltic Concrete ...	79
4.6.3. Thermal Conductivity of Granular Bases and Subgrade Soils	80
4.6.4. Heat Capacity of Granular Bases and Subgrade Soils	82
4.7. Summary	86
 CHAPTER V. PREDICTED TEMPERATURES IN ASPHALTIC CONCRETE PAVEMENT STRUCTURES	 92
5.1. Introduction	92
5.2. The Finite Difference Approach	92
5.3. Previous Investigations	94
5.4. Formulation of the Finite Difference Equations ...	97
5.4.1. Finite Difference Equation for Temperatures within a Component Layer..	97
5.4.2. Finite Difference Equation for Temperatures at an Air-Pavement Surface Boundary	99
5.4.3. Finite Difference Equation for Temperatures at the Interface of Component Layers	100
5.5. Input Variables for Temperature Prediction	102
5.5.1. Meteorological Variables	102
5.5.2. Structural and Physical Properties	104
5.5.3. Thermal Properties	104
5.6. Predicted Versus Recorded Temperatures	106
5.6.1. Asphaltic Concrete Temperatures	108
5.6.2. Subgrade Temperatures	110
5.7. Summary	111

TABLE OF CONTENTS - (Cont'd.)

	<u>Page</u>
CHAPTER VI. MATERIAL CHARACTERIZATION	128
6.1. Introduction	128
6.2. Pavement Test Sections Included in Study	129
6.3. Determination of Stiffness Modulus	130
6.3.1. Stiffness Modulus-Reduced Time Relationships for Manitoba Asphaltic Concretes	137
6.3.2. Stiffness Modulus-Reduced Time Relationships for Alberta Asphaltic Concretes	138
6.4. Test Method Used for Determining Low Temperature Tensile Properties of Asphaltic Concrete Cores ...	139
6.4.1. Tensile Properties of Manitoba Asphaltic Concrete Cores	142
6.4.2. Tensile Properties of Alberta Asphaltic Concrete Cores	144
6.5. Tensile Strengths of Mixes and Asphalt Stiffness	146
6.6. Summary	147
CHAPTER VII. STRESS PREDICTION AND LOW TEMPERATURE FRACTURE SUSCEPTIBILITY OF ASPHALTIC CONCRETE	177
7.1. Introduction	177
7.2. Stress Predictive Methods	178
7.2.1. Pseudo-Elastic Beam Analysis	179
7.2.2. Pseudo-Elastic Slab Analysis	180
7.2.3. Viscoelastic Slab Analysis	181
7.2.4. Viscoelastic Beam Analysis	182
7.2.5. Approximate Viscoelastic Slab Analysis	183
7.3. Computation of Thermal Stresses	183
7.3.1. Input Variables for Thermal Stress Computations	183

TABLE OF CONTENTS - (Cont'd.)

	<u>Page</u>
7.3.2. Numerical Integration for Pseudo-Elastic Analyses	185
7.3.3. Numerical Integration for Viscoelastic Analyses	186
7.4. Computed Stresses and a Cracking Criterion	187
7.5. Comparison of Observed and Predicted Low Temperature Performance	189
7.5.1. Manitoba Test Sections	190
7.5.1.1. Structure D, Low Viscosity 150-200 Asphalt Pavement	190
7.5.1.2. Structure B, Low Viscosity 300-400 Asphalt Pavement	191
7.5.1.3. Structure B, Low Viscosity 150-200 Asphalt Pavement	191
7.5.1.4. Structure C, Low Viscosity 150-200 Asphalt Pavement	192
7.5.1.5. Structure B, High Viscosity 150-200 Asphalt Pavement	192
7.5.1.6. Other Manitoba Test Sections	192
7.5.2. Alberta Test Sections	193
7.5.2.1. Results of Stress Analyses for First Winter of Service	193
7.5.2.2. Results of Stress Analyses for Third Winter of Service	193
7.6. Evaluation of Results	194
7.6.1. Approximations and Assumptions	194
7.6.2. Comparison of Stress Analyses	195
7.7. Summary	197
 CHAPTER VIII. GUIDELINES FOR REDUCING TRANSVERSE CRACKING OF ASPHALTIC CONCRETE PAVEMENTS	 220
8.1. Introduction	220
8.2. Previous Design Approaches	220

TABLE OF CONTENTS - (Cont'd.)

	<u>Page</u>
8.2.1. Setting Asphalt Specification Limits	221
8.2.2. Limiting Asphalt or Mix Stiffness Values	222
8.2.3. Prediction of Asphaltic Concrete Fracture Temperature	223
8.2.4. Prediction of Crack Frequency	223
8.3. Proposed Design Guideline	224
8.4. Comparisons Between Proposed and Previously Suggested Guidelines	228
8.5. Summary	229
 CHAPTER IX. SUMMARY, CONCLUSIONS AND RECOMMENDATIONS	 234
9.1. Summary and Conclusions	234
9.2. Recommendations	241
 LIST OF REFERENCES	 243
 APPENDIX A. COMPUTER PROGRAM FOR PAVEMENT TEMPERATURE PREDICTIONS	 A1
A.1. Introduction	A1
A.2. Program Operations	A2
A.2.1. Main Program	A3
A.2.2. Subroutine Boundary	A5
A.2.3. Subroutine Nodal	A6
A.2.4. Subroutine Depth	A6
A.2.5. Subroutine Output	A7
A.2.6. Subroutine Airsun	A7
A.2.7. Subroutine Temperature	A7
A.2.8. Subroutine Graphs	A9
A.2.9. Subroutine Graph1	A9
A.2.10. Subroutine Graph2	A10

TABLE OF CONTENTS - (Cont'd.)

	<u>Page</u>
APPENDIX B. COMPUTER PROGRAM FOR THERMAL STRESS PREDICTIONS USING PSEUDO-ELASTIC ANALYSES	B1
B.1. Introduction	B1
B.2. Program Operations	B2
B.2.1. Main Program	B2
B.2.2. Subroutine Readin	B2
B.2.3. Subroutine Linear	B2
B.2.4. Subroutine Stress	B3
APPENDIX C. COMPUTER PROGRAM FOR THERMAL STRESS PREDICTIONS USING VISCOELASTIC ANALYSES WITH VARIABLE TIME INCREMENTS	C1
C.1. Introduction	C1
C.2. Program Operations	C3
C.2.1. Main Program	C3
C.2.2. Subroutine Readin	C3
C.2.3. Subroutine Linear	C3
C.2.4. Subroutine XI15M	C4
C.2.5. Subroutine Str2	C4
C.2.6. Subroutine Str15	C4
C.2.7. Subroutine XI5M	C5
C.2.8. Subroutine Str5	C5
APPENDIX D. COMPUTER PROGRAM FOR CALCULATING THE MODULUS FUNCTION $R(\xi)$	D1
D.1. Introduction	D1
D.2. Numerical Method for Evaluating $R(\xi)$	D1
APPENDIX E. LISTING OF A COMPUTER PROGRAM FOR THERMAL STRESS PREDICTIONS USING VISCOELASTIC ANALYSES WITH CONSTANT TIME INCREMENTS	E1
E.1. Introductory Remarks	E1

LIST OF TABLES

<u>TABLE</u>		<u>Page</u>
III-1	Time Period of Temperature Data Included in the Analyses	47
III-2	Summary of Air and Asphaltic Concrete Temperatures	48
III-3	Relationships Between Air and Asphaltic Concrete Daily Temperature Ranges	49
III-4	Relationships Between Air and Asphaltic Concrete Temperatures at a Time of Minimum Daily Air Temperature	50
IV-1	Unfrozen Water Content in Typical Nonsaline Soils ..	88
V-1	Input Variables for Temperature Prediction of Structure B	112
V-2	Input Variables for Temperature Prediction of Structure C	113
V-3	Input Variables for Temperature Prediction of Structure D	114
V-4	Input Variables for Temperature Prediction of the Edmonton Structure	115
V-5	Relationships Between Maximum Daily Recorded and Predicted Asphaltic Concrete Temperatures of Structures B, C and D	116
V-6	Relationships Between Minimum Daily Recorded and Predicted Asphaltic Concrete Temperatures of Structures B, C and D	117
V-7	Relationships Between Recorded and Predicted Asphaltic Concrete Temperatures of the Edmonton Structure	118
VI-1	Summary of Properties of Asphalts Included in Manitoba Test Project	148

LIST OF TABLES - (Cont'd.)

<u>TABLE</u>		<u>Page</u>
VI-2	Summary of Properties of Asphalts Included in Alberta Test Project	149
VI-3	Physical Properties of Asphaltic Concrete Cores Obtained from the Manitoba Test Project	150
VI-4	Physical Properties of Asphaltic Concrete Cores Obtained from the Alberta Test Project	151
VI-5	Transverse Crack Frequencies of Pavements Included in the Manitoba Test Project	152
VI-6	Transverse Crack Frequencies of Pavements Included in the Alberta Test Project	153
VI-7	Summary of Tensile Splitting Test Results Manitoba Asphaltic Concrete Cores	154
VI-8	Summary of Tensile Splitting Test Results Alberta Asphaltic Concrete Cores at Construction	155
VI-9	Summary of Tensile Splitting Test Results Alberta Asphaltic Concrete Cores at 34 Months	156
VII-1	Predicted Thermal Stresses in LV 150/200 Asphaltic Concrete Using Viscoelastic Beam Analysis and Various Time Increments	198
VII-2	Predicted and Observed Times and Temperatures of Thermal Fracture of Manitoba Asphaltic Concrete Pavements Composed of LV 150/200 Asphalt Cement	199
VII-3	Predicted and Observed Times and Temperatures of Thermal Fracture of Asphaltic Concrete Pavements Composed of LV 300/400, HV 150/200 and SC-5 Asphalts	200
VII-4	Temperatures During Crack Initiation at Alberta Test Project	201

LIST OF TABLES - (Cont'd.)

<u>TABLE</u>	<u>Page</u>
VII-5 Correlation of Predicted and Observed Initial Times of Fracture Using the Pseudo-Elastic Beam Analysis	202
VIII-1 Maximum Mix Stiffness for Selecting Asphalt Grade ..	230

LIST OF FIGURES

<u>FIGURE</u>	<u>Page</u>
I-1 Block Diagram of the Pavement System	8
I-2 Major Elements of the Solution Analysis and Evaluation Phases for the Design Subsystem	9
II-1 Types of Transverse Pavement Cracks	29
II-2 Comparison of Predicted and Actual Performance Losses in Pavements Exhibiting Transverse Cracking	30
II-3 Factors Associated to Transverse Cracking	31
II-4 Correlation Between Viscosity at 140 F and Penetration at 77 F for Currently Used Asphalt Cements	32
III-1 Asphaltic Concrete Pavement Structures	51
III-2 Daily Mean Maximum and Minimum Air Temperatures for Edmonton, Alberta	52
III-3 Cumulative Frequencies of Maximum Monthly Air Temperatures for Edmonton, Alberta	53
III-4 Cumulative Frequencies of Minimum Monthly Air Temperatures for Edmonton, Alberta	54

LIST OF FIGURES - (Cont'd.)

<u>FIGURE</u>		<u>Page</u>
III-5	Bihourly Air and Pavement Surface Temperature Distributions of Structure B	55
III-6	Bihourly 4 Inch Temperature Distributions in Structures B and C	56
III-7	Daily Range of Temperatures at Various Depths in Asphaltic Concrete Pavement Surfaces Versus Daily Range in Pavement Surface Temperature	57
III-8	Asphaltic Concrete Pavement Temperatures at Various Depths Versus Minimum Daily Air Temperature	58
III-9	Time Rate of Temperature Change Distributions of the Asphaltic Concrete Temperature of Structure C ..	59
III-10	Time Rate of Temperature Change Distributions of the Asphaltic Concrete Temperatures of Structure D	60
III-11	Thermal Regime in the Subgrade of Structure B	61
III-12	Thermal Regime in the Subgrade of Structure C	62
III-13	Thermal Regime in the Subgrade of Structure D	63
III-14	Bihourly 18 in. and 10 in. Temperature Distributions of Structures B and D	64
IV-1	Heat Transfer Between Ground Surface and Air on Sunny Day	89
IV-2	Influence of Initial Moisture Content and Temperature on Unfrozen Water Content of Clay and Silt Soils	90
IV-3	Influence of Temperature on Apparent Specific Heat Capacity	91
V-1	Nodal Elements in a Pavement Section	119
V-2	Depth-Time Grid of a Layered System	120

LIST OF FIGURES - (Cont'd.)

<u>FIGURE</u>		<u>Page</u>
V-3	Influence of Depth on Maximum and Minimum Recorded Subgrade Temperatures	121
V-4(A)	Comparison Between Predicted and Recorded Asphaltic Concrete Temperatures of Structure B	122
V-4(B)	Comparison Between Predicted and Recorded Asphaltic Concrete Temperatures of Structure D	122
V-5(A)	Comparison Between Predicted and Recorded Asphaltic Concrete Temperatures of Structure C	123
V-5(B)	Comparison Between Predicted and Recorded Temperatures of Structure C During Seasonal Maximum Ambient Temperatures	123
V-6	Comparison Between the Predicted and Recorded Thermal Regime in the Subgrade of Structure B	124
V-7	Comparison Between the Predicted and Recorded Thermal Regime in the Subgrade of Structure C	125
V-8	Comparison Between the Predicted and Recorded Thermal Regime in the Subgrade of Structure D	126
V-9	Comparison Between the Predicted and Recorded Thermal Regime in the Subgrade of the Edmonton Structure	127
VI-1	Nomograph for Determining the Stiffness Modulus of Bitumens	157
VI-2	Effect of Time and Temperature on the Stiffness Modulus for a Thermorheologically Simple Material	158
VI-3	Master Stiffness Modulus Curves for Manitoba Asphaltic Concretes at a Reference Temperature of 0 F	159
VI-4	Shift Factor Versus Temperature Relationships for Manitoba Asphaltic Concretes	160

LIST OF FIGURES - (Cont'd.)

<u>FIGURE</u>		<u>Page</u>
VI-5	Master Stiffness Modulus Curves for Asphaltic Concrete Composed of Supplier No. 1 Asphalt Cement	161
VI-6	Master Stiffness Modulus Curves for Asphaltic Concrete Composed of Supplier No. 2 Asphalt Cement	162
VI-7	Master Stiffness Modulus Curves for Asphaltic Concrete Composed of Supplier No. 3 Asphalt Cement	163
VI-8	Shift Factor Versus Temperature Relationships for Alberta Asphaltic Concretes at Construction	164
VI-9	Shift Factor Versus Temperature Relationships for Alberta Asphaltic Concretes at 34 Months	165
VI-10	Stress-Strain Relationships for Manitoba Asphaltic Concrete Cores Composed of LV 150/200 Penetration Grade Asphalt Cement	166
VI-11	Stress-Strain Relationships for Manitoba Asphaltic Concrete Cores Composed of LV 300/400 Penetration Grade Asphalt Cement	167
VI-12	Stress-Strain Relationships for Manitoba Asphaltic Concrete Cores Composed of HV 150/200 Penetration Grade Asphalt	168
VI-13	Stress-Strain Relationships for Manitoba Asphaltic Concrete Cores Composed of SC-5 Liquid Asphalt	169
VI-14	Average Failure Strain-Temperature Relationships of Manitoba Asphaltic Concrete Cores	170
VI-15	Average Tensile Failure Strength-Temperature Relationships of Manitoba Asphaltic Concrete Cores..	171
VI-16	Stress-Strain Relationships for Asphaltic Concrete Cores Composed of Supplier No. 1 Asphalt Cement	172

LIST OF FIGURES - (Cont'd.)

<u>FIGURE</u>		<u>Page</u>
VI-17	Stress-Strain Relationships for Asphaltic Concrete Cores Composed of Supplier No. 2 Asphalt Cement	173
VI-18	Stress-Strain Relationships for Asphaltic Concrete Cores Composed of Supplier No. 3 Asphalt Cement	174
VI-19	Average Tensile Failure Strength-Temperature Relationships of Alberta Asphaltic Concrete Cores ..	175
VI-20	Tensile Strength of Mixes as a Function of the Stiffness Modulus of the Asphalt Cement	176
VII-1	Pavement Element	203
VII-2	Influence of Time Increment on Calculated Thermally Induced Stresses in LV 150-200 Asphaltic Concrete Using Elastic Beam Analysis	204
VII-3	Numerical Integration Procedure for Viscoelastic Analyses	205
VII-4	Thermally Induced Stress at Various Depths in the LV 150-200 Asphaltic Concrete Pavement Surface of Structure D Using Viscoelastic Beam Analysis	206
VII-5	Thermally Induced Stress at 1/2 Inch Depth of the LV 150-200 Asphaltic Concrete Pavement Surface of Structure D	207
VII-6	Thermally Induced Stress at 1/2 Inch Depth of the LV 300-400 Asphaltic Concrete Pavement Surface of Structure B	208
VII-7	Thermally Induced Stress at 1/2 Inch Depth of the LV 150-200 Asphaltic Concrete Pavement Surface of Structure B	209
VII-8	Thermally Induced Stress at 1/2 Inch Depth of the LV 150-200 Asphaltic Concrete Pavement Surface of Structure C	210

LIST OF FIGURES - (Cont'd.)

<u>FIGURE</u>		<u>Page</u>
VII-9	Thermally Induced Stress at 1/2 Inch Depth of the IV 150-200 Asphaltic Concrete Pavement Surface of Structure B	211
VII-10	Thermally Induced Stress at 1/2 Inch Depth of the LV 300-400 Asphaltic Concrete Pavement Surface of Structure C	212
VII-11	Thermally Induced Stress at the 1/2 Inch Depth of the HV 150-200 Asphaltic Concrete Pavement Surface of Structure C	213
VII-12	Thermally Induced Stress at the 1/2 Inch Depth of the HV 150-200 Asphaltic Concrete Pavement Surface of Structure D	214
VII-13	Thermally Induced Stress at 1/2 Inch Depth of the SC-5 Asphaltic Concrete Pavement Surface of Structure B	215
VII-14	Thermally Induced Stress at 1/2 Inch Depth of the SC-5 Asphaltic Concrete Pavement Surface of Structure C	216
VII-15	Thermally Induced Stress at 1/2 Inch Depth of Asphaltic Concrete Pavement Surface Composed of Supplier No. 1 Asphalt Cement	217
VII-16	Thermally Induced Stress at 1/2 Inch Depth of Asphaltic Concrete Pavement Surface Composed of Supplier No. 2 Asphalt Cement	218
VII-17	Thermally Induced Stress at 1/2 Inch Depth of Asphaltic Concrete Pavement Surface Composed of Supplier No. 3 Asphalt Cement	219
VIII-1	Stiffness Modulus of Asphaltic Concrete Versus Maximum Predicted Thermally Induced Stress	231
VIII-2	Relationships Between Asphalt and Asphaltic Concrete Stiffness Moduli	232

LIST OF FIGURES - (Cont'd.)

<u>FIGURE</u>		<u>Page</u>
VIII-3	Volume Concentration of Aggregate Versus Maximum Predicted Thermally Induced Stress for Various Asphalt Stiffness Moduli	233
A-1	Generalized Flow Diagram of Temperature Prediction Program	A27
A-2	Flow Diagram for Main Program	A28
A-3	Flow Diagram for Subroutine Boundary	A29
A-4	Flow Diagram for Subroutine Temperature	A30
B-1	Flow Diagram for Main Program (Pseudo-Elastic Stress Analyses)	B9
C-1	Flow Diagram for Main Program (Viscoelastic Stress Analyses)	C15

CHAPTER I

INTRODUCTION

1.1. Introductory Remarks

The performance of asphaltic concrete pavements is dependent on many individual and interacting load, environment, construction and maintenance variables. In areas subjected to low temperature climatic environments, significant deterioration in riding quality and increase in maintenance cost of these pavements, commonly referred to as flexible pavements, have been attributed, in part, to non-traffic load associated distress mechanisms. One manifestation of such distress is low temperature transverse cracking. During the past decade many agencies and individuals have expended considerable effort towards developing solutions to the transverse cracking problem. The majority of investigations related to the problem have involved the collection of detailed field inventory data, observation of controlled field test projects and the testing of pavement component materials under various laboratory conditions.

Documented field inventories and observations of controlled field test projects have enabled many significant factors associated with low temperature cracking of asphaltic concrete pavements to be defined. These test projects have also yielded specific information on

the temperature distributions within pavement structures during periods of observed fracture. The low temperature properties of constituent materials of pavements, determined by various material characterization techniques, have been compared with observed field behavior. Such comparisons have permitted the influence of material properties on the low temperature fracture susceptibility of asphaltic concrete mixtures to be assessed and have enabled many factors contributing to subsequent pavement performance losses to be identified.

The form of pavement distress associated with low temperature cracking is but one of a series of distress mechanisms that must be considered in an overall pavement design process. Since a pavement is a complex structure, subjected to a variety of loading and environmental conditions, the solution of the overall pavement design problem requires the development of a comprehensive and coordinated framework in which various components of the problem can be organized. In recent years, systems engineering principles, such as those presented by Hudson et al. (1969) and Hutchinson and Haas (1968), have been employed to structure pavement design processes.

The significant elements of the pavement design system proposed by Hudson et al. (1969) are shown in FIGURE I-1 and include: 1) individual and interacting load, environment, construction and maintenance input variables; 2) physical characteristics of pavements, which include the basic properties which characterize material behavior; 3) primary and limiting output functions of the system; 4) a decision criteria based on economic and performance considerations; and 5) feedback and

interaction between the various units of the system.

The pavement design process proposed by Hutchinson and Haas (1968) is subdivided into six major phases which include: 1) problem definition; 2) solution generation; 3) solution analysis; 4) evaluation and optimization; 5) implementation; and 6) performance assessment. These authors reviewed existing knowledge within each of the six phases of the design system and concluded that one of the most important deficiencies in current knowledge is a quantitative understanding of non-load associated factors which cause progressive deterioration in pavement serviceability.

Within the proposed pavement design systems, component design subsystems may be structured in which one or a combination of forms of pavement distress are considered. One such subsystem which considers the response of flexible pavements at low temperatures has been proposed by Haas and Anderson (1969). These authors organized existing knowledge of pavement distress associated with low temperature cracking within the design framework proposed by Hutchinson and Haas (1968), and concluded that the primary aspect of low temperature response of flexible pavements that must be considered in such a design subsystem is their susceptibility to fracture.

With reference to the subsystem presented by Haas and Anderson (1969), possible causes of low temperature cracking were grouped into the following three categories:

- 1) Exceeding the tensile strength (or tolerable strain) of the bituminous surface as a result of thermally induced stresses

(and strains),

a) without considering traffic loads,

b) when considering traffic loads.

2) Freezing shrinkage and cracking of the subgrade, followed by crack propagation through the base and asphaltic concrete component layers.

3) Freezing shrinkage and cracking of the base or subbase materials, followed by crack propagation through the asphaltic concrete.

Considering category 1(a), the major elements of the solution analysis and evaluation phases of the aforementioned subsystem are shown in FIGURE I-2. As illustrated in this figure, an assessment of the low temperature fracture susceptibility of asphaltic concrete paving mixtures requires a knowledge of the thermal regimes to which asphaltic concrete are subjected, definition of the low temperature stiffness and strength properties of asphaltic concretes, and a model by which the low temperature response of paving mixtures can be realistically evaluated.

1.2. Purpose and Scope

The objectives of this investigation are:

- 1) to summarize, in a statistical manner, recorded temperatures in asphaltic concrete pavement structures subjected to low temperature climatic environments;
- 2) to develop an analytical model for predicting temperatures in asphaltic concrete pavement structures and to compare

- (and strains),
- a) without considering traffic loads,
 - b) when considering traffic loads.
- 2) Freezing shrinkage and cracking of the subgrade, followed by crack propagation through the base and asphaltic concrete component layers.
- 3) Freezing shrinkage and cracking of the base or subbase materials, followed by crack propagation through the asphaltic concrete.

Considering category 1(a), the major elements of the solution analysis and evaluation phases of the aforementioned subsystem are shown in FIGURE I-2. As illustrated in this figure, an assessment of the low temperature fracture susceptibility of asphaltic concrete paving mixtures requires a knowledge of the thermal regimes to which asphaltic concrete are subjected, definition of the low temperature stiffness and strength properties of asphaltic concretes, and a model by which the low temperature response of paving mixtures can be realistically evaluated.

1.2. Purpose and Scope

The objectives of this investigation are:

- 1) to summarize, in a statistical manner, recorded temperatures in asphaltic concrete pavement structures subjected to low temperature climatic environments;
- 2) to develop an analytical model for predicting temperatures in asphaltic concrete pavement structures and to compare

predicted and recorded temperatures;

- 3) to characterize the stiffness and low temperature tensile strengths of various asphaltic concrete paving mixtures which are known to exhibit different low temperature behavior;
- 4) to assess various stress predictive methods by comparing predicted and observed field fracture times and temperatures of various asphaltic concrete pavement surfaces; and
- 5) to develop quantitative guidelines for the design of asphaltic concrete paving mixtures subjected to climatic conditions, where, neglecting all other loading mechanisms, the thermally induced tensile stress may exceed the tensile strength of the asphaltic concrete.

In the present study data obtained from two extensive field test projects in Western Canada, designed to study the low temperature response of asphaltic concrete pavements, have been analyzed to meet these objectives.

1.3. Outline of Contents

The results of previous laboratory and field investigations related to the low temperature cracking problem of asphaltic concrete pavements are briefly reviewed in CHAPTER II.

In CHAPTER III recorded temperatures in asphaltic concrete pavements, during selected time periods of low temperature climatic environments, are summarized. The summary includes daily temperature

variations, temperature gradients and time rates of temperature change in pavement surfaces and subgrade thermal regimes.

CHAPTER IV contains a review of heat transfer concepts as applied to pavement structures. Methods employed to quantify the influence of various heat transfer modes on temperature regimes of pavement structures are discussed and thermal properties of materials comprising such structures are presented.

Assuming a one-dimensional heat conduction problem, a finite difference model for predicting temperatures in layered systems, in response to imposed climatic conditions, is developed in CHAPTER V. Details of the temperature prediction computer program are contained in APPENDIX A. Computed temperatures are compared with measured temperatures in various pavement structures.

Tensile strength and stiffness properties of various asphaltic concrete paving mixtures are presented in CHAPTER VI. These properties are discussed in relation to observed low temperature behavior of pavements in which the mixtures are incorporated.

In CHAPTER VII, numerical methods used to predict thermal stresses in asphaltic concrete pavements are discussed and theoretical considerations for the formulation of the stress prediction methods are reviewed. The various stress analyses are then used to compute thermally induced stresses within the asphaltic concretes whose strength and stiffness properties are given in CHAPTER VI. Details of the computer programs developed for these stress computations are contained in APPENDICES B, C, D and E. Employing a postulated fracture criterion,

predicted times and temperatures of fracture of the paving mixtures are compared with times and temperatures of observed cracking of the corresponding pavements in the field projects. From the results of such comparisons, the stress predictive methods are assessed and a correlation between observed and predicted low temperature fracture susceptibility of the asphaltic concretes is derived.

Utilizing field data currently available, together with the results of the comparisons between observed and predicted pavement fracture, presented in CHAPTER VII, tentative guidelines for the design of asphaltic concrete paving mixtures with respect to low temperature cracking are developed in CHAPTER VIII. A short summary, the conclusions of this investigation, and recommendations for further study are contained in CHAPTER IX.

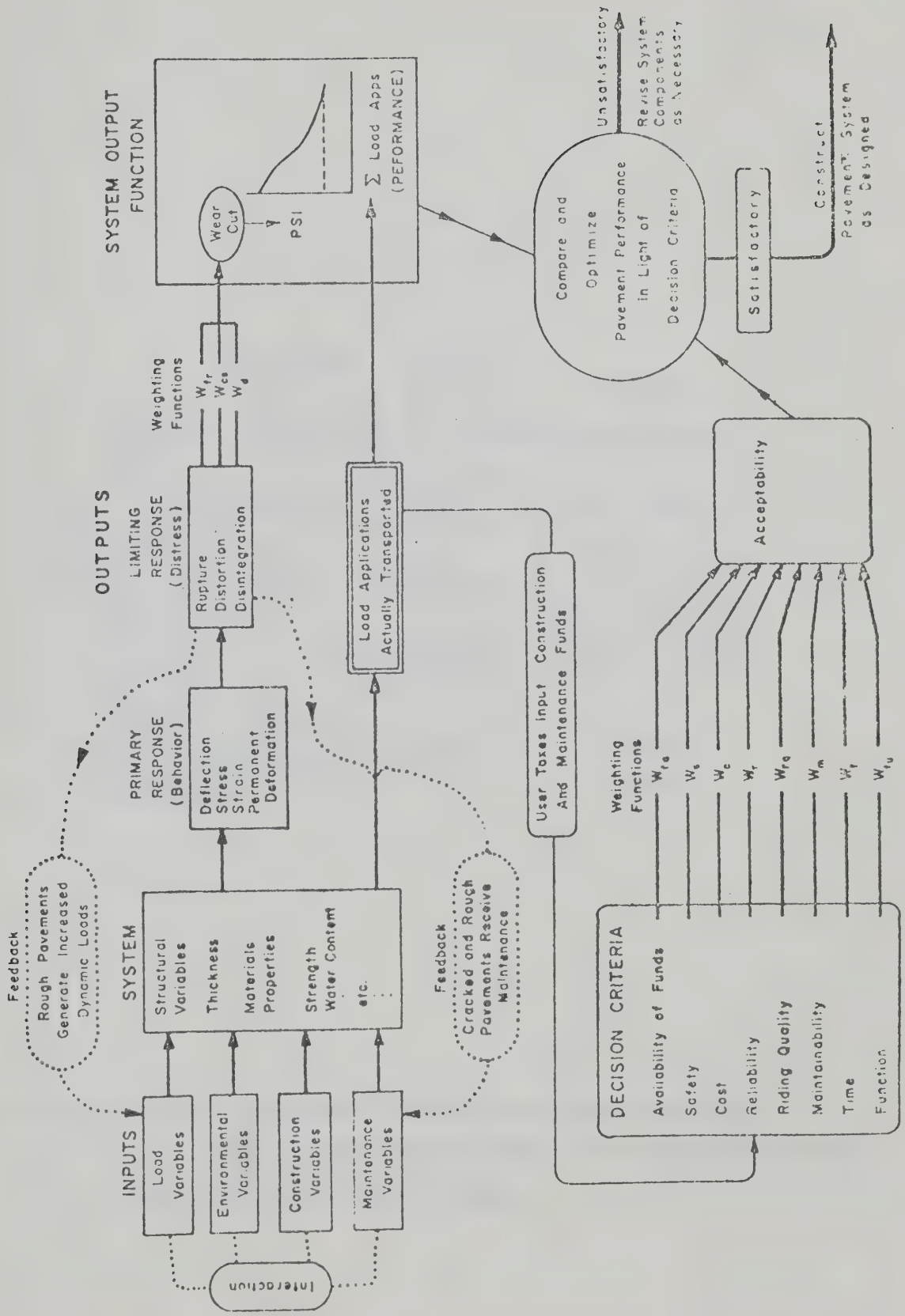


FIGURE I-1 BLOCK DIAGRAM OF THE PAVEMENT SYSTEM (after Hudson et al., 1969)

CHAPTER II

A SELECTED REVIEW OF VARIOUS FACTORS RELATED TO LOW TEMPERATURE CRACKING OF FLEXIBLE PAVEMENTS

2.1. Introduction

Non-load associated fracture of flexible pavements subjected to low temperature climatic environments, such as experienced in the Northern United States, was recognized as a serious problem by Rader (1935). The problem of low temperature cracking became acute in Canada during the mid-1950's and early 1960's when the highway network was rapidly expanding and performance requirements for pavements increased. During this period of time both field and laboratory investigations were initiated in an attempt to define the extent and the causes of transverse cracking. Among the first results of these early studies were those reported by Shields (1964), Shields and Anderson (1964), and Domaschuk et al. (1964).

In 1965, the Canadian Good Roads Association (CGRA) recognized the severity of the transverse cracking problem and placed it within the top priority of research needs in Canada. The paper presented by Monismith et al. (1965) to the Association of Asphalt Paving Technologists concerning thermally induced stresses in asphaltic concrete paving

mixtures and the Association's 1966 Symposium on Non-Traffic Load Associated Cracking gave further recognition to the problem. Since the mid 1960's field test projects designed to study the low temperature response of asphaltic concrete pavements have been constructed and various laboratory studies related to the problem have been either initiated or continued. An ad hoc committee on Low Temperature Behavior of Flexible Pavements was established within CGRA in 1969, the purpose of which was to dimension the low temperature pavement cracking problem in Canada and to document used or suggested design approaches to the problem. The results of this comprehensive review of the subject area has been presented by Haas et al. (1970). In view of this comprehensive review, the content of this chapter is limited to a brief description of low temperature transverse cracks, a review of performance and economic considerations pertaining to the problem, and a summary of some variables which have been found to be associated with transverse crack development.

2.2. Description of Low Temperature Transverse Cracks

In areas of low temperature climatic environment, the fracture pattern of asphaltic concrete surfaces placed on granular base courses or directly on prepared subgrades is commonly one of regular spaced transverse cracks in association with longitudinal cracks along the center line and shoulders of paved surfaces. Such a fracture pattern differs from the more irregular pattern generally exhibited by pavement structures that incorporate portland cement treated or stabilized bases. The irregular spacing of transverse and longitudinal cracks within the

surface of such structures may partially be the result of hydration cracks within the treated base being reflected through the asphaltic concrete. The following discussion is confined to transverse cracks associated with the former pavement structures.

Four types of transverse cracks, as identified by McLeod (1968), are shown in FIGURE II-1. Each type is commonly found in pavements where low temperature cracking has become a serious problem. From continuous crack mapping of different pavement structures included in an extensive field test project designed to study the low temperature response of asphaltic concrete pavements, Young et al. (1969) found that the pattern of transverse crack development often follows a systematic process. This process involves the formation of initial cracks spaced at relatively large intervals followed by the development of subsequent transverse cracks spaced at approximately regular intervals between the initially formed cracks. As transverse crack frequency increases longitudinal cracks may develop in the wheel paths causing a block fracture pattern to develop. Such a fracture pattern of pavements located in Northern Ontario was reported by Kingham (1966).

Results of transverse crack surveys, such as presented by Culley (1966), Shields (1964), Shields et al. (1964) and (1969), Anderson et al. (1966), Fromm (1966), and Young et al. (1969), have shown that within a given locale asphaltic concrete pavements commonly exhibit a wide range in transverse crack frequencies. Typical of the range experienced is that reported by Shields (1964). This particular survey included all main paved highways within a fifty mile radius of

the City of Edmonton, Alberta, in which crack frequencies were found to range from pavements exhibiting no transverse cracks to others exhibiting 400 cracks per mile. Factors believed contributing to such a range in crack frequency are discussed in Section 2.4 of this chapter.

2.2.1. Crack Initiation

Continuously monitoring temperature and crack detection systems, employed in field test projects located in Southern Manitoba and Central Alberta, have enabled temperature conditions conducive to transverse cracking of various pavement structures to be defined. Young et al. (1969) reported that transverse cracking of pavement structures located at the Manitoba test site resulted from the effects of prolonged low temperatures with the majority of cracks being initiated at a time approximately equivalent to the time at which minimum daily air temperatures were recorded. Shields et al. (1969) reported that initial transverse cracking at the Alberta test site was confined to periods of seasonal minimum pavement temperatures. Further evidence of an apparent relationship between transverse crack development and low temperature climatic environment has been presented by Fromm (1966) and Kingham (1966). These investigators reported that pavements located in the northern regions of the Province of Ontario commonly exhibit higher crack frequencies than pavements located in southern areas of the province. Although it is generally agreed that the majority of transverse pavement cracks in Canada initiate during severe winter climatic conditions Culley (1966), Domaschuk et al. (1964)

and Iluculak (1964), reported that transverse cracks become evident after prolonged cold temperatures followed by a sudden rise in temperature.

2.2.2. Crack Width Development

Among the most extensive studies related to transverse crack development have been those reported by Rix (1969), and Shields et al. (1969). From measurements between surface gauge points, installed at transverse crack locations within various mature pavement structures in Alberta and made using a mechanical extensometer, Rix (1969) found that seasonal crack width changes could not be accounted for by simple contraction and expansion of the asphaltic concrete surfaces. Maximum crack widths tended to increase with increased depth of frost penetration within the subgrades of the pavement structures and minimum crack widths, measured during summer months, generally exceeded minimum seasonal widths of the previous year. Permanent crack width increases, for pavements located in Northern Ontario, have also been reported by Kingham (1966).

Employing measurement techniques as used by Rix (1969), Shields et al. (1969) reported that initial surface crack widths of a pavement in Central Alberta were in the order of 0.4 millimeters. Following a period of low temperature, an increase in pavement surface temperature resulted in generally larger crack widths and approximately fifty days after crack initiation a sudden cold spell resulted in further contraction with maximum crack widths in the order of 6.0 millimeters. During the second winter crack openings became much more apparent and maximum

widths of approximately 12.0 millimeters were observed at a time closely related to the time of maximum recorded depth of frost penetration. The authors concluded that since a direct relationship between crack opening and surface temperature was not apparent some mechanism other than simple surface contraction must be operative.

With the exception of these investigations, the influence of subgrade, base and subbase material properties on crack width development has not been included in field studies directly related to the transverse cracking problem. However, Young et al. (1969) reported that initial crack widths of 0.19 inches were measured at the surface of asphaltic concrete structures incorporating a highly plastic clay subgrade, while, surface cracks in structures incorporating a sand subgrade were very minute and difficult to detect by visual observation. Further evidence of the influence of subgrade soil type on crack width development has been presented by Hamilton (1966). Employing uni-directional closed system freezing tests, Hamilton (1966) found that various soils exhibit shrinkage normal to the direction of freezing and that the magnitude of freezing shrinkage is dependent on soil density, plasticity and degree of saturation.

2.2.3. Crack Depth

Asphaltic concrete coring data supplemented by general field observations, such as reported by Huculak (1964), Anderson et al. (1966), Kingham (1966), Shields et al. (1969) and Young et al. (1969), have indicated that in some cases transverse cracks are limited in depth to the asphaltic concrete, while in others, cracks extend through the

surface and into subsurface layers. Deep subsurface cracks are generally found in pavement structures having clay subgrade soils. In both the preceding cases the influence of subsurface layers on promoting transverse cracking of the asphaltic concrete is unknown. However, from results of detailed field and laboratory studies, Anderson et al. (1966) concluded that mechanisms promoting transverse cracking cannot be simply and explicitly stated but undoubtedly involves thermal contraction of surface components which may be masked by the behavior of the subgrade under certain conditions.

The possibility of transverse cracking due to thermal contraction of the asphaltic concrete surface has been supported by results of experimental studies presented by Monismith et al. (1965), Hills and Brien (1966), Haas (1968) and Haas and Topper (1969). Employing various material characterization techniques, theoretical considerations and stress predictive methods, these investigators have all found that at low temperatures predicted thermally induced stresses within asphaltic concrete surfaces may be of a magnitude far exceeding the tensile strength of asphaltic concrete.

2.2.4. Vertical Displacement

The initial effect of transverse cracking on pavement riding quality is generally minor. However, the intrusion of water at crack locations into subgrades exhibiting high potential swelling characteristics can result in heaving at crack locations. On sand subgrades, removal of fine particles by water can result in depressions at crack locations. Kingham (1966) presented data showing that the differential

heave parallel to transverse cracks can be as much as 0.44 inches, with the maximum and minimum vertical movement occurring at the pavement edge and pavement center line, respectively. Vertical displacements at transverse cracks located in various pavements have been reported by Rix (1969). Rix found that such displacements are primarily controlled by the moisture content of the subgrade, while the direction of movement appears related to soil plasticity as well as moisture content.

In addition to vertical displacement, the loss of load transfer at crack locations can result in additional cracks being formed immediately adjacent to the original cracks. As cracking progresses, spalling may develop with progressive removal of surface material by traffic and the eventual formation of potholes. Such events can readily lead to rapid pavement performance losses, increased maintenance costs and decreased pavement surface life.

2.3. Performance and Economic Considerations

Anderson et al. (1966) presented data showing the severe performance losses that can occur in pavements exhibiting ineffectively maintained transverse cracks. The performance-age history of one such pavement is shown in FIGURE II-2. In this figure the predicted performance-age history was determined by means of a mathematical model relating performance to age, strength as measured by deflection and to traffic conditions. The model was developed from data collected on approximately 469 inventory pavement sections on clay subsoils in Alberta. Assuming a terminal serviceability of 4.5, the pavement reached this level in approximately one fourth of its expected life

span. Resurfacing of such a pavement will raise the level of pavement serviceability, however, existing cracks generally reflect through the new surface causing increased maintenance problems and continued performance losses.

Haas (1968) reviewed the economic importance of the low temperature cracking problem in Canada. Based on approximate 1967 costs of crack filling operations in the prairie provinces of Canada, Haas concluded that a conservative estimate of annual maintenance costs of these operations would be at least one million dollars.

In addition to being a source of maintenance expenditures, the reduction in pavement service life caused by transverse cracking may be of much more importance in an economic sense. To the author's knowledge an objective analysis of such costs has not been performed. However, based on a simplified economic evaluation of 1966-67 annual costs of pavement construction in Western Canada, Haas (1968) concluded that it is not unreasonable to suggest that low temperature cracking of pavements in Canada is an annual multi-million dollar problem.

2.4. Factors Related to Transverse Crack Development

From the results of extensive field inventory data and field observations Shields (1964) postulated possible mechanisms promoting transverse cracking which included simple contraction of the asphaltic concrete and/or shrinkage of the subgrade. Considering these possible mechanisms, together with the wide range of materials and climatic conditions encountered, Shields categorized the many factors believed

pertinent to transverse crack development by means of FIGURE II-3.

Factors of possible significance to transverse crack development have also been summarized by Haas (1968). In this latter summary, external and component variables of possible significance were summarized with respect to the pavement component layer in which cracking may initiate. Some factors which have been found to be of recognized significance to the low temperature cracking problem, and which are reviewed in following subsections, include;

- 1) asphalt source,
- 2) asphalt grade,
- 3) asphalt stiffness,
- 4) asphaltic concrete fracture characteristics,
- 5) asphaltic concrete age,
- 6) asphaltic concrete thickness, and
- 7) subsurface materials.

2.4.1. Asphalt Source

Results of transverse crack frequency surveys have shown that one of the most significant variables associated with the occurrence of low temperature cracking is the crude source of the asphalt cement, as indicated by differences in low temperature field behavior of asphaltic concretes composed of similar asphalts but obtained from different suppliers. Shields (1964), Shields and Anderson (1964) and Anderson et al. (1966) presented crack count data for many miles of the Alberta highway system. The data indicated a definite relationship between frequency of cracking and asphalt supplier, although exceptions were

noted. Fromm (1966) reported a similar relationship for pavements within the Province of Ontario. The results of field test projects, such as reported by Culley (1966), McLeod (1969) and Shields et al. (1969), have also shown that pavement structures of similar properties but composed of asphalts from different crude sources exhibit different crack frequencies. Although field observations suggest relationships between crack frequencies and asphalt sources, results of extensive laboratory investigations such as reported by Anderson et al. (1966), have revealed that individual asphalt properties obtained by conventional laboratory testing methods cannot be definitely correlated with this observed behavior.

2.4.2. Asphalt Grade

Incorporated within field test projects in the Provinces of Ontario, Manitoba, Saskatchewan and Alberta were asphaltic concrete pavement surfaces composed of asphalts of different penetrations as measured at 77 F and different absolute viscosity values as determined at 140 F. The results of these test projects, presented by McLeod (1969), Young et al. (1969), Culley (1966) and Shields et al. (1969), respectively, have shown that those asphaltic concretes composed of similar penetration grade asphalts but having different viscosities exhibit significantly different crack frequencies. Asphaltic concretes which incorporated asphalts of the same relative viscosity but of different penetrations were also found to exhibit different crack frequencies. In the former case, cracking was found to be most predominate in the asphaltic concretes composed of the lowest viscosity

asphalt, while in the latter, highest crack frequencies were associated with pavements incorporating the lowest penetration asphalt.

Relationships between absolute viscosity and penetration values of asphalts, measured at 140 and 77 F, respectively and as presented by McLeod (1967), are shown in FIGURE II-4. McLeod denoted lines A, B and C as being representative of high, low and intermediate viscosity asphalts, respectively. From this figure, the wide range in absolute viscosity which may be experienced when grading asphalt by penetration and the range in asphalt penetration when grading by viscosity is apparent. On the basis of the results of the previously mentioned field studies and in particular those presented by Young et al. (1969) the low temperature fracture susceptibility of an asphaltic concrete paving mixture is dependent on both the penetration and the viscosity of the asphalt comprising the mixture.

2.4.3. Asphalt Stiffness

In recent years the stiffness concept, introduced by Van der Poel (1954), has received fairly extensive attention in relation to the low temperature cracking problem. Stiffness, as defined by Van der Poel, is a time and temperature dependent ratio of tensile stress to strain of asphalt materials subjected to various loading conditions. Further details of the stiffness concept are contained in CHAPTER VI. Various methods used to determine stiffness moduli of asphalts at low temperatures have been summarized by Anderson and Haas (1970) and Hajek (1971). These methods may be classified as direct methods, based on direct testing of the asphalt, and indirect methods which make

use of nomographs for estimating low temperature stiffness values from a knowledge of asphalt properties determined at higher temperatures.

Employing a direct tension test on thin films of two typical asphalts used in Canada, Haas (1968) found that the stiffness moduli thus determined could be subjectively related to observed differences in low temperature behavior of asphalt concrete paving mixtures incorporating the asphalts. Using an indirect method of stiffness determination Young et al. (1969) found that the crack frequency of particular asphaltic concrete pavements could be related to the low temperature stiffness moduli of the asphalts comprising the mixtures. In both of these studies, asphalts which exhibited highest stiffness moduli at low temperatures were associated with pavements which exhibit highest transverse crack frequencies.

At the present time, direct means of measuring the low temperature stiffness of asphalt in a simple and repeatable manner are not available. Therefore, low temperature asphalt specification requirements, based on a stiffness approach, have not yet been developed.

2.4.4. Asphaltic Concrete Fracture Characteristics

Visual observations of asphaltic concrete cores taken at transverse crack locations have indicated that the majority of fracture takes place through the asphalt phase. Shields (1966) reported that within three separate pavements approximately 95 per cent of the fracture was through the asphalt phase. He further suggested that, because of the soft stone used in the asphaltic concretes, the observed stone fracture may have occurred during compaction procedures.

Puzinauskas (1966) found that asphaltic concrete cores taken from some Ontario pavements exhibited fractured aggregate particles, although to a variable degree. Burgess (1966) reported having observed varying degrees of large stone fracture where transverse cracks had occurred.

From observations of asphaltic concrete specimens subjected to direct tension tests at temperatures ranging from 30 F to -30 F, Hajek (1971) reported that the percentage of aggregate fracture decreased with increasing test temperature. He stated that these observations, together with those reported by Puzinauskas (1966), lend support to the initiation of transverse cracks at low temperatures because it would be unlikely that such cracking would occur through the aggregate at high temperatures.

From the results of detailed field inventories and test projects various investigators, such as Anderson et al. (1966), Shields et al. (1969) and Young et al. (1969), have shown that no apparent relationship exists between individual asphaltic concrete mix variables, such as asphalt content and aggregate gradation, and crack frequency. However, Christianson (1970) and Anderson and Shields (1971) have presented data showing that tensile fracture properties of field cores and laboratory prepared asphaltic concrete specimens, which are dependent on such variables, can be correlated with low temperature cracking.

From results of tensile splitting tests performed at 0 F on various asphaltic concrete specimens Anderson and Shields (1971) found that the tensile failure strain capability of the specimens increased

with increasing viscosity at 140 F for a given penetration grade asphalt, and increased with increasing asphalt penetration value at 77 F for a given viscosity. The authors suggested that these findings reflect the experience gained with high and low viscosity asphalt cements, but is not readily deduced from conventional asphalt tests at higher test temperatures. The authors also indicated that although a definite limiting failure strain cannot be stated, previous correlations with field behavior suggest that values less than 10×10^{-4} in per in are generally associated with paving mixtures having high potential for cracking under climatic conditions of Western Canada.

Based on results of various test projects, McLeod (1969) prepared a tentative design guide for asphaltic concretes with respect to low temperature cracking. Within this guide, levels of asphaltic concrete stiffness at which cracking is expected and levels at which cracking should be eliminated are given for various minimum expected temperatures. The guide, as more fully described in CHAPTER VIII, is based on asphalt cement stiffness moduli determined by indirect means and dense, well-graded asphaltic concrete mixtures. Such a design approach to the problem reflects the findings of field inventories, full-scale test sections and laboratory investigations that have shown that the major variable contributing to the low temperature fracture susceptibility of an asphaltic concrete paving mixture is the asphalt used.

2.4.5. Asphaltic Concrete Age

Results of transverse crack frequency surveys involving more than 1900 miles of asphaltic concrete pavements in Alberta, summarized by Kathol (1968), have indicated a general increase in crack frequency with increasing pavement age. Kingham (1966) suggested a similar relationship for pavements in the Province of Ontario. Although regional transverse crack surveys have suggested a relationship between crack frequency and surface age, surveys of specific field projects, such as those described by Shields et al. (1969) and Young et al. (1969), suggest that climatic conditions, asphalt source, asphalt grade and subgrade soil type are more important factors influencing initial as well as subsequent crack frequencies.

Studies of changes in asphalt properties with time as related to transverse crack development have been reported by Anderson and Shields (1971) and Culley (1969). From a comparison of the in-service performance of three sources of similar penetration grade asphalts, but ranging from low to high viscosity materials at 140 F, the former authors found that the low viscosity source exhibited the largest variation in conventional physical properties, most rapid densification under traffic and the earliest and largest amount of low temperature cracking. Culley (1969) found that changes in asphalt properties, within five different projects and after twelve months of service, showed no definite relationship with the extent of transverse cracking within the projects.

From the results of these investigations it would appear that a general increase in crack frequency with age may partially be due to an increase in asphaltic concrete stiffness caused by densification under traffic and by an increase in the probability of occurrence of low temperature climatic condition conducive to transverse cracking, which increases with pavement age.

2.4.6. Asphaltic Concrete Thickness

Young et al. (1969) have presented data showing that, when a paving mixture susceptible to low temperature cracking is used, crack frequency is dependent on the structural thickness of the asphaltic concrete. At the Manitoba test site, described by these authors, a 10 inch full depth pavement section was found to exhibit approximately one-half the crack frequency as that associated with a 4 inch asphaltic concrete surface of identical material properties.

Hajek (1971) suggested that such differences in pavement behavior may be explained by the relatively good insulating properties of asphaltic concrete and the resulting influence of these properties on thermally induced stresses within asphaltic concrete surfaces of various thicknesses. In a theoretical study of depth and spacing of tension cracks in semi-infinite elastic solids, Lachenbruch (1961) has presented data showing that the zone of stress relief in such a material increases as crack depth increases. Such data may also aid in explaining the dependency of crack frequency on asphaltic concrete thickness.

2.4.7. Subsurface Materials

In studies related to low temperature cracking of asphaltic concrete pavements the role of the subsurface component layers on promoting or retarding cracking has largely been ignored. However, from observations and data obtained from field test projects and inventory sections various investigators, such as Fromm (1966), Anderson et al. (1966), McLeod (1968) and Young et al. (1969), have recognized that the subgrade can have a significant effect in some cracking situations. The most apparent of these situations is evidenced by pavement structures having sand subgrades generally exhibiting considerably higher crack frequencies than pavements placed over clay subgrades, all other variables being the same. Comparisons between such pavement structures have been reported by Young et al. (1969), where, the transverse crack frequencies of pavement structures having sand subgrades were found to be approximately three times the crack frequencies of pavements with clay subgrades.

The physical properties of granular bases and subgrades of pavements, representing twenty individual inventory sections in the Province of Alberta, have been included in the study presented by Anderson et al. (1966). The authors reported that no explicit relationship could be detected between the properties of the subsurface materials and the crack frequencies within the control sections. Haas et al. (1970) indicated the need for the development of techniques that are quantitatively able to relate soil parameters to cracking susceptibility and crack frequency.

2.5. Summary

In this chapter a description of low temperature transverse cracks, a brief review of performance and economic considerations related to the transverse cracking problem, and a summary of some of the factors which have been found by various agencies and individuals to be associated with the occurrence of low temperature cracking have been presented. It should be emphasized that reference has been made to only a limited number of published references and a more comprehensive review of the subject area has been presented by Haas et al. (1970).

From the studies reported, the low temperature fracture susceptibility of an asphaltic concrete paving mixture appears primarily dependent on the asphalt used. This dependency is reflected by differences in crack frequencies of pavements composed of asphalts obtained from different crude sources, incorporating asphalts of various grades as specified in terms of viscosity and/or penetration and including asphalts which exhibit different low temperature stiffness properties. Once transverse cracking of an asphaltic concrete has initiated the extent of cracking appears to be not only dependent on the asphalt but also on such variables as asphaltic concrete thickness and subsurface materials.

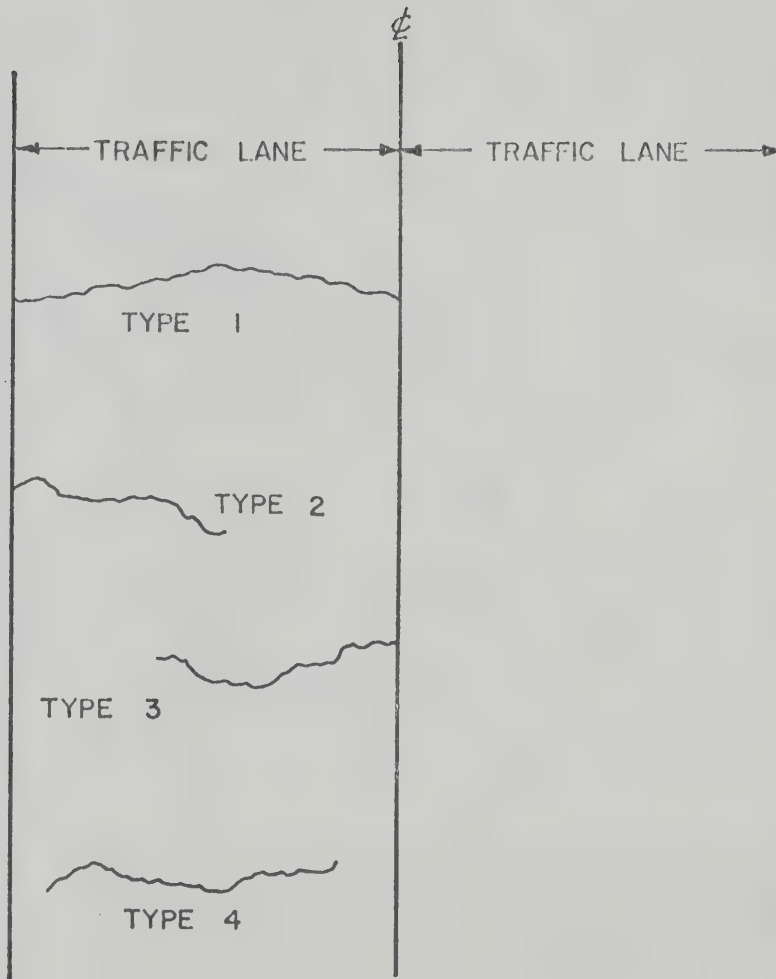


FIGURE II-1 TYPES OF TRANSVERSE PAVEMENT CRACKS (after McLeod; 1968)

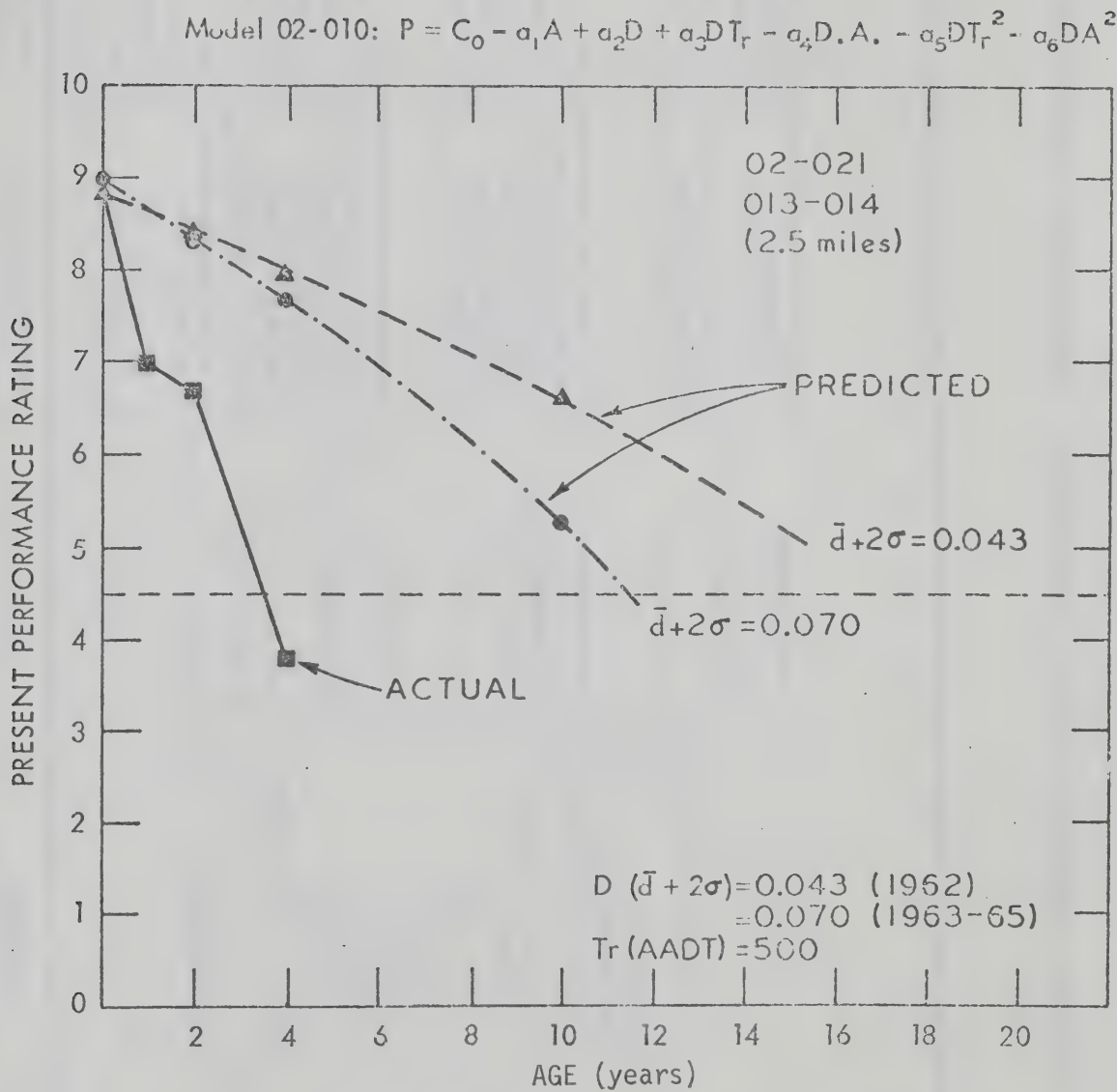


FIGURE. II-2 COMPARISON OF PREDICTED AND ACTUAL PERFORMANCE LOSSES IN PAVEMENTS EXHIBITING TRANSVERSE CRACKING. (after Anderson et al. 1966)

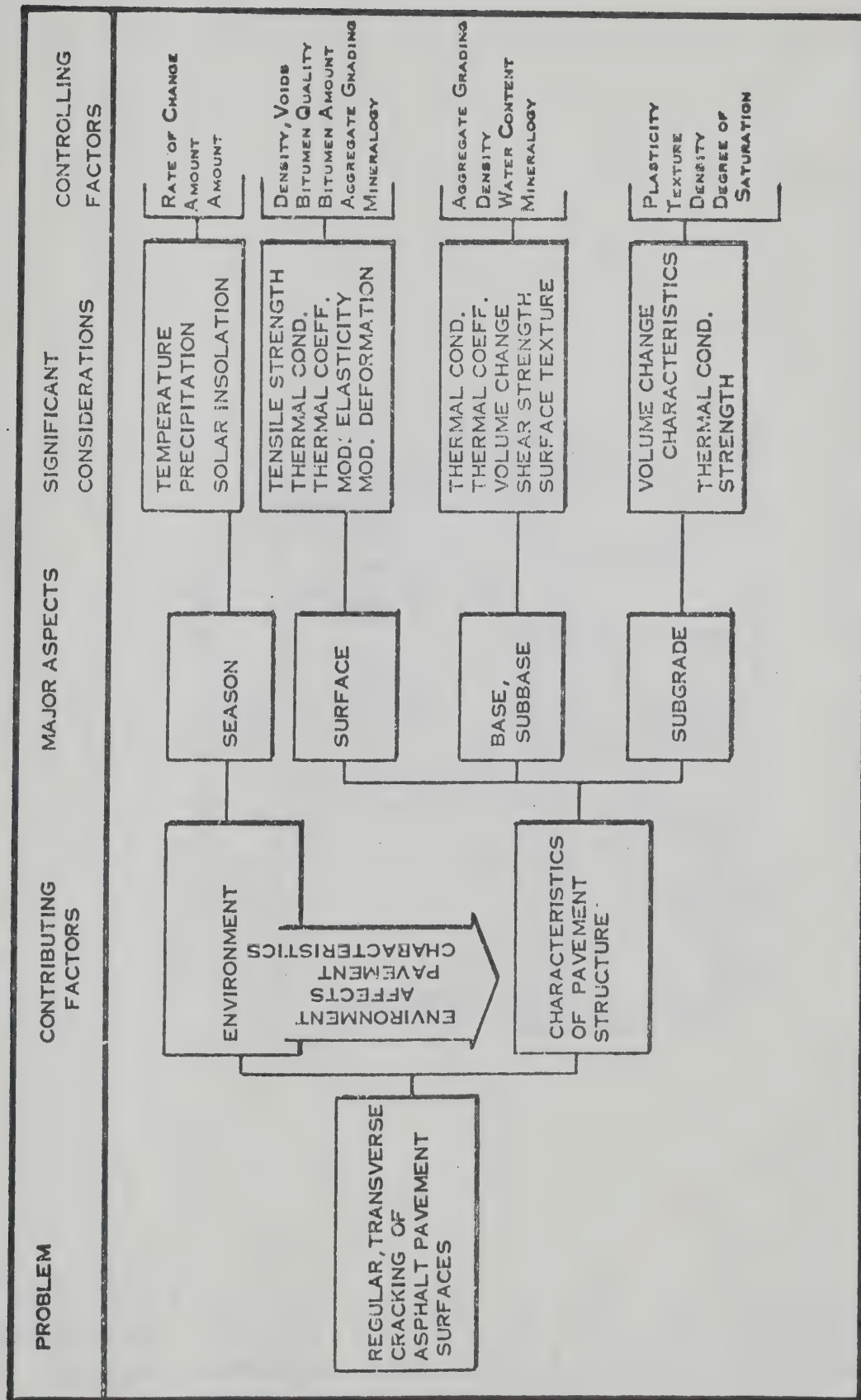


FIGURE II - 3 FACTORS ASSOCIATED WITH TRANSVERSE CRACKING (after Shields, 1964)

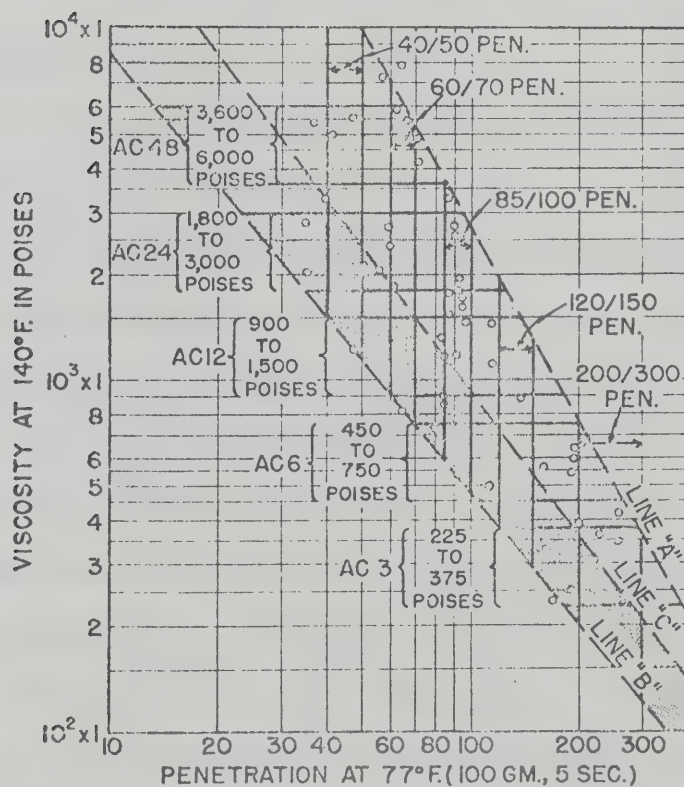


FIGURE II - 4
CORRELATION BETWEEN VISCOSITY AT 140 F. AND PENETRATION
AT 77 F FOR CURRENTLY USED ASPHALT CEMENTS (after McLeod, 1967)

CHAPTER III

TEMPERATURES IN ASPHALTIC CONCRETE PAVEMENT STRUCTURES SUBJECTED TO LOW TEMPERATURE CLIMATIC ENVIRONMENTS

3.1. Introduction

The importance of temperature as related to the behavior of asphaltic concrete paving mixtures has long been recognized. At high temperatures asphaltic concrete paving mixtures require sufficient stability to resist deformations resulting from various rates and modes of traffic loading, while pavement distress resulting from fatigue due to repetitive loadings may be encountered over a wide range of temperatures. In areas of low temperature climatic environment the fracture strength of asphaltic concrete must be sufficient to support traffic during spring thaw periods. Stability, fatigue and fracture strength considerations have become of increased importance as highway and air-field facilities are being subjected to greater traffic volumes coupled with increased allowable loadings. In addition to pavement distress associated with traffic loadings, pavement fracture due to thermal effects is a serious form of distress in areas subjected to low temperatures. The response of a pavement system to these traffic and environmental conditions, as measured in terms of deflection, stress and strain, can

only be expressed in a quantifiable manner if the temperature dependence of the asphaltic concrete pavement component is defined.

Two field studies in Western Canada have yielded continuous surface and subsurface temperature records in several asphaltic concrete pavement structures subjected to climatic temperatures approaching a low of -40 F. In this chapter, the results of statistical analyses of temperatures within the pavement structures, during periods of low temperature climatic conditions, are presented.

3.2. Description of Test Sites

Detailed descriptions and preliminary results of the two field test projects, located in Alberta and Manitoba, have been presented by Shields et al. (1969) and Young et al. (1969), respectively. Temperature as well as other data made available by the agencies involved in these projects has provided the necessary information to carry out the present study.

3.2.1. Alberta Test Project - Shields et al. (1969)

The Alberta test site is located approximately 60 miles south of Edmonton and forms a portion of a four-lane divided freeway in Central Alberta. In order to evaluate more precisely the possible environmental conditions contributing to low temperature transverse cracking, and the influence of asphalt source, the Provincial Department of Highways in cooperation with the Research Council of Alberta decided to incorporate within one 13 mile contract three different sources of 200-300 penetration grade asphalt cement. These three asphalt sources,

obtained from the major refiners in the province, represented high, intermediate and low viscosity materials, as measured at 140 F. It was felt that within a single paving contract, with uniform subgrade and base materials, it would be possible to obtain reasonably homogeneous, contiguous surfaces, wherein the relative behavior of the asphalt cements could be evaluated. By careful planning it was possible to change the asphalt supply so that one source was present on one roadway and the other two sources abutted at a common point on the other roadway.

The geometrics of the pavement system at the site include two 40 foot wide paved surfaces separated by a 64 foot depressed median. The pavement structure, shown in FIGURE III-1(A), consists of a 12 inch granular base course surfaced with a two inch asphalt bound base and a four inch asphaltic concrete surface. The asphalt bound base and granular base was placed in the summer of 1965 with the surfacing the following year. The subsoils are low plasticity tills and alluvial-lacustrine deposits overlying till.

During the first two winters of service, measurements of air, surface and subsurface temperatures were obtained by means of a continuously recording multi-position thermograph used in conjunction with thermistors placed at various depths in the pavement structure. Also, during this period, continuity circuits, consisting of a high conductivity silver base paint, placed in a longitudinal sawn cut on the paved shoulder, enabled temperature conditions conducive to thermal fracture of the pavement sections to be defined. These conditions have

been briefly reviewed in Section 2.2.1 of the previous chapter.

3.2.2. Manitoba Test Project - Young et al. (1969)

The Manitoba test project, more commonly referred to as the Ste. Anne Test Road, is a joint research project of the Manitoba Department of Transportation and Shell Canada Limited. The test road was constructed during the summer of 1967 and constitutes a portion of the westbound two lanes of the four-lane divided Trans-Canada Highway approximately 25 miles east of Winnipeg.

The project consists of twenty-nine 400 foot pavement sections, each having a 24 foot paved surface width, constructed on highly plastic clay and sand subgrades. The primary variables included in the test project are; three pavement structures, four different asphalt binders, two asphalt contents and two aggregate gradations. The three structures are shown in FIGURE III-1 (B), (C) and (D). The asphalts used were a low viscosity (LV) 150-200 penetration grade asphalt, a high viscosity (HV) 150-200 penetration grade asphalt, a LV 300-400 penetration grade asphalt and a slow curing, SC-5, liquid asphalt. Optimum asphalt contents of approximately five per cent by weight of dry aggregate, determined by the Marshall design method, and one per cent below optimum, were the main asphalt contents included in the test project. For some test sections the gradation of the asphaltic concrete aggregate, which was used in the majority of the sections, was modified by the addition of portland cement.

Continuous measurements of air and pavement temperatures were obtained by means of electronic temperature recorders monitoring thermocouples placed at various depths through each of the three pavement structures. In seven of the twenty-nine pavement sections, crack detection circuits were used in an attempt to define initial times of cracking. Details of the temperature and crack detection systems have been described by Deme and Fisher (1968).

3.2.3. Climatic Environment at Test Sites

Shields et al. (1969) indicated that air temperatures recorded at the Alberta test site, during the winters of 1966-67 and 1967-68, could be considered equivalent to long-term average conditions for Central Alberta. Long-term daily mean minimum and maximum air temperatures, determined from meteorological records for the Edmonton area, are shown in FIGURE III-2. As shown in this figure, daily mean minimum and maximum air temperatures are less than 30 F for approximately five and three months of the year, respectively. Such temperature data emphasizes the need of establishing procedures for the design, testing and evaluation of asphaltic concrete pavements at low temperatures, as experienced in the Edmonton area.

Various proposed asphaltic concrete design procedures attempt to incorporate climatic environment by defining a critical temperature with reference to a particular distress criterion. In the design of asphaltic concrete paving mixtures for stability, the critical temperature is generally considered an extreme high temperature to which the asphaltic concrete is likely to be subjected. The

frequencies of occurrence of extreme maximum and minimum monthly air temperatures for the Edmonton area, calculated using records for the period 1881 to 1968, are shown in FIGURES III-3 and 4, respectively. During winter months in the Edmonton area, extreme maximum and minimum monthly air temperatures of 30 F and -50 F, respectively, may be expected. Fromm and Phang (1971) have suggested that minimum expected temperatures for a particular region be chosen on a probabilistic basis. The authors have presented iso-temperature contours, for Canada, based on a one per cent recurrence interval, from which a winter design temperature of -40 F, for Central Alberta, is suggested. This temperature is in close agreement with an air temperature of -50 F, as asphaltic concrete temperatures are generally somewhat higher than air temperatures during periods of extreme cold.

Extreme maximum and minimum air temperatures in the Winnipeg area are similar to those of Edmonton. Bihourly air and pavement surface temperature frequencies for Structure B, identified in Section 3.2.2, for the time period from November 21, 1967 to March 31, 1968, are shown in FIGURE III-5. During this time, air and surface temperatures were less than 30 F for approximately 85 per cent of the time and a minimum air temperature of -45 F was recorded.

For ease of presentation, the one Alberta structure together with the three Manitoba structures, as shown in FIGURE III-1, will be referred to as Structures A, B, C and D, respectively.

3.3. Asphaltic Concrete Temperatures

For each of the four structures, temperature data included in the analyses were for the time periods given in TABLE III-1. Malfunctions of the recording apparatus resulted in incomplete temperature data at the two inch depth of Structure B and only those days with complete asphaltic concrete temperature records were included in the following summaries.

A summary of the daily mean maximum and minimum air and asphaltic concrete temperatures of each structure is given in TABLE III-2. The average temperatures of Structure B were less than those of Structures C and D. This difference can mainly be attributed to the fact that the time period of complete temperature records for Structure B was limited to days of seasonal minimum temperature. However, as shown in FIGURE III-6, at equivalent depths and times, asphaltic concrete temperatures of Structure B were less than those of Structure C. Young et al. (1969) suggested that such temperature differences may partially be accounted for by the fact that Structure B is located in an area void of shelter, while Structure C is located in a wooded area and sheltered from prevailing winter winds.

As observed from TABLE III-2, the daily mean maximum and minimum temperatures of Structure C approximated those within the upper inches of Structure D. This approximation is made by interpolating the temperatures of Structure D to depths equivalent to depths at which temperatures were measured in the asphaltic concrete surface of Structure C. Similar results have been reported by Kallas (1966),

who found that temperatures at depths of 2, 4 and 6 inches in 6 and 12 inch asphaltic concrete surfaces were essentially the same when subjected to similar climatic environments.

3.3.1. Daily Temperature Variations

Although average temperatures, such as summarized in TABLE III-2, are useful in describing the general climatic conditions to which pavements in Western Canada are subjected, during periods of low ambient temperatures, such an analysis does not yield specific information as to the daily temperature variations within such pavement surfaces. Linear regression analyses, using the method of least squares, were employed to develop relationships between daily air and surface temperature ranges and daily ranges of temperature at the depths of temperature recordings in the four pavement surfaces. The results of these analyses are given in TABLE III-3. The relatively high standard errors of estimate of those equations relating daily air-surface temperature variations were expected, since, climatic factors other than just air temperature influence pavement temperature. A review of some of these factors is given in Section 4.4 of CHAPTER IV.

The regression equations, shown in TABLE III-3, relating daily pavement temperature ranges were equated to daily surface temperature variations experienced at the test sites. FIGURE III-7 shows the resulting daily pavement temperature variations with respect to depth. The daily temperature ranges at the two inch depth of Structures A, B and C were approximately 80 per cent of any particular daily pavement surface temperature variation. With increased depth, the daily

temperature variations decreased, and with the exception of the six inch depth shown for Structure A, this decrease appears independent of pavement structure.

3.3.2. Temperature Gradients

As mentioned in Section 2.2.1 of CHAPTER II, Shields et al. (1969) and Young et al. (1969) reported that transverse cracking at the Alberta and Manitoba test sites occurred during times of minimum recorded air and pavement temperatures. The time of daily minimum air temperatures was chosen as a reference time and further linear regression analyses were performed, relating daily minimum air temperatures and asphaltic concrete temperatures at this particular reference point in time. The resultant relationships are shown in TABLE III-4. The standard errors of estimate of equations relating daily minimum air temperature to pavement surface temperature are approximately one-half those relating daily temperature ranges, as previously presented in TABLE III-3. The improved correlations may be attributed to the fact that at the test sites minimum daily temperatures were generally recorded during early morning hours at which time shortwave radiation does not have a direct influence on pavement temperatures.

The regression equations given in TABLE III-4 were equated to daily minimum air temperatures experienced at the test sites and the resulting minimum air-pavement temperature relationships are shown in FIGURE III-8. These relationships indicate that the temperature gradients increased with a decrease in daily minimum air temperature.

Such an increase of temperature gradient is especially noted for Structure D, where, at a minimum daily air temperature of 0 F a temperature differential between the surface and 10 inch depth of 15 F could be expected while, at -35 F the corresponding temperature differential is increased to approximately 25 F. Such changes in temperature gradients with respect to daily minimum air temperatures can be attributed to the particular climatic conditions to which the pavement structures were subjected. Examination of the temperature records revealed that the structures were not subjected to prolonged periods of extreme low temperatures. Therefore, even though the minimum recorded pavement surface temperature of Structure D, during the 1967-68 winter, was -37 F, the minimum recorded 10 inch depth temperature was -6 F.

3.3.3. Rates of Temperature Change

The decrease of daily temperature variations with respect to depth, as shown in FIGURE III-7, implies a decrease in the time rate of temperature change with increased depth. The time rate of temperature change corresponds to a strain rate, which is directly proportional to the temperature change provided that the thermal coefficient of expansion of asphaltic concrete is assumed temperature independent. Various investigators, Domaschuk et al. (1964), Monismith et al. (1965) and Littlefield et al. (1967) have determined the expansion coefficient of asphaltic concretes over various temperature ranges. The reported coefficients vary from approximately 1.2×10^{-5} to 1.7×10^{-5} per degree

Fahrenheit. Recently, Burgess et al. (1971) reported test results on asphaltic concrete specimens simulating those mixtures incorporated in the Manitoba test project. The average coefficient of expansion of the specimens over a temperature range from 68 to -40 F was approximately 1.1×10^{-5} per degree Fahrenheit. The results of these studies suggest that, for practical purposes, the coefficient of thermal expansion of a given asphaltic concrete may be assumed temperature independent and, therefore, a strain rate may be considered directly proportional to a time rate of temperature change.

The rates of temperature change which occurred in the asphaltic concretes of Structures C and D are shown in FIGURES III-9 and III-10, respectively. During the 1967-68 winter season, the rate of surface temperature change of each structure was equal to or less than +3 degrees Fahrenheit per hour for approximately 90 per cent of the time, and equal to or less than -3 degrees Fahrenheit per hour for 10 per cent of the time. At depths of four inches the corresponding rates of temperature change were reduced by a factor of three and at the 10 inch depth of Structure D the rates of temperature change were greatly reduced and were generally within ± 0.5 degrees Fahrenheit per hour. Maximum time rates of surface temperature change recorded at the Manitoba test site were in the order of 8 to 10 degrees Fahrenheit per hour.

A knowledge of such time rates of temperature change is of great value in establishing realistic and meaningful laboratory testing environments. Investigators, such as Hills and Brien (1966),

Haas (1968) and Fromm and Phang (1971), have assumed various time rates of temperature change in studies related to the low temperature fracture susceptibility of asphaltic concrete paving mixtures. Hills and Brien (1966) subjected restrained asphaltic concrete specimens to a cooling rate of 10 degrees Centigrade per hour, while, Haas (1968) used a cooling rate of 30 degrees Fahrenheit per hour, for determining thermally induced stress-temperature relationships of asphaltic concrete paving mixtures. Fromm and Phang (1971) proposed a method of determining the relative low temperature fracture susceptibility of different paving mixtures, in which a rate of 10 degrees Fahrenheit per hour is utilized. This value was determined from an examination of hourly temperature records from various locations within the Province of Ontario which indicated that the ambient temperature drop during a one hour period does not exceed 10 degrees Fahrenheit per hour at temperatures below 0 F.

The results of the present study suggest that, for the climatic environment experienced at the Manitoba test site, time rates of asphaltic concrete temperature change are generally less than those assumed in the preceding laboratory studies, while, a maximum cooling rate of approximately 10 degrees Fahrenheit per hour is consistent with that utilized by Fromm and Phang (1971).

3.4. Subgrade Temperatures

The thermal regimes which existed in the subgrades of Structures B, C and D, during the 1967-68 winter, are shown in FIGURES

III-11, III-12 and III-13, respectively. The isotherms shown in these figures were determined by linear interpolation between recorded temperatures measured at two foot intervals in each of the subgrades. Minimum ambient temperatures at the Manitoba test site were measured during late December and early January during which time maximum subgrade temperature gradients were recorded. Uncertainty exists as to whether these subgrade temperature gradients had a direct influence on initial transverse cracking of the asphaltic concrete pavement surfaces. However, as mentioned in Section 2.4.5 of CHAPTER II, transverse crack frequencies at the Manitoba test site were found to be dependent on subgrade soil type, and since the strength and volume change characteristics of soil are temperature dependent, subgrade thermal regimes may have contributed to crack initiation as well as subsequent crack development.

The maximum depth of frost penetration, as calculated from the position of the 32 F isotherm below the subgrade surface, within the clay subgrade of Structures B and D was 70 inches, while, the maximum depth of frost penetration in the sand subgrade of Structure C was 110 inches. Such a difference in frost penetration depth reflects the influence of the different thermal properties and latent heat of water of the two soil types. The thermal properties referred to are discussed in Section 4.6 of the following chapter.

The bihourly 18 inch and 10 inch depth temperature frequencies of Structures B and D, respectively, are shown in FIGURE III-14. The similarity of these temperature frequencies, together with the equal

depths of frost penetration within the two structures, suggests that, for the prolonged subfreezing subgrade temperatures experienced at the Manitoba test site, the 10 inch asphaltic concrete pavement surface of Structure D and the four inch surface plus 16 inch granular base course of Structure B may be considered equivalent with respect to their influence on subgrade temperatures.

3.5. Summary

In this chapter recorded temperatures in various asphaltic concrete pavement structures subjected to low temperature climatic environments experienced in Western Canada have been summarized. Relationships between daily air and asphaltic concrete temperature variations, and between daily minimum air temperatures and asphaltic concrete temperatures have been developed using linear regression techniques. Time rates of temperature change within two asphaltic concrete pavement surfaces and thermal regimes which existed in subgrades of three pavement structures, subjected to near identical climatic environments, have been presented.

TABLE III-1
TIME PERIOD OF TEMPERATURE DATA
INCLUDED IN THE ANALYSES

Structure	Time Period
A	October 1, 1966 - March 31, 1967, January 1, 1968 - February 29, 1968
B	November 15, 1967 - February 29, 1968
C	November 15, 1967 - March 31, 1968
D	November 21, 1967 - March 31, 1968

TABLE III-2
SUMMARY OF AIR AND ASPHALTIC
CONCRETE TEMPERATURES

Structure	Location of Temperature Measurement	Daily Mean Maximum Temperature (F)	Daily Mean Minimum Temperature (F)
A	Air Surface 2 in 6 in	32.0 (15.5) (a) 34.2 (17.4) 33.1 (16.2) 29.2 (12.5)	11.3 (13.6) 16.5 (11.4) 18.0 (11.1) 22.1 (10.7)
B	Air Surface 2 in 4 in	14.2 (18.7) 16.5 (17.0) 19.6 (16.3) 13.8 (14.7)	-2.4 (22.2) 1.6 (18.5) 7.7 (17.6) 8.5 (15.5)
C	Air Surface 2 in 4 in	23.8 (19.9) 35.1 (22.9) 30.3 (20.2) 25.6 (16.0)	2.5 (20.5) 9.6 (16.2) 12.2 (16.3) 17.7 (14.6)
D	Air Surface 3 in 7 in 10 in	22.3 (19.0) 33.7 (22.4) 26.8 (17.3) 24.2 (15.1) 22.6 (11.4)	1.2 (19.7) 8.4 (15.7) 13.9 (14.5) 16.1 (13.6) 19.9 (11.7)

(a) Figures in brackets indicate one standard deviation.

TABLE III-3
RELATIONSHIPS BETWEEN AIR AND ASPHALTIC
CONCRETE DAILY TEMPERATURE RANGES

Structure	Linear Regression Equation*	Coefficient of Correlation	Standard Error of Estimate (F)
A	$T_{RS} = 1.30 + .79 T_{RA}$	0.61	8.4
	$T_{R2} = 0.90 + .81 T_{RS}$	0.95	2.9
	$T_{R6} = 0.75 + .42 T_{R2}$	0.88	2.0
B	$T_{RS} = 7.09 + .47 T_{RA}$	0.70	3.6
	$T_{R2} = -2.60 + .97 T_{RS}$	0.88	2.7
	$T_{R4} = 2.12 + .27 T_{R2}$	0.38	3.6
C	$T_{RS} = 3.52 + 1.03 T_{RA}$	0.74	8.8
	$T_{R2} = 0.17 + .70 T_{RS}$	0.89	4.6
	$T_{R4} = 1.40 + .36 T_{R2}$	0.79	2.8
D	$T_{RS} = 7.50 + .85 T_{RA}$	0.61	10.0
	$T_{R3} = 0.47 + .49 T_{RS}$	0.95	2.0
	$T_{R7} = 0.50 + .59 T_{R3}$	0.95	1.3
	$T_{R10} = 0.82 + .23 T_{R7}$	0.57	1.3

* T_{RA} = Daily range in air temperature (F)

T_{RS} = Daily range in surface temperature (F)

T_{R2} , T_{R4} , etc. = Daily range in 2 and 4 inch asphaltic concrete temperatures (F)

TABLE III-4
RELATIONSHIPS BETWEEN AIR AND ASPHALTIC
CONCRETE TEMPERATURES AT A TIME OF
MINIMUM DAILY AIR TEMPERATURE

Structure	Linear Regression Equation*	Coefficient of Correlation	Standard Error of Estimate (F)
A	$T_S = 8.00 + .78 T_{MA}$	0.94	4.15
	$T_2 = 2.46 + .96 T_S$	0.99	1.67
	$T_6 = 5.32 + .97 T_2$	0.97	2.59
B	$T_S = 6.02 + .87 T_{MA}$	0.97	4.85
	$T_2 = 1.80 + .95 T_S$	0.99	2.58
	$T_4 = 6.89 + .85 T_2$	0.98	2.46
C	$T_S = 8.44 + .76 T_{MA}$	0.97	4.16
	$T_2 = 3.19 + .98 T_S$	0.99	1.85
	$T_4 = 7.52 + .91 T_2$	0.99	2.64
D	$T_S = 7.64 + .77 T_{MA}$	0.96	4.35
	$T_3 = 7.20 + .93 T_S$	0.98	2.74
	$T_7 = 3.37 + .95 T_3$	0.99	1.35
	$T_{10} = 7.47 + .78 T_7$	0.96	2.95

* T_{MA} = Minimum daily air temperature (F)

T_S = Pavement surface temperature (F)

T_2, T_4 , etc. = Asphaltic concrete temperature at 2 and 4 inch depths (F)

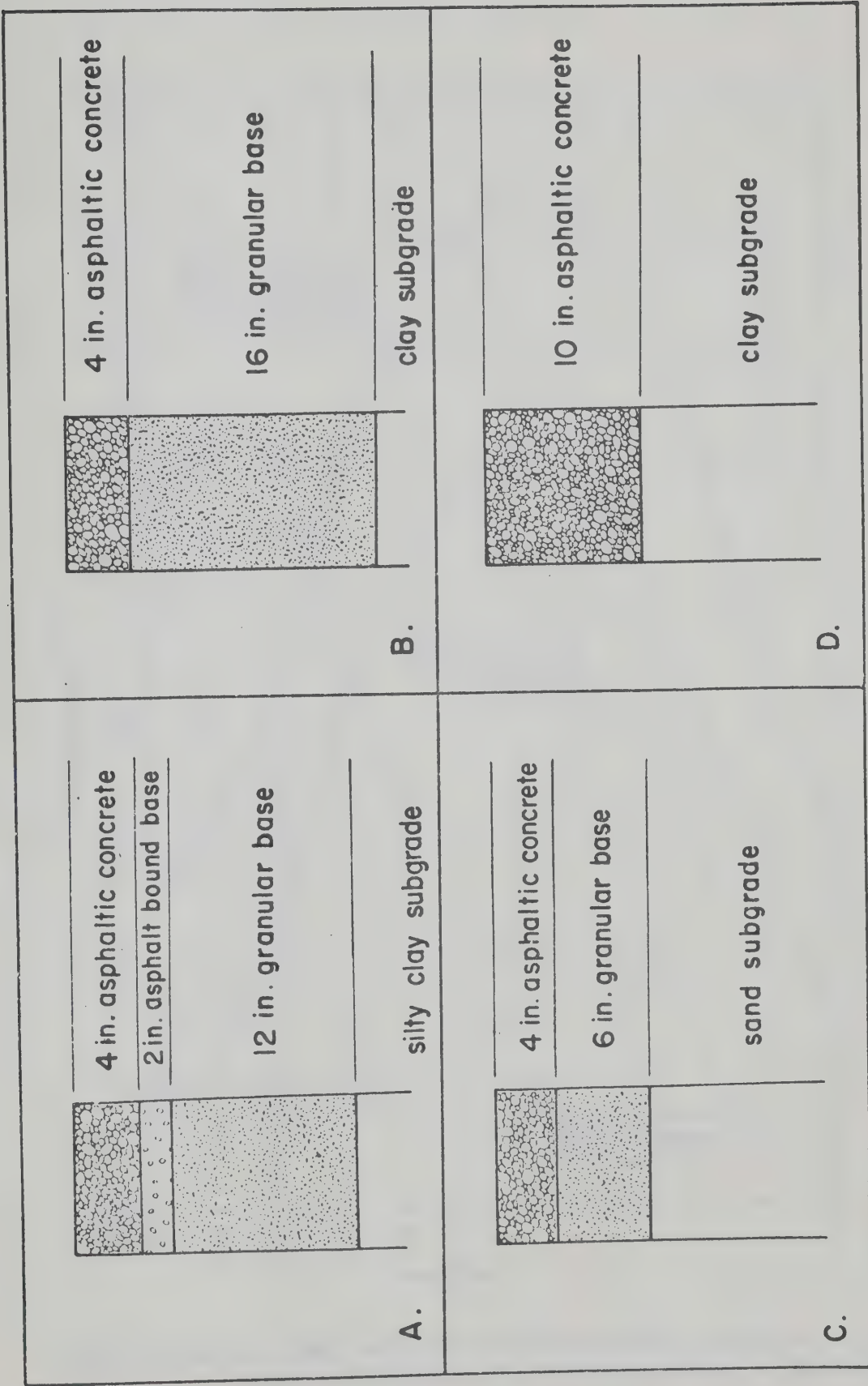


FIGURE III-1 ASPHALTIC CONCRETE PAVEMENT STRUCTURES.

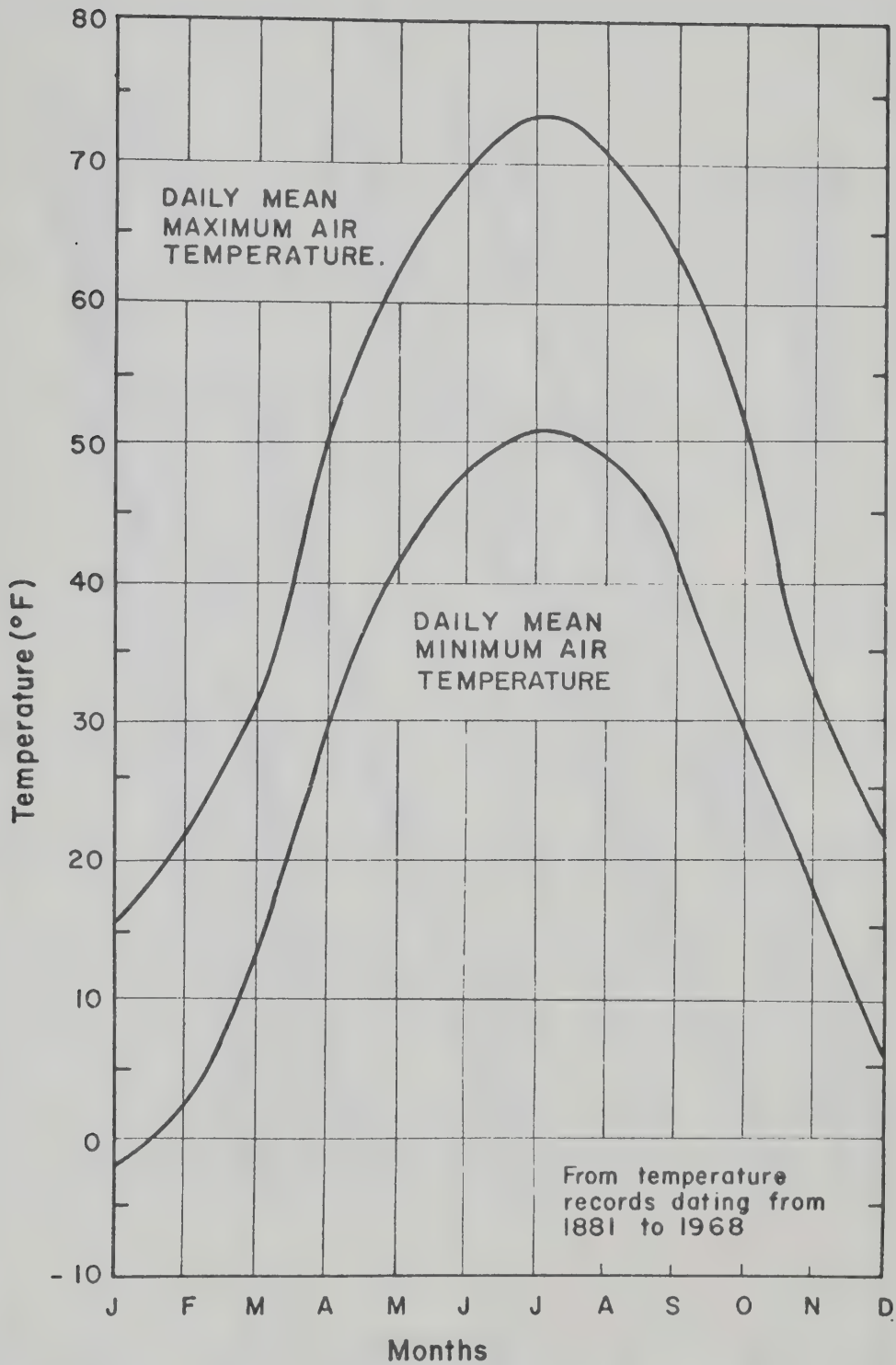


FIGURE III-2 DAILY MEAN MAXIMUM AND MINIMUM
AIR TEMPERATURE FOR EDMONTON, ALBERTA.

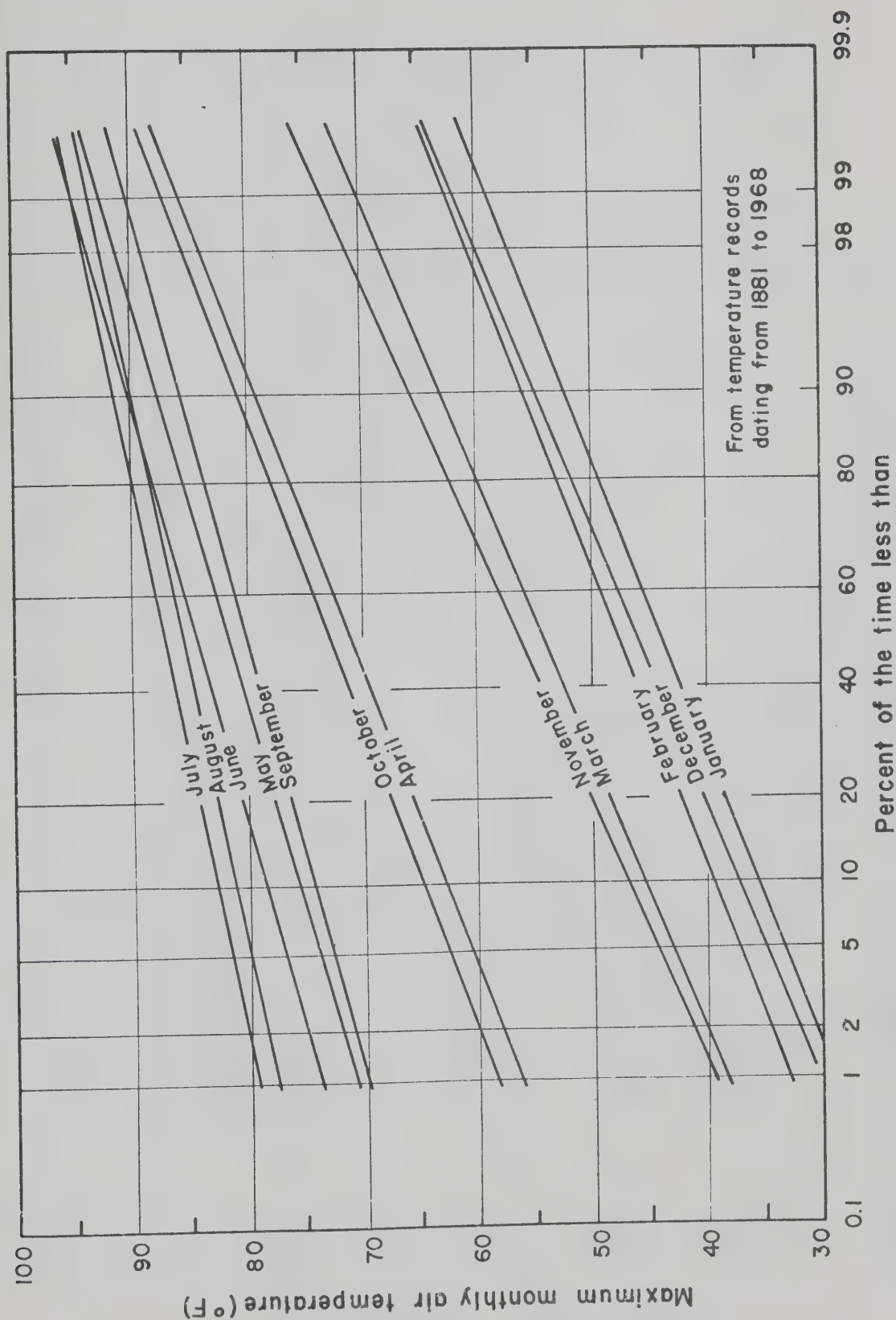


FIGURE III-3 CUMULATIVE FREQUENCIES OF MAXIMUM MONTHLY AIR TEMPERATURES FOR EDMONTON, ALBERTA.

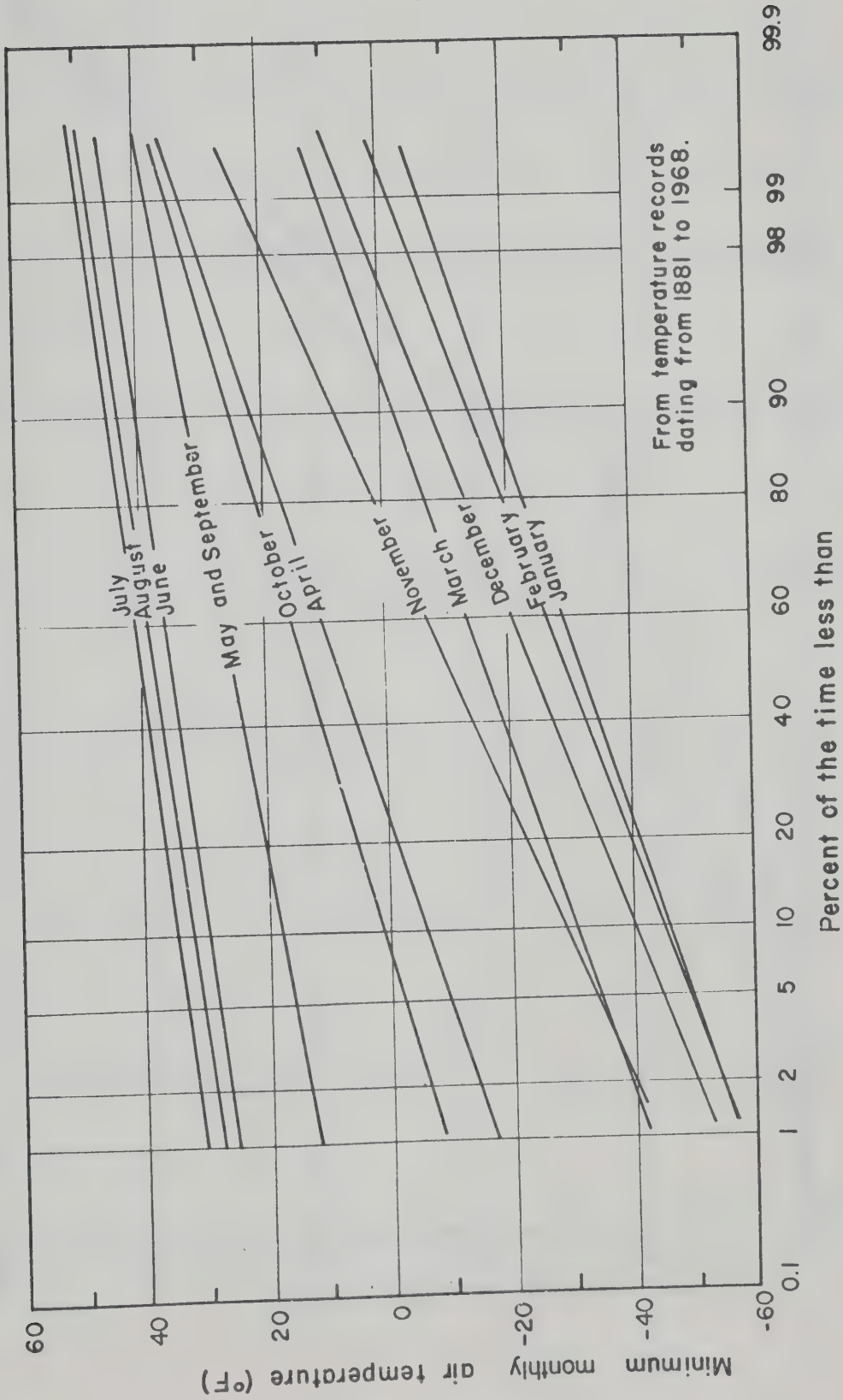


FIGURE III-4 CUMULATIVE FREQUENCIES OF MINIMUM MONTHLY AIR TEMPERATURES FOR EDMONTON, ALBERTA.

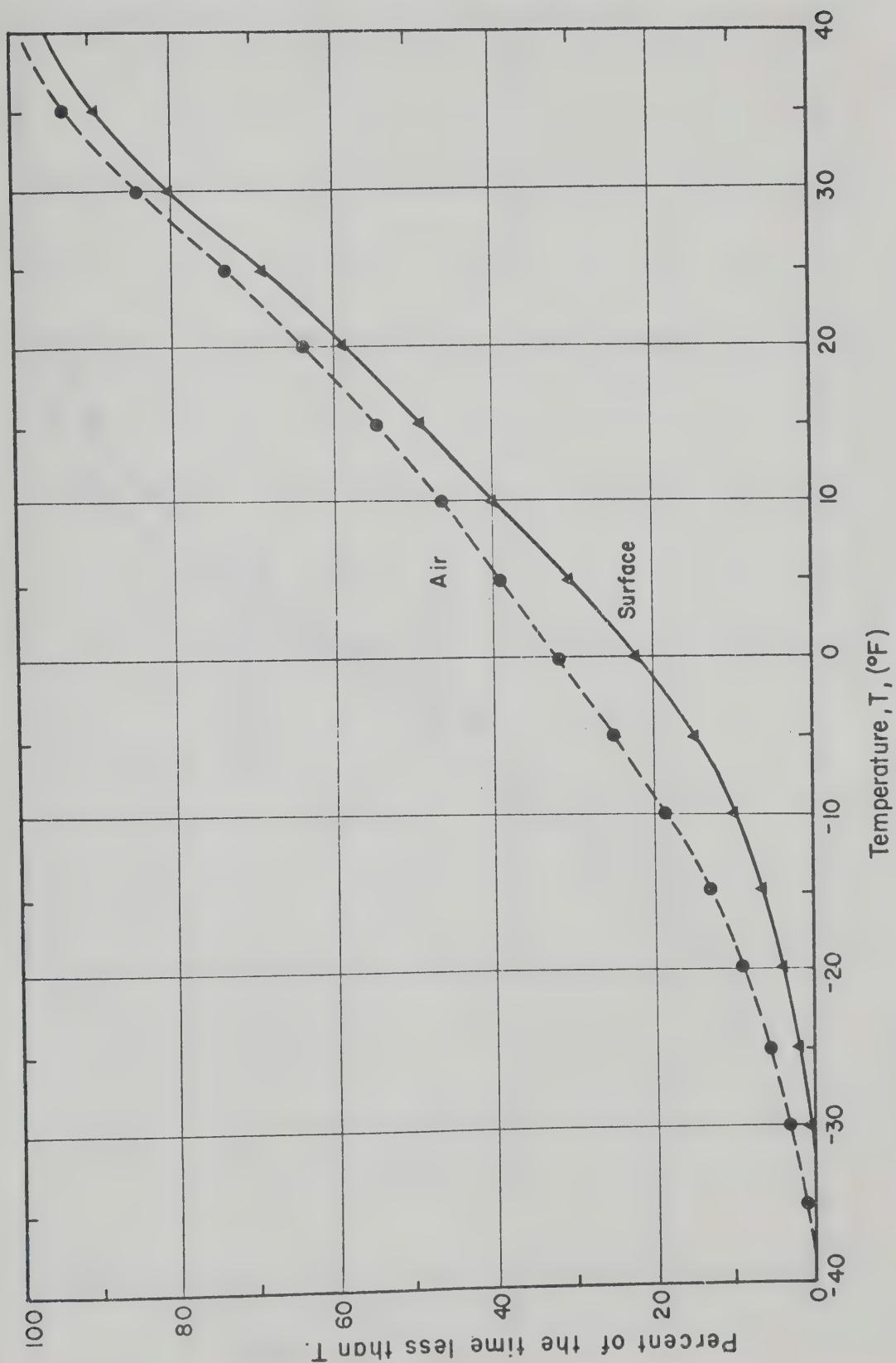


FIGURE III-5 BIHOURLY AIR AND PAVEMENT SURFACE TEMPERATURE DISTRIBUTIONS
OF STRUCTURE B. (Nov. 21, 1967 to Mar. 31, 1968)

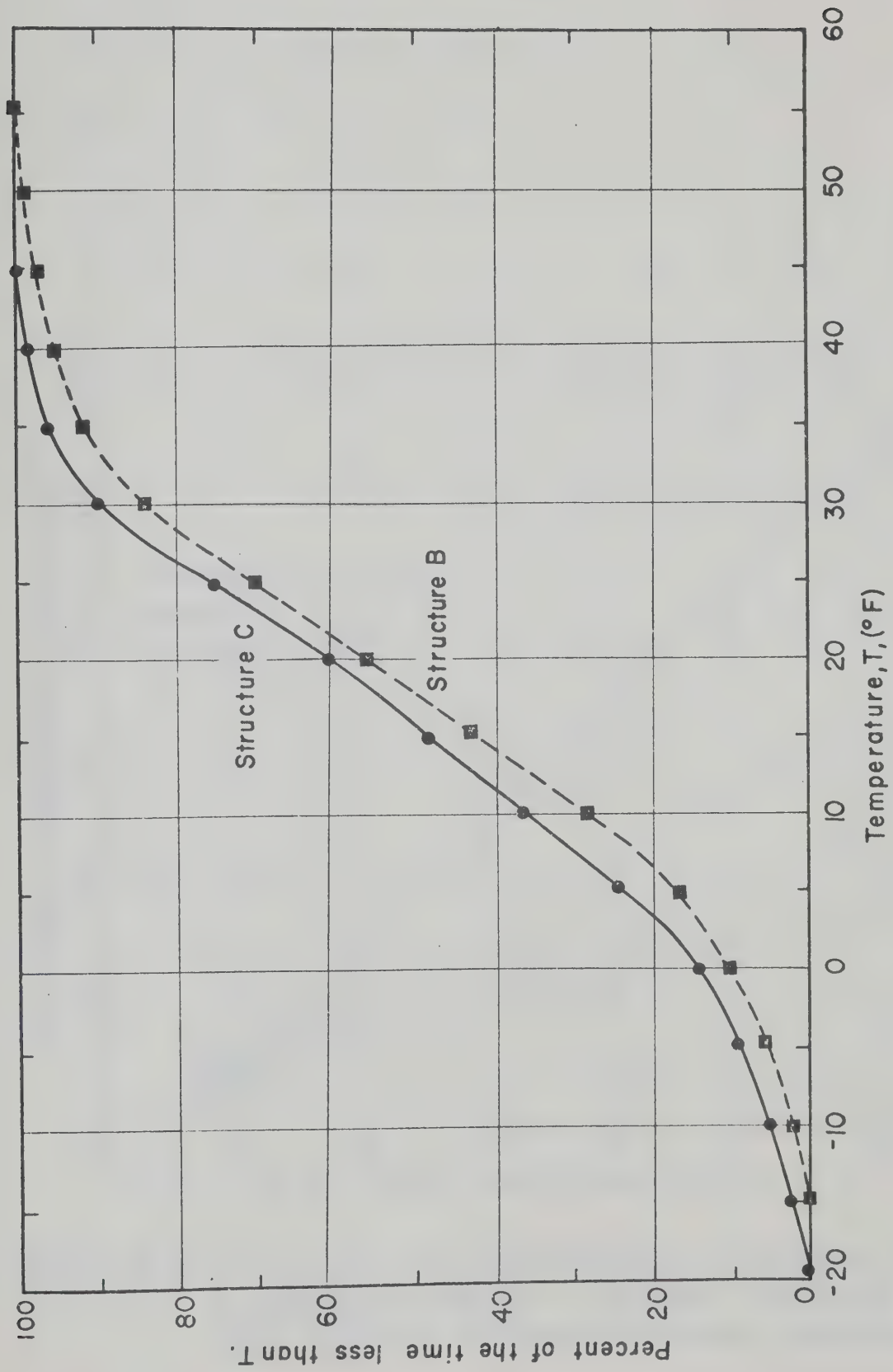


FIGURE III - 6 BIHOURLY 4 INCH TEMPERATURE DISTRIBUTIONS IN STRUCTURES
B AND C. (Nov. 21, 1967 to Mar. 31, 1968)

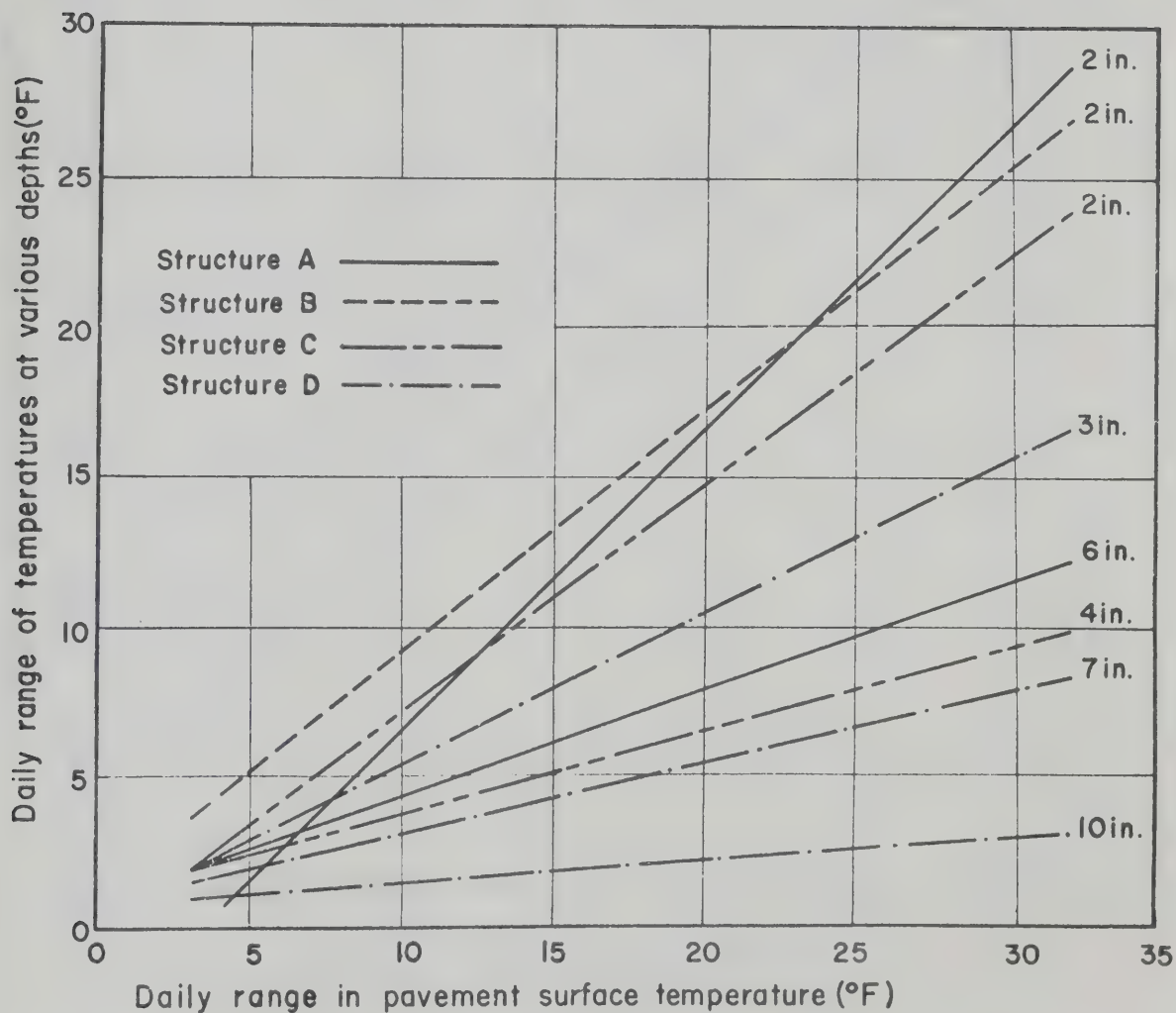


FIGURE III -7 DAILY RANGE OF TEMPERATURES AT VARIOUS DEPTHS IN ASPHALTIC CONCRETE PAVEMENT SURFACES VERSUS DAILY RANGE IN PAVEMENT SURFACE TEMPERATURE.

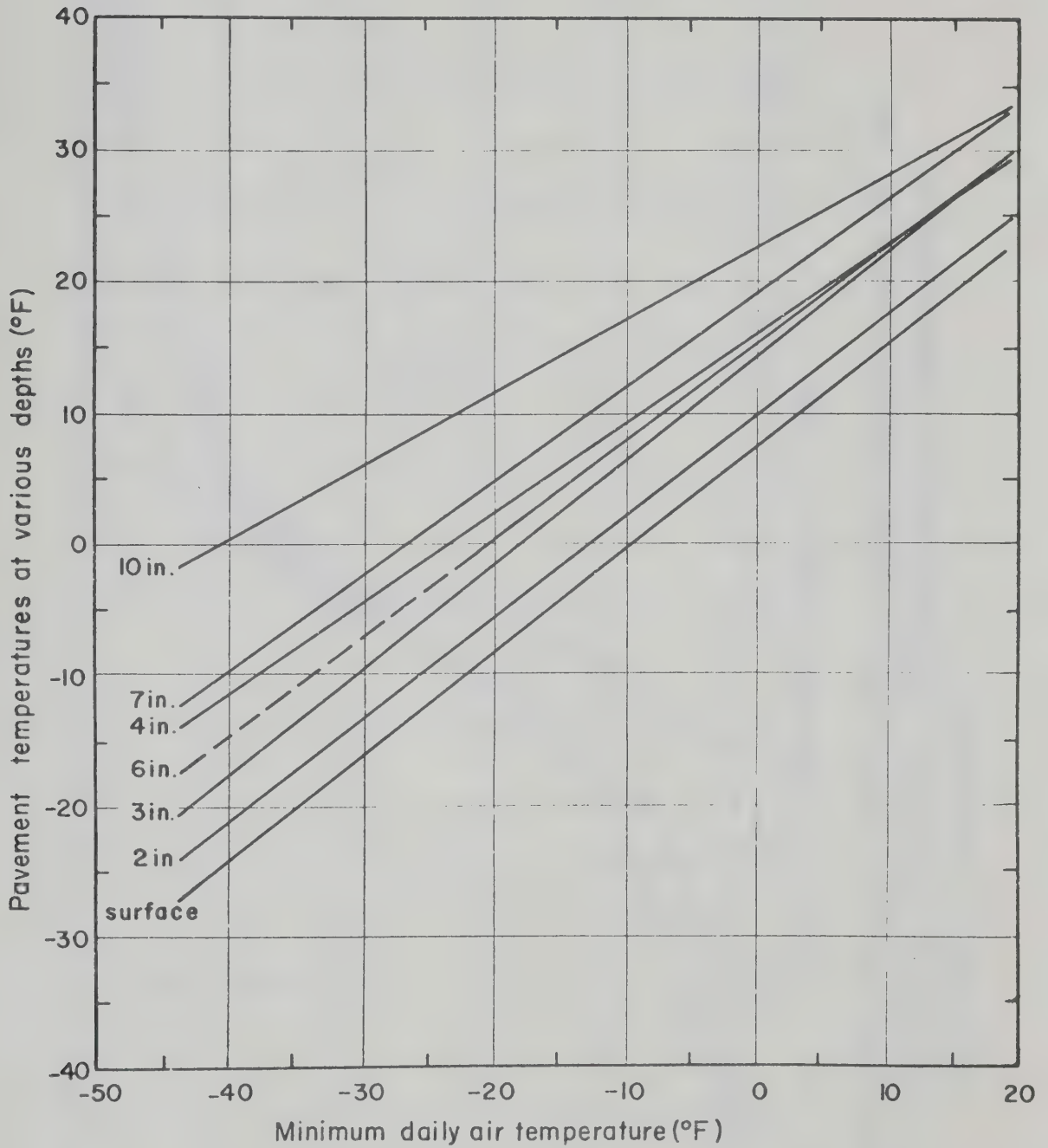


FIGURE III-8 ASPHALTIC CONCRETE PAVEMENT TEMPERATURES AT VARIOUS DEPTHS VERSUS MINIMUM DAILY AIR TEMPERATURE.

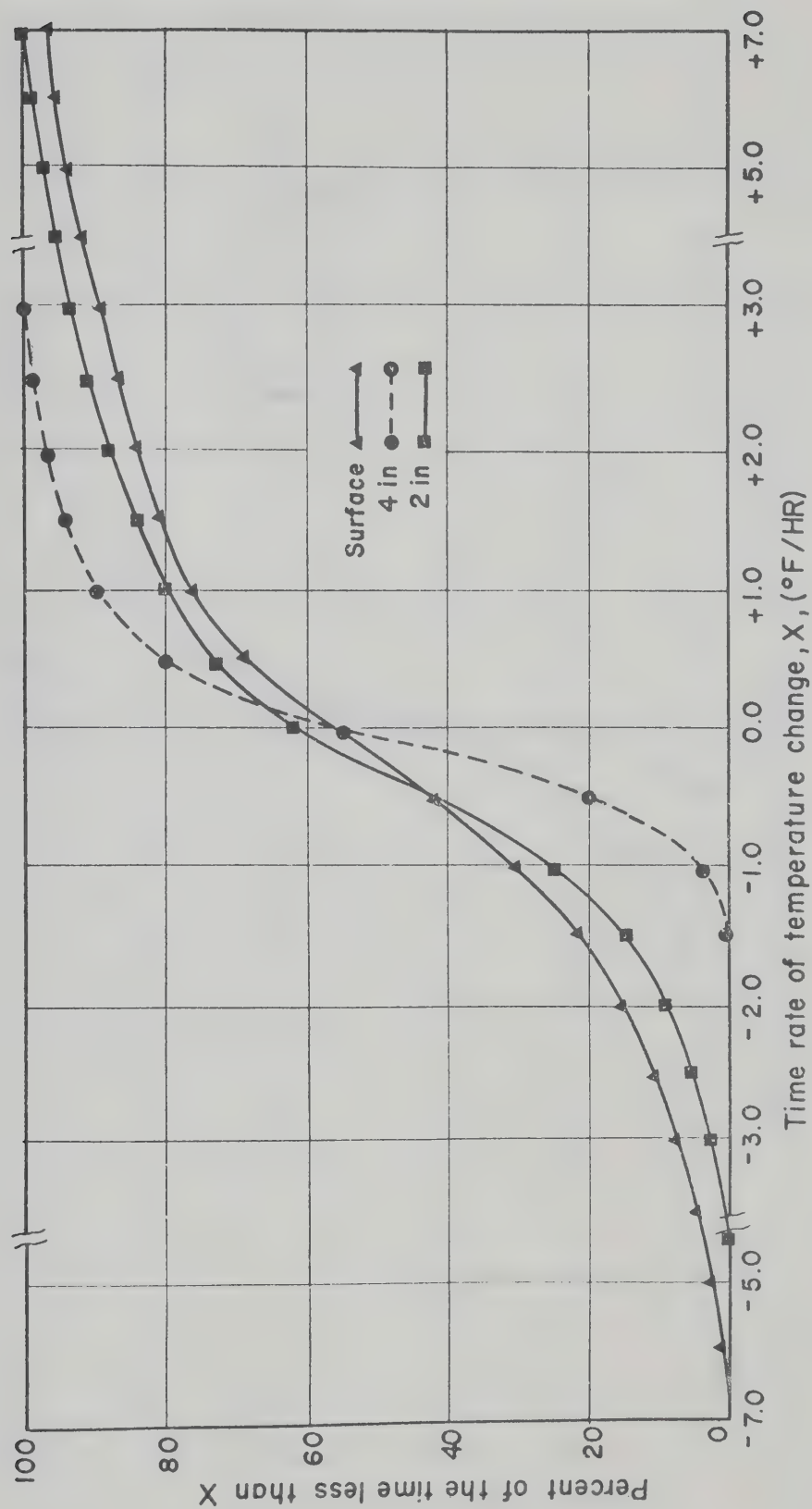


FIGURE III-9 TIME RATE OF TEMPERATURE CHANGE DISTRIBUTIONS OF THE ASPHALTIC CONCRETE TEMPERATURES OF STRUCTURE C.

(Nov. 21, 1967 to Mar. 31, 1968)

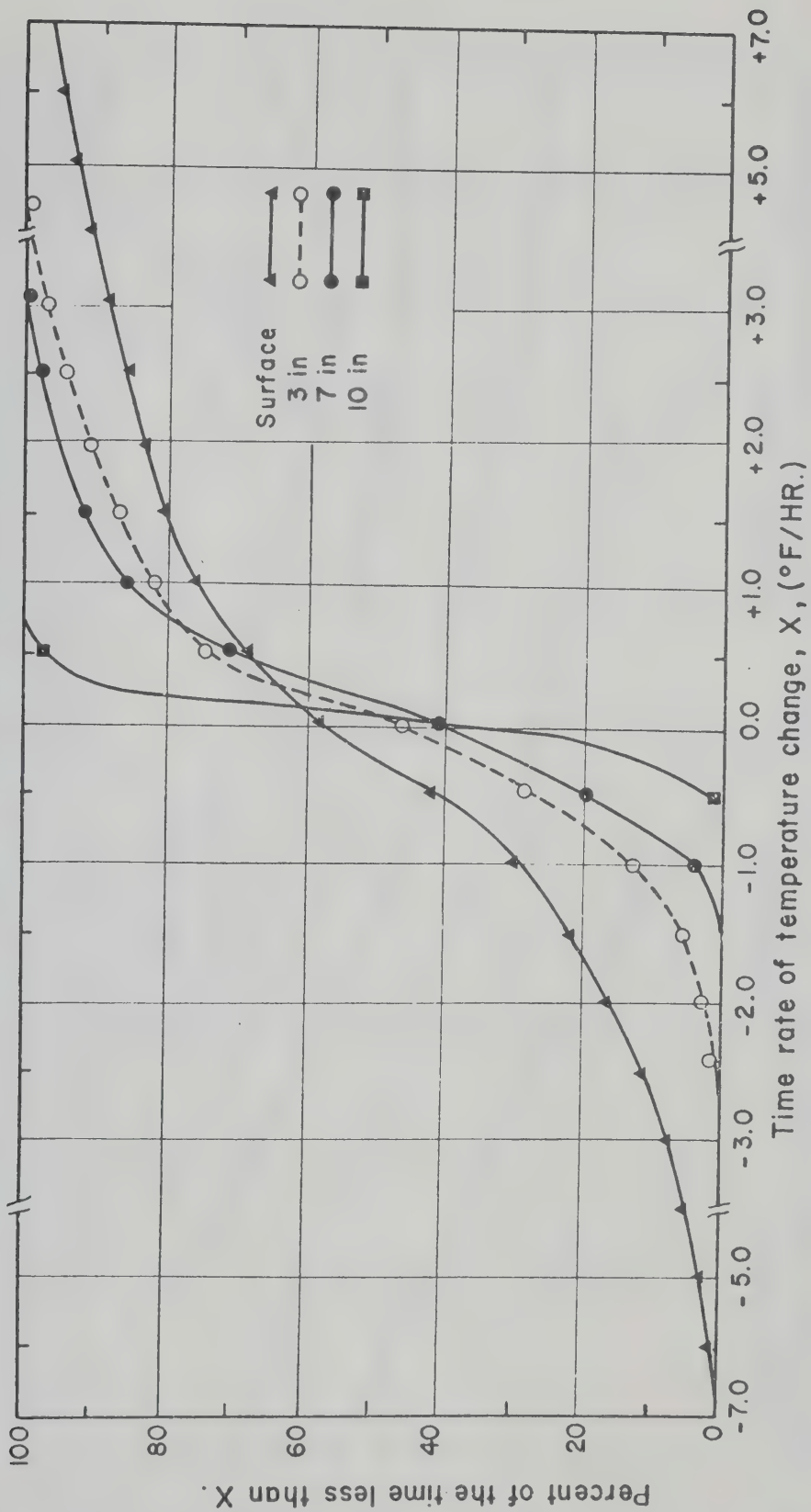


FIGURE III-10 TIME RATE OF TEMPERATURE CHANGE DISTRIBUTIONS OF THE ASPHALTIC CONCRETE TEMPERATURES OF STRUCTURE D.
(Nov. 21, 1967 to Mar. 31, 1968)

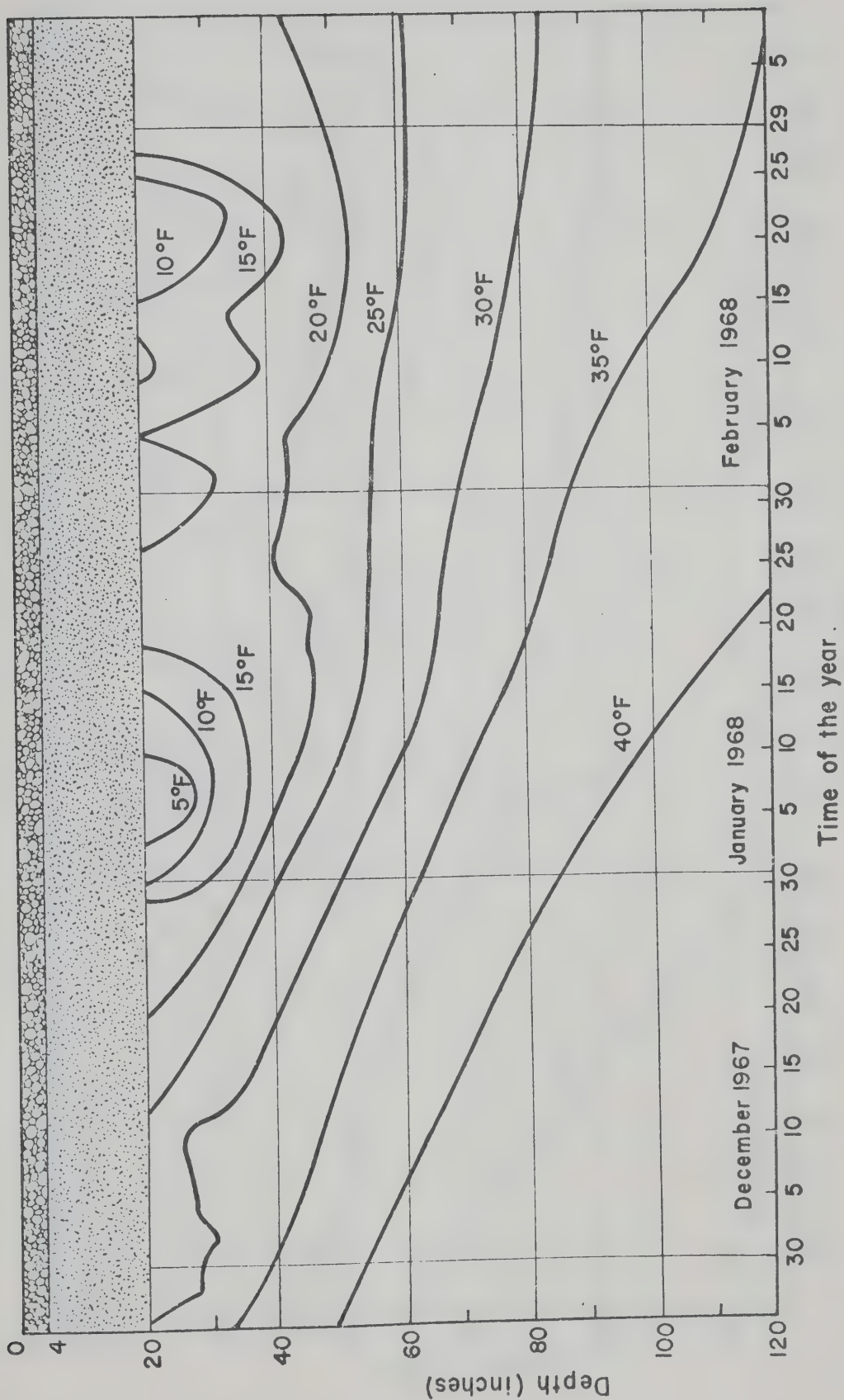


FIGURE. III-11 THERMAL REGIME IN THE SUBGRADE OF STRUCTURE B .

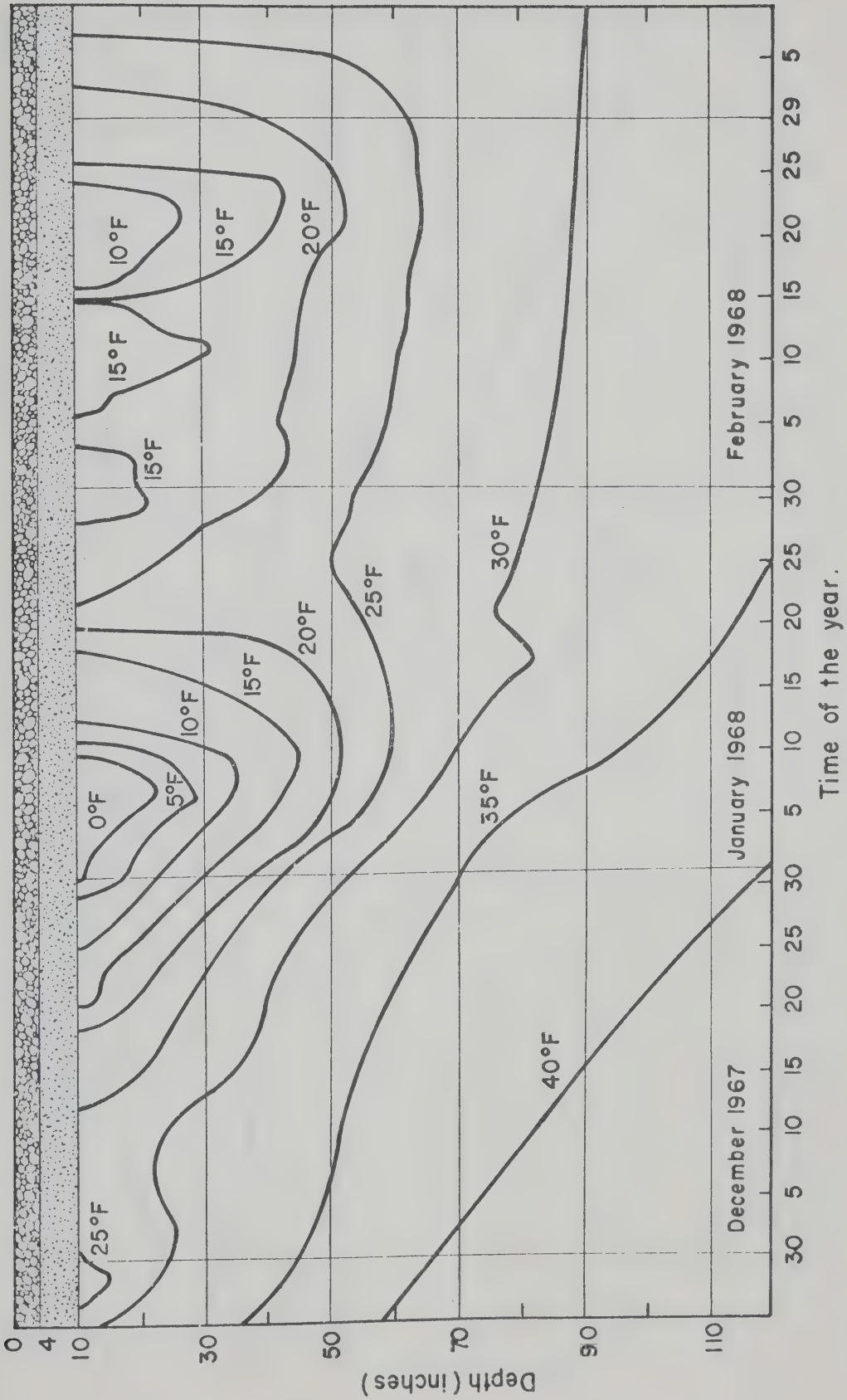


FIGURE III-12 THERMAL REGIME IN THE SUBGRADE OF STRUCTURE C.

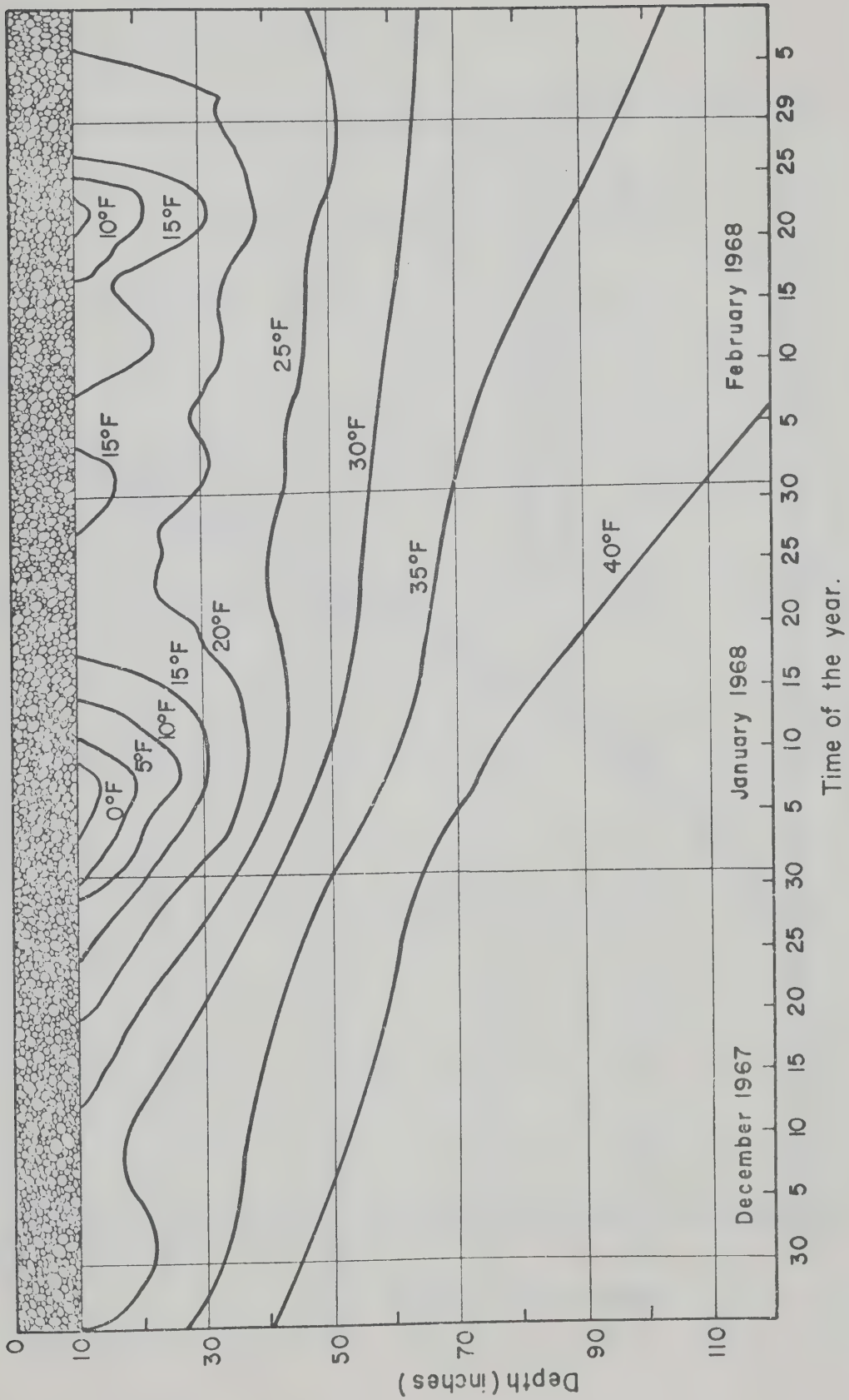


FIGURE III - 13 THERMAL REGIME IN THE SUBGRADE OF STRUCTURE D.

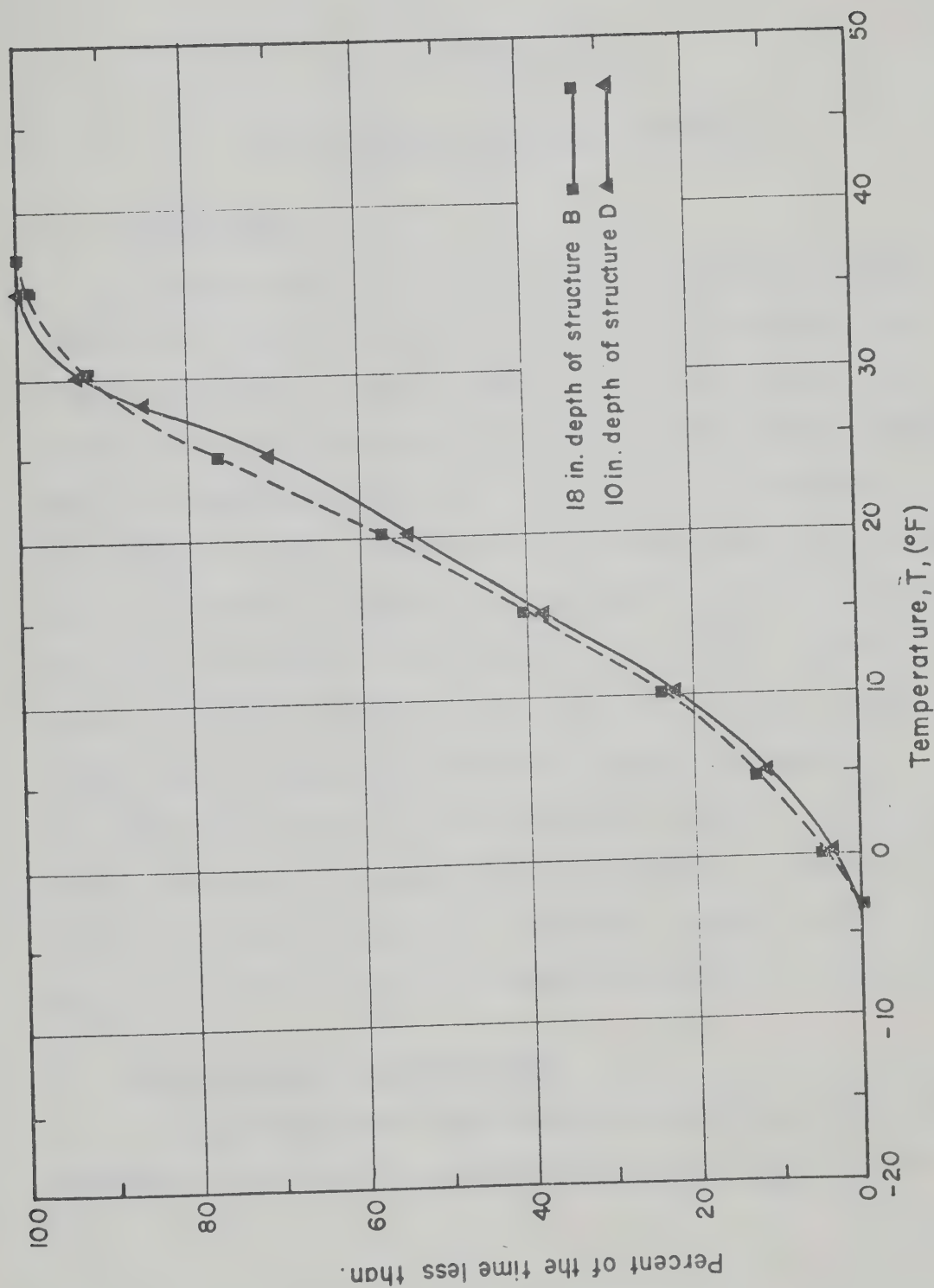


FIGURE III-14 BIHOURLY 18 IN. AND 10 IN. TEMPERATURE DISTRIBUTIONS OF STRUCTURES B AND D, RESPECTIVELY. (Nov. 21, 1967 to Mar. 31, 1968)

CHAPTER IV

HEAT TRANSFER IN PAVEMENT STRUCTURES

4.1. Introduction

In the absence of recorded pavement temperatures, such as summarized in the previous chapter, a realistic assessment of the response of asphaltic concrete pavements to various climatic and loading conditions is dependent on a method whereby pavement temperatures can be reliably predicted. The application of principles of heat transfer in which the influence of climatic factors and pavement material properties on pavement temperatures are considered enable such predictive methods to be developed. In a study of asphaltic concrete fracture temperatures constitute a primary input variable for thermal stress computations and tensile strength determinations. In this chapter heat transfer concepts applied to pavement structures and thermal properties of pavement component materials are reviewed. These concepts and properties have been employed in CHAPTER V where an analytical model for predicting pavement temperatures is developed.

4.2. Governing Heat Transfer Equation

The one-dimensional heat conduction equation governing the dissipation of heat in a homogeneous body is expressed as follows:

$$\alpha \frac{\partial^2 T}{\partial x^2} = \frac{\partial T}{\partial t} \quad (IV-1)$$

where: α = diffusivity of the body,

T = the temperature of the body at a specific depth x and time t .

In a pavement structure the assumption of one-dimensional heat transfer is most likely approximated near the pavement surface where the depth to width ratio of the structure is small. Other simplifying assumptions, concerning negligible moisture and volume changes due to temperature variations, are also inherent in the governing heat conduction equation. As mentioned in Sections 2.2.2 and 2.2.5 of CHAPTER II, substantial volume changes are known to occur in certain subgrade soil types and such changes are often found to be most prevalent in subgrades subjected to frost action. When solving Equation (IV-1) for the pavement temperature regimes errors introduced by assuming constant volume and moisture conditions are difficult to quantify. However, such errors are probably small in comparison to the errors introduced when attempting to define the thermal properties of the component layers and the influence of various climatic variables on pavement surface temperature.

The solution of Equation (IV-1) is dependent on prescribed initial and boundary conditions. In heat conduction problems the temperature distribution throughout a body is generally stipulated as an initial condition, and in relation to a pavement structure, this requires that the temperature gradient at a particular time be known or

estimated. The boundary conditions describe the influence of the surroundings of a body on its surface. At extreme depths in a pavement structure changes in temperature with respect to depth and time become small as compared to temperature variations near the pavement surface. Therefore, the assumption of a constant temperature at a specified depth and for a given time period constitutes a possible boundary condition when determining the temperature distribution in a pavement structure as a function of time. A relationship between various climatological factors and pavement surface temperature forms a second required boundary condition when solving Equation (IV-1) for the thermal regime in a pavement system.

4.3. Ambient and Pavement Surface Temperatures

The most readily recognized climatic variable influencing the thermal regime of a pavement structure is atmospheric temperature. Methods of predicting frost penetration depths in pavement structures, such as those presented by Aldrich (1956) and Sanger (1963), express atmospheric temperature in terms of the parameters degree-days and freezing index. These parameters, together with a knowledge of the thermal properties of the component layers, permit approximate depths of frost penetration to be calculated.

The degree-days of freezing for any one day equals the difference between the average daily air temperature and a reference temperature, provided that the average daily air temperature is less than the reference temperature. The reference temperature is generally assumed equal to 32 F. The freezing index is defined as the difference between

the maximum and minimum points on a cumulative degree-day plot and is a measure of the combined duration and magnitude of below freezing temperatures. The freezing index can be calculated on the basis of air or pavement surface temperature. However, since air temperature data is generally more readily available, the air freezing index is commonly computed and converted to a surface freezing index by assuming a constant ratio between average air and pavement surface temperatures.

Although air and pavement surface temperatures are related, various investigators, Carlson and Kersten (1953), Kersten and Johnson (1955), Sanger (1963) and Penner et al. (1966) have found that this relationship is dependent on such factors as geographic location, thermal properties of the pavement materials and surface type.

Carlson and Kersten (1953) suggested a value of 0.6 as the ratio of surface freezing index to air freezing index, commonly termed the "n-factor", for asphaltic concrete, portland cement concrete and gravel surfaces in Alaska. Kersten and Johnson (1955) concluded that a n-factor of 0.80 was applicable for asphaltic concrete pavement surfaces in the Minneapolis, Minnesota area. Sanger (1963) reviewed the results of frost penetration studies performed by the United States Corps of Engineers and concluded that, for climatic conditions experienced in the northern states, the surface freezing index for bare pavements and smooth soil surfaces is approximately 90 per cent of the air freezing index. Penner et al. (1966) found n-factors of 0.68 and 0.58 for foam plastic insulated and uninsulated asphaltic concrete pavement structures, respectively, at a test site in Sudbury, Ontario.

Methods of predicting depths of frost penetration that incorporate the degree-day concept have the disadvantage of yielding only total frost penetration depths and not temperature variations in a pavement as a function of time and position. Coupled with this factor are the difficulties involved in converting an air freezing index to a surface freezing index. As observed from the relatively wide range of reported n -factors, the relationship between air and pavement surface temperatures is complex. A rational approach to the development of such a relationship involves defining heat transfer phenomena occurring at an air-pavement surface boundary.

4.4. Heat Transfer at an Air-Pavement Surface Boundary

Thermal energy is transferred to and from a pavement surface by means of radiation, conduction and convection. Aldrich (1956) suggested that the transfer of thermal energy between the air and a pavement surface is most affected by direct and diffuse solar radiation, net longwave radiation between the pavement and atmosphere, and convection. The interacting radiation and convection heat transfer modes, as presented by Aldrich (1956), are shown in FIGURE IV-1.

The influence of individual climatic variables such as solar radiation, wind velocity and cloud cover, on the heat economy of a pavement surface is difficult to quantify because of their variation in intensity, time and geographic location. Therefore, predictive methods of defining the influence of such climatic variables on pavement surface temperatures rely heavily on empirical relationships determined from laboratory and field investigations. Also, the availability of

meteorological data at a particular location often dictates the choice of methods used to predict the radiation, conduction and convection heat "quantities".

4.4.1. Shortwave Radiation

Shortwave radiation includes the complete spectrum of solar radiation and is the principal source of heat energy received by a pavement surface during daylight hours. Only a portion of the solar radiation received by the earth's atmosphere reaches the surface of the earth. The intensity of direct and diffuse incident shortwave radiation is dependent on such factors as latitude, altitude, cloud cover, time of year and the time of day at the particular observation site.

Major meteorological stations record the intensity of direct and diffused solar radiation in terms of Btu per sq ft per hr or langley's per sq ft per hr. Where such data is not available the shortwave radiation heat flux at a pavement surface can be estimated by computing the theoretical shortwave radiation received at the site for a clear day and applying a reduction factor based on the per cent of possible daily sunshine received at the site.

Dempsey and Thompson (1970) observed that the intensity of shortwave radiation received by the earth's surface varies parabolically from the time of sunrise to the time of sunset. Based on this observation, the authors developed a computer program from which the intensity of shortwave radiation on pavement surfaces, during finite time intervals, can be readily predicted.

Employing a system of solar radiation cells, Straub et al. (1968) measured the incident solar radiation on an asphaltic concrete pavement surface located at Potsdam, New York. From a comparison of measured solar radiation values and recorded air and pavement temperatures, Straub et al. (1968) concluded that for cloudless days and climatic conditions experienced at the test site, variations in solar radiation have a greater effect on asphaltic concrete pavement temperatures than caused by changes in air temperature.

A semiempirical method of simulating maximum pavement temperatures was developed by Barber (1957). This method includes the effect of solar radiation on pavement temperatures by defining an effective air temperature as follows:

$$T_e = T_a + aI/h \quad (IV-2)$$

where: T_e = effective air temperature, F

T_a = air temperature, F

a = absorptivity of the pavement surface

I = solar radiation, Btu per sq ft per hr

h = surface coefficient, Btu per sq ft per hr per F.

The absorptivity, a , of a pavement surface equals the ratio of solar radiation absorbed to that received by the surface and the distribution of incident energy is independent of the temperature or physical nature of the surface. In previous pavement temperature studies absorptivity values ranging from 0.35 to 1.00 have been assumed.

The shortwave radiation heat flux influencing temperatures at an air-pavement surface boundary may be expressed as follows:

$$Q_{sw} = a Q_{isw} \quad (IV-3)$$

where: Q_{sw} = shortwave radiation heat flux contributing to the thermal regime of a pavement structure, Btu per sq ft per hr

a = absorptivity of the pavement surface

Q_{isw} = solar energy incident on the pavement surface, Btu per sq ft per hr.

4.4.2. Longwave Radiation

Bodies emit energy at a rate proportional to the fourth power of their absolute temperature and the radiation emitted at a given wavelength is found by Planck's spectral distribution. The transfer of the thermal energy by means of longwave radiation at an air-pavement surface boundary is most evident during cold cloudless nights. As shown in FIGURE IV-1, during the day a pavement surface is warmed by shortwave radiation. However, at night the shortwave radiation incident on a pavement surface is reduced to zero and thermal energy transferred by longwave radiation from the pavement results in a rapid cooling of the pavement surface.

Straub et al. (1968) approximated the longwave radiation heat flux at an air-pavement surface boundary by means of the following relationship.

$$Q_{lw} = \sigma e (T_s^4 - T_a^4) \quad (IV-4)$$

where: Q_{lw} = the heat flux resulting thermal energy
transferred by longwave radiation,
Btu per sq ft per hr

e = emissivity of the pavement surface

σ = Stefan-Boltzmann constant,
 0.1714×10^{-8} Btu per sq ft per hr per T

T_s = pavement surface temperature, R

T_a = air temperature, R.

The emissivity of a surface equals the ratio of emitted radiant heat flux per unit area to that of a blackbody at the same temperature and is dependent on such variables as temperature, wavelength and surface composition. Previous asphaltic concrete pavement temperature simulation studies have incorporated emissivity values ranging from 0.93 to 1.00.

Scott (1957) indicated that longwave radiation at the earth's surface is not only dependent on air and surface temperatures but also on cloud cover and vapour pressure. Meteorological stations generally record the duration of bright sunshine during a day which is determined by measuring cloud cover duration. Therefore, when applying a cloud cover correction to the longwave radiation entering the energy balance at an air-pavement surface boundary, it is necessary to assume that the measured cloud cover duration is also representative of that which occurs during nighttime hours.

Geiger (1959) developed an empirical equation in which the longwave radiation emitted by the atmosphere is expressed as a function

of air temperature and vapour pressure. This relationship is as follows:

$$Q_{1wa} = \sigma T_a^4 [G - J (10^{-\rho p})] \quad (IV-5)$$

In Equation (IV-5), Q_{1wa} is the heat flux resulting from longwave radiation emitted by the atmosphere with no cloud cover correction. The terms σ and T_a are as defined in Equation (IV-4) and Geiger assigned the following values to the constants G , J , and ρ : $G = 0.77$, $J = 0.28$ and $\rho = 0.074$. Geiger (1959) suggested that the vapour pressure, p , varies from approximately 1 to 10 millimeters of mercury for climates near the earth's surface.

4.4.3. Conduction

The existence of a temperature gradient between a pavement surface and the layer of air immediately above the surface results in a transfer of thermal energy from the high temperature medium to the low temperature medium. The heat transfer mode is that of conduction and the rate of heat transfer is proportional to the normal temperature gradient at the air-pavement surface boundary. The resulting heat flux can be expressed as follows:

$$Q_{cond} = -K \frac{dT}{dx} \quad (IV-6)$$

where: Q_{cond} = the heat flux resulting from heat transfer by conduction, Btu per sq ft per hr

K = thermal conductivity, Btu per hr per ft per F

dT/dx = temperature gradient, F/ft.

Conduction is the primary mode of heat transfer in a pavement structure and the energy balance of other heat "quantities", interacting at a pavement surface, determines the quantity of thermal energy remaining for conductive heat transfer within a pavement.

Geiger (1959) and Barry (1968) suggested that since air is a poor conductor heat transfer by conduction in the atmosphere can be virtually neglected. The authors also suggested that the low viscosity of air and its consequent ease of motion makes convection the primary method of atmospheric heat transfer.

4.4.4. Convection

The temperature gradient at an air-pavement surface boundary is influenced by the mixing motion of the air immediately above the surface. Convective heat transfer at the boundary is a process of energy transport by the combined action of heat conduction and the mixing motion of the air and, therefore, a pseudo heat conduction process. Newton's Law of Cooling states that the heat flux across the boundary of a surface, being cooled by forced convection, is proportional to the temperature difference between the surface and the surrounding medium. This heat flux can be expressed as follows:

$$Q_{\text{conv}} = H \Delta T \quad (\text{IV-7})$$

where: Q_{conv} = heat flux resulting from convective heat transfer, Btu per sq ft per hr

H = surface convection coefficient,
Btu per sq ft per hr per $^{\circ}\text{F}$

ΔT = temperature difference between the surface
and the surrounding medium, F.

The surface convection coefficient, H, which depends upon such factors as wind velocity, surface type and surface roughness, is difficult to evaluate. Carroll et al. (1966) suggested a value of 2.7 Btu per sq ft per hr per F for granular surfaces and wind velocities ranging from 0 to 10 miles per hour. Vehrencamp (1953) developed the following empirical formula for estimating the convection coefficient at an air-soil boundary.

$$H = 0.00144 T_m^{0.3} U^{0.7} + 0.00097 (T_s - T_a)^{0.3} \quad (IV-8)$$

where: H = surface convection coefficient,
Cal per sq cm per min per C

T_m = average of the air and surface temperatures, K

U = average daily wind velocity, m per sec

T_s = surface temperature, C

T_a = air temperature, C.

The data used to formulate Equation (IV-8) was collected from a study of the air temperature distribution close to the surface of a smooth, level, dry lake bed. Vehrencamp (1953) indicated that Equation (IV-8) yielded results within 10 per cent of experimental data.

The temperature of a pavement surface is also dependent on such phenomena as precipitation and evaporation. However, the time of occurrence and the influence of such hydrologic variables on pavement temperature cannot be readily defined. Therefore, heat fluxes resulting from such variables have not been considered in previously mentioned

asphaltic concrete temperature simulation studies. Sanger (1959) concluded that phase changes of water, at an air-pavement surface boundary, could be safely ignored when calculating frost penetration depths beneath highway and airfield pavements. A similar opinion was held by Aldrich (1956).

4.5. The Energy Balance Approach

Utilizing an energy balance approach, the algebraic sum of all heat "quantities" at an air-pavement surface boundary is equated to zero. Neglecting heat transfer resulting from phase changes in water and precipitation, and considering heat transfer towards a pavement surface as positive and away from the pavement surface as negative, the energy balance equation involving the previously defined heat fluxes is as follows:

$$Q_{sw} \pm Q_{lw} \pm Q_{cond} \pm Q_{conv} = 0 \quad (IV-9)$$

Equation (IV-9) provides a basis for establishing a realistic relationship between many climatic variables and pavement surface temperatures. The degree of accuracy of such a relationship for predicting pavement surface temperatures is largely dependent on the method and parameters used to predict the influence of the various climatic variables on the individual heat fluxes. Furthermore, Equation (IV-9) furnishes a second possible boundary condition for the numerical solution of Equation (IV-1), from which, the thermal regime in a pavement structure can be predicted provided that the thermal properties of the component layers are defined.

4.6. Thermal Properties of Component Layers

In order to calculate the thermal regime in a pavement system a knowledge of two independent thermal properties, namely, thermal conductivity and heat capacity of each component layer is required. Thermal conductivity, K , expresses the rate of heat flow through a unit area under a unit temperature gradient. Most commonly used units of thermal conductivity are Btu per hr per ft per F or Cal per sec per cm per C. Thermal conductivity is generally evaluated by measuring the temperature gradient along a specimen of the material conducting heat at a known rate.

The heat capacity, C , is the amount of thermal energy required to cause a one degree change in a unit mass of the material. The units of heat capacity depend on whether volumetric or mass heat capacity is used. The units of volumetric heat capacity are Btu per cu ft per F or Cal per cc per C while mass heat capacity units are Btu per lb per F or Cal per g per C. Often specific heat capacity is specified. The specific heat of a material is dimensionless and equals the ratio of the heat capacity of the material to the heat capacity of water. Generally, the heat capacity of a material is computed from a heat balance between the heat gained by water in a calorimeter and the heat gained by the material.

The thermal conductivity and heat capacity of a heterogeneous material can be approximated by summing the thermal properties of the constituents comprising the material. The volume or weight fractions of the individual constituents must be considered in such a summation

process. The thermal conductivity and heat capacity of pavement materials subjected to freezing and thawing conditions are somewhat more difficult to define since latent heat associated with these conditions must also be evaluated.

4.6.1. Thermal Conductivity of Asphaltic Concrete

Kersten (1949) determined the thermal conductivity of an asphaltic concrete paving mixture having a density of 138 pcf and an asphalt content of 6 per cent by dry weight of aggregate. The thermal conductivity was found to range from 0.82 Btu per hr per ft per F at -20 F to 0.86 Btu per hr per ft per F at 40 F.

Johnson (1952) reported a thermal conductivity of 0.82 Btu per hr per ft per F for an asphaltic concrete mixture having a density of 150 pcf and an asphalt content of 4.5 per cent by dry weight of aggregate.

Aldrich (1956) suggested a value of 0.84 be used for asphaltic concrete paving mixtures near freezing temperatures, and Penner et al. (1966) assumed this value when calculating frost penetration depths within various asphaltic concrete pavement structures. In recent asphaltic concrete temperature prediction analyses, such as presented by Corlew and Dickson (1968), Kasianchuk (1968) and Straub et al. (1968), a value of 0.70 was assumed, a value suggested by Barber (1957).

4.6.2. Heat Capacity of Asphaltic Concrete

Due to the relatively large weight fraction of aggregate in asphaltic concrete mixtures, as compared to the weight fraction of

asphalt, the heat capacity of such a mixture is generally assumed to approximate the heat capacity of the aggregate comprising the mixture. As discussed in Section 4.6.4 in this chapter, the heat capacity of dry aggregate has been found to vary from approximately 0.16 to 0.25 Btu per lb per F. From an extensive literature review Johnson (1952) concluded that a value of 0.20 Btu per lb per F was representative for most dry soils and rocks, and Dempsey and Thompson (1970) suggested a heat capacity of between 0.20 and 0.22 Btu per lb per F as being realistic for most asphaltic concrete paving mixtures.

4.6.3. Thermal Conductivity of Granular Bases and Subgrade Soils

The most widely used method of estimating the thermal conductivity and heat capacity of subsurface pavement materials is based on the results of an extensive laboratory investigation reported by Kersten (1949). Kersten determined the thermal conductivity of 19 different soils and related the effect of density, moisture content, temperature, texture and mineral composition to the resulting thermal conductivities. From the test results, Kersten (1949) developed equations which express the thermal conductivity of frozen and unfrozen soils in terms of soil type, moisture content and dry density. The equations are as follows:

Fine Textured Soils:

$$\text{Unfrozen } K_u = \frac{(0.9 \log w - 0.2) 10^{0.01\gamma_d}}{12} \quad (\text{IV-10})$$

$$\text{Frozen } K_f = \frac{0.01(10)^{0.022\gamma_d} + 0.085(10)^{0.008\gamma_d}(w)}{12} \quad (\text{IV-11})$$

Granular Soils:

$$\text{Unfrozen } K_u = \frac{(0.07 \log w + 0.4) 10^{0.01 \gamma_d}}{12} \quad (\text{IV-12})$$

$$\text{Frozen } K_f = \frac{0.076(10)^{0.013 \gamma_d} + 0.032(10)^{0.146 \gamma_d (w)}}{12} \quad (\text{IV-13})$$

where: K_u = thermal conductivity of unfrozen soil,
Btu per hr per ft per F

K_f = thermal conductivity of frozen soil,
Btu per hr per ft per F

γ_d = dry density, pcf

w = moisture content, percent by dry weight of soil.

Kersten (1949) considered the above equations to be accurate within ± 25 per cent and suggested that soils with 50 per cent or more silt and clay sizes, particles less than 0.05 mm, be defined as fine textured soils and those with less than 50 per cent silt and clay size particles be defined as granular soils. Kersten indicated that Equations (IV-10) and (IV-11) are valid for soils having moisture contents equal to or greater than 7 per cent, and Equations (IV-12) and (IV-13) are valid for soils having moisture contents equal to or greater than 1 per cent.

As shown by Equations (IV-10) through (IV-13), the thermal conductivity of a soil depends upon whether the soil is in a frozen or unfrozen condition and difference in thermal conductivity between these two conditions is largely dependent on the moisture content of the soil. At low moisture contents, the difference between unfrozen and frozen thermal conductivity of a given soil is small. However, with

increasing moisture contents the thermal conductivity of a frozen soil becomes progressively greater than the thermal conductivity of the soil in an unfrozen condition. Since the percentage of water frozen in a soil-water system is temperature dependent, the thermal conductivity of such a system in a freezing condition is also dependent on temperature. Sanger (1963) suggested that the thermal conductivity of soil in a freezing condition could be approximated by averaging unfrozen and frozen thermal conductivity values.

Kersten (1949) concluded that an increase in dry density of a soil, while maintaining a constant moisture content, resulted in an increase in thermal conductivity. In a later summary, Kersten (1959), suggested that as a general rule a 1 pcf change in dry density will result in approximately three per cent change in thermal conductivity.

The influence mineral composition on the thermal conductivity of soils has been studied by such investigators as Kersten (1949) and Farauki (1966). Kersten (1949) found that the thermal conductivity of a soil increased as quartz content increased. Farouki (1966) determined the thermal conductivity of quartz, sand and kaolinite clay mixtures and found that the maximum thermal conductivity was obtained at optimum clay contents. Kersten (1959) concluded that the lack of experimental results makes it difficult to take mineral composition into account when estimating the thermal conductivity of a soil.

4.6.4. Heat Capacity of Granular Bases and Subgrade Soils

Kersten (1949) determined the heat capacity of various dry soils over a temperature range of 140 F. The heat capacity of each soil was

found to vary from approximately 0.15 to 0.19 Btu per lb per F at 0 F and 140 F, respectively. However, base and subgrade materials comprising a pavement structure are seldom, if ever, in a moisture free condition. Kersten (1949) suggested that the following relationships be used to estimate the specific heat of a soil-water system.

$$C_u = \frac{100 C_s + 1.0 w}{100 + w} \quad (IV-14)$$

$$C_f = \frac{100 C_s + 0.5 w}{100 + w} \quad (IV-15)$$

where: C_u = heat capacity of unfrozen soil, Btu per lb per F
 C_f = heat capacity of frozen soil, Btu per lb per F
 C_s = heat capacity of dry soil, Btu per lb per F
 w = moisture content of soil, per cent by dry weight of soil.

The values 1.0 and 0.5 in the above equations are the heat capacities, expressed in units of Btu per $\frac{1}{lb}$ per F, of water and ice, respectively.

From Equation (IV-14), the heat capacity of an unfrozen soil can be estimated provided that the dry density, moisture content and the heat capacity of the soil in a dry state are known. Since the heat capacities of dry soils vary within narrow limits an approximated value of C_s would appear meaningful for practical purposes. However, in the derivation of Equation (IV-15) the assumption is made that the total moisture in a soil-water system is in a frozen state. The results of laboratory studies, such as reported by Lovell (1957) and Yong (1965),

have shown that practically all water in granular materials freezes at approximately 32 F, while, in soils containing substantial quantities of silt and clay size particles a large portion of the water may remain unfrozen at temperatures below 32 F.

Unfrozen moisture content-temperature relationships of various soil types have been established by Yong (1965), Nerseova and Tsytoovich (1963), Williams (1968) and Dillon and Andersland (1966). Although general agreement exists concerning the influence of silt and clay size particles on unfrozen moisture contents, there are differences of opinion as to the influence of initial moisture content on the percentage of water frozen at a given temperature.

Yong (1965) found that as the initial moisture content of a clay having a liquid limit of 67 per cent, and a plastic limit of 28 per cent, was increased the unfrozen moisture content at temperatures below 32 F also increased. The unfrozen moisture content-temperature relationships for a clay and silt soil, as obtained by Yong (1965), are shown in FIGURE IV-2. Williams (1968) presented similar unfrozen moisture content-temperature relationships for various soils. However, Williams reported that different total moisture contents had no significant effect on unfrozen moisture contents.

Nerseova and Tsytoovich (1963) suggested that the unfrozen moisture content in a soil-water system is dependent on temperature, specific surface area of the soil particles, the mineral and chemical composition of the soil and the soluble compounds present in the water phase. Nerseova and Tsytoovich suggested that for practical purposes

unfrozen moisture contents can be assumed to be primarily a function of temperature. Unfrozen moisture content-temperature relationships for nonsaline soils, as proposed by Nerseova and Tsytovich (1963), are given in TABLE IV-1.

Dillon and Andersland (1966) developed an empirical relationship to predict unfrozen moisture contents of frozen clay soils. This relationship is as follows:

$$W_u = \frac{S \cdot T}{T_0} \cdot \frac{1}{A_c} \cdot l \cdot k \cdot 100 \quad (\text{IV-16})$$

where: W_u = unfrozen moisture content, per cent by dry weight of soil

S = a measure of the average specific surface of the soil particles, sq m per g (M)

T = temperature of frozen soil, K

T_0 = temperature of initial freezing of soil pore water, K

A_c = activity ratio, plasticity index/percent < 2 μ

l = a constant, equal to 1 and 2 for soils having non-expanding and expanding lattice structures, respectively

k = 2.8×10^{-4} , g of water per sq M.

Dillon and Andersland (1966) collected data on various soils, for which unfrozen moisture content information was available, and concluded that Equation (IV-16) yielded unfrozen moisture contents which were in close agreement with experimental values.

The results of the preceding investigations enable approximate temperature limits of a frozen and unfrozen condition of soil-water system to be defined. Between these temperature limits the heat capacity of such a system is made large by the latent heat of fusion released upon freezing. Williams (1968) determined the apparent specific heat capacity of various silt, clay and organic soils. Apparent specific heat capacity is distinguished from specific heat capacity in that the former takes into account the latent heat of fusion, whereas, "true" specific heat capacity is not associated with a phase change. A typical apparent specific heat-temperature relationship of a soil, as presented by Williams (1968), is shown in FIGURE IV-3. With reference to this figure, at temperatures above the freezing temperature of a soil-water system the apparent specific heat is equivalent to the unfrozen heat capacity of the system. Upon freezing, the apparent specific heat is made large by latent heat, and as freezing progresses, unfrozen moisture content decreases and the apparent specific heat capacity approaches the heat capacity of a frozen system. The latent heat component of the apparent specific heat capacity can be approximated provided that an unfrozen moisture content-temperature relationship is known since the difference in unfrozen moisture content between any two temperatures gives the latent heat involved in such a temperature change.

4.7. Summary

In this chapter heat transfer concepts applied to pavement structures and thermal properties of pavement component materials have

been briefly reviewed.

The influence of climatic variables on pavement surface temperature is difficult to quantify. A rational approach to this problem involves an energy balance procedure in which surface temperatures are related to various meteorological parameters. The accuracy of such a relationship is dependent on the method used to describe the influence of changing climatic conditions on surface temperatures, which will generally be governed by available meteorological data at a given locale.

From the studies reported, thermal conductivity and heat capacity values of asphaltic concrete paving mixtures have been found to vary within narrow limits and, therefore, estimated values would appear meaningful for practical purposes. Also, considering the moisture content of such paving mixtures to be negligible, these thermal properties may be assumed temperature independent.

Thermal conductivities and heat capacities of granular bases and subgrade soils are primarily dependent on moisture content, density and temperature. In temperature prediction analyses of pavement structures subjected to low temperature climatic environments three different sets of these thermal properties must be recognized, depending on whether the material is in an unfrozen, freezing or frozen condition.

TABLE IV-1
UNFROZEN WATER CONTENT IN TYPICAL NONSALINE SOILS
(Nerserva and Tsytovich, 1963)

Soil	Maximum Molecular Water Capacity, %	Unfrozen Water, % by Dry Weight				
		-0.2C to -0.5C	-1C to -2C	-4.5C to -5C	-9C to -10C	below -10C
Sand	1 - 7	0.5 - 2	0.5	0.5	0.5	0.5
Sandy Loam	9 - 13	3 - 10	3 - 6	3 - 6	3 - 6	3 - 6
Clayey Loam	15 - 23	10 - 20	5 - 15	5 - 10	4 - 8	4 - 8
Clay	23 - 35	15 - 25	10 - 20	10 - 15	5 - 10	5 - 10
Clay Containing Montmorillonite	> 35	30 - 40	20 - 30	15 - 25	15 - 20	15 - 20

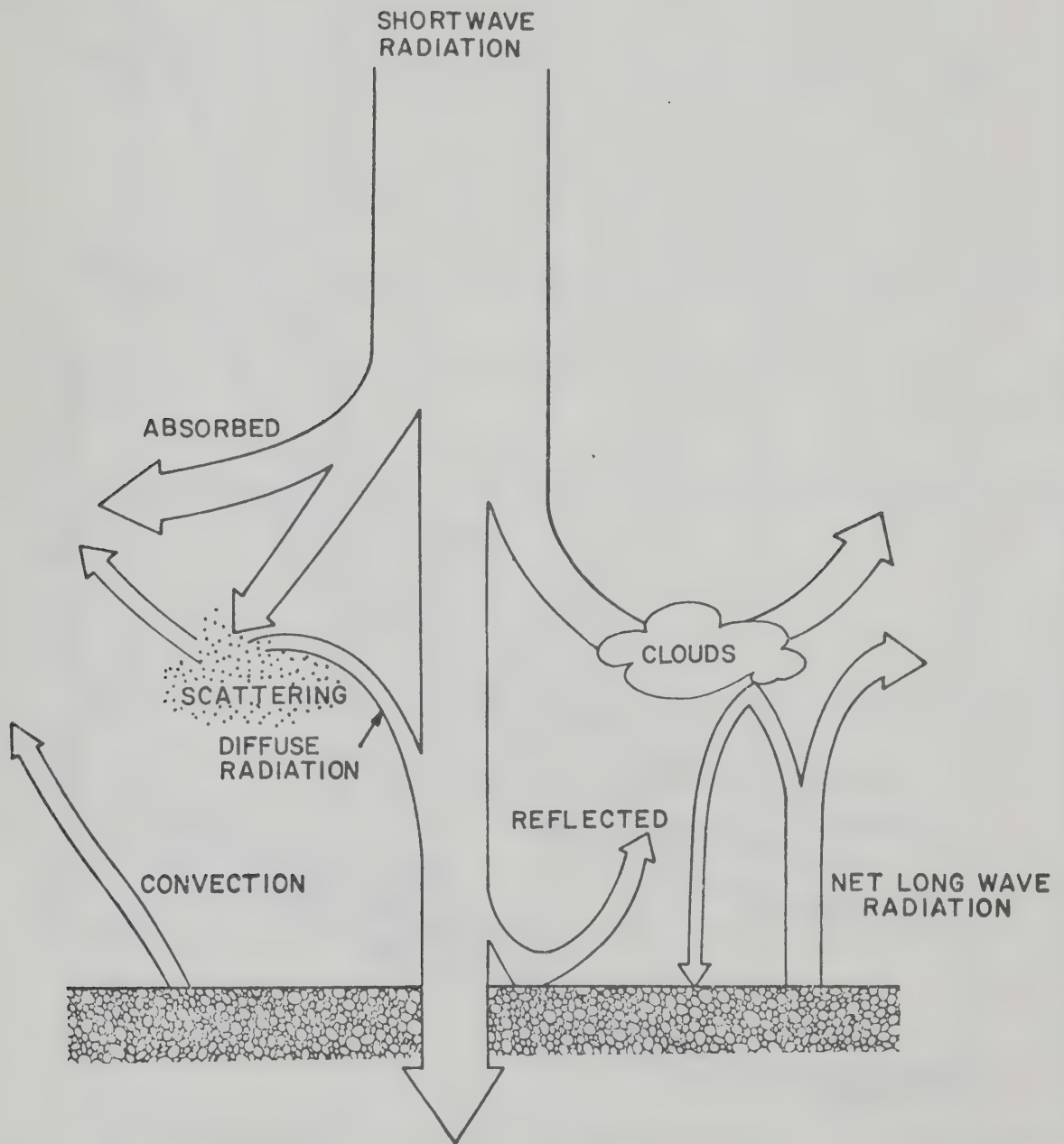


FIGURE IV-1 HEAT TRANSFER BETWEEN GROUND SURFACE AND AIR ON SUNNY DAY. (after Aldrich, 1956)

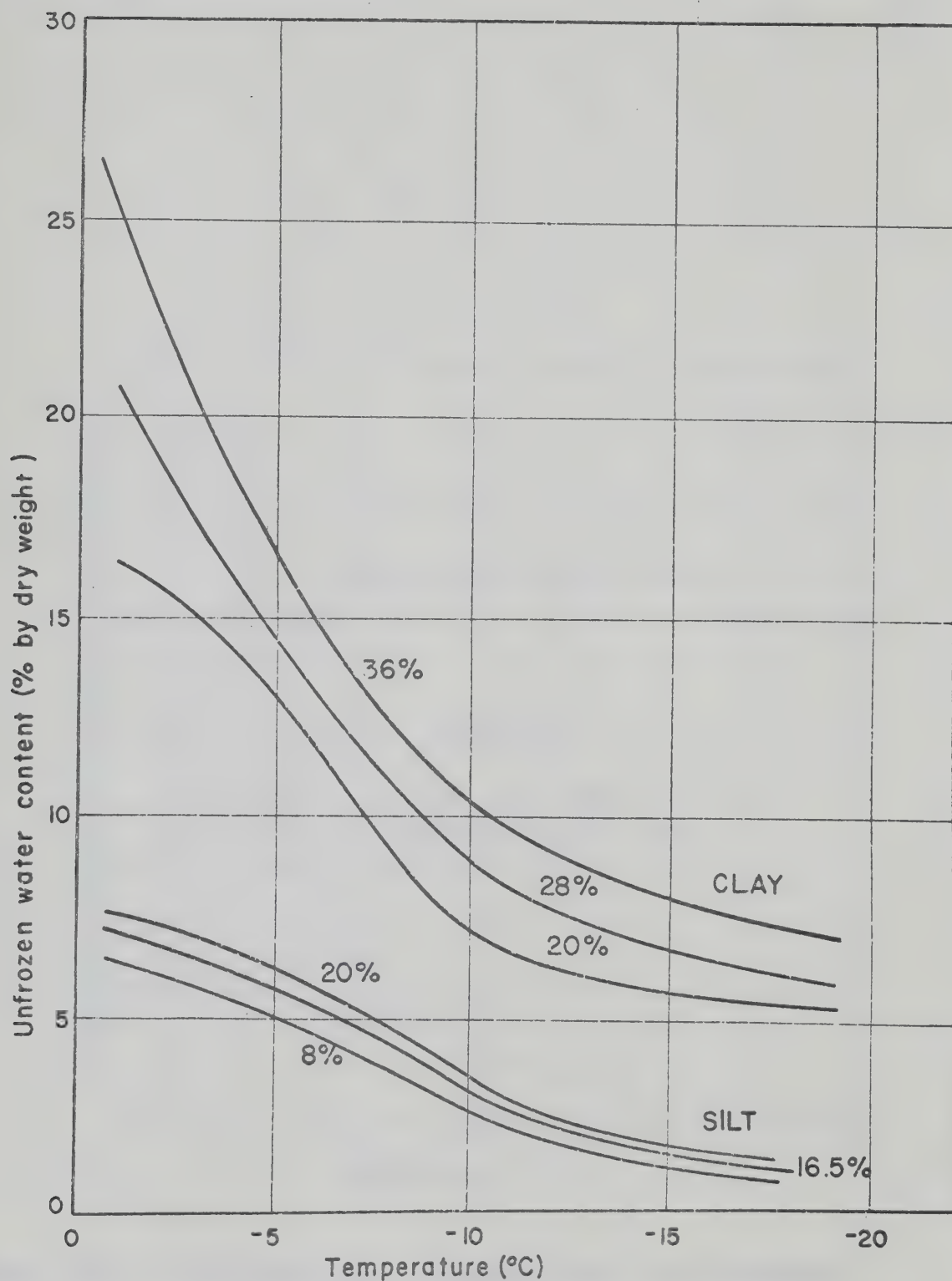


FIGURE IV-2 INFLUENCE OF INITIAL MOISTURE CONTENT AND TEMPERATURE ON UNFROZEN WATER CONTENT OF CLAY AND SILT SOILS. (after Yong, 1965)

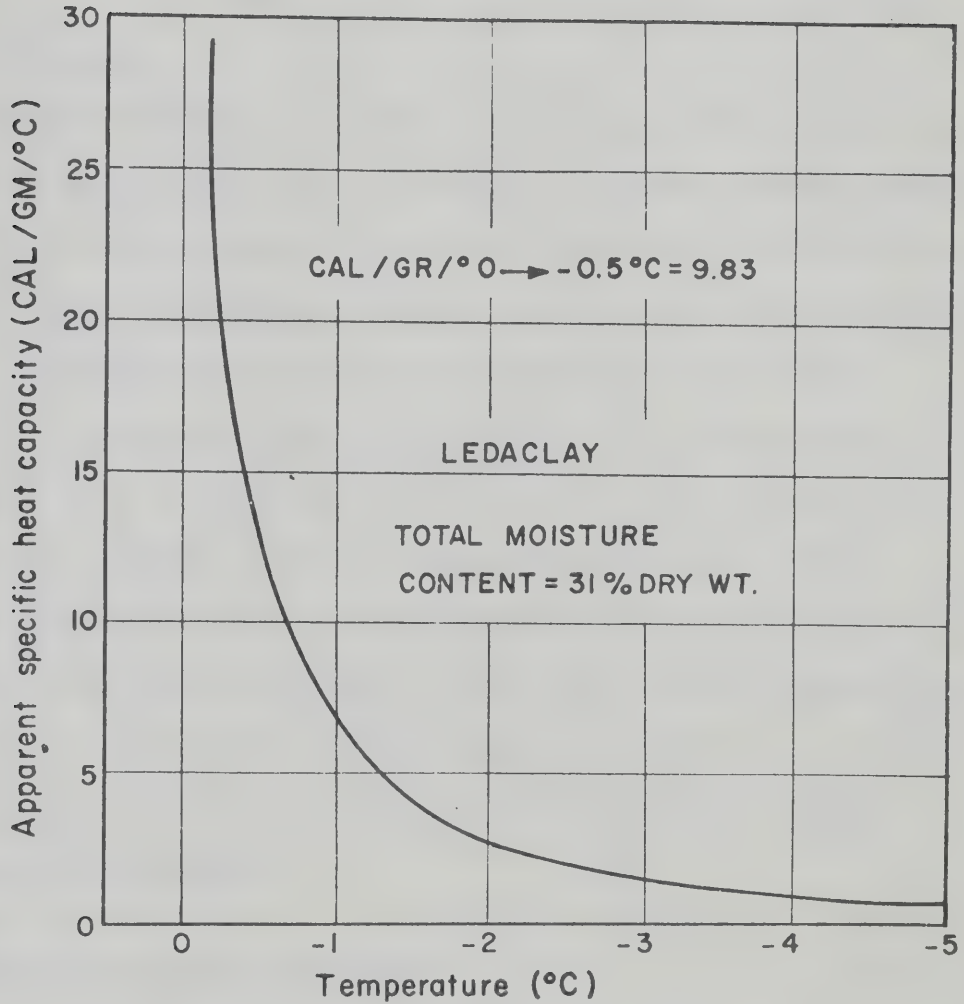


FIGURE IV-3 INFLUENCE OF TEMPERATURE ON APPARENT SPECIFIC HEAT CAPACITY. (after Williams, 1968)

CHAPTER V

PREDICTED TEMPERATURES IN ASPHALTIC CONCRETE PAVEMENT STRUCTURES

5.1. Introduction

Numerical solution techniques, such as the method of finite differences, coupled with the use of digital computers provide a means of readily solving heat transfer problems which cannot ordinarily be evaluated analytically because of complex boundary conditions or geometrics. The prediction of temperature variations in a pavement structure as a function of time and position is one such problem. In this chapter heat transfer concepts and thermal properties presented in the previous chapter, together with a finite difference approximation of the governing heat transfer equation, have been used in the development of an analytical model for predicting pavement temperatures. Comparisons of predicted and recorded temperatures in various asphaltic concrete pavement structures subjected to low temperature climatic environments are presented.

5.2. The Finite Difference Approach

The basic approach in a finite difference approximation of the governing differential equation of conductive heat transfer, Equation (IV-1) of the previous chapter, is the expansion of the temperature

functions in terms of a Taylor's series. Various methods, ranging from explicit to fully implicit methods, are available to express the differential equation in finite difference form. Independent of the choice of methods the problem reduces to a set of algebraic equations which can be rapidly solved by computer operations.

The explicit method provides a noniterative process of determining the temperature at a given position and time in relation to known preceding temperatures and assuming a one-dimensional analysis, only one algebraic equation is required to solve for the unknown temperature. However, the time increment at which the temperatures are evaluated is restricted by the mathematical stability criteria of the finite difference equation.

Implicit procedures generally involve a matrix type of numerical solution at each time step since the unknown temperature is expressed in terms of present as well as preceding temperatures. The implicit method has no restrictions on the time increment at which the temperatures are evaluated. However, the resulting finite difference equations become difficult to formulate and program when two- or three-dimensional or complex one-dimensional heat transfer problems are to be solved. Such is the case in pavement systems where variations of thermal properties of the pavement materials with respect to temperature and location are required during program operations.

Various investigators, Carroll et al. (1966), Straub et al. (1968), Corlew and Dickson (1968), Dempsey and Thompson (1970) and Ilo et al. (1970) have successfully used the explicit method of the finite

difference approximation to predict temperatures in asphaltic concrete pavement structures. Many of the concepts and findings of these investigations have been incorporated in the developed heat transfer model.

5.3. Previous Investigations

Carroll et al. (1966) used an explicit finite difference method to predict the depth of frost penetration in a pavement structure during a single winter. Daily average air temperatures and a constant convection coefficient of 2.7 Btu per sq ft per hr per F were incorporated within the air-pavement surface boundary condition. The position of the constant temperature lower boundary condition was found to influence the predicted thermal regime. The investigators concluded that for accurate deep temperature simulation studies, temperatures well below the region of interest must be known or carefully estimated.

Straub et al. (1968) modified the computer program used by Carroll et al. (1966) in order that extreme daily temperatures in asphaltic concrete pavement surfaces could be predicted. The air-pavement surface boundary condition was formulated using an energy balance approach similar to that presented in Section 4.5 of CHAPTER IV. The lower boundary condition of a constant temperature was positioned at a depth of 24 inches below the pavement surface. At this depth no diurnal temperature variations were measured. The intensity of solar radiation was found to have a great influence on extreme daily asphaltic concrete temperatures and the authors suggested that when initial temperature conditions are unknown approximate temperature gradients

can best be estimated at a time prior to sunrise when the influence of solar radiation on pavement temperature is a minimum. Initial pavement temperatures of ± 10 F from measured temperatures were found to have little influence on predicted maximum daily surface temperatures. However, with increased depth such input errors resulted in significantly large deviations between measured and predicted temperatures.

Corlew and Dickson (1968) computed the thermal energy transferred in asphaltic concrete paving mixtures at the time of paving operations. The air-pavement surface boundary condition incorporated the radiation, conduction and convection modes of heat transfer. The results of the study indicated that, during paving operations, temperatures of asphaltic concrete paving mixtures may decrease more rapidly at the pavement-subsurface interface than at the air-pavement surface boundary.

Dempsey and Thompson (1970) developed a heat transfer model for predicting thermal regimes in pavement structures subjected to frost action. The solar radiation heat flux was accounted for by means of a semi-empirical relationship between solar position and the time of day at a particular geographic location. The longwave radiation heat flux and the convection coefficient were approximated by Equations (IV-5) and (IV-8) presented in the previous chapter. The latent heat released upon freezing of subsurface layers was estimated by varying the heat capacity of the component layers in accordance with a frozen water content-temperature relationship presented by Yong (1965). All soil water freezing was assumed to occur between 32 F and 30 F.

Ho et al. (1970) compared predicted and measured temperatures in various insulated pavement structures subjected to subfreezing climatic conditions. Mean daily air temperatures were employed as an upper surface boundary condition and the latent heat of fusion was considered by specifying a nonlinear frozen moisture content-temperature relationship for each component layer. Predicted sub-surface temperatures were found to be influenced by the position of the constant temperature lower boundary condition. The authors compared recorded pavement temperatures with those predicted from one- and two-dimensional analyses and concluded that if temperature variations in the vicinity of the center line of a pavement structure are of interest, a good approximation of the thermal regime can be obtained using the one-dimensional analysis.

The results of these investigations indicate that the meteorological variables required in the formulation of an air-pavement surface boundary condition are dependent on the problem to be analyzed. When predicting asphaltic concrete temperatures major meteorological variables should be specified. However, when predicting subgrade temperatures, such a boundary condition may be somewhat generalized without greatly influencing the accuracy of the predicted temperatures. In both short-term and long-term temperature prediction studies the constant temperature lower boundary condition must be positioned at a depth well below the region in which predicted temperatures are of interest.

5.4. Formulation of the Finite Difference Equations

When using the finite difference technique to obtain an approximate solution of the thermal regime existing in a pavement system, the system is divided into a series of nodal elements as shown in FIGURE V-1. The cross-sectional area of each nodal element is assumed equal to unity and the nodal depth (Δx) is so chosen as to satisfy the mathematical stability of the resulting finite difference equations. Also, the nodal depth is selected so that the pavement layer interfaces are located at the centroids of the nodal elements and at any time (t) the temperature at the centroid of a nodal element is assumed to represent the average temperature of the element. The prediction of temperatures of nodal elements located within a pavement component layer, at an air-pavement surface boundary and at the interface of adjacent component layers, requires the formulation of three general finite difference equations.

5.4.1. Finite Difference Equation for Temperatures within a Component Layer

The one-dimensional equation of transient heat transfer by conduction, can readily be expressed in explicit finite difference form with the aid of the space-time grid shown in FIGURE V-2. The nodal points in FIGURE V-2 represent the centroids of the nodal elements at which the temperatures are to be predicted. The second order partial derivative of temperature with respect to depth can be approximated by:

$$\frac{\partial^2 T}{\partial x^2} = \frac{T(x-\Delta x, t) - 2T(x, t) + T(x+\Delta x, t)}{(\Delta x)^2}$$

and the change in temperature with respect to time can be approximated by:

$$\frac{\partial T}{\partial t} = \frac{T(x, t+\Delta t) - T(x, t)}{\Delta t} .$$

Multiplying the former expression by the diffusivity of the component layer, α , which is equal to the thermal conductivity divided by the product of the heat capacity and total unit weight of the material, the resulting finite difference equation can be expressed as follows:

$$\begin{aligned} & \frac{K}{\Delta x} [T(x-\Delta x, t) - T(x, t)] + \frac{K}{\Delta x} [T(x+\Delta x, t) - T(x, t)] \\ & = \frac{\gamma C \Delta x}{\Delta t} [T(x, t+\Delta t) - T(x, t)] \end{aligned} \quad (V-1)$$

The left hand side of Equation (V-1) represents the thermal energy transferred to and from a nodal element, during a time increment (Δt) whose centroid is located at a space and time coordinate of (x) and (t), respectively. The expression on the right hand side of Equation (V-1) equals the thermal energy stored in the element during the time increment (Δt). Assuming that an initial temperature gradient throughout a pavement structure is specified, the unknown temperature $T(x, t+\Delta t)$ can be calculated from a knowledge of the preceding temperatures. Rearranging the terms of Equation (V-1) and solving for the unknown temperature yields:

$$\begin{aligned} T(x, t+\Delta t) &= [R] T(x-\Delta x, t) + [1-2R] T(x, t) \\ &+ [R] T(x+\Delta x, t) \end{aligned} \quad (V-2)$$

where: $R = \alpha \Delta t / (\Delta x)^2$.

Carnahan et al. (1969) indicated that a sufficient condition for the convergence of Equation (V-2) is $0 < R \leq 1/2$. The selection of a time and depth increment which satisfy this condition is dependent on the thermal properties of the pavement component layers.

5.4.2. Finite Difference Equation for Temperatures at an Air-Pavement Surface Boundary

An approximation of the thermal energy balance at an air-pavement surface boundary is given by Equation (IV-9) presented in Section 4.5 of the previous chapter. Using a central difference technique, the thermal energy transferred by conduction can be equated to the thermal energy transferred by radiation and convection by the following expression.

$$\frac{K}{2\Delta x} [T(x-\Delta x, t) - T(x+\Delta x, t)] = Q_{\text{rad}} \pm Q_{\text{conv}}$$

The term Q_{rad} equals the algebraic sum of the shortwave and longwave radiation heat fluxes of the energy balance equation. Solving for the fictitious temperature $T(x-\Delta x, t)$ in the above equation and substituting into Equation (V-2) yields:

$$\begin{aligned} T(x, t+\Delta t) = & [2R] T(x+\Delta x, t) + [1-2R] T(x, t) \\ & + \frac{2\Delta x R}{K} [Q_{\text{rad}} \pm Q_{\text{conv}}] \end{aligned} \quad (\text{V-3})$$

The longwave radiation heat flux, incorporated in the Q_{rad} term of Equation (V-3), is dependent on the fourth power of temperature.

To the author's knowledge, the stability of such a finite difference equation, incorporating a non-linear temperature function, can only be evaluated by adopting a trial procedure in which various time and depth increments are specified.

5.4.3. Finite Difference Equation for Temperatures at the Interface of Component Layers

The development of a finite difference equation to approximate temperatures at the interface of two layers is based upon the assumption of a continuous heat flux existing at the interface. With reference to the i^{th} layer, FIGURE V-2, Taylor's expansion yields the approximate relationship

$$T(x-\Delta x, t) = T(x, t) - \Delta x \left(\frac{\partial T}{\partial x} \right)_i + \frac{(\Delta x)^2}{2} \left(\frac{\partial^2 T}{\partial x^2} \right)_i$$

and the time derivative is approximated by

$$\left(\frac{\partial T}{\partial t} \right)_i = \frac{T(x, t+\Delta t) - T(x, t)}{\Delta t} .$$

Solving the former expression for $\frac{\partial^2 T}{\partial x^2}$ and substituting the result together with the latter expression into the one-dimensional Fourier heat transfer equation yields:

$$\Delta x \left(\frac{\partial T}{\partial x} \right)_i = \frac{T(x, t+\Delta t) - T(x, t)}{2R_i} + T(x, t) - T(x-\Delta x, t)$$

Similarly, for the $i^{\text{th}}+1$ layer:

$$-\Delta x \left(\frac{\partial T}{\partial x} \right)_{i+1} = \frac{T(x, t+\Delta t) - T(x, t)}{2R_{i+1}} + T(x, t) - T(x+\Delta x, t)$$

In order for the heat flux to be continuous at the interface the following condition must be satisfied.

$$K_i \left(\frac{\partial T}{\partial x} \right)_i = K_{i+1} \left(\frac{\partial T}{\partial x} \right)_{i+1}$$

Substituting the above relationship into the two previous equations and solving for the unknown temperature $T(x, t+\Delta t)$ yields:

$$\begin{aligned} T(x, t+\Delta t) = & \frac{2K_{i+1} \Delta t}{I} T(x+\Delta x, t) \\ & + \left(1 - \frac{2K_i \Delta t}{I} - \frac{2K_{i+1} \Delta t}{I} \right) T(x, t) \\ & + \frac{2K_i \Delta t}{I} T(x-\Delta x, t) \end{aligned} \quad (V-4)$$

In Equation (V-4), $I = (\Delta x)^2 (\gamma_i C_i + \gamma_{i+1} C_{i+1})$ and for stability, the temperature coefficient of $T(x, t)$ is positive when $\frac{(K_i + K_{i+1})\Delta t}{I} \leq \frac{1}{2}$.

Although the selection of the time and depth increment is generally governed by the stability requirements of Equations (V-2), (V-3) and (V-4), the use of small mesh sizes increase the accumulative effect of round-off errors. It is difficult to determine exactly the order of magnitude of the cumulative departure of the solution due to round-off errors, however, such errors are probably far outweighed by those errors introduced when defining thermal properties and climatic variables.

Equations (V-2), (V-3) and (V-4) form the numerical basis of the analytical model developed for predicting pavement temperatures.

The equations are well suited for programming on a digital computer and thereby allow rapid solutions to large amounts of input data. The required input data consists of meteorological variables together with structural, physical and thermal properties of the pavement component layers.

5.5. Input Variables for Temperature Prediction

A detailed description, flow diagrams and program listing of a computer program developed to predict thermal regimes in layered systems is presented in APPENDIX A. The basic computer program consists of a main program and six subroutines whose operations interact to calculate temperatures over a specified time period and at depths and time increments of (Δx) and (Δt) , respectively. Three other subroutines, whose operations are independent of the above six, permit computer plotting of the generated temperatures at specified depths as a continuous function of time.

5.5.1. Meteorological Variables

Meteorological variables such as air temperature, solar radiation, cloud cover and wind velocity are often unknown quantities with respect to a particular geographic location and time. Therefore, these variables must be estimated from data collected at nearby meteorological stations. The extrapolation of meteorological data from one location to another may result in errors between predicted and field temperatures. The only time dependent meteorological variables incorporated in the computer program were solar radiation values and air temperatures.

Major meteorological stations throughout Canada record the hourly direct and diffuse solar radiation received by the earth's surface and these values are published in the Monthly Radiation Summary by the Department of Transport - Meteorological Branch - Canada. In order to approximate the incident shortwave radiation on a pavement surface at time increments of (Δt) a linear relationship between hourly input solar radiation values was assumed. At each increment of time, the shortwave radiation influencing pavement temperatures was computed by multiplying the incident shortwave radiation by the absorptivity of the pavement surface. The absorptivity of asphaltic concrete was assumed equal to 0.90.

The net longwave radiation and convective heat transfer entering the air-pavement surface energy balance relationship were approximated by Equations (IV-4) and (IV-7) presented in CHAPTER IV. The emissivity of asphaltic concrete was assumed equal to 0.95 and the surface coefficient of convection was assumed equal to 2.7 Btu per sq ft per hr per F. Such approximations do not consider the effects of vapour pressure and cloud cover on the net longwave radiation or the influence of wind velocity variations on the heat flux resulting from conductive heat transfer. Changes to the computer program can readily be implemented when attempting to account for the influence of these climatic variables on pavement surface temperatures.

In order to compute the net longwave radiation heat flux and the heat flux resulting from convective heat transfer, at time steps of (Δt), a linear air temperature-time relationship was assumed.

5.5.2. Structural and Physical Properties

The number of layers in the pavement structure in which temperatures are to be predicted together with the thickness, moisture content and dry density of each layer must be specified. The moisture content of each component layer was assumed constant throughout the time period in which the temperatures were calculated. Dempsey and Thompson (1970) suggested that the assumption of a constant moisture content is reasonable for predicting temperatures in unfrozen soils, while greater errors may be expected in frozen soil temperature predictions because the diffusivity of frozen soils is more sensitive to moisture content changes than the diffusivity of unfrozen soils.

5.5.3. Thermal Properties

From the literature review presented in the previous chapter, the thermal conductivity and heat capacity of asphaltic concrete paving mixtures have been found to vary within narrow limits and for practical purposes can be considered temperature independent. In the temperature prediction studies presented in Section 5.6, thermal conductivity and heat capacity values of asphaltic concrete paving mixtures were assumed to be 0.84 Btu per hr per ft per F and 0.22 Btu per lb per F, respectively.

The thermal properties of subsurface pavement components are dependent on whether the material is in an unfrozen, frozen or freezing condition. In order to distinguish between these three conditions, a freezing temperature range was specified for each subsurface layer.

Unfrozen moisture content-temperature relationships, such as summarized in Section 4.6.4 of CHAPTER IV, aid in estimating the temperature range in which various soil-water systems may be considered to be in a freezing condition.

The method used to incorporate a moving zone of freezing in the model is most readily described with reference to FIGURE V-2. When solving for the unknown temperature $T(x, t + \Delta t)$ "while freezing" thermal properties were used if the preceding temperatures, $T(x - \Delta x, t)$ and $T(x + \Delta x, t)$, were within the specified temperature limits of freezing of the particular component layer. If this condition was not satisfied, the unknown temperature was calculated using frozen or unfrozen thermal properties depending on the temperature $T(x, t)$.

The unfrozen and frozen thermal conductivities of subsurface materials were estimated from figures presented by Aldrich (1956) and Sanger (1963), illustrating the influence of moisture content and dry density on the thermal conductivity of various soils as determined by Kersten (1949). The thermal conductivity of a component layer in a state of being frozen was assumed equal to the average frozen and unfrozen conductivity of the layer.

The heat capacities of subsurface materials in the previously mentioned states were approximated by means of Equations (IV-14) and (IV-15) and the apparent specific heat concept proposed by Williams (1968), discussed in Section 4.6.4 of the previous chapter. The apparent specific heat at the specified initial freezing temperature of a component layer was assumed equal to the total latent heat released

upon freezing divided by the total unit weight of the component material. At the lower temperature limit of the freezing zone the apparent specific heat was assumed equal to the frozen heat capacity of the material. A similar approach to the problem of accounting for latent heat released upon freezing was employed by Dempsey and Thompson (1970).

As shown in FIGURE IV-3 of the previous chapter, apparent specific heat decreases rapidly with decreasing temperature. Therefore, during freezing of a subsurface material a linear relationship was assumed between the logarithm of apparent specific heat and temperature. This relationship was established using the previously calculated specific heat values determined at upper and lower temperature limits defining the freezing zone.

5.6. Predicted Versus Recorded Temperatures

In order to assess the predictive capability of the analytical model a comparison was made between predicted and recorded temperatures in four asphaltic concrete pavement structures. Three of the structures were those incorporated in the Manitoba test section, and are referred to as Structures B, C and D, shown in FIGURE III-1 of CHAPTER III. Temperatures in each of these three structures were predicted over a time period extending from mid-November, 1967 to the end of March, 1968, and at depths corresponding to the depths at which temperatures were measured.

Bihourly air temperatures measured at the test site and hourly solar radiation values recorded at the Winnipeg International Airport, located approximately 35 miles west of the test site, constituted the meteorological input variables. The depth and magnitude of the constant

temperature lower boundary condition was approximated by means of FIGURE V-3, which shows the maximum and minimum recorded temperatures at various depths in each of the three structures during the 1967-68 winter. From this figure, a constant temperature of 50 F was imposed at a depth of 18 feet below the pavement surface of each structure. This depth is 6 feet below the maximum depth at which temperatures were recorded and approximately 9 feet below maximum recorded depth of frost penetration. Initial temperature gradients were determined from recorded temperatures at the start of the prediction period when all component layers were in an unfrozen condition. Input parameters for the temperature prediction of Structures B, C and D are given in TABLES V-1, V-2 and V-3, respectively.

The fourth pavement structure in which a comparison was made between predicted and recorded temperatures is located approximately 10 miles east of Edmonton, Alberta. Input parameters for the temperature prediction of the structure are summarized in TABLE V-4. Within this structure, temperatures at the 1/2, 2-1/2, 5 and 7 inch depths in the asphaltic concrete pavement surface and at 1 foot intervals, to a depth of 9-1/2 feet, in the subgrade were recorded on approximately a weekly basis during the 1968-69 winter. The time period of temperature prediction extended from November, 1968 to April 1969, during which time an identical lower boundary condition to that imposed at the Manitoba site was assumed. The initial temperature gradient existing in the pavement structure on November 1st was estimated and the hourly air temperatures and solar radiation values used were obtained from records

taken at the Edmonton Industrial Airport and Stony Plain Meteorological Stations. These stations are located approximately 10 and 25 miles west of the pavement structure, respectively.

Time and depth increments of 0.125 hours and 2 inches, respectively, were employed in each of the temperature prediction analyses. These values were found to be compatible with the stability requirements of Equations (V-2), (V-3) and (V-4).

5.6.1. Asphaltic Concrete Temperatures

Comparisons between predicted and recorded temperatures in the asphaltic concrete surfaces of Structures B, D and C, during low temperature climatic conditions, are presented in FIGURES V-4 (A) and (B) and FIGURE V-5 (A), respectively. Since all meteorological input variables and asphaltic concrete thermal properties used for the temperature predictions of the Manitoba pavement surfaces were identical, predicted temperatures at equivalent depths and times in each of the three structures were similar. However, recorded asphaltic concrete temperature distributions in each structure at any particular time were found to differ. As mentioned in Section 3.3 of CHAPTER III, Young et al. (1969) suggested that such differences may partially be accounted for by micro-climatic variables existing at the test site. In the prediction analyses, no attempt was made to account for the influence of micro-climatic conditions, such as differences in wind velocity at the air-pavement surface boundaries, on pavement temperatures.

During the period of seasonal minimum ambient temperatures, predicted temperatures of Structure B were approximately 4 F higher than

recorded temperatures, while, during the same period predicted temperatures of Structure C were approximately 4 F lower than recorded temperatures. The difference between recorded and predicted temperatures of these two structures partially reflects the difference in measured temperatures in the structures at equivalent depths and times.

Temperature predictions for Structure C were continued into the month of June, 1968. A typical comparison between predicted and recorded asphaltic concrete temperatures, during a time period in which ambient temperatures were approaching seasonal maximum values, is shown in FIGURE V-5 (B). Excellent agreement between predicted and measured temperatures during such a time period is evident.

In order to obtain a measure of the accuracy of the predicted asphaltic concrete temperatures of Structures B, C and D over the entire 1967-68 winter, linear regression analyses were employed to relate maximum daily recorded and predicted asphaltic concrete temperatures and minimum daily recorded and predicted temperatures in each of the three structures. The results of these analyses are presented in TABLES V-5 and V-6, respectively.

A similar approach was used to compare the predicted and measured temperatures in the asphaltic concrete pavement surface located near Edmonton. However, in the latter analyses, predicted and recorded temperatures were compared at times corresponding to times of temperature measurement. The recorded-predicted temperature relationships of the Edmonton structure are presented in TABLE V-7.

As observed from TABLES V-5, V-6 and V-7, maximum standard errors of estimate were associated with temperatures at and immediately below the air-pavement surface boundary. This result was expected since many meteorological variables such as snow cover, wind velocity variations and cloud cover, which are known to influence the pavement temperatures, were not included in the formulation of the air-pavement surface boundary condition. Also, such errors may partially be due to the extrapolation of meteorological data from one locale to another and errors in assumed thermal properties of the pavements. Despite the many assumptions involved in the development of the analytical model, the comparisons between recorded and predicted temperatures suggest that the model enables temperatures in asphaltic concrete pavement surfaces to be predicted within limits of practical significance.

5.6.2: Subgrade Temperatures

Isotherms depicting the predicted and recorded thermal regimes which existed in Structures B, C and D and the Edmonton Structure are shown in FIGURES V-6, V-7, V-8 and V-9, respectively. The depths of the isotherms were calculated assuming a linear relationship to exist between temperatures at various thermocouple positions. Due to the relatively small temperature gradients in the subgrades, small differences between predicted and recorded temperatures at a given depth and time may result in large variations between the positions of the recorded and predicted isotherms. Therefore, it may be considered fortuitous that the distance between corresponding measured and

predicted isotherms at a given time was generally less than the distance between thermocouple positions in each of the subgrades.

5.7. Summary

In this chapter an analytical model for predicting thermal regimes in pavement structures has been developed and comparisons between predicted and recorded temperatures of four pavement structures, located in Western Canada, have been presented.

The close agreement between predicted and recorded temperatures in each of the four structures suggests that the model can be used to obtain reliable predictions of thermal regimes existing in various pavement structures in different geographical locations. Such temperature data aids in realistically assessing the influence of climatic environment on the response of pavement systems to various loading conditions. In relation to the present study of low temperature transverse cracking of asphaltic concretes known or predicted asphaltic concrete temperatures, constitute primary inputs for thermal stress computations and tensile strength determinations.

TABLE V-1

INPUT VARIABLES FOR THE TEMPERATURE PREDICTION OF
STRUCTURE B

Meteorological	Bihourly Air Temperatures (F) Solar Radiation (Langleys/hr)			
	Number of Layers = 3			
Structural		Asphaltic Concrete	Base Course	Subgrade
	Thickness (in)	4	16	196
Physical	Dry Density (pcf)	147.0	145.0	81.0
	Moisture Content (% by dry wt.)	-	3.0	37.0
Thermal	Conductivity (Btu/hr/ft/F) Unfrozen Frozen	0.84 0.84	2.00 2.60	0.60 1.25
	Heat Capacity (Btu/lb/F) Unfrozen Frozen	0.22 0.22	0.23 0.20	0.40 0.26
	Freezing Zone	-	32 F → 30 F	29 F → 24 F
	% Moisture Frozen	-	99.0	80.0

TABLE V-2
INPUT VARIABLES FOR THE TEMPERATURE PREDICTION OF
STRUCTURE C

Meteorological	Bihourly Air Temperature (F) Solar Radiation (Langleys/hr)			
Structural	Number of Layers = 3			
		Asphaltic Concrete	Base Course	Subgrade
	Thickness (in)	4	6	206
Physical	Dry Density (pcf)	146.0	143.0	124.0
	Moisture Content (% by dry wt.)	-	3.0	5.0
Thermal	Conductivity (Btu/hr/ft/F) Unfrozen Frozen	0.84 0.84	2.00 2.60	1.30 1.60
	Heat Capacity (Btu/lb/F) Unfrozen Frozen	0.22 0.22	0.23 0.20	0.21 0.19
	Freezing Zone	-	32 F → 30 F	32 F → 30 F
	% Moisture Frozen	-	99.0	99.0

TABLE V-3
INPUT VARIABLES FOR THE TEMPERATURE PREDICTION OF
STRUCTURE D

Meteorological	Bihourly Air Temperatures (F) Solar Radiation (Langleys/hr)		
Structural	Number of Layers = 2		Subgrade
		Asphaltic Concrete	
	Thickness (in)	10	206
Physical	Dry Density (pcf)	146.0	81.0
	Moisture Content (% by dry wt.)	-	37.0
Thermal	Conductivity (Btu/hr/ft/F) Unfrozen Frozen	0.84 0.84	0.60 1.25
	Heat Capacity (Btu/lb/F) Unfrozen Frozen	0.22 0.22	0.40 0.26
	Freezing Zone	-	29 F → 24 F
	% Moisture Frozen	-	80.0

TABLE V-4
INPUT VARIABLES FOR THE TEMPERATURE PREDICTION OF
THE EDMONTON STRUCTURE

Meteorological	Hourly Air Temperatures (F) Solar Radiation (Langleys/hr)		
Structural	Number of Layers = 2		
		Asphaltic Concrete	Subgrade
	Thickness (in)	11	205
Physical	Dry Density (pcf)	143.0	100.0
	Moisture Content (% by dry wt.)	-	16.0
Thermal	Conductivity (Btu/hr/ft/F) Unfrozen Frozen	0.84 0.84	0.74 0.85
	Heat Capacity (Btu/lb/F) Unfrozen Frozen	0.22 0.22	0.29 0.20
	Freezing Zone	-	29 F → 24 F
	% Moisture Frozen	-	85.0

TABLE V-5
RELATIONSHIPS BETWEEN MAXIMUM DAILY RECORDED AND
PREDICTED ASPHALTIC CONCRETE TEMPERATURES OF
STRUCTURES B, C AND D

Structure	Linear Regression Equation*	Coefficient of Correlation	Standard Error of Estimate (F)
B	$T_{SR} = -1.86 + 1.06 T_{SP}$	0.99	2.70
	$T_{2R} = -1.66 + 1.06 T_{2P}$	0.99	2.33
	$T_{4R} = -2.26 + 1.02 T_{4P}$	0.99	1.40
C	$T_{SR} = 2.09 + 1.01 T_{SP}$	0.97	4.50
	$T_{2R} = 1.57 + 1.00 T_{2P}$	0.98	3.36
	$T_{4R} = -0.78 + 1.14 T_{4P}$	0.99	4.50
D	$T_{SR} = 4.17 + 1.04 T_{SP}$	0.95	4.43
	$T_{3R} = 2.12 + 1.01 T_{3P}$	0.96	3.55
	$T_{7R} = 0.18 + 1.02 T_{7P}$	0.98	2.59
	$T_{10R} = 0.24 + 0.94 T_{10P}$	0.99	1.54

* T_{SR}, T_{SP} = Maximum daily recorded and predicted surface temperatures (F).

T_{2R}, T_{2P} = Maximum daily recorded and predicted 2 inch temperatures (F).

TABLE V-6
RELATIONSHIPS BETWEEN MINIMUM DAILY RECORDED AND
PREDICTED ASPHALTIC CONCRETE TEMPERATURES OF
STRUCTURES B, C AND D

Structure	Linear Regression Equation*	Coefficient of Correlation	Standard Error of Estimate (F)
B	$T_{SR} = -2.09 + 0.98 T_{SP}$	0.98	3.37
	$T_{2R} = -5.09 + 1.05 T_{2P}$	0.99	2.79
	$T_{4R} = -2.51 + 1.01 T_{4P}$	0.99	1.50
C	$T_{SR} = -0.11 + 1.10 T_{SP}$	0.99	2.74
	$T_{2R} = -1.37 + 1.03 T_{2P}$	0.99	2.26
	$T_{4R} = -1.42 + 1.08 T_{4P}$	0.99	2.08
D	$T_{SR} = -0.06 + 0.98 T_{SP}$	0.99	2.15
	$T_{3R} = 1.27 + 0.87 T_{3P}$	0.99	2.40
	$T_{7R} = -0.45 + 0.97 T_{7P}$	0.99	1.75
	$T_{10R} = 1.07 + 0.92 T_{10P}$	0.99	1.56

* T_{SR} , T_{SP} = Minimum daily recorded and predicted surface temperatures (F).

T_{2R} , T_{2P} = Minimum daily recorded and predicted 2 inch temperatures (F).

TABLE V-7
RELATIONSHIPS BETWEEN RECORDED AND
PREDICTED ASPHALTIC CONCRETE TEMPERATURES OF
THE EDMONTON STRUCTURE

Depth (inches)	Linear Regression Equation*	Coefficient of Correlation	Standard Error of Estimate (F)
0.5	$T_R = 1.60 + 1.03 T_P$	0.97	2.93
2.5	$T_R = 1.36 + 1.01 T_P$	0.98	2.51
5.0	$T_R = 1.31 + 1.08 T_P$	0.99	1.92
7.0	$T_R = 1.10 + 0.97 T_P$	0.99	1.42

* Predicted temperatures calculated by assuming a linear relationship between calculated temperatures at 2 inch depth increments.

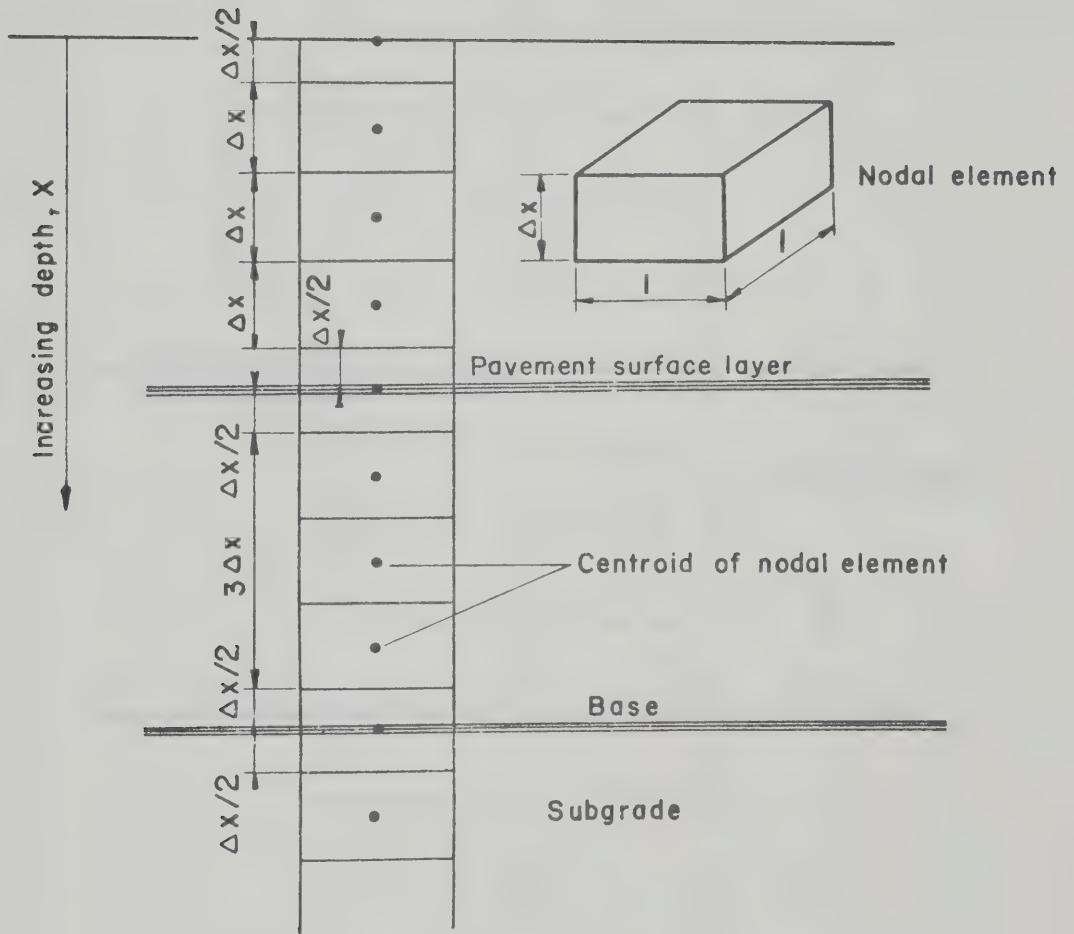


FIGURE V - 1 NODAL ELEMENTS IN A PAVEMENT SECTION.

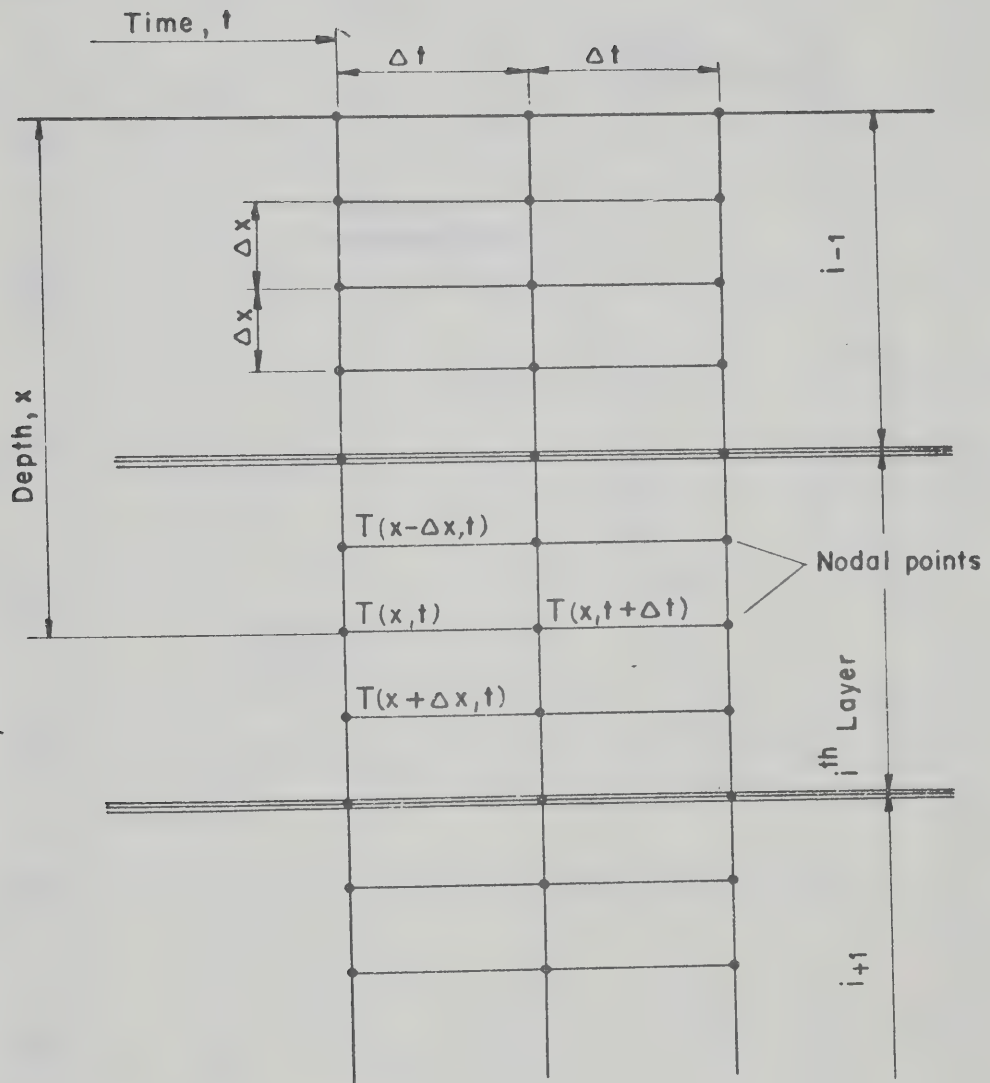


FIGURE V-2 DEPTH-TIME GRID OF A LAYERED SYSTEM.

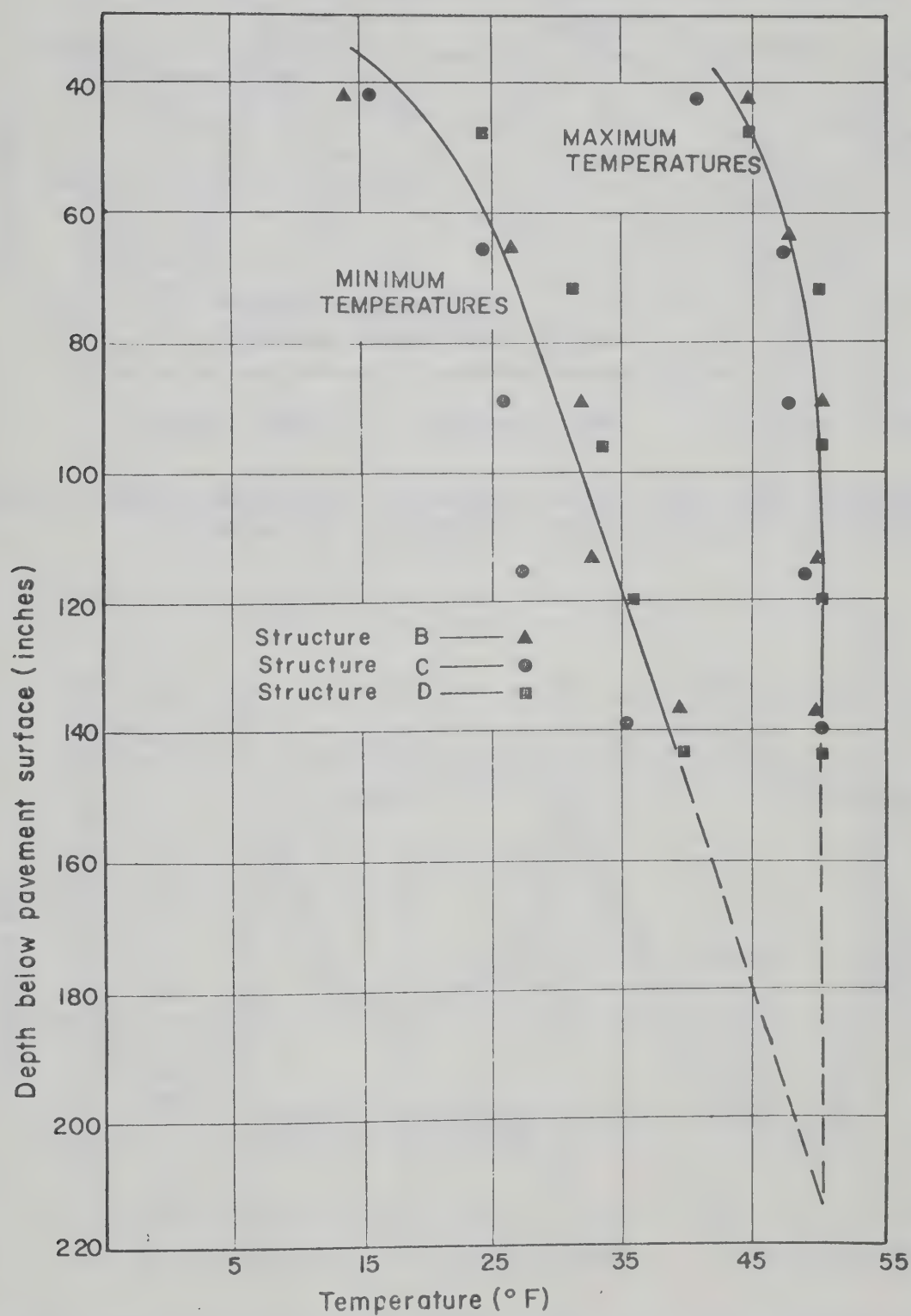


FIGURE V-3 INFLUENCE OF DEPTH ON MAXIMUM AND MINIMUM RECORDED SUBGRADE TEMPERATURES.

(Nov. 21, 1967 to Mar. 31, 1968)

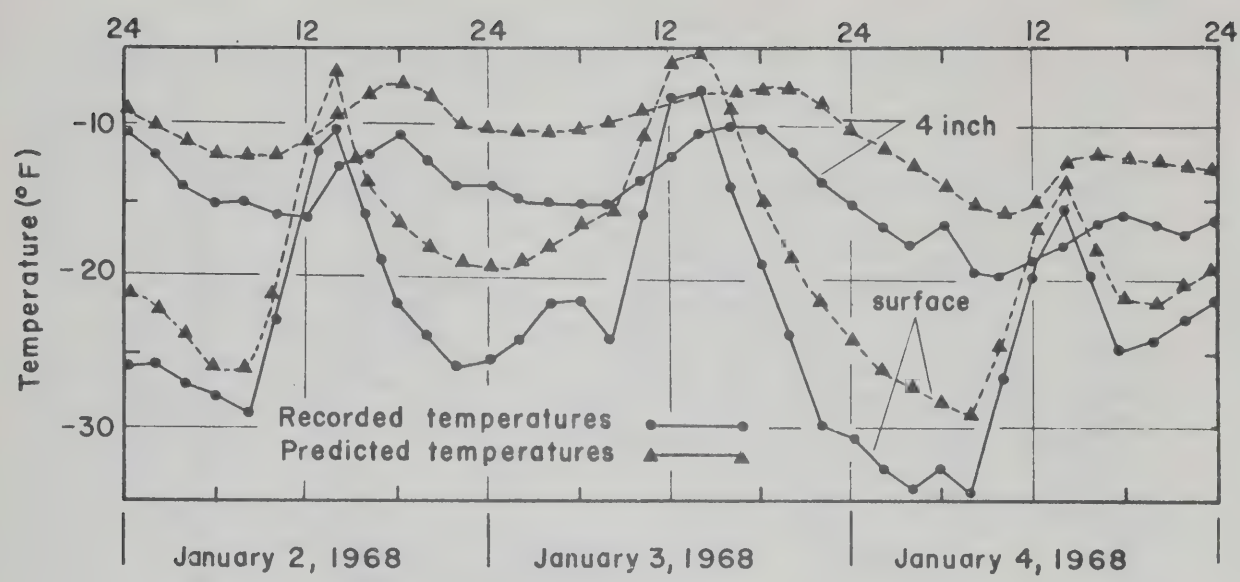


FIGURE V-4(A) COMPARISON BETWEEN PREDICTED AND RECORDED ASPHALTIC CONCRETE TEMPERATURES OF STRUCTURE B

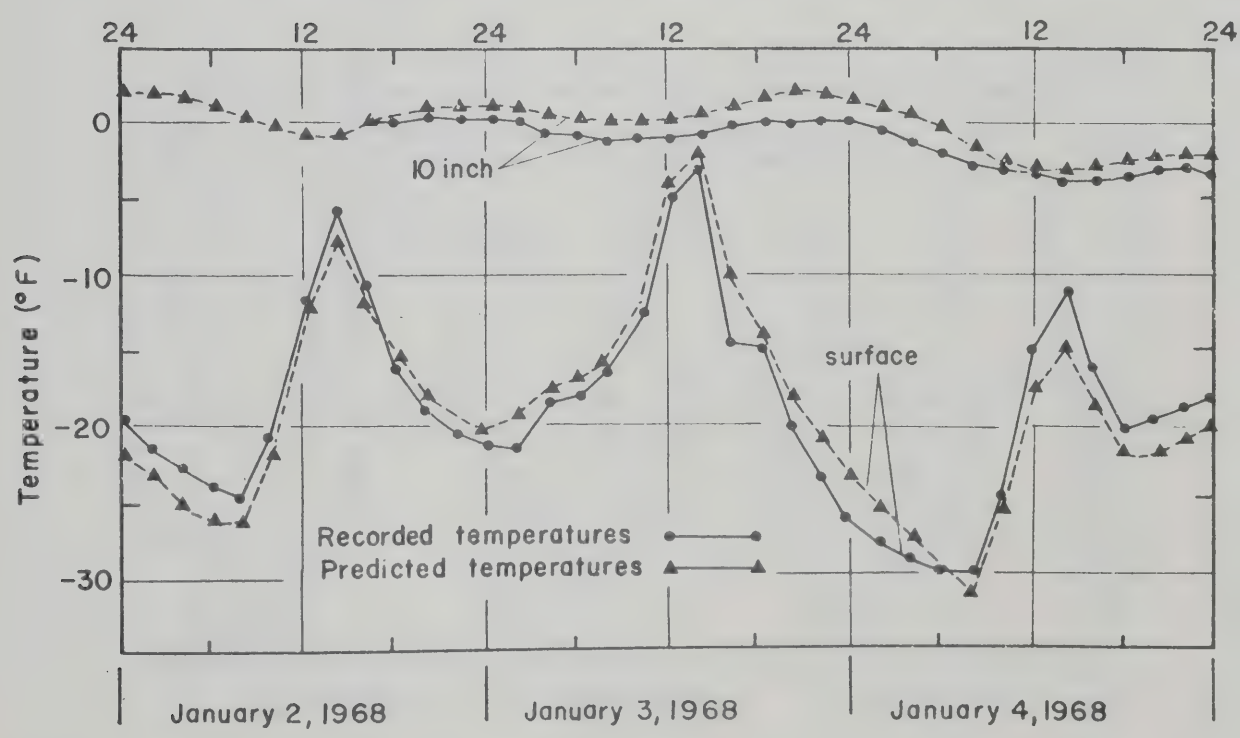


FIGURE V-4(B) COMPARISON BETWEEN PREDICTED AND RECORDED ASPHALTIC CONCRETE TEMPERATURES OF STRUCTURE D.

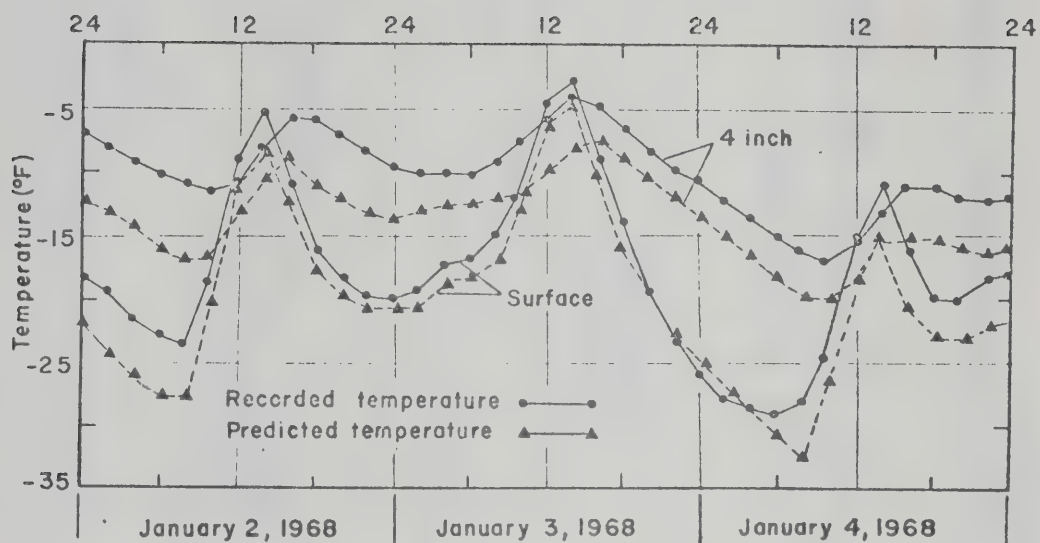


FIGURE V-5(A) COMPARISON BETWEEN PREDICTED AND RECORDED ASPHALTIC CONCRETE TEMPERATURES OF STRUCTURE C.

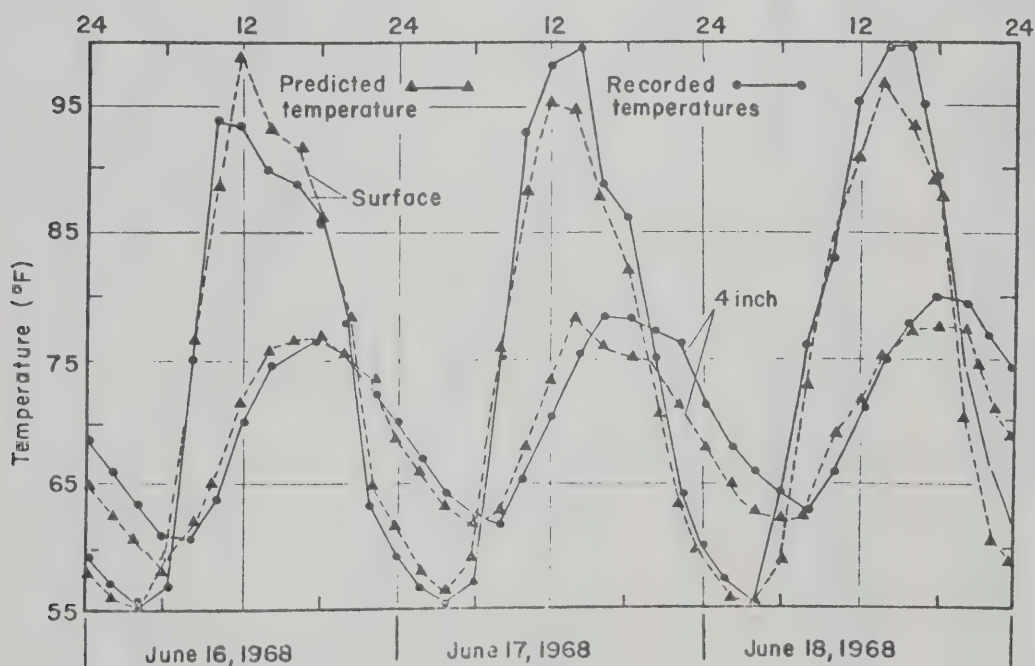


FIGURE V-5(B) COMPARISON BETWEEN PREDICTED AND RECORDED TEMPERATURES OF STRUCTURE C DURING SEASONAL MAXIMUM AMBIENT TEMPERATURES.

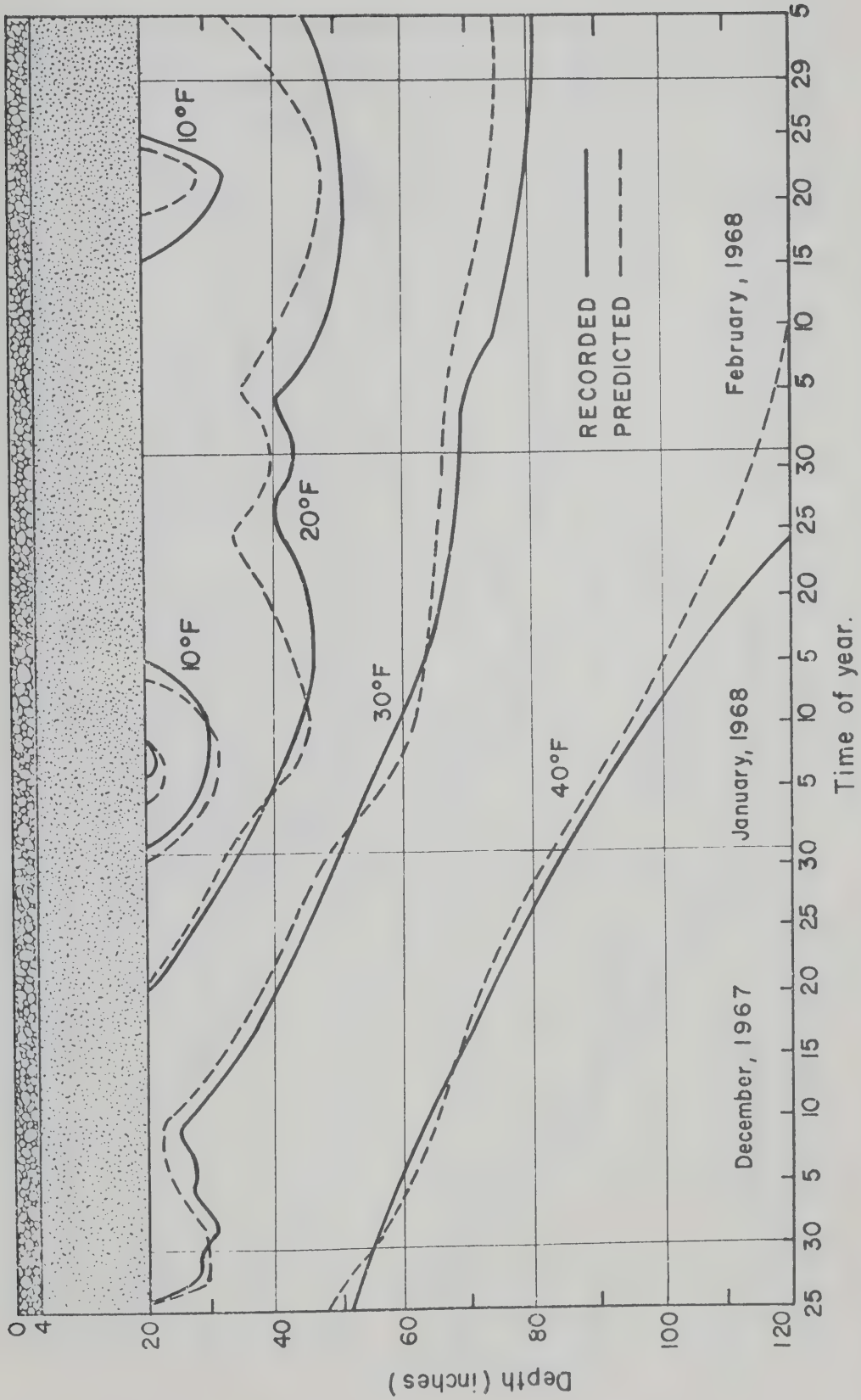


FIGURE V-6 COMPARISON BETWEEN THE PREDICTED AND RECORDED THERMAL REGIME IN THE SUBGRADE OF STRUCTURE B.

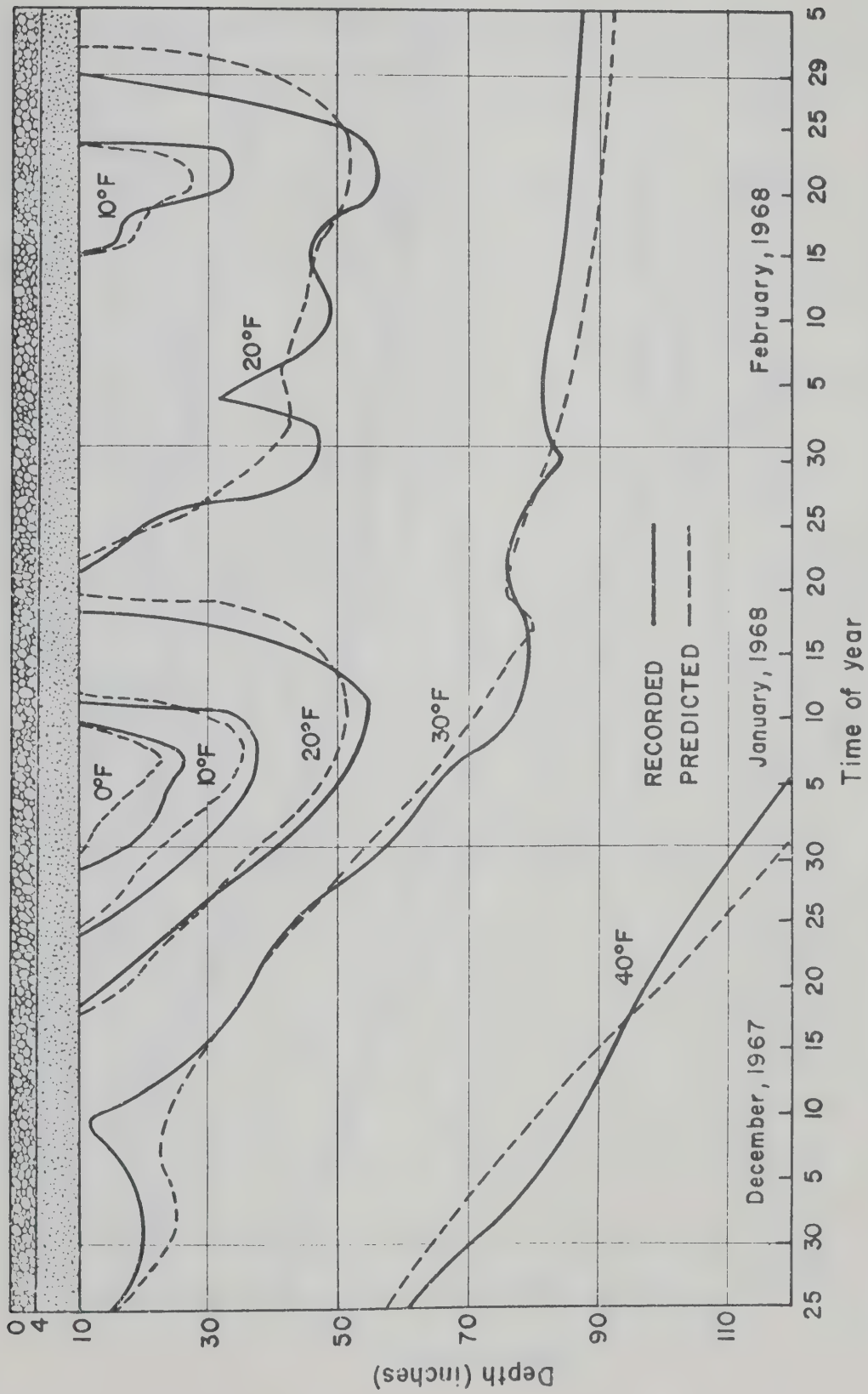


FIGURE V-7 COMPARISON BETWEEN THE PREDICTED AND RECORDED THERMAL REGIME IN THE SUBGRADE OF STRUCTURE C.

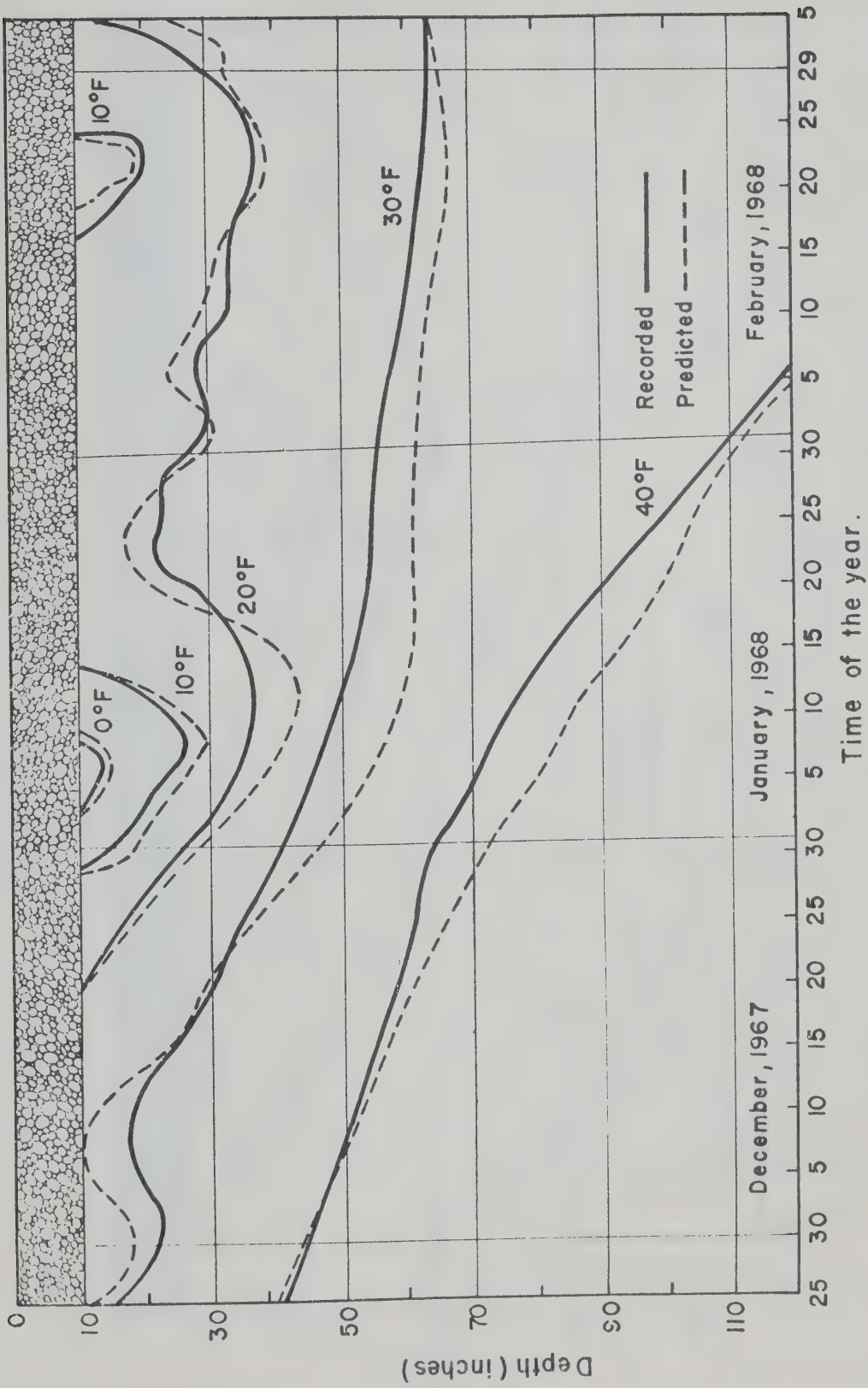


FIGURE V-8 COMPARISON BETWEEN THE PREDICTED AND RECORDED THERMAL REGIME IN THE SUBGRADE OF STRUCTURE D.

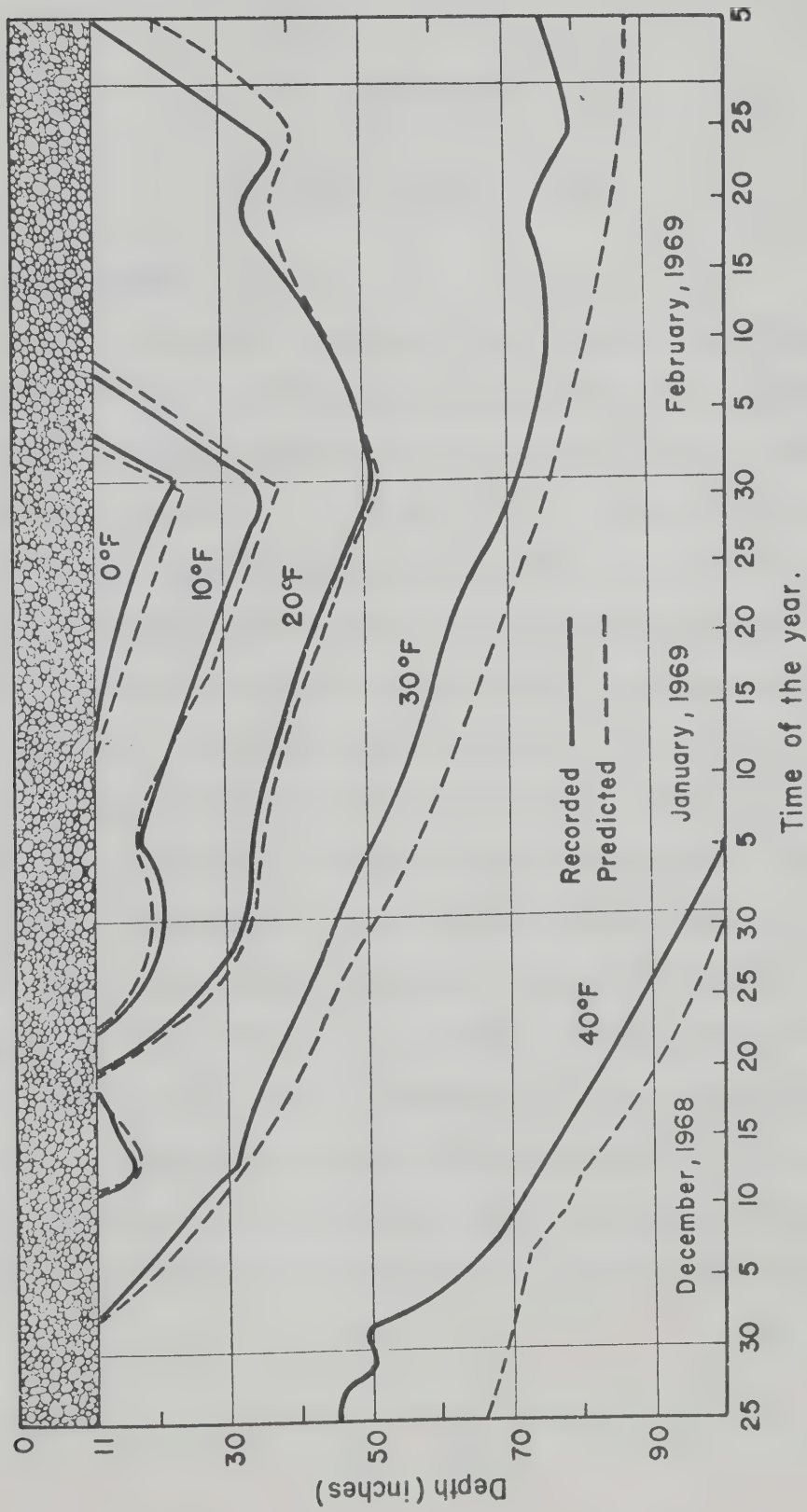


FIGURE V-9 COMPARISON BETWEEN THE PREDICTED AND RECORDED THERMAL REGIME IN THE SUBGRADE OF THE EDMONTON STRUCTURE.

CHAPTER VI

MATERIALS CHARACTERIZATION

6.1. Introduction

During the past two decades various methods of determining the time and temperature dependence of the deformation characteristics of asphalts and asphaltic concrete paving mixtures have been developed. As mentioned in Section 2.4.3 of CHAPTER II, these methods involve direct laboratory testing techniques as well as indirect procedures which utilize nomographs from which the time and temperature dependent stiffnesses can be estimated from a knowledge of the physical properties of the material. Previous studies related to the transverse cracking problem have made use of both direct and indirect procedures to characterize the behavior of asphalt materials subjected to low temperature climatic environments. In the present study numerical methods used to predict thermal stresses in asphaltic concrete pavements require definition of the stiffness characteristics of the asphaltic concretes and in order to assess the low temperature fracture susceptibility of an asphaltic concrete paving mixture subjected to a particular temperature history, assuming a stress fracture criterion, the fracture strength-temperature relationship of the asphaltic concrete must be defined.

In this chapter the concepts which were used to characterize the stiffness and low temperature tensile strengths of asphaltic concrete paving mixtures incorporated in the Manitoba and Alberta test projects are reviewed and values of the necessary parameters to characterize the materials are presented. The stiffness values, together with laboratory determined tensile properties of asphaltic concrete cores obtained from the test sites, are briefly discussed in relation to observed differences in low temperature behavior of the various pavement test sections included in the projects.

6.2. Pavement Test Sections Included in Study

A brief description of the Alberta test project has been presented in Section 3.2.1 of CHAPTER III. In the following chapter comparisons are made between observed and predicted times and temperatures of fracture of each of the three test sections having a pavement structure as shown in FIGURE III-1 (A). For these comparisons tensile strength-temperature relationships of asphaltic concrete cores, obtained from the test project at the time of construction and at a service age of 34 months, were determined using the tensile splitting test procedure reported by Christianson (1970).

The design variables included in the Manitoba test project have been reviewed in Section 3.2.2 of CHAPTER III. In the present study observed and predicted low temperature fracture of ten of the twenty-nine pavement sections, during the 1967-68 winter, are compared. With the exception of asphalt and pavement structures, the design variables of each of the ten sections are effectively the same. The asphaltic

concrete paving mixtures of the ten sections were those having optimum asphalt contents and a non-modified aggregate gradation. The sections under consideration include; three test sections of Structures B, C and D, shown in FIGURE III-1, which incorporated the low viscosity (LV) 150-200 penetration grade asphalt, three test sections of Structures B, C and D which incorporated the high viscosity (HV) penetration grade asphalt, two test sections of Structures B and C which included the LV 300-400 penetration grade asphalt and two test sections of Structures B and C which included the slow curing SC-5 liquid asphalt. Fracture strength-temperature relationships of asphaltic concrete cores obtained from the test project during the summer of 1968, and composed of the four asphalts, have been utilized in the fracture predictive analyses of the pavement test sections.

Due to a limited number of asphaltic concrete cores obtained from the test projects, laboratory testing conditions were restricted and, therefore, indirect nomographic procedures were used to estimate the stiffness of the asphaltic concrete paving mixtures over time and temperature ranges necessary for the thermal stress predictions.

6.3. Determination of Stiffness Modulus

An extensive review and assessment of various procedures used to characterize the viscoelastic behavior of asphaltic concrete mixtures has been presented by Monismith et al. (1966). Included in this review were the concepts of stiffness proposed by Van der Poel (1954) and the concept of time-temperature superposition, both of which were used in the present investigation.

Van der Poel (1954) introduced the concept of a "stiffness modulus", which is time and temperature dependent, to characterize the response of asphalt materials to various loading conditions. This stiffness modulus, commonly shortened to stiffness, is defined as:

$$S(t,T) = \frac{\sigma}{\epsilon} \quad (VI-1)$$

where

$S(t,T)$ = stiffness at a particular time and temperature
 σ, ϵ = axial tensile stress and strain, respectively.

On the basis of correlations obtained between results of creep and dynamic tests on various asphalts and results of routine tests on the asphalts, which included penetrations and ring and ball softening points, Van der Poel developed a nomograph from which the stiffness of an asphalt can be estimated as a function of time and temperature. This nomograph is shown in FIGURE VI-1. The required characterizing asphalt parameters for computing stiffness from the nomograph include asphalt penetration and penetration index. Assuming that the penetration at the temperature of the ring and ball softening point equals 800 dmm, as suggested by Van der Poel (1954), the penetration index, as defined by Pfeiffer and Van Doormaal (1936), can be computed by means of the following equation.

$$\frac{20 - PI}{10 + PI} = 50 \frac{\log 800 - \log Pen}{T_{R\&B} - T_P} \quad (VI-2)$$

where

PI = penetration index

Pen = penetration of asphalt, dmm

$T_{R\&B}$ = ring and ball softening point, C

T_p = temperature at which penetration is determined, C.

From comparisons of experimental values of asphalt stiffness with values read from the nomograph, Van der Poel found that nomograph stiffness values were generally within a factor of two of those determined from direct tests.

Heukelom (1966) presented a version of Van der Poel's nomograph with a slight correction for asphalts having very low penetration index values. Further modifications to the original method of determining stiffness have been suggested by Heukelom (1969) and McLeod (1969). These modifications, together with the use of the stiffness concept as applied to the characterization of asphalt paving materials, have been reviewed by Anderson and Haas (1970). Included in this review was the particular method used in the present study to characterize the time and temperature dependence of asphaltic concrete paving mixtures included in the test projects.

Van der Poel (1954) recommended that FIGURE VI-1 not be used to estimate stiffness values of asphalts having relatively high wax contents since the ring and ball softening point of such an asphalt is influenced by the presence of paraffin wax. Recently, Heukelom (1969) suggested that the ring and ball softening point of waxy and/or blown asphalts be modified and developed a Bitumen Test Data Chart from which a modified softening point can be derived and used in association with Van der Poel's nomograph for estimating the stiffness of such an

asphalt. This modification, as applied to some Canadian asphalts, has been described in detail by Kopvillem and Heukelom (1969) and was used for estimating stiffness values of the paving mixtures.

Properties of asphalts included in the Manitoba test project, sampled prior to plant mix operations and after being recovered from uncompacted field mixes, have been summarized by Young et al. (1969). Stiffness computations for the penetration grade asphalts at the Manitoba test project were based on index values, shown in TABLE VI-1, which were derived using as-supplied asphalt samples. The choice of using as-supplied asphalt properties rather than the properties of the asphalts extracted from uncompacted field mixes was made in view of results reported by Shields et al. (1969) and Bright et al. (1969). These investigators suggested that asphalts recovered from uncompacted field mixes may exhibit premature hardening characteristics unless special sampling procedures are used and, therefore, the physical properties of such asphalts may not be indicative of the actual physical properties of asphalts within newly constructed pavements.

Comparisons between estimated stiffness values of the asphalt cements included in the Manitoba test project, and determined using as-supplied and recovered asphalt properties, have been reported by Young et al. (1969). The low temperature stiffness values of a given asphalt cement, determined using the two sets of asphalt properties, were found to be approximately equivalent. This finding reflects the offsetting influence of the lower ring and ball softening points and

penetration index values of the as-supplied asphalts, as compared to the corresponding properties of the recovered asphalts, on estimated stiffness values of various asphalts.

The properties of the asphalts incorporated in the Alberta test project and determined at various service ages have been reported by Anderson and Shields (1971). For stiffness computations associated with the Alberta test project both as-supplied properties and properties of asphalts extracted from pavement cores at a service age of 34 months were used with modifications to the index values associated with Van der Poel's nomograph in a manner suggested by Heukelom (1969). Properties of the asphalts used for stiffness computations are given in TABLE VI-2.

Using Van der Poel's nomograph, together with penetration index and ring and ball softening point values given in TABLE VI-1 and VI-2, the stiffness of each asphalt was determined at loading times ranging from 10 to 100,000 seconds and over a temperature range of 40 to -40 F. The corresponding asphaltic concrete stiffness values were computed by means of the following equation, proposed by Heukelom and Klomp (1964).

$$\frac{S_{\text{mix}}}{S_{\text{asphalt}}} = \left[1 + \frac{2.5}{n} \cdot \frac{C_v}{1-C_v} \right]^n \quad (\text{VI-3})$$

where

S_{mix} = mixture stiffness, kg per sq cm

S_{asphalt} = stiffness of asphalt, kg per sq cm

C_v = volume concentration of aggregate
defined as

$$\frac{\text{volume of aggregate}}{\text{volume of (aggregate + asphalt)}}$$

$$n = 0.83 \log \frac{4 \times 10^5}{S_{\text{asphalt}}}$$

Heukelom and Klomp indicated that Equation (VI-3) is valid for asphaltic concrete mixtures with C_v values ranging from 0.7 to 0.9 and air void contents in the order of three per cent.

The volume concentration of aggregate values for the Manitoba asphaltic concrete paving mixtures were computed using specific gravity values and average asphalt contents of uncompacted field mixes, reported by Young et al. (1969), together with determined densities of asphaltic concrete cores obtained from the test project. The C_v values of the Alberta pavements were computed using similar properties reported by Shields et al. (1969). For those paving mixtures having air void contents greater than three per cent the C_v values were modified in accordance with the procedure proposed by Van Draat and Sommer and described by McLeod (1969). This modification involves correcting the determined C_v value of such a paving mixture by means of the following equation

$$C_v' = \frac{C_v}{1 + \Delta V} \quad (\text{VI-4})$$

where

C_v' = corrected volume concentration of aggregate of those mixtures having air void contents greater than three per cent

ΔV = difference, expressed as a decimal fraction, between the volume of air voids in the paving mixture and an air voids volume of three per cent for the same paving mixture.

Physical properties of the asphaltic concrete paving mixtures associated with Manitoba and Alberta test projects and included in the present study are summarized in TABLES VI-3 and VI-4, respectively.

Having estimated the stiffness modulus of each asphaltic concrete paving mixture over the previously mentioned time and temperature ranges, the time-temperature equivalency hypothesis was used to establish a master stiffness modulus versus reduced time relationship for each of the mixtures. The use of this hypothesis, as applied to materials characterization of asphaltic concrete, has been summarized in the review presented by Monismith et al. (1966). Briefly, according to the hypothesis, all basic time dependent response functions, such as stiffness modulus, are affected by a temperature change only within a corresponding uniform shift of the logarithmic time scale. To illustrate this concept, stiffness curves as shown in FIGURE VI-2 may be shifted along the time axis to a selected reference temperature, T_0 , and a reduced time, ξ , is defined such that stiffness curves for various temperatures superimposed when plotted as a function of ξ . Materials exhibiting such behavior are termed "thermorheologically simple".

The reduced time ξ is defined by the equation

$$\xi = t \exp[f(T)] \quad (VI-5)$$

where

ξ = reduced time corresponding to a
real time, t , at temperature T_0

$f(T)$ = a temperature function giving the shift
of the response curve.

The temperature function $f(T)$ is generally termed the shift factor, a_T , and equals the ratio of the time to observe a phenomenon at a temperature T to the time to observe the same phenomenon at the reference temperature T_0 .

6.3.1. Stiffness Modulus-Reduced Time Relationships for Manitoba Asphaltic Concretes

The determined stiffness modulus versus reduced time relationships and the shift factor versus temperature relationships for the Manitoba asphaltic concrete mixtures are shown in FIGURES VI-3 and VI-4, respectively. Such relationships permit the stiffness of the asphaltic concretes to be readily evaluated at any time and temperature and constitute the primary inputs of the stress predictive methods used in the following chapter.

As observed from FIGURE VI-3, at 0 F and a given reduced time, which is equivalent to real time at this reference temperature, the four Manitoba asphaltic concrete paving mixtures were found to exhibit large differences in estimated stiffness values. This would suggest correspondingly large differences between the magnitude of thermally induced stresses within the various pavement surfaces when subjected to similar low temperature climatic environments.

Although a realistic assessment of the low temperature fracture susceptibility of an asphaltic concrete paving mixture, based on a stress fracture criterion, requires a knowledge of both thermally induced stresses and tensile strengths of the mixture, a correlation was found between relative stiffness values of the Manitoba asphaltic concretes, shown in FIGURE VI-3, and transverse crack frequencies of the pavement sections in which the paving mixtures are incorporated. These frequencies, as reported by Young et al. (1969), are summarized in TABLE VI-5. Differences in crack frequencies between pavement sections which incorporated the same asphalt cement may partially be attributed to differences in asphaltic concrete thickness and subgrade soil type, as discussed in Sections 2.4.6 and 2.4.7 of CHAPTER II. However, those paving mixtures composed of the low viscosity asphalts exhibited the highest estimated stiffness values, at low temperatures and/or short loading times, and the highest crack frequencies, while, those mixtures composed of the high viscosity penetration grade asphalt and the SC-5 liquid asphalt exhibited the lowest stiffness values and no transverse cracks.

6.3.2. Stiffness Modulus-Reduced Time Relationships for Alberta Asphaltic Concretes

The stiffness modulus-reduced time relationships and the shift factor-temperature relationships for the "at construction" and 34 month asphaltic concrete mixtures of the Alberta test project are presented in FIGURES VI-5 to VI-9. As shown in these figures, each of the three asphaltic concrete mixtures exhibited an increase in estimated stiffness

values during the 34 month service period. Such increases can largely be attributed to the increase in density and resulting increase in volume concentration of aggregate values of the asphaltic concretes during this time period as shown in TABLE VI-4. Shields et al. (1969) presented data showing that the most rapid rate of density increase of the asphaltic concretes occurred during the first year of service.

The extent of transverse cracking at various service ages of the Alberta test project is summarized in TABLE VI-6. Anderson and Shields (1971) attributed the marked increase in cracking in all three sections during the third winter to the fact that this winter was considered to be one of the most severe in Central and Northern Alberta in the past 75 years.

6.4. Test Method Used for Determining Low Temperature Tensile Properties of Asphaltic Concrete Cores

Laboratory procedures most extensively used to characterize the tensile properties of asphaltic concrete paving mixtures with respect to their low temperature fracture susceptibility have been the direct tension test, described by Haas (1968), and the tensile splitting test described by Anderson and Hahn (1968) and Christianson (1970). In the present study use has been made of the latter test method to determine the low temperature tensile properties of the asphaltic concrete cores obtained from the test projects. Briefly, the test method involves loading cylindrical asphaltic concrete specimens across a diameter in a compression frame, and within a chamber maintained at a constant low temperature. Output signals from a load cell and series connected

linear variable differential transformers attached to opposite faces of the specimen were continuously monitored on a two-channel recorder. Such recordings enabled the induced tensile stress and strain to be calculated at any time during the test.

Assuming the specimen to exhibit elastic properties and also assuming a state of plane stress exists, the strain in the direction of a diameter at right angles to the applied load and at the center of the face of the specimen is equated to the normal stresses by means of the following equation.

$$\epsilon_x = \frac{1}{E} (\sigma_x - \nu \sigma_y) \quad (VI-6)$$

where

- ϵ_x = horizontal strain
- E = modulus of elasticity
- σ_x = induced tensile stress
- σ_y = induced compressive stress
- ν = Poisson's ratio.

When employing loading strips of width less than one-tenth the diameter of the specimen the induced tensile and compressive stress at the center of the specimen is given by

$$\sigma_x = \frac{2P}{\pi DL} \quad \sigma_y = -\frac{6P}{\pi DL}$$

where

- P = applied load
- D = diameter of specimen, and
- L = thickness of specimen.

Substituting the above relationships into Equation (VI-6) yields

$$\epsilon_x = \frac{1}{E} \left[\frac{2P}{\pi DL} + \frac{\nu 6P}{\pi DL} \right] \quad (\text{VI-7})$$

In order to calculate the strain due to the tensile stress, $2P/ DL$, Poisson's ratio must be defined. With the exception of results reported by Monismith and Secor (1962) and Sayegh (1967), there is little published information defining the time and temperature dependence of Poisson's ratio, ν , of asphaltic concrete paving mixtures. Monismith and Secor (1962) found that Poisson's ratio of an asphaltic concrete paving mixture varied from approximately 0.35 to 0.50 between temperatures of 40 and 140 F, respectively. Sayegh (1967) found Poisson's ratio to increase from 0.10 at low temperatures, high frequencies and small deformations to 0.50 at high temperatures, low frequencies and large deformations. In view of these results a value of 0.30 was assumed representative for the employed test conditions. Upon substituting this value into Equation (VI-7), the strain resulting from the induced tensile stress is approximately equal to one half the measured horizontal deformation over the one inch gauge length employed in the test.

Due to the limited number of asphaltic concrete cores obtained from the test projects, testing conditions were restricted to a nominal cross-head loading rate of 0.06 in per min and temperatures ranging from 20 to -20 F. The test data was analyzed by means of computer programs developed by Christianson (1970), and in order to summarize much of the data, average tensile stress-strain relationships of cores

belonging to a given test population were determined by averaging induced tensile stress values at specific strain levels.

6.4.1. Tensile Properties of Manitoba Asphaltic Concrete Cores

The stress-strain relationships of asphaltic concrete cores obtained from the Manitoba test project are shown in FIGURES VI-10 to VI-13, and a summary of the tensile properties of the cores, at failure conditions, is given in TABLE VI-7. As observed from this table, each of the four asphaltic concretes exhibited a decrease in failure strain with a decrease in test temperature. The average failure strain-temperature relationships of the cores are shown in FIGURE VI-14. Within the range of test temperatures, the asphaltic concrete composed of the LV 150-200 penetration grade asphalt exhibited the lowest failure strains, while, cores composed of the HV 150-200 penetration grade asphalt and those of the LV 300-400 penetration grade asphalt yielded somewhat lower failure strains than cores composed of the SC-5 liquid asphalt.

A comparison between measured failure strains and crack frequencies of pavement sections given in TABLE VI-5 reveals that lowest failure strain values are associated with the asphaltic concrete which exhibited highest crack frequencies. As mentioned in Section 2.4.4 of CHAPTER II, Anderson and Shields (1971) reported that the expected failure strain of a paving mixture, determined by the tensile splitting test, may be related to the penetration and viscosity of the asphalt comprising the paving mixture, and suggested a failure strain value less than 10×10^{-4} in per in, at 0 F, to be indicative of a paving mixture

having a high potential for cracking under climatic conditions of Western Canada. The results of the present study are consistent with these findings and suggested strain value.

The average tensile failure strength-temperature relationships of the Manitoba paving mixtures are shown in FIGURE VI-15. Considering the moderately rapid loading rate, together with the low test temperatures and observed brittle fracture mode of the specimens, rate effects on fracture strengths were believed minimized. Data presented by Tons and Krokosky (1963) and Haas (1968) indicate that variations in loading rate have little influence on the resulting low temperature tensile failure strengths of asphaltic concrete paving mixtures. Such results suggest that similar fracture strength-temperature relationships as shown in FIGURE VI-15 would have been obtained had test conditions not been limited to a single loading rate.

As test temperatures were decreased from 20 F to 0 F the tensile failure strength of each of the asphaltic concrete paving mixtures increased. However, at a temperature of approximately -5 F, those cores composed of the LV and IIV 150-200 penetration grade asphalt cements exhibited a decrease in failure strength with a decrease in test temperature. Similar decreases in failure strengths with decreasing temperatures have been reported by Tons and Krokosky (1963). These investigators attributed such reduced tensile strengths to the presence of an uneven distribution of stress in paving mixtures at low temperatures. Heukelom (1966) suggested that the tensile strength of an asphaltic concrete could be related to the stiffness of the asphalt

comprising the paving mixture. This suggested relationship is discussed in the following section of this chapter.

As shown in TABLE VI-7, at test temperatures of 20 and 0 F the asphaltic concrete composed of the LV 150-200 penetration grade asphalt exhibited the highest average failure stiffness. Failure stiffness values of the asphaltic concretes were also computed by means of Equation (VI-3), in which stiffness values of the asphalts were determined using Van der Poel's nomograph and a loading time corresponding to the time to failure of the asphaltic concrete cores. As shown in TABLE VI-7, stiffness values determined directly from tests were generally higher than stiffness values estimated by this indirect procedure. Differences between these two sets of stiffness values may partially be attributed to the assumptions involved in the analysis of the test results as well as those associated with the indirect stiffness computation method. Also, at low test temperatures measured deformations of individual cores belonging to a given test population were extremely small and often found to be a factor of two from the average of the population. Such measured deformations reflect large differences in computed stiffness values.

6.4.2. Tensile Properties of Alberta Asphaltic Concrete Cores

The results of the tensile splitting tests performed on asphaltic concrete cores obtained from the Alberta test project have been reported in detail by Christianson (1970). The average test stress-strain relationships of asphaltic concrete cores obtained from the test project and composed of asphalts obtained from Suppliers 1,

2 and 3 as denoted in TABLE VI-2, are shown in FIGURES VI-16, VI-17 and VI-18, respectively. The tensile properties of the cores at failure are summarized in TABLES VI-8 and VI-9.

From a comparison of crack frequency associated with the three pavement sections and the results of the tensile splitting test, Christianson (1970) concluded;

- a) An increase in crack frequency is accompanied by a decrease in failure strain and an increase in failure stress and failure stiffness.
- b) An increase in density with service life is accompanied by a decrease in failure strain, and an increase in failure stress, failure stiffness and crack frequency.
- c) In terms of relative comparisons, the pavement section with the highest crack frequency (that section which included Supplier 1 asphalt as shown in TABLE VI-6) also has the lowest failure strain and the highest failure stress and failure stiffness.
- d) In terms of service life, the low viscosity asphalt cement exhibits the greatest change in density, failure strain and failure stiffness, and highest crack frequency.

The average tensile failure strength-temperature relationships of the asphaltic concrete cores are shown in FIGURE VI-19. These relationships have been employed in the fracture prediction analyses presented in the following chapter.

6.5. Tensile Strengths of Mixes and Asphalt Stiffness

Heukelom (1966) presented data which shows that the tensile strength of asphaltic concrete paving mixtures is a function of asphalt stiffness. The tensile strength-stiffness relationships for two asphaltic concrete paving mixtures, as presented by Heukelom (1966), are shown in FIGURE VI-20. Heukelom suggested that the curve marked Type I is an example of paving mixes with poor grading and/or compaction, whereas, the curve marked Type II represents paving mixes with better grading and/or compaction. Superimposed on FIGURE VI-20 are the tensile fracture strengths, obtained in this investigation, versus asphalt stiffness values of the asphalts comprising the mixes. The stiffness values were computed by means of Van der Poel's nomograph and using loading times corresponding to the fracture times of the asphaltic concrete cores. The scatter in results may partially be attributed to the many variables, such as asphalt types and contents, air void contents and aggregate gradations, of the asphaltic concrete cores included in the study. At high stiffness values, corresponding to low test temperatures, the tensile strengths of the cores were generally less than those strengths which could be expected assuming the cores to be representative of Type I mixes. However, the measured tensile strengths are consistent with those given by Haas (1968). Using a direct tension test Haas reported tensile strengths of asphaltic concrete mixes composed of different Western Canadian asphalts of approximately 320 psi (22 kg per sq cm) at test temperatures of -10 and -40 F.

6.6. Summary

In this chapter concepts used to characterize the time and temperature dependence of asphaltic concrete paving mixtures incorporated within two field test projects in Western Canada have been presented and stiffness modulus-reduced time relationships for the paving mixtures have been developed. Results of tensile splitting tests on pavement cores obtained from the test projects have been summarized and briefly discussed in relation to observed differences in low temperature behavior of test control sections within the projects.

TABLE VI-1
SUMMARY OF PROPERTIES OF ASPHALTS INCLUDED IN MANITOBA TEST PROJECT
(Young et al., 1969)

Asphalt Type and Grade	Penetration at 77 F, 100 gm 5 sec (dmm)	Absolute Viscosity at 140 F (poise)	T _{R&B} (F) Modified (a)	Penetration Index
LV 150-200 (b)	192	253	95	-2.5
LV 300-400 (b)	313	141	88	-2.4
HV 150-200 (b)	159	591	102	-1.0
SC-5 (c)	193	-	106	+0.5

- (a) Modified using method described by Heukelom (1969).
- (b) As supplied asphalt properties.
- (c) After plant mix asphalt properties.

TABLE VI-2
SUMMARY OF PROPERTIES OF ASPHALTS INCLUDED IN ALBERTA TEST PROJECT
(Anderson and Shields, 1971)

Supplier	Age	Penetration (dmm) 77 F 39.2 F	Absolute Viscosity at 140 F (poise)	T _{R&B} (F) Modified (a)	Penetration Index
1	As Supplied 34 mo.	265 68	237	95	-1.2
		144 29	343	99	-2.7
2	As Supplied 34 mo.	215 62	610	98	-1.1
		105 30	1,281	111	-1.0
3	As Supplied 34 mo.	217 58	544	102	-0.1
		70 26	1,801	117	-1.2

(a) Estimated values using method described by Heukelom (1969).

TABLE VI-3
PHYSICAL PROPERTIES OF ASPHALTIC CONCRETE CORES
OBTAINED FROM THE MANITOBA TEST PROJECT

Asphalt Type and Grade	Asphalt (a) Content (1b/100 1b)	Unit Weight (pcf)	Air Voids (per cent)	Volume Concentration of Aggregate C_v'
LV 150-200	4.8	148.0	4.9	0.88
LV 300-400	4.8	148.9	5.0	0.88
HV 150-200	5.3	151.8	3.0	0.90
SC-5	4.8	145.8	6.8	0.87
Aggregate (a) Gradation	Per Cent Passing			
	3/4 in	No. 4	No. 10	No. 200
	100	56.6	43.3	19.8
				2.9

(a) Average of extracted samples reported by Young et al. (1969).

TABLE VI-4
PHYSICAL PROPERTIES OF ASPHALTIC CONCRETE CORES
OBTAINED FROM THE ALBERTA TEST PROJECT

Supplier No.	Age	Asphalt Content (1b/100 1b)	Unit Weight (pcf)	Air Voids (per cent)	Volume Concentration of Aggregate C_v
1	At Construction	5.2 (0.5)	138.6 (4.3)	8.2 (2.1)	0.852
2		5.3 (0.4)	137.1 (2.3)	9.3 (1.5)	0.845
3		4.4 (0.4)	134.1 (2.2)	12.1 (1.5)	0.838
1	34 Months	5.2 (0.6)	147.6 (0.5)	2.1 (0.9)	0.898
2		5.3 (0.8)	142.9 (1.2)	5.4 (0.8)	0.877
3		4.4 (0.4)	142.6 (0.6)	6.5 (0.4)	0.876
Aggregate (a) Gradation	Per Cent Passing				
	3/4 in	No. 4	No. 10	No. 40	No. 200
	100	50.5	37.4	15.8	6.3

(a) Average of gradations reported by Shields et al. (1969).

TABLE VI-5
 TRANSVERSE CRACK FREQUENCIES OF PAVEMENTS
 INCLUDED IN THE MANITOBA TEST PROJECT
 (Young et al., 1969)

Structure	Asphalt Binder			
	LV 150/200	HV 150/200	LV 300/400	SC-5
B	285 (a)	0	143	0
C	1,056	0	0	0
D	107	0	-	-

(a) Cracks per mile.

TABLE VI-6
 TRANSVERSE CRACK FREQUENCIES
 OF PAVEMENTS INCLUDED IN THE
 ALBERTA TEST PROJECT
 (Anderson and Shields, 1971)

Asphalt Supplier	Age (months)		
	12	24	34
1	4 (a)	87	187
2	0	0	126
3	0	4	88

(a) Cracks per mile.

TABLE VI-7
SUMMARY OF TENSILE SPLITTING TEST RESULTS
MANITOBA ASPHALTIC CONCRETE CORES

Asphalt Binder	Test Temp. (a) (F)	No. of Cores	Failure Strain (in/in x 10 ⁻⁴)	Maximum Tensile Stress (psi)	Time to Failure (sec)	Failure Stiffness Measured (psi x 10 ⁴)	Failure Stiffness Calculated (psi x 10 ⁴)
LV 150/200	20	5	19.0 (5.6) (b)	320 (45)	252 (46)	33.3 (12.0)	21.3
	0	4	3.0 (1.2)	444 (27)	165 (6)	318.0 (163.0)	148.0
	-20	4	1.0 (0.3)	362 (38)	297 (30)	687.0 (288.0)	550.0
LV 300/400	20	5	26.0 (4.2)	341 (15)	281 (18)	25.0 (4.6)	8.9
	0	4	10.0 (2.1)	448 (12)	165 (13)	78.8 (21.0)	74.2
	-20	4	(1.2) (0.4)	531 (70)	301 (31)	841.0 (408.0)	341.0
HV 150/200	20	4	38.0 (3.0)	331 (25)	294 (17)	15.7 (1.2)	13.1
	0	5	11.0 (1.8)	641 (52)	172 (12)	111.0 (18.6)	74.2
	-20	4	1.0 (0.2)	551 (31)	299 (11)	793.0 (136.0)	233.0
SC-5	20	6	83.0 (17.0)	108 (27)	244 (35)	2.5 (0.8)	4.3
	10	4	47.0 (3.0)	168 (5)	256 (9)	6.6 (0.5)	11.0
	0	5	25.0 (7.0)	270 (22)	160 (9)	21.2 (5.5)	19.4
	-10	4	14.0 (2.0)	371 (18)	334 (18)	50.1 (4.6)	43.8
	-20	3	2.8 (1.0)	386 (15)	157 (13)	267.0 (80.0)	74.4

(a) All tests performed at a loading rate of 0.06 in/min.

(b) Figures in brackets indicate one standard deviation.

TABLE VI-8
SUMMARY OF TENSILE SPLITTING TEST RESULTS
ALBERTA ASPHALTIC CONCRETE CORES
AT CONSTRUCTION

Supplier No.	Test Temp. (a) (F)	No. of Cores	Failure Strain (in/in x 10 ⁻⁴)	Maximum Tensile Stress (psi)	Time to Failure (sec)	Failure Stiffness Measured (psi x 10 ⁴)	Failure Stiffness Calculated (psi x 10 ⁴)
1	20	5	20.0 (5.4) (b)	220 (39)	175 (28)	19.9 (10.4)	3.7
	10	5	11.0 (3.9)	265 (63)	167 (30)	48.1 (11.1)	6.6
	0	5	8.4 (2.3)	320 (20)	172 (34)	69.5 (17.7)	31.5
	-10	3	3.7 (2.1)	363 (27)	167 (10)	226.0 (125.0)	65.9
2	20	4	46.0 (10.0)	159 (9)	178 (25)	6.4 (1.2)	2.9
	10	4	23.0 (10.0)	218 (47)	151 (30)	17.5 (8.2)	9.8
	0	6	8.2 (4.9)	302 (36)	169 (10)	67.4 (30.4)	30.3
	-10	2	8.5 (2.1)	310 (33)	162 (9)	67.9 (10.0)	64.7
3	20	5	40.0 (11.0)	146 (14)	161 (14)	6.9 (1.7)	3.1
	10	6	22.0 (8.6)	186 (28)	176 (35)	18.7 (10.3)	7.0
	0	6	14.0 (6.7)	194 (40)	131 (23)	36.6 (23.8)	14.5
	-10	4	5.0 (2.9)	174 (33)	168 (41)	79.6 (36.9)	29.9

(a) All tests performed at a loading rate of 0.06 in/min.

(b) Figures in brackets indicate one standard deviation.

TABLE VI-9
SUMMARY OF TENSILE SPLITTING TEST RESULTS
ALBERTA ASPHALTIC CONCRETE CORES
AT 34 MONTHS

Supplier No.	Test Temp. (a) (F)	No. of Cores	Failure Strain (in/in x 10 ⁻⁴)	Maximum Tensile Stress (psi)	Time to Failure (sec)	Failure Stiffness Measured (psi x 10 ⁴)	Failure Stiffness Calculated (psi x 10 ⁴)
1	20	6	18.0 (3.2) (b)	377 (23)	183 (17)	40.5 (8.6)	32.1
	10	6	13.0 (2.2)	428 (65)	168 (22)	62.0 (16.4)	145.6
	0	7	5.6 (1.8)	437 (69)	153 (18)	143.0 (79.0)	339.2
	-10	4	2.8 (1.2)	469 (67)	153 (5)	357.0 (142.0)	542.1
2	20	6	37.0 (9.0)	239 (36)	186 (15)	12.8 (5.9)	31.2
	10	6	26.0 (7.9)	253 (28)	154 (27)	19.7 (6.9)	43.9
	0	8	10.0 (2.6)	305 (18)	136 (9)	57.9 (15.6)	117.4
	-10	4	8.4 (1.9)	335 (19)	140 (2)	82.9 (18.7)	148.5
3	20	5	24.0 (1.9)	165 (14)	158 (9)	12.8 (1.3)	42.9
	10	5	21.0 (4.2)	224 (9)	153 (15)	19.3 (4.3)	163.8
	0	7	8.3 (1.9)	270 (18)	130 (10)	62.3 (14.9)	261.4
	-10	4	8.0 (1.1)	296 (28)	120 (7)	71.9 (6.9)	408.5

(a) All tests performed at a loading rate of 0.06 in/min.

(b) Figures in brackets indicate one standard deviation.

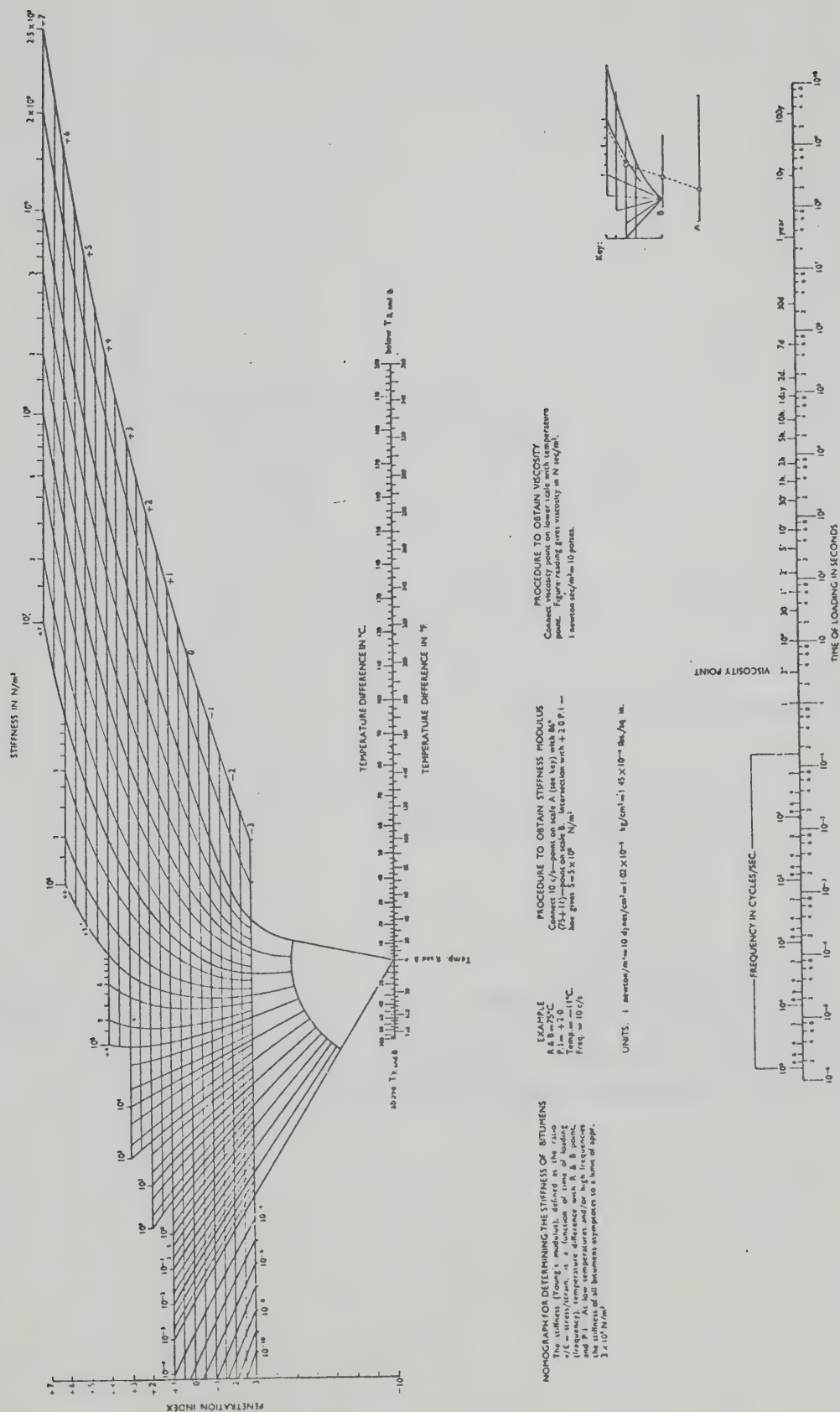


FIGURE VI-1 NOMOGRAPH FOR DETERMINING THE STIFFNESS OF BITUMENS. (after Van der Poel, 1954)

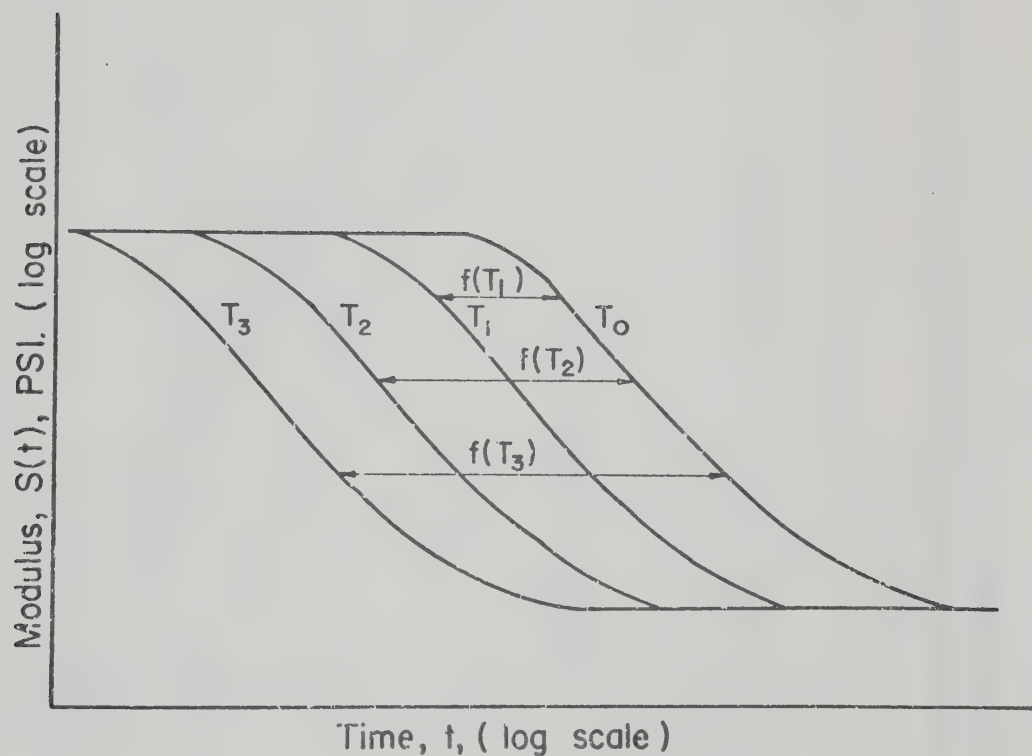


FIGURE VI-2 EFFECT OF TIME AND TEMPERATURE ON THE STIFFNESS MODULUS FOR A THERMORHEOLOGICALLY SIMPLE MATERIAL (after Monismith et al., 1966)

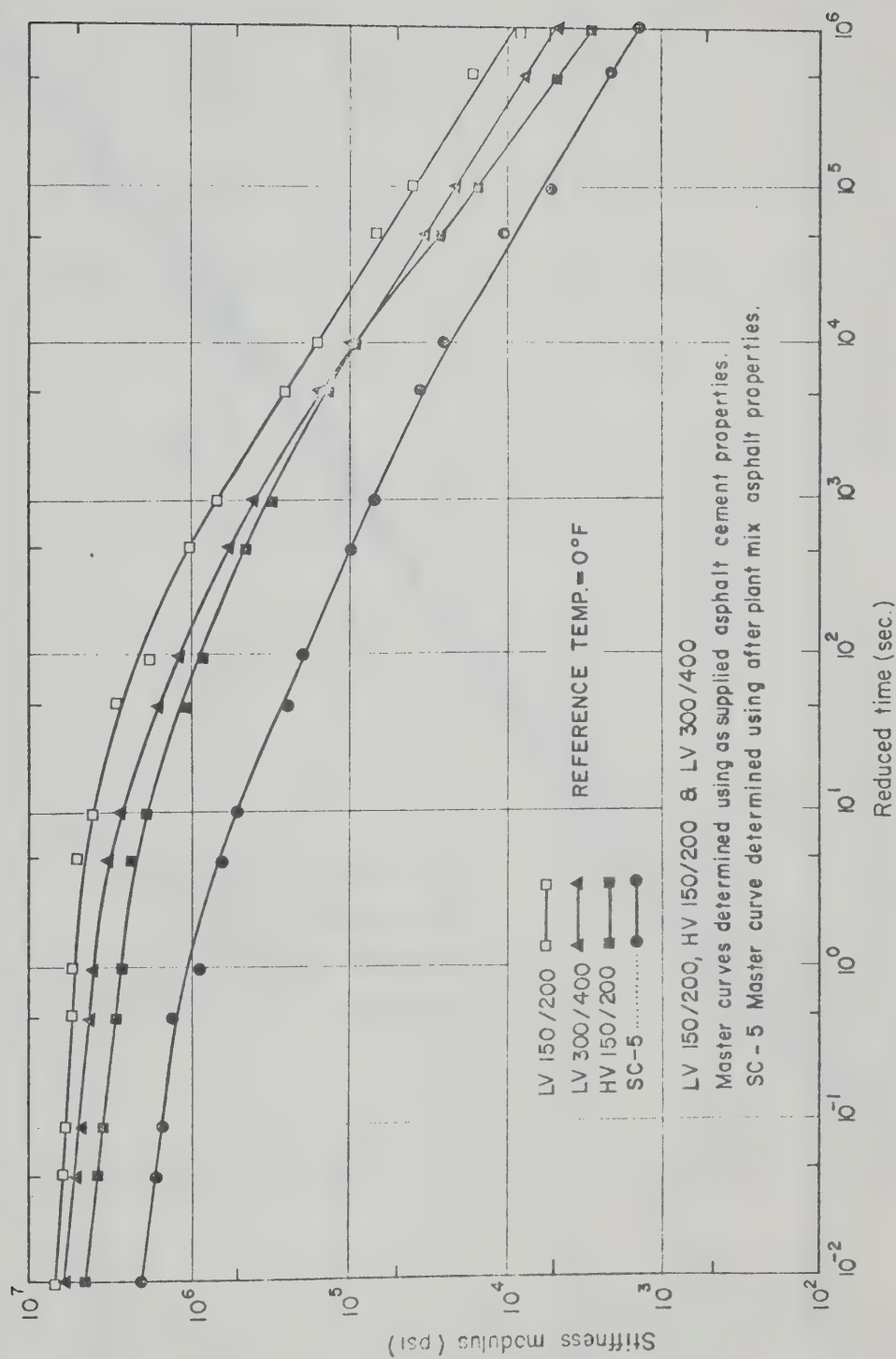


FIGURE VI-3 MASTER STIFFNESS MODULUS CURVES FOR MANITOBA ASPHALTIC CONCRETES
 AT A REFERENCE TEMPERATURE OF 0°F.

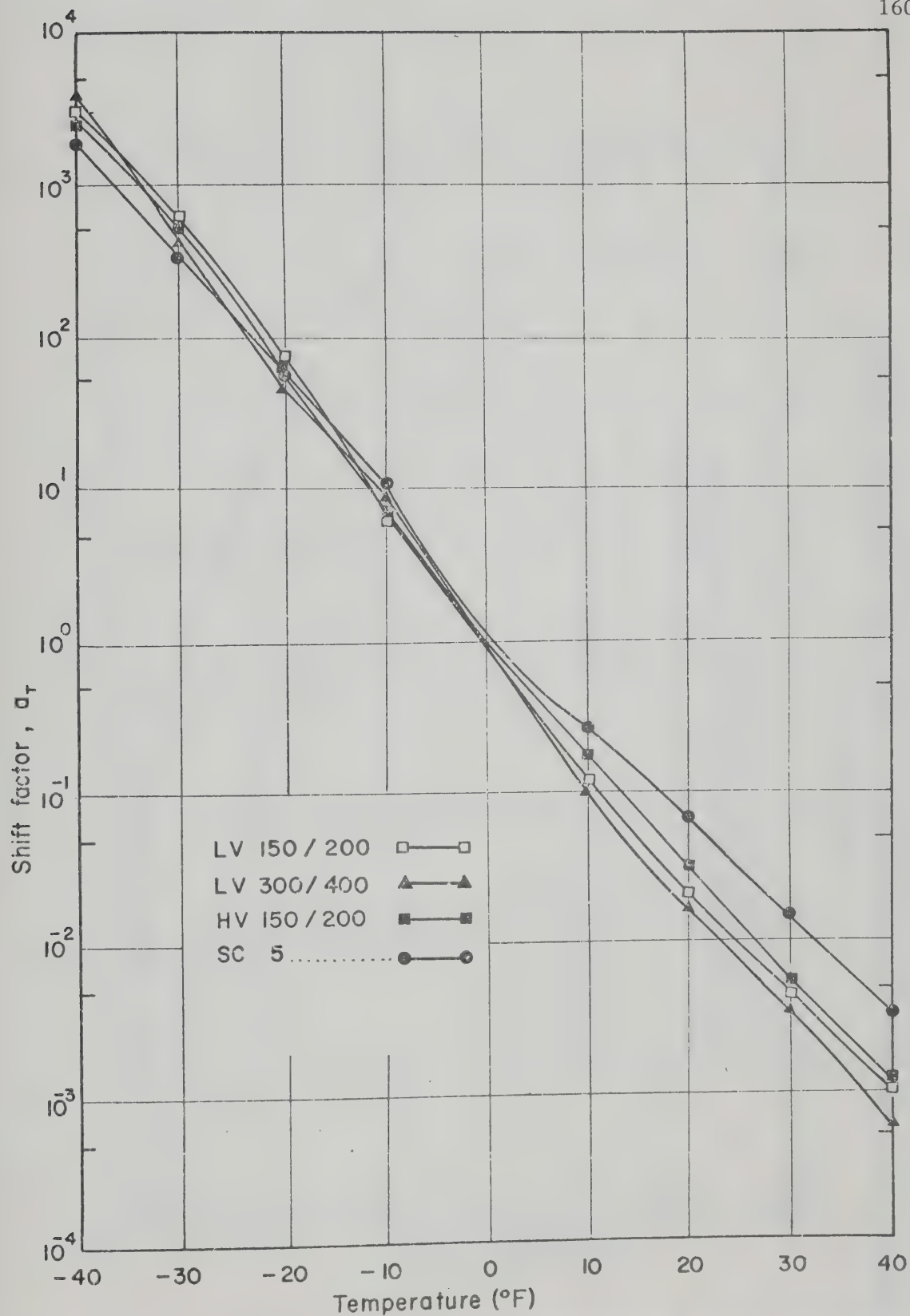


FIGURE VI-4 SHIFT FACTOR VERSUS TEMPERATURE RELATIONSHIPS FOR MANITOBA ASPHALTIC CONCRETES.

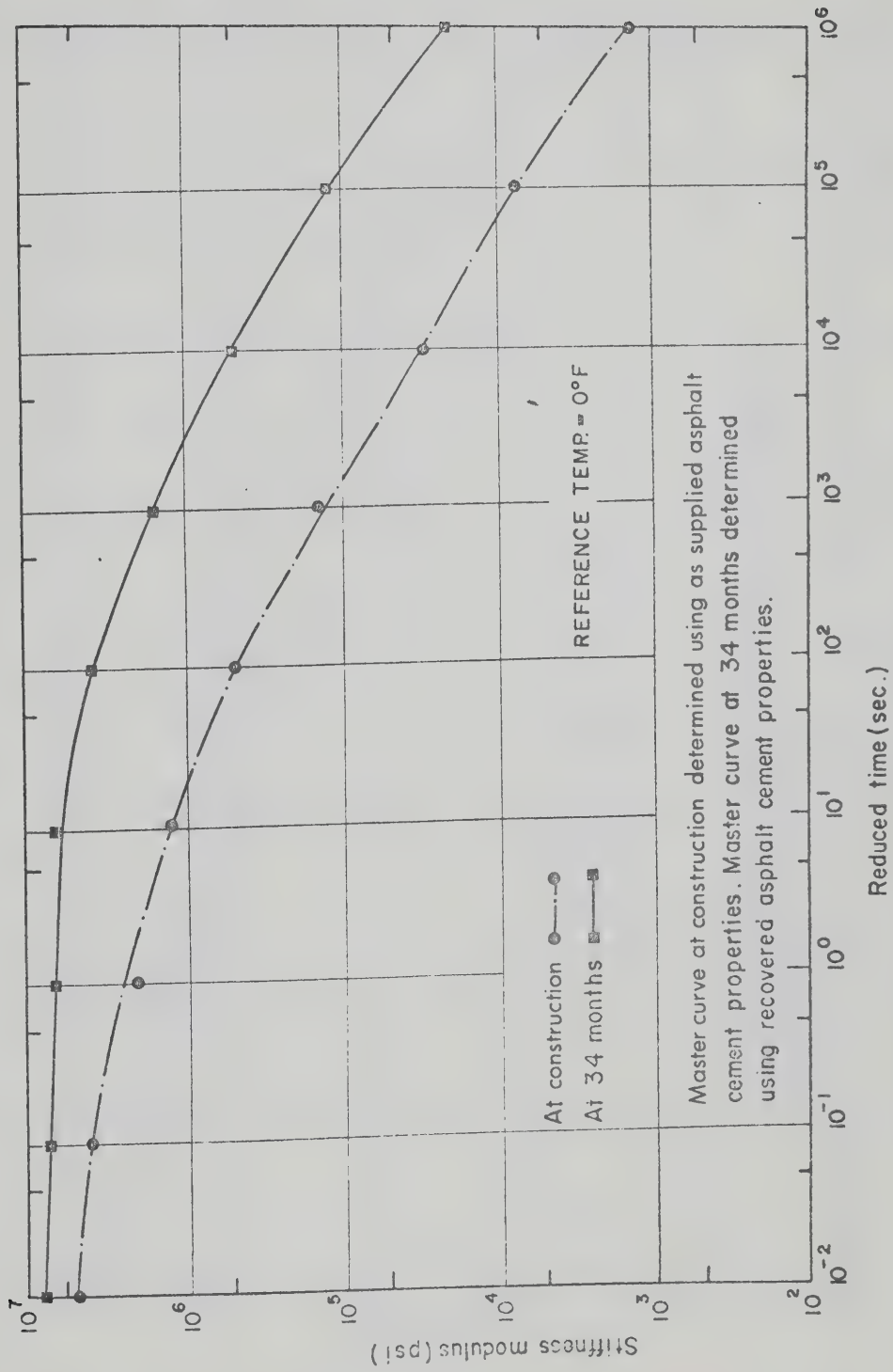


FIGURE VI-5 MASTER STIFFNESS MODULUS CURVES FOR ASPHALTIC CONCRETE
COMPOSED OF SUPPLIER NO. 1 ASPHALT CEMENT.

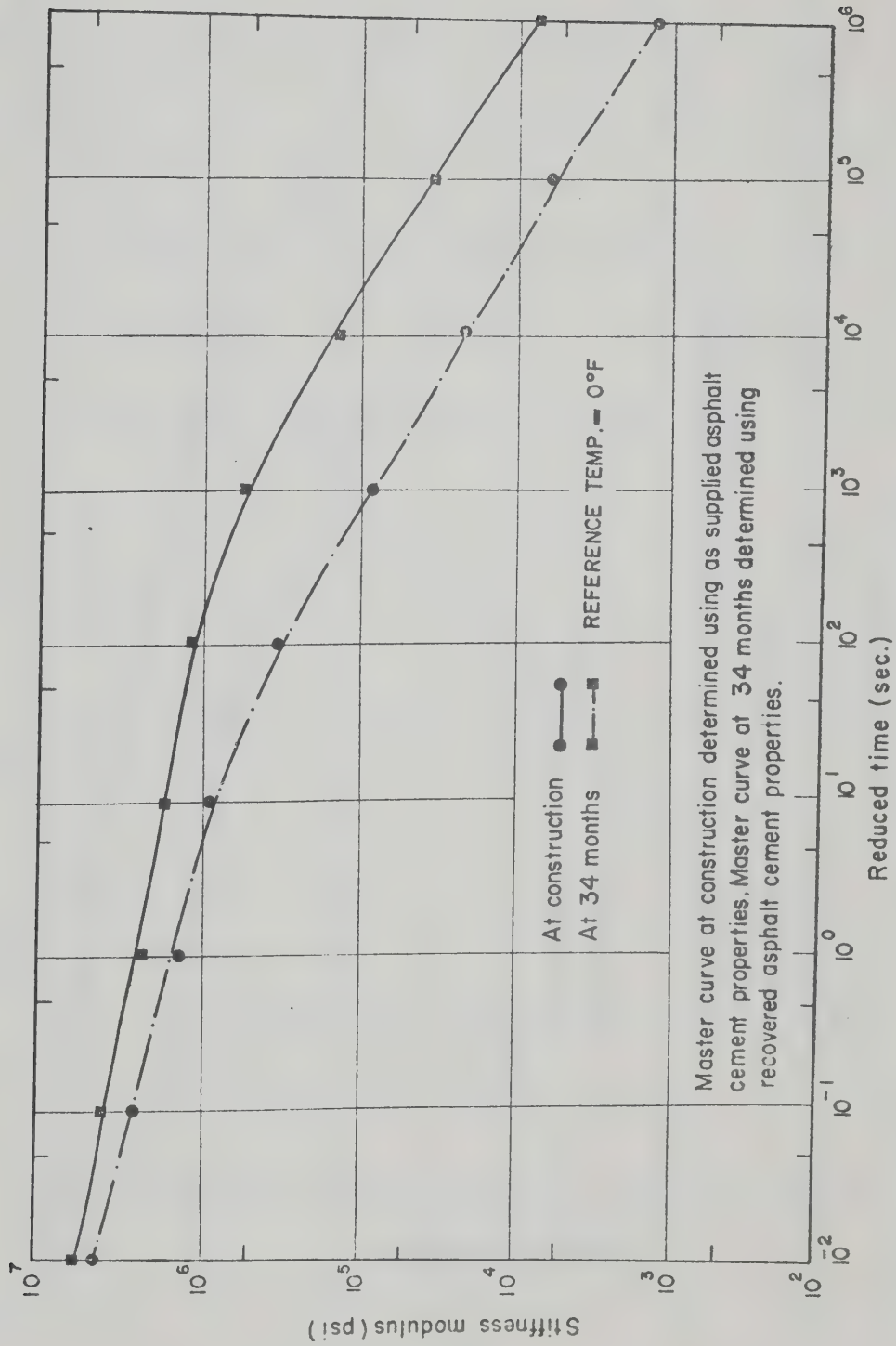


FIGURE VI-6 MASTER STIFFNESS MODULUS CURVES FOR ASPHALTIC CONCRETE COMPOSED OF SUPPLIER NO. 2 ASPHALT CEMENT.

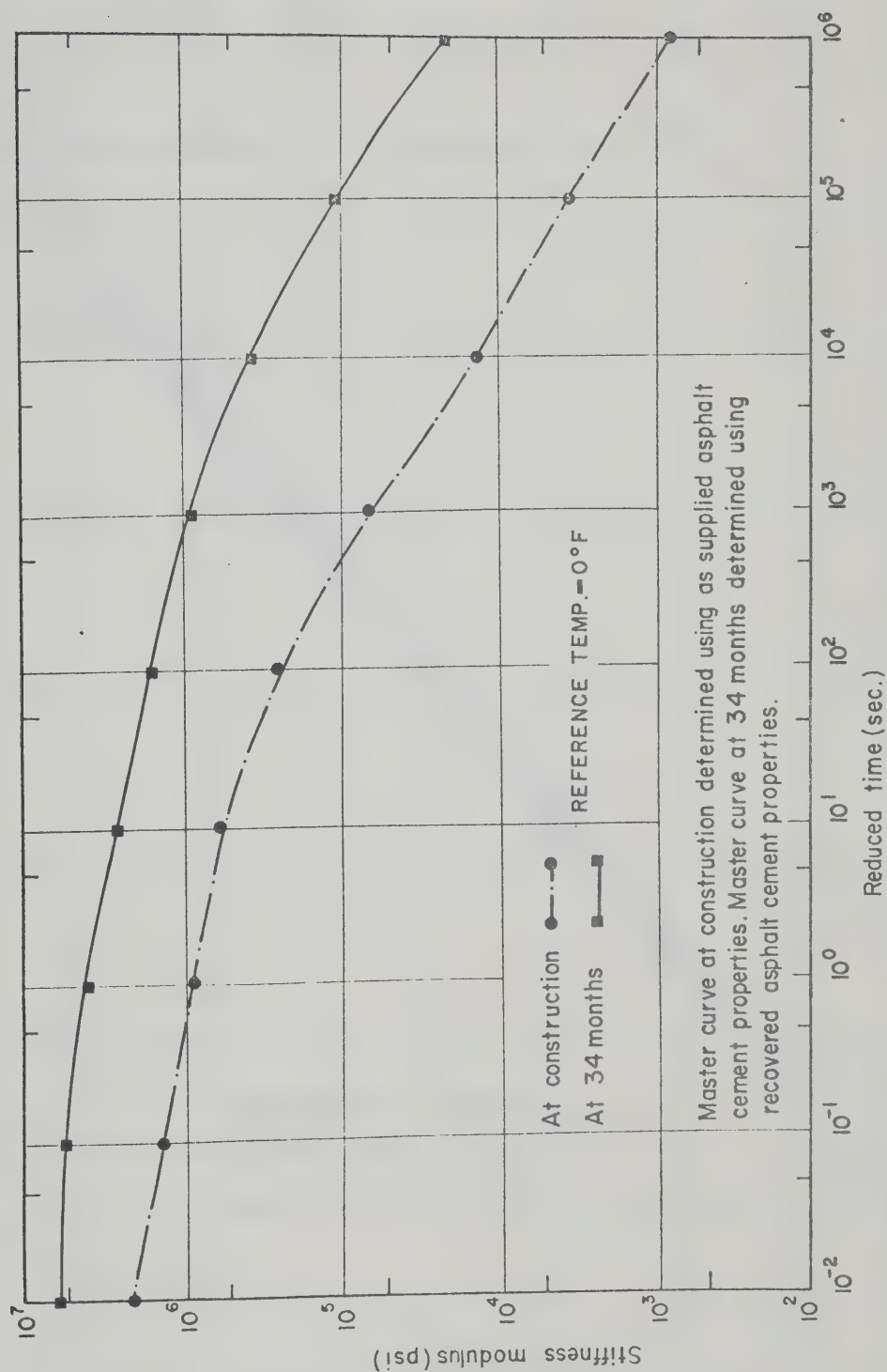


FIGURE VI-7 MASTER STIFFNESS MODULUS CURVES FOR ASPHALTIC CONCRETE COMPOSED OF SUPPLIER NO.3 ASPHALT CEMENT.

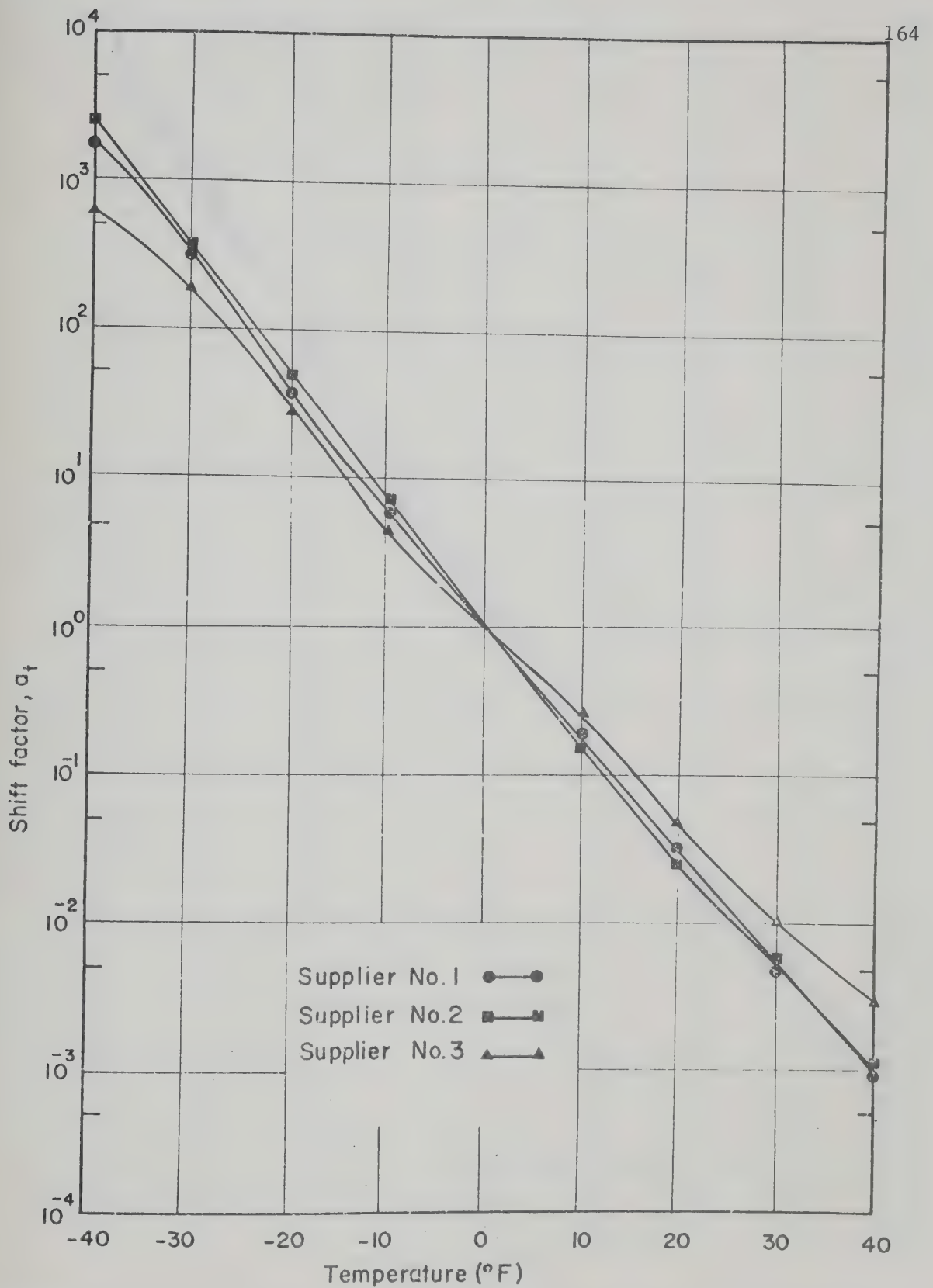


FIGURE VI-8 SHIFT FACTOR VERSUS TEMPERATURE RELATIONSHIPS
FOR ALBERTA ASPHALTIC CONCRETES AT CONSTRUCTION.

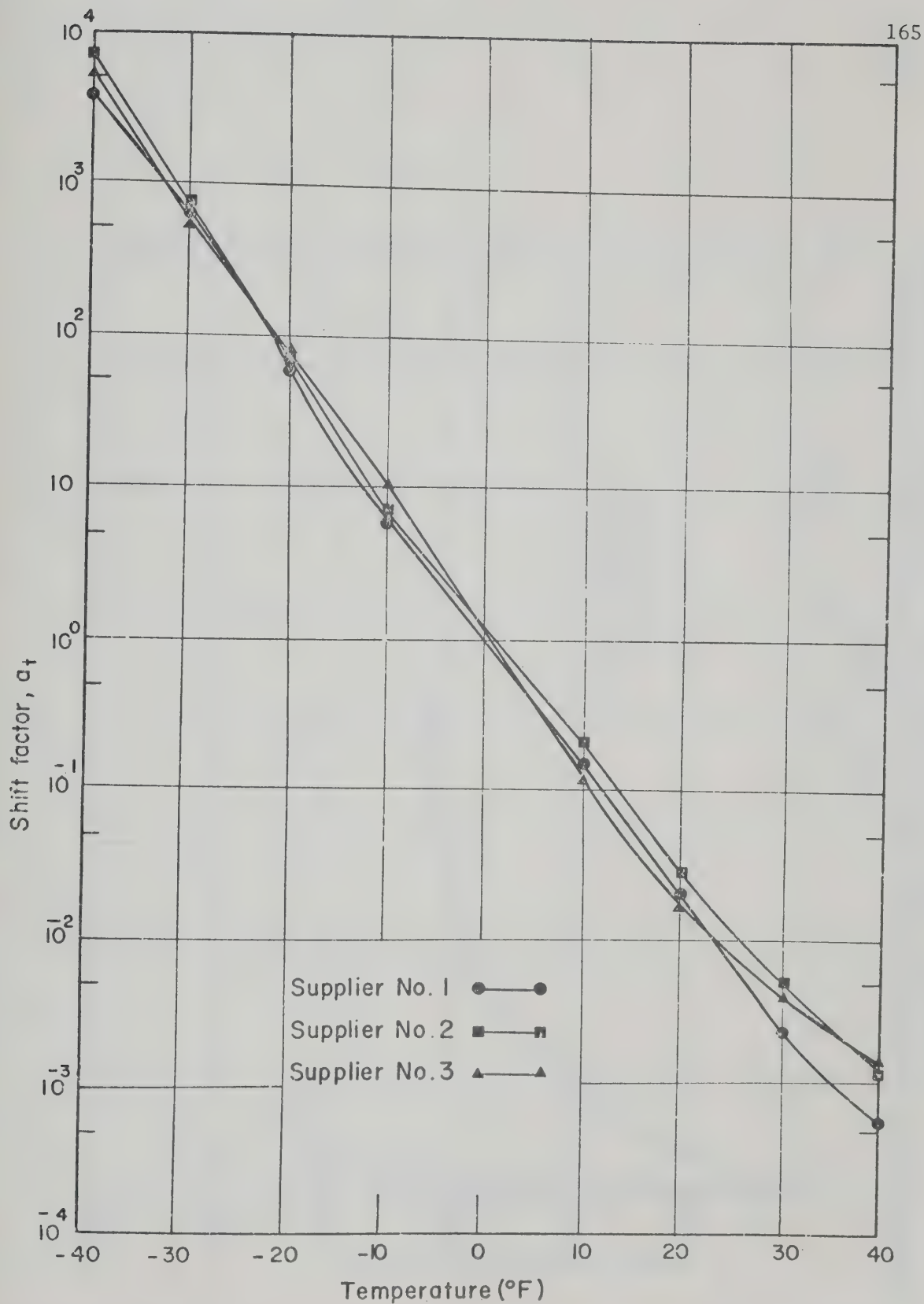


FIGURE VI-9 SHIFT FACTOR VERSUS TEMPERATURE RELATIONSHIPS
FOR ALBERTA ASPHALTIC CONCRETES AT 34 MONTHS.

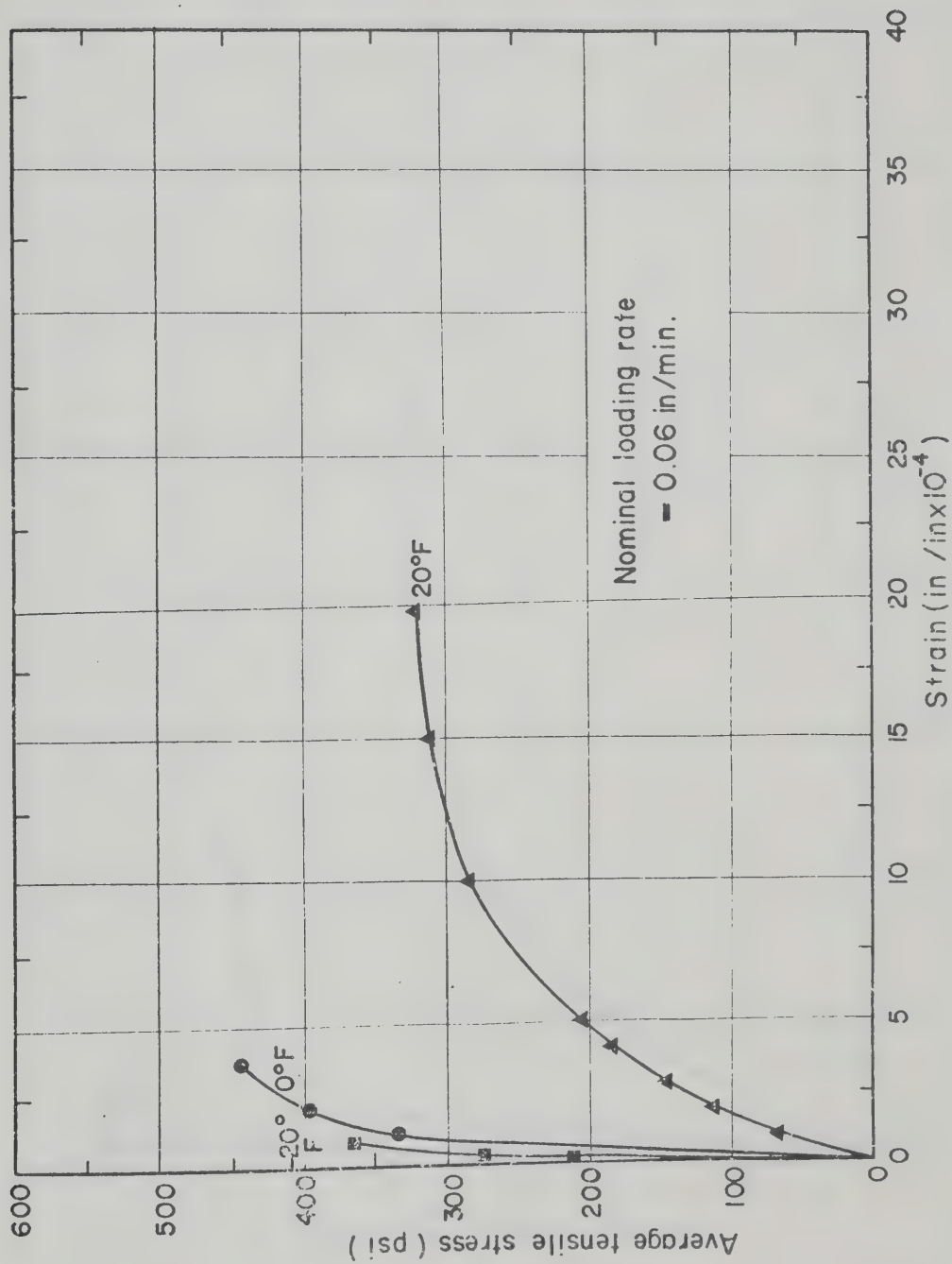


FIGURE VI-10 STRESS-STRAIN RELATIONSHIPS FOR MANITOBA ASPHALTIC CONCRETE CORES COMPOSED OF LV 150 / 200 PENETRATION GRADE ASPHALT CEMENT.

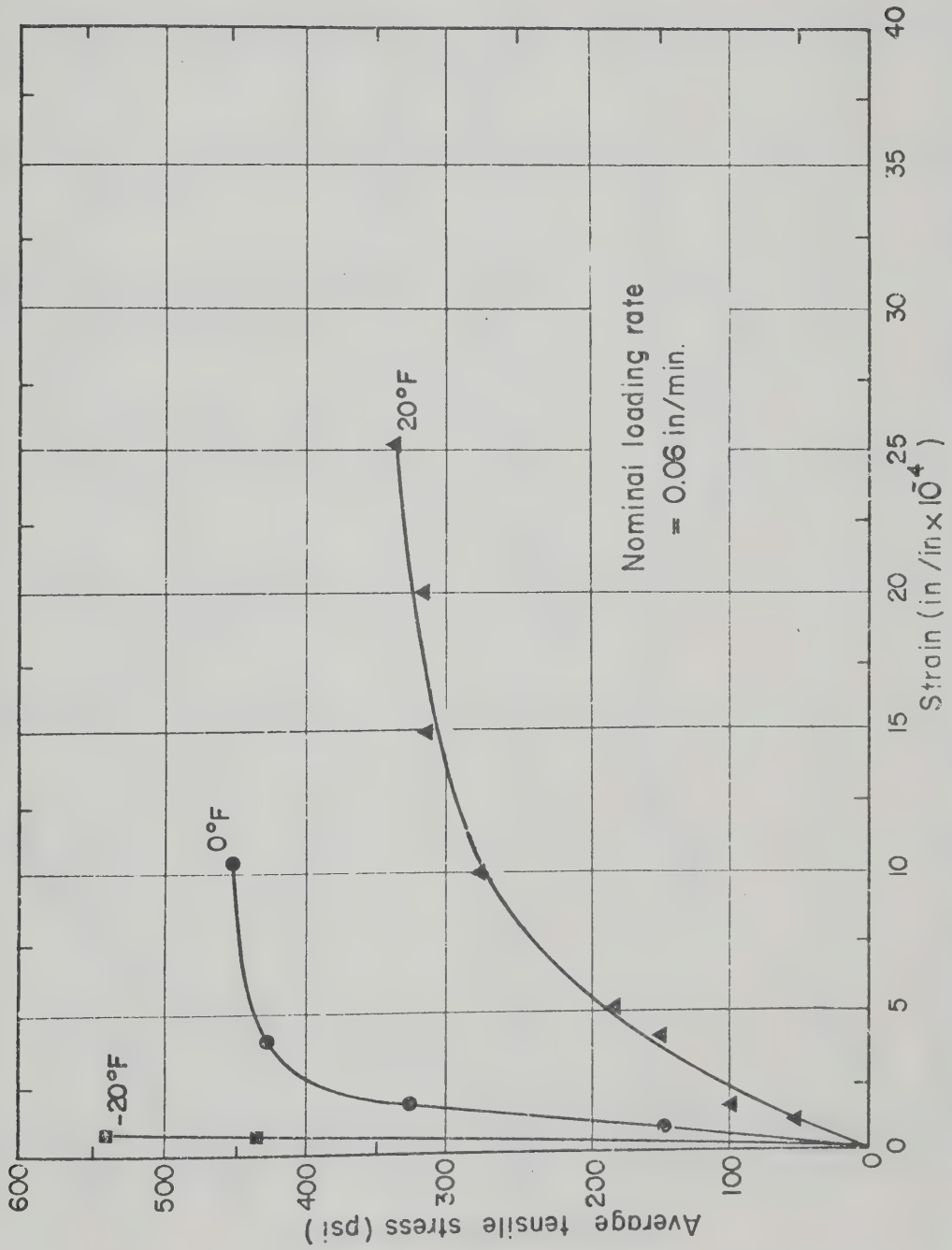


FIGURE VI-11 STRESS - STRAIN RELATIONSHIPS FOR MANITOBA ASPHALTIC CONCRETE CORES COMPOSED OF LV 300/400 PENETRATION GRADE ASPHALT CEMENT.

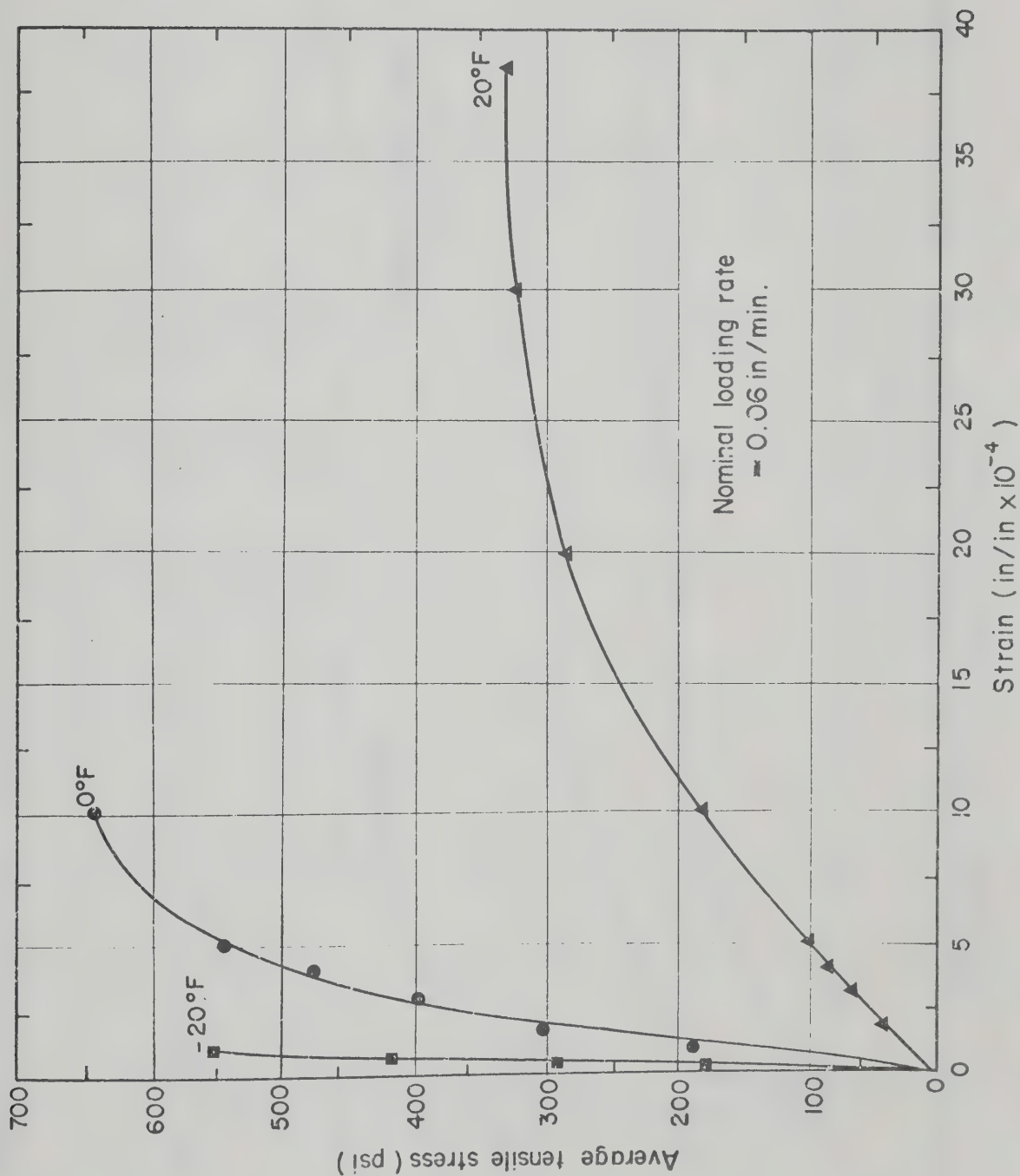


FIGURE VI-12 STRESS-STRAIN RELATIONSHIPS FOR MANITOBA ASPHALTIC CONCRETE
CORES COMPOSED OF HV 150/200 PENETRATION GRADE ASPHALT
CEMENT

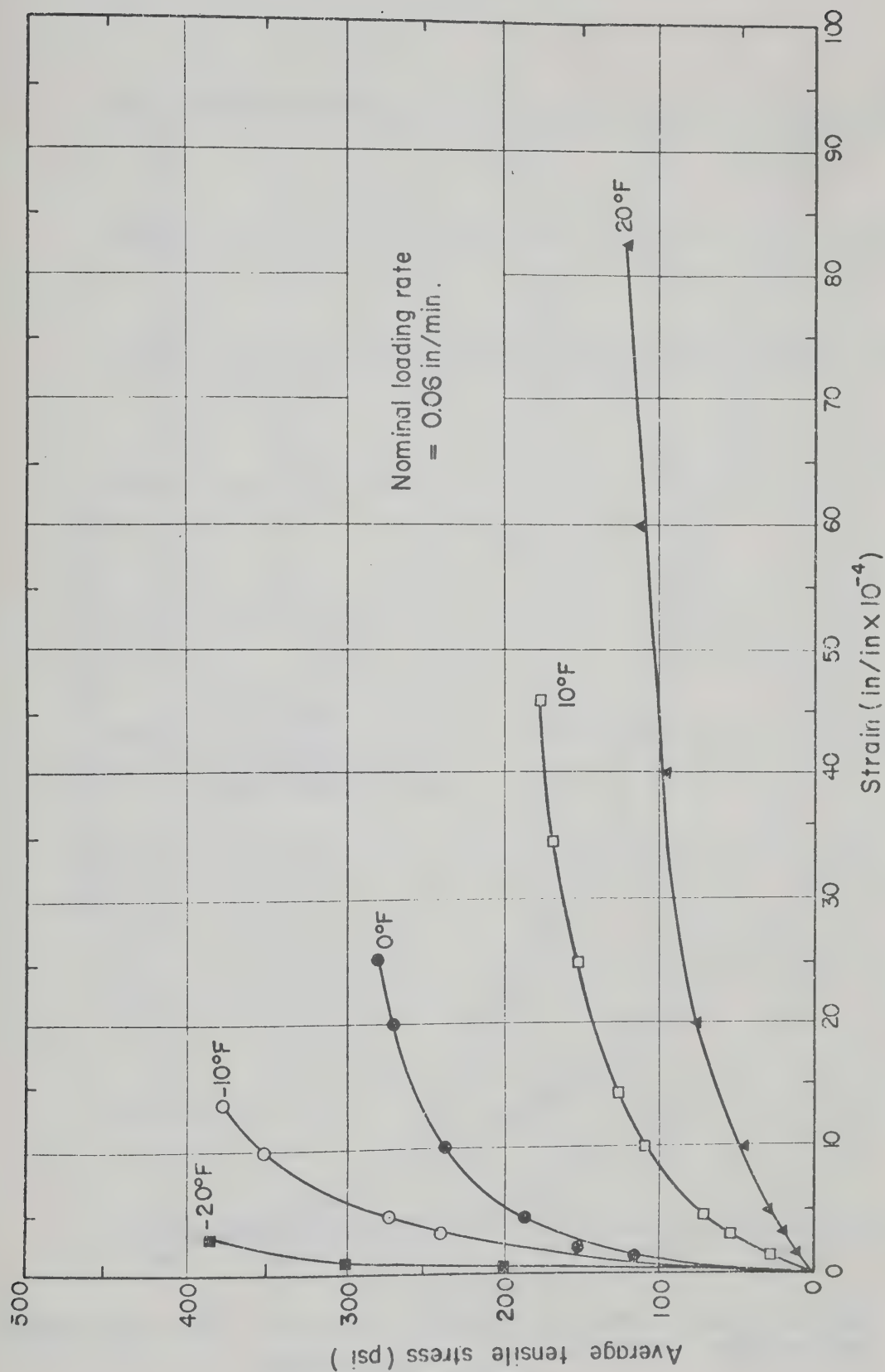


FIGURE VI-13 STRESS-STRAIN RELATIONSHIPS FOR MANITOBA ASPHALTIC CONCRETE CORES COMPOSED OF SC-5 LIQUID ASPHALT.

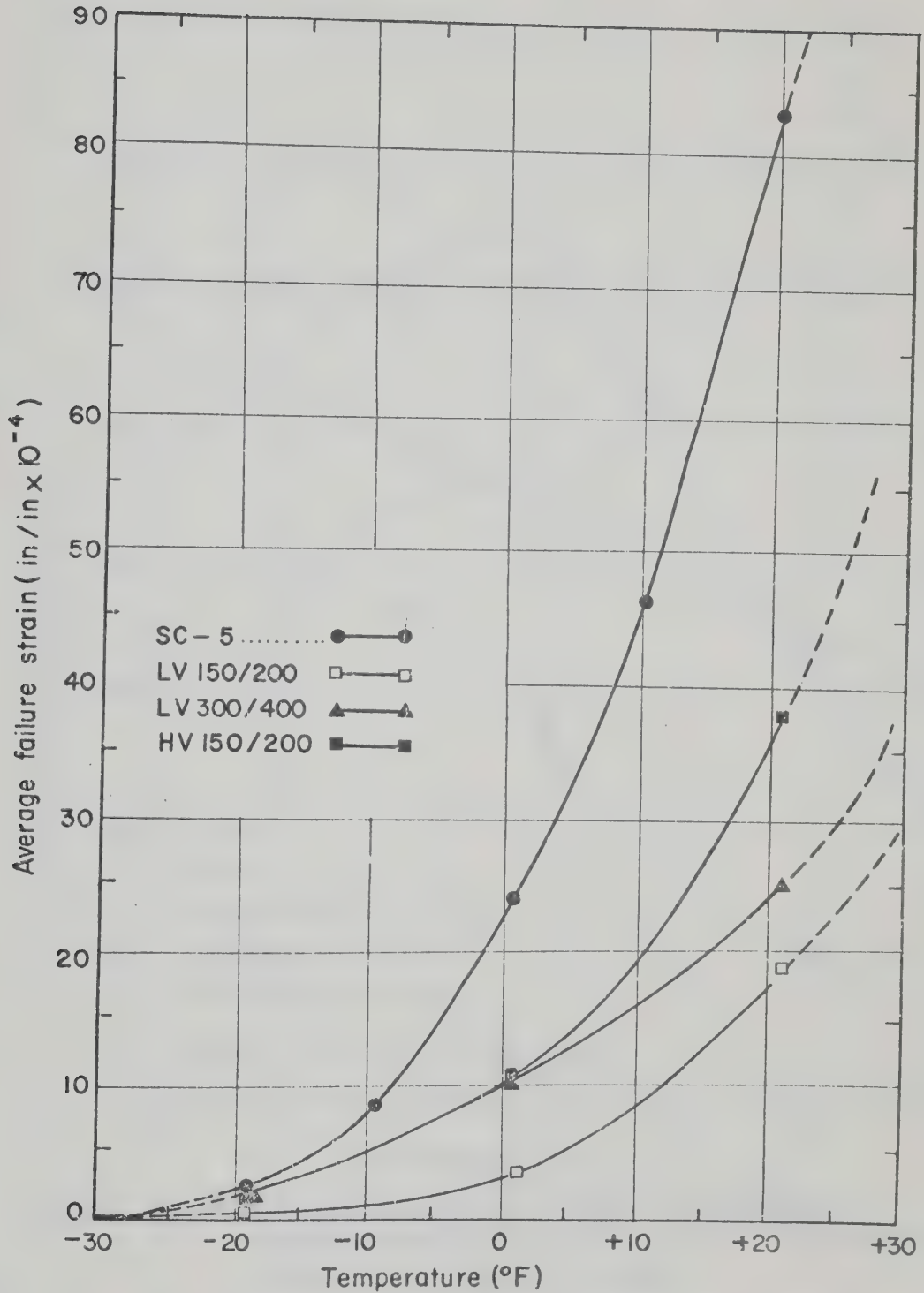


FIGURE VI-14 AVERAGE FAILURE STRAIN-TEMPERATURE RELATIONSHIPS OF MANITOBA ASPHALTIC CONCRETE CORES.

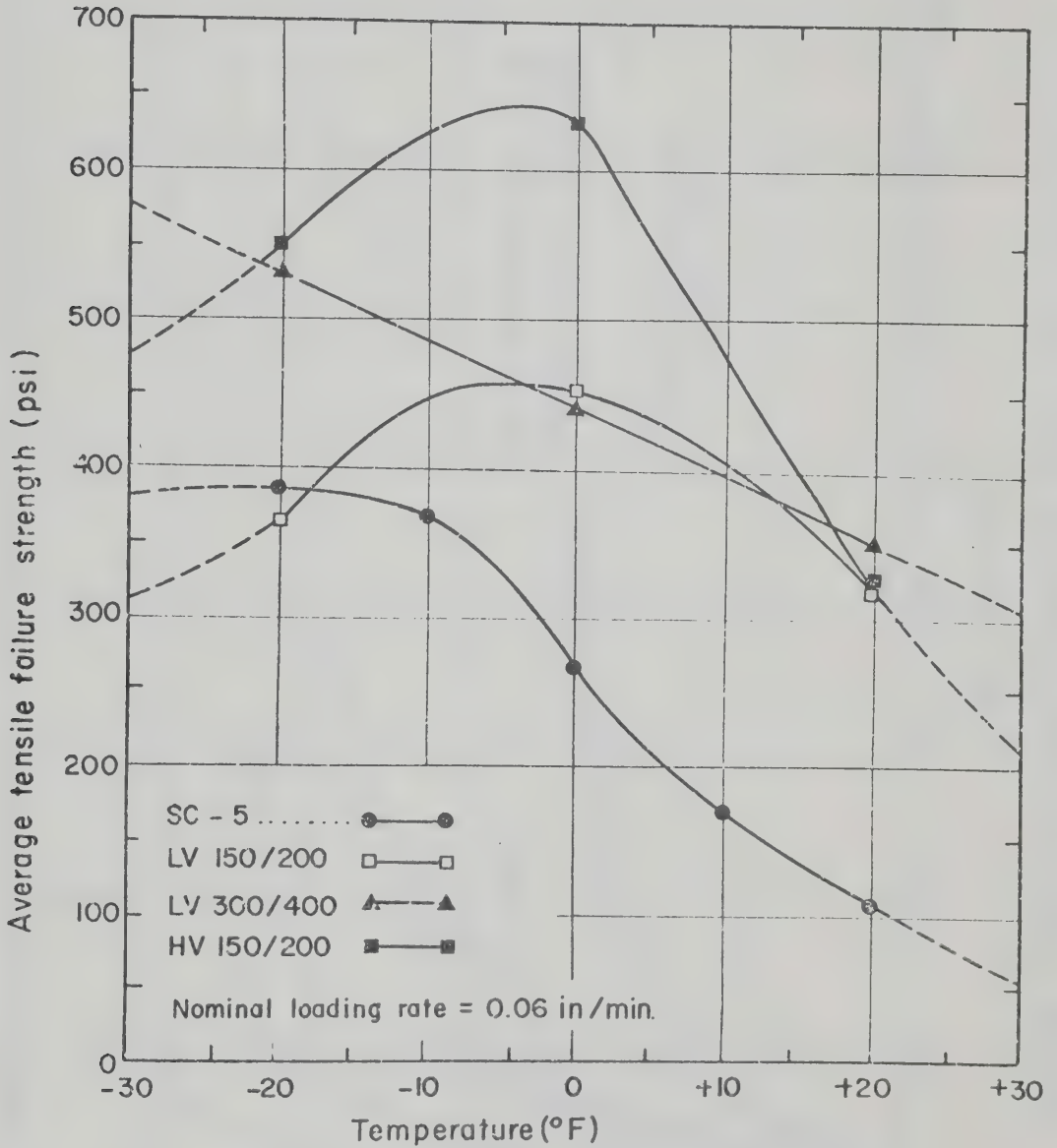


FIGURE VI-15 AVERAGE TENSILE FAILURE STRENGTH-TEMPERATURE RELATIONSHIPS OF MANITOBA ASPHALTIC CONCRETE CORES.

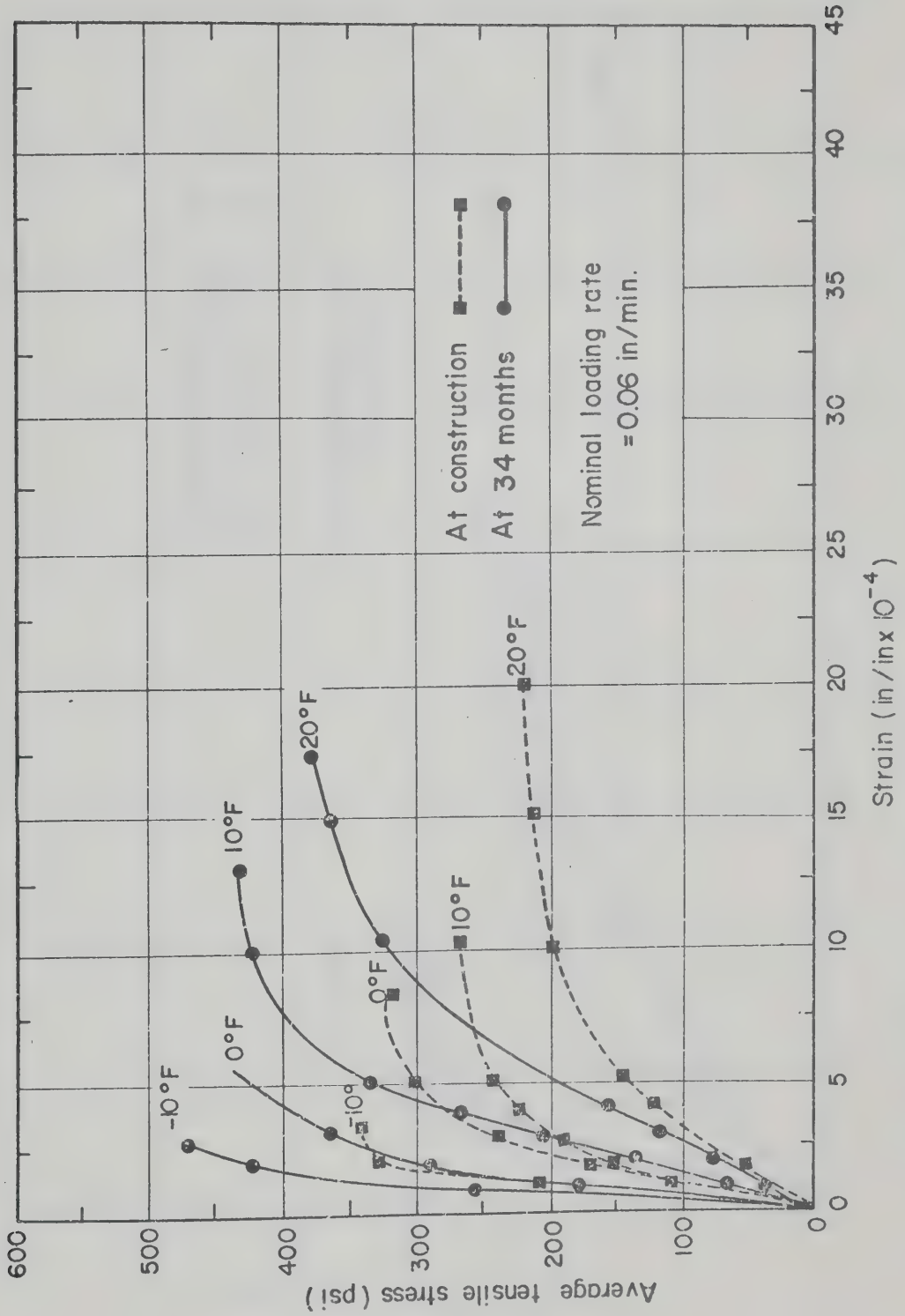


FIGURE VI-16 STRESS - STRAIN RELATIONSHIPS FOR ASPHALTIC CONCRETE CORES COMPOSED OF SUPPLIER NO.1 ASPHALT CEMENT.

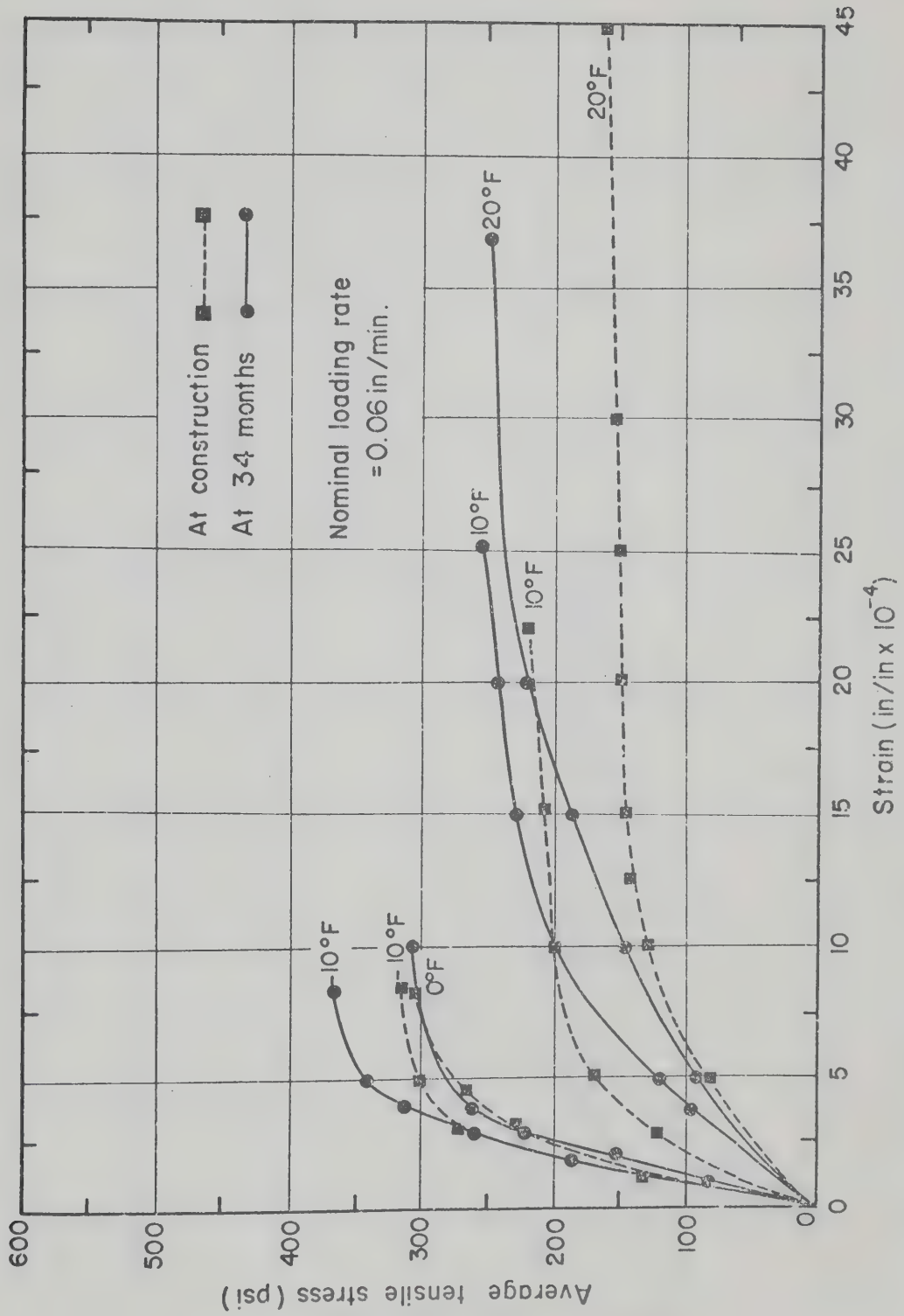


FIGURE VI-17 STRESS-STRAIN RELATIONSHIPS FOR ASPHALTIC CONCRETE CORES COMPOSED OF SUPPLIER NO. 2 ASPHALT CEMENT.

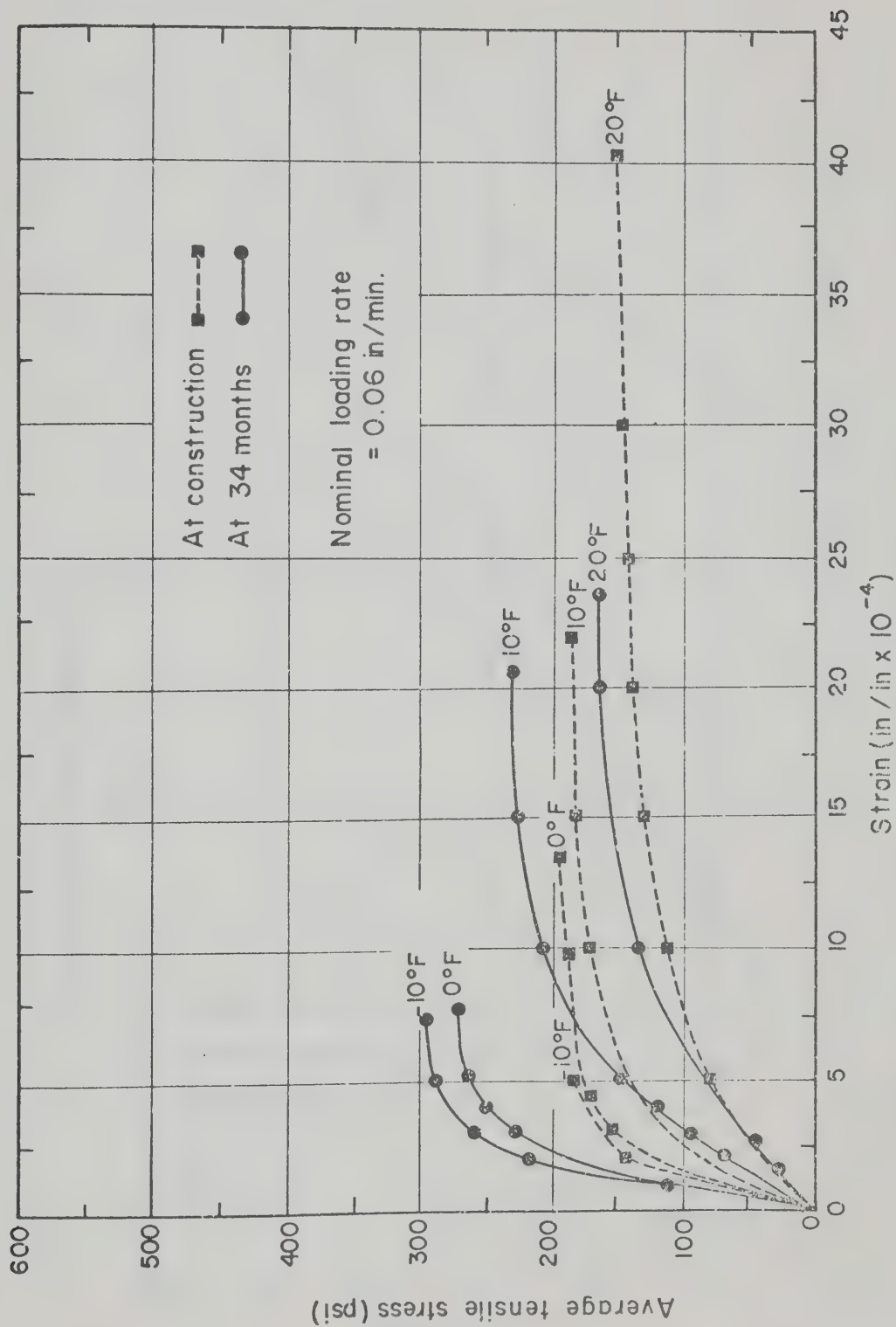


FIGURE VI-18 STRESS-STRAIN RELATIONSHIPS FOR ASPHALTIC CONCRETE CORES COMPOSED OF SUPPLIER NO. 3 ASPHALT CEMENT.

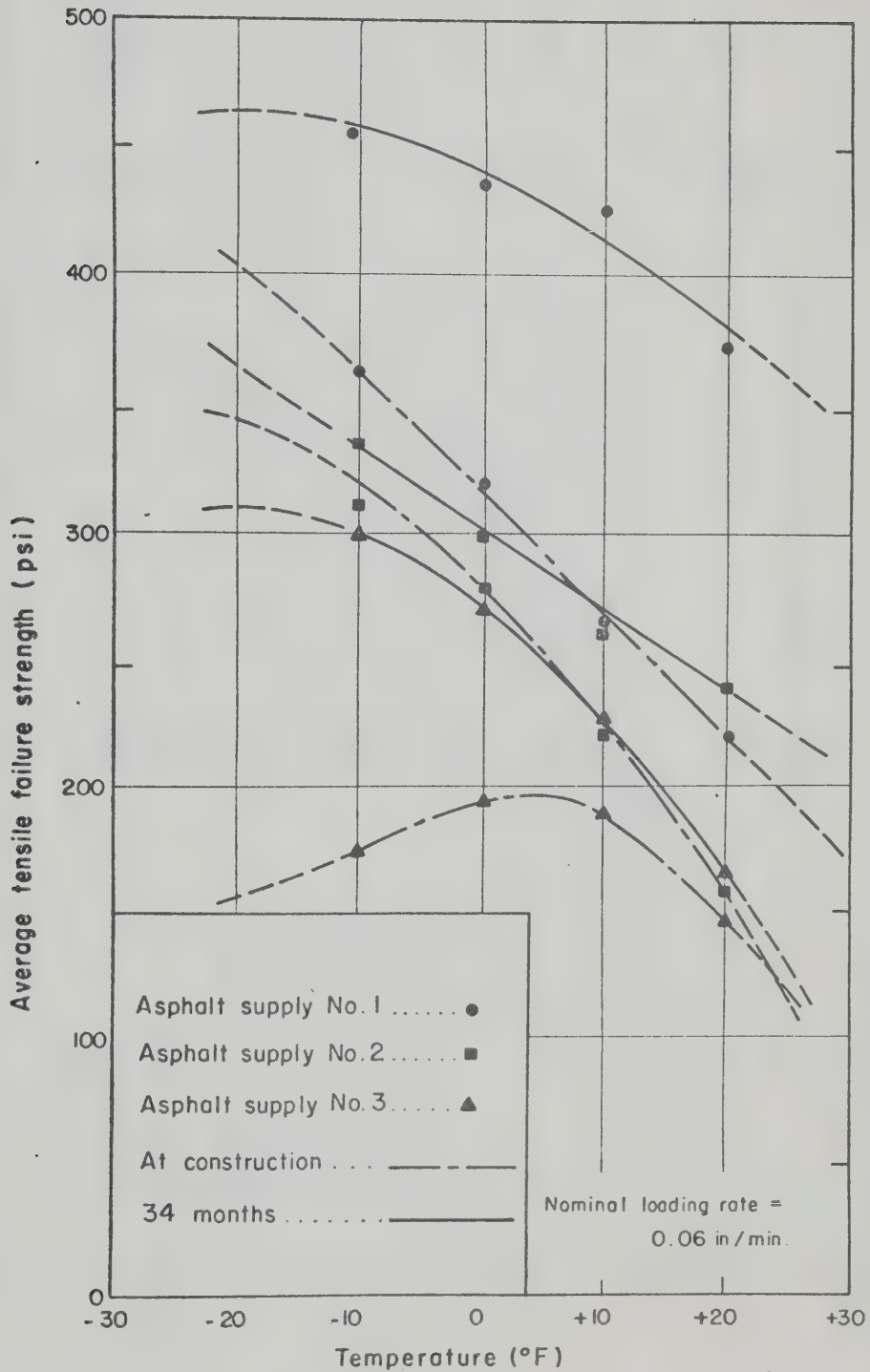


FIGURE VI-19 AVERAGE TENSILE FAILURE STRENGTH-TEMPERATURE RELATIONSHIPS OF ALBERTA ASPHALTIC CONCRETE CORES.

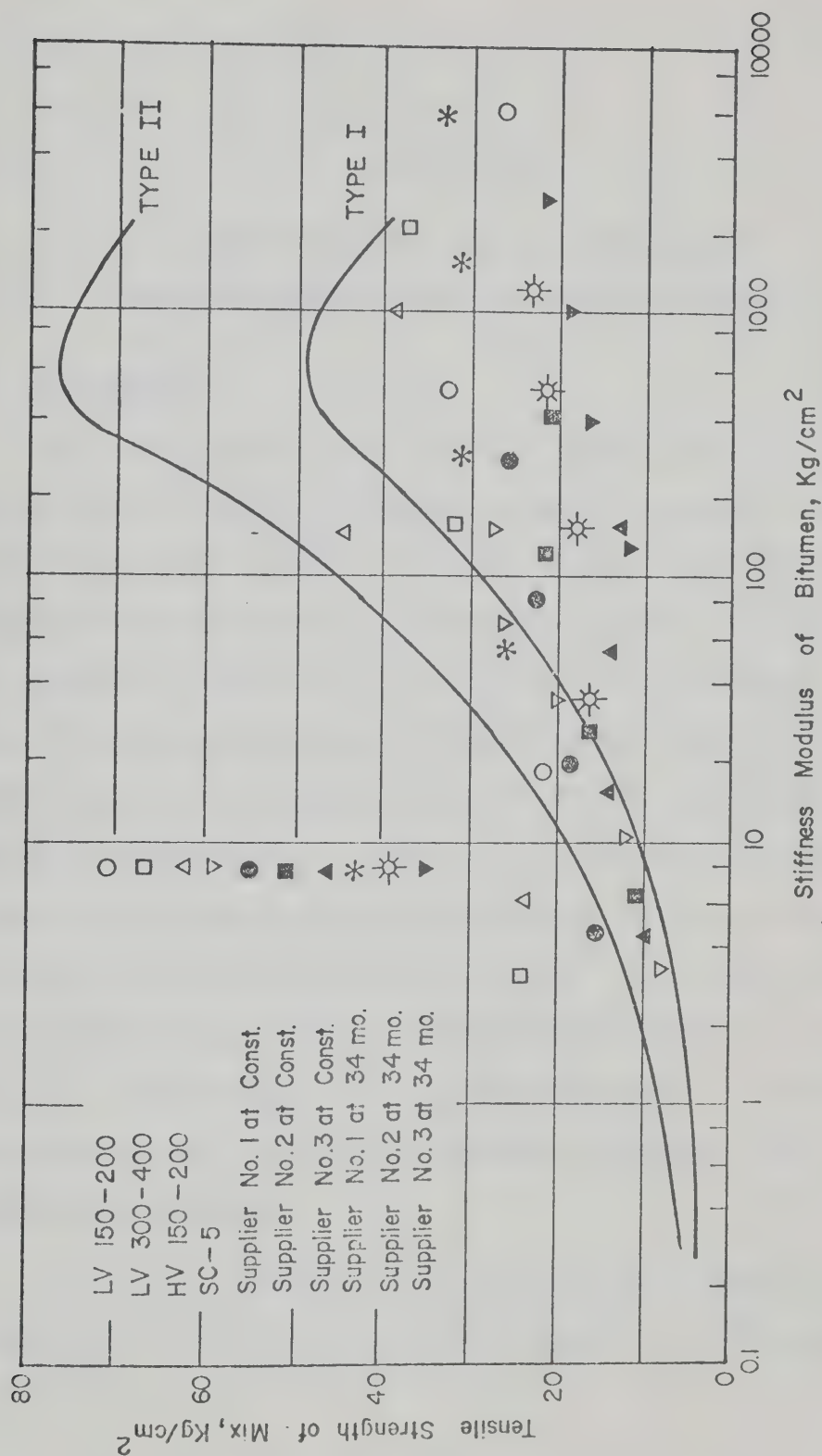


FIGURE. VI-20 TENSILE STRENGTH OF MIXES AS A FUNCTION OF THE STIFFNESS MODULUS OF THE ASPHALT CEMENT (after Heukelom, 1966)

CHAPTER VII

STRESS PREDICTION AND LOW TEMPERATURE FRACTURE SUSCEPTIBILITY OF ASPHALTIC CONCRETE

7.1. Introduction

In recent years various numerical methods have been used to predict thermal stresses in asphaltic concrete pavements subjected to assumed temperature regimes. It is only recently that information has become available as to the real temperature regimes occurring in pavement structures prior to and at the time of crack initiation. In this chapter such temperature data, obtained from the field test projects in Manitoba and Alberta, together with the stiffness and fracture strength-temperature relationships of asphaltic concrete mixes incorporated in the test projects and described in CHAPTER VI, is used to assess the results of various stress prediction methods. The stress prediction methods include pseudo-elastic and viscoelastic beam and slab analyses. Theoretical considerations for the formulation of the stress prediction methods are reviewed and numerical solutions of the stress equations are presented.

Employing a postulated fracture criterion, computed stresses are compared with the fracture strength-temperature relationships of

the asphaltic concrete cores obtained from the individual field test projects to predict times of fracture. These times of fracture are then compared with times of observed low temperature cracking of the corresponding pavements in the field projects. Such comparisons provide a means of assessing the stress predictive methods in relation to observed differences in the low temperature fracture susceptibility of asphaltic concrete paving mixtures included in the test projects.

7.2. Stress Predictive Methods

A review of a number of different methods used to compute thermal stresses in asphaltic concrete pavements has been presented by Haas and Topper (1969). These analyses may be classified according to the boundary constraints on a pavement element. Considering an element of pavement as shown in FIGURE VII-1, the term "beam analysis" implies the conditions

$$\epsilon_x = 0 \quad \sigma_y = \sigma_z = 0 \quad (\text{VII-1})$$

and the term "slab analysis" implies the conditions

$$\epsilon_x = \epsilon_y = 0 \quad \sigma_z = 0 \quad (\text{VII-2})$$

For pavement structures the beam assumptions approximate conditions at the edge of a pavement while the slab assumptions are more severe than those which would be anticipated in the center of the pavement.

Five analyses have been used in this study for stress computations. These analyses are designated as:

- 1) Pseudo-elastic beam.

- 2) Approximate pseudo-elastic slab.
- 3) Viscoelastic slab.
- 4) Viscoelastic beam.
- 5) Approximate viscoelastic slab.

A description of these analyses follows.

7.2.1. Pseudo-Elastic Beam Analysis

The stress equation for the pseudo-elastic beam analysis is

$$\sigma_x(t) = - \int_{t_0}^t S(\Delta t, T) \alpha_0(T) dT(t) \quad (\text{VII-3})$$

where $S(\Delta t, T)$ is the time and temperature dependent stiffness modulus. If the coefficient of the thermal expansion, α_0 , and S are independent of time and temperature this equation reduces to the simple elastic thermal stress equation. To evaluate stress numerically Equation (VII-3) is written as

$$\sigma_x(t_i) = \sigma_x(t_{i-1}) + (\Delta\sigma_x)_i \quad (\text{VII-4})$$

where

$$(\Delta\sigma_x)_i = - \int_{t_{i-1}}^{t_i} S(\Delta t, T) \alpha_0(T) dT(t) \quad (\text{VII-5})$$

Hills and Brien (1966) suggested that the stiffness modulus in Equation (VII-5) be determined for a loading time (Δt) equal to the time interval, $t_i - t_{i-1}$, over which the change of stress $(\Delta\sigma_x)_i$ is computed, and at a mean temperature during this time interval. McLeod (1969) recommended that the stiffness be evaluated at a loading time (Δt) of

20,000 seconds. Fromm and Phang (1971) used stiffness values determined at a loading time of 10,000 seconds.

In this study the pseudo-elastic beam stress increments were computed using the trapezoidal rule with stiffnesses evaluated at the temperatures for times t_i and t_{i-1} , and a loading time (Δt) equal to the time step ($t_i - t_{i-1}$). With the assumption that the coefficient of thermal expansion is temperature independent the approximation to Equation (VII-5) then becomes

$$(\Delta\sigma_x)_i = \frac{\alpha_o}{2} (S_i + S_{i-1})(T_i - T_{i-1}) \quad (\text{VII-6})$$

where the subscripts i and $i-1$ indicate quantities at times t_i and t_{i-1} , respectively.

7.2.2. Pseudo-Elastic Slab Analysis

A pseudo-elastic slab analysis may be evaluated to satisfy conditions (VII-2) by inserting the factor $1/[1-\nu(T,t)]$ within the integral sign of Equation (VII-3). As mentioned in Section 6.4 of CHAPTER VI, with the exception of results reported by Monismith et al. (1962) and Sayegh (1967), there is little published information defining the time and temperature dependence of Poisson's ratio, ν , of asphaltic concrete paving mixtures. The approximate pseudo-elastic slab stress was therefore evaluated by assuming Poisson's ratio to be a constant and equal to 0.30. The stress obtained from Equation (VII-4) was therefore simply multiplied by the factor $1/(1-\nu)$ to obtain an approximate pseudo-elastic slab stress.

7.2.3. Viscoelastic Slab Analysis

Humphreys and Martin (1963) proposed a method of determining thermal stresses in a slab with temperature dependent viscoelastic properties. Using the time-temperature equivalence hypothesis of a thermorheologically simple material described in Section 6.3 of CHAPTER VI, these authors expressed deviatoric and hydrostatic stresses (s_{ij} and σ) in terms of the deviatoric and volumetric strains (e_{ij} and ϵ) by the following relationships

$$s_{ij} = \int_{-\infty}^t G_1(\xi - \xi') \frac{\partial}{\partial t'} [e_{ij}(t')] dt' \quad (\text{VII-7})$$

$$\sigma(t) = \int_{-\infty}^t G_2(\xi - \xi') \frac{\partial}{\partial t'} [\epsilon(t') - 3 \alpha_0 \theta(t')] dt' \quad (\text{VII-8})$$

where ξ is the reduced time introduced in the discussion of material characterization in Section 6.3 of CHAPTER VI, G_1 and G_2 are deviatoric and volumetric relaxation moduli and θ is a pseudo-temperature defined as

$$\theta = \frac{1}{\alpha_0} \int_{T(t_0)}^{T(t)} \alpha_0(T') dT' \quad (\text{VII-9})$$

Assuming the dilatational response to stress remains elastic, Humphreys and Martin (1963) presented a numerical technique for evaluating an effective modulus of a slab, $R(\xi)$, from stiffness modulus-reduced time relationships such as those presented in CHAPTER VI. For a constant

coefficient of thermal expansion, $\alpha(T') = \alpha_0$, Equations (VII-7), (VII-8) and (VII-9) yield

$$\sigma_x = -3\alpha_0 \int_0^t R[\xi - \xi'] dT(t') \quad (\text{VII-10})$$

Monismith et al. (1965) used the trapezoidal rule to evaluate Equation (VII-10) numerically, according to the expression

$$\sigma_x(t) = -\frac{3\alpha_0}{2} \sum_{i=1}^N [R(\xi - \xi_i) + R(\xi - \xi_{i-1})](T_i - T_{i-1}) \quad (\text{VII-11})$$

where N is the number of time steps from 0 to t . Equation (VII-11) is the equation used in the present study to compute viscoelastic slab stresses.

7.2.4. Viscoelastic Beam Analysis

The stresses in a viscoelastic beam are conceptually simpler than those in a slab and follow directly from the superposition principle once the time-temperature equivalency hypothesis has been introduced. Thus, for a constant α_0 , we may write

$$\sigma_x(t) = -\alpha_0 \int_{t_0}^t S(\xi - \xi') dT(t') \quad (\text{VII-12})$$

which, when evaluated by the trapezoidal rule, results in

$$\sigma_x(t) = -\frac{\alpha_0}{2} \sum_{i=1}^N [S(\xi - \xi_i) + S(\xi - \xi_{i-1})](T_i - T_{i-1}) \quad (\text{VII-13})$$

7.2.5. Approximate Viscoelastic Slab Analysis

Assuming that Poisson's ratio remains constant an approximate estimate of stresses in a viscoelastic slab may be obtained by multiplying the stresses predicted from Equation (VII-13) by the factor $1/(1-\nu)$. This assumption for ν , which is purely for analytical simplicity, yields results considerably different than those obtained from Equation (VII-11). [Humphreys and Martin (1963).]

7.3. Computation of Thermal Stresses

Thermal stress predictions based on the numerical solutions of the pseudo-elastic and viscoelastic stress equations were obtained by computer operations. Details of the computer programs developed for these analyses are contained in APPENDICES B and C, respectively. The primary input variables for the programs and the numerical integration procedures associated with the analyses are described in the following subsections.

7.3.1. Input Variables for Thermal Stress Computations

The primary inputs to the computer programs include

- 1) a stiffness modulus-reduced time relationship for the asphaltic concrete,
- 2) the corresponding shift factor-temperature relationship,
- 3) a temperature field,
- 4) a coefficient of thermal expansion, and
- 5) Poisson's ratio, for slab analyses.

The pavement test sections included in the present study have been described in Section 6.2 of CHAPTER VI. Derived stiffness modulus-reduced time relationships and shift factor-temperature relationships of asphaltic concretes associated with these test sections are shown in FIGURES VI-3 to VI-9 of the same chapter.

For computer operations, stiffness values are specified at small increments of reduced time and a linear relationship is assumed between the logarithm of stiffness and the logarithm of reduced time. Similarly, shift factors, a_T , are specified at small temperature increments and a linear relationship assumed between the logarithm of a_T and the input temperatures.

For Structure A of the Alberta test project monitored temperatures during the first winter of service were used for stress computations while during the third winter, the winter of 1968-69, stresses were computed using a temperature history predicted by means of the analytical model described in CHAPTER V. For Structures B, C and D, the temperature histories available for stress computations were those transcribed at 2 hour intervals from the continuously monitored field temperatures of the Manitoba test project.

The results of a number of investigations related to defining the coefficient of thermal expansion of asphaltic concrete have been reviewed in Section 3.3.3 of CHAPTER III. In the present study the coefficient of thermal expansion of all the asphaltic concrete paving mixtures was assumed temperature independent and equal to 1.5×10^{-5} per degree Fahrenheit. For slab analyses, Poisson's ratio of the asphaltic

concretes was assumed constant and equal to a value of 0.30.

7.3.2. Numerical Integration for Pseudo-Elastic Analyses

One of the difficulties in applying pseudo-elastic analyses based on the Hills and Brien approach of 1966 is that the predicted stress is dependent on the time interval used in the numerical evaluation. A comparison of stresses computed by Equations (VII-4) and (VII-5) for 15 minute and 2 hour intervals using the characterizing stiffness properties of the low viscosity 150-200 penetration grade asphalt pavement of the Manitoba test project is shown in FIGURE VII-2. The maximum computed stress using the 15 minute time increment is approximately 50 per cent greater than that computed using the 2 hour time increment. This difference is primarily due to the change of stiffness with loading time, since at a given temperature the stiffness of an asphaltic concrete increases with decreasing loading times. The previously mentioned methods of McLeod (1969) and Fromm and Phang (1971) eliminate the dependency on the time interval of numerical integration by specifying loading times. However, the results of the stress computations are directly influenced by the loading time specified. For these pseudo-elastic analyses stresses were computed using a 2 hour time increment.

In addition to the dependency of the pseudo-elastic stresses on assumed loading time, such methods do not make allowance for the relaxation of stresses subsequent to the time interval in which stresses are computed. Although thermal stresses within pavements are unknown, the assumption of a constant stress over extended time periods is not

compatible with the known viscous behavior of bituminous materials. A viscoelastic model of material characteristics would therefore be expected to produce more reliable results.

7.3.3. Numerical Integration for Viscoelastic Analyses

The modulus function, $R(\xi)$, appearing in Equations (VII-10) and (VII-11) was evaluated numerically, for the asphalt concretes under consideration, by the method proposed by Humphreys and Martin (1963). Details of a computer program developed for this purpose are contained in APPENDIX D. A study of convergence of stress results with different time increments of numerical integration and the computation times on an IBM-360 computer are summarized in TABLE VII-1. The stresses shown are those predicted using the viscoelastic beam analysis and the material properties of the low viscosity 150-200 asphalt pavement incorporated in the Manitoba test project and subjected to the temperature history shown in FIGURE VII-2. Since the viscoelastic stress equations require numerical computation over the entire previous temperature history to which the asphaltic concrete is subjected, long computer runs and large storage requirements are involved if stresses are to be predicted over extended periods of time. Because the most recent temperature history is the most significant for stress evaluation, the following scheme of variable time increments was adopted:

- a) For times up to (t-24) hours a time increment of 2 hours was employed.
- b) For the following 22 hours a time increment of 15 minutes was employed.

- c) For the 2 hours immediately prior to t , a time increment of 5 minutes was employed.

This scheme, illustrated in FIGURE VII-3, made it reasonably economical to evaluate stresses over extended periods of time and, as shown in TABLE VII-1, the resulting accuracy is comparable to that for a constant 15 minute time increment. Details of the computer program which incorporates these variable time increments are presented in APPENDIX C, while a similar program, but one in which a constant time increment of numerical integration may be specified is contained in APPENDIX E.

It should be noted that further economy in computing time could be obtained by deriving closed form expressions for the characterizing properties of the asphalt concretes.

7.4. Computed Stresses and a Cracking Criterion

Stresses at 1/2 inch depth intervals throughout each of the asphaltic concrete surfaces included in the present study were computed by each of Equations (VII-6), (VII-11) and (VII-13). Stresses for the approximate slab analyses were determined by multiplying the beam results by $1/(1-\nu)$, where, as previously mentioned, Poisson's ratio was assumed equal to 0.30.

For all pseudo-elastic analyses stresses were computed using a 2 hour time increment, a time increment corresponding to the time interval of temperature input. Viscoelastic analyses were evaluated using the combination of 120, 15 and 5 minute increments previously described.

The analyses were initiated in late autumn or early winter when the temperature data indicated a uniform temperature of 30 F throughout the pavement surfaces, at which time the stress was assumed equal to zero.

Thermally induced stresses within the low viscosity 150-200 asphalt pavement of Structure D, for the period December 30, 1967 to January 4, 1968, computed by the viscoelastic beam analysis, are shown in FIGURE VII-4. It is apparent that the maximum tensile stress occurs at or near the upper surface and that a relatively high stress gradient exists during periods of maximum stress. Since this stress gradient is typical, the stress at the 1/2 inch depth was adopted as a measure of the severity of the stress condition to which the asphaltic concretes were subjected.

The computed stresses at the 1/2 inch depth resulting from the pseudo-elastic beam, viscoelastic slab and viscoelastic beam analyses are shown in FIGURES VII-5 to VII-14, for the initial time periods of critical stress within asphalt pavement surfaces of the Manitoba test project. In addition, the fracture strength for the corresponding temperature, obtained from FIGURE VI-15 of CHAPTER VI, is also shown on these figures. Similar stress-time plots were determined for the asphaltic concretes incorporated in the Alberta test project. FIGURES VII-15, VII-16 and VII-17, show stresses computed at the 1/2 inch depth of the three Alberta test sections. The stresses shown are those computed using the pseudo-elastic beam analysis together with the predicted third winter of service temperature history.

For the purpose of comparing times of predicted and observed cracking the following criterion is postulated. Cracking is assumed to occur when the computed stress at the 1/2 inch depth equals or exceeds the fracture strength of the asphaltic concrete for the corresponding temperature. According to this criterion the predicted time of initial cracking of the asphaltic concretes may be obtained for each of the stress analyses by locating the first point of intersection of the fracture strengths with the computed stresses on the stress-time plots. It is also postulated that the degree of cracking is related to the amount by which the computed stresses exceed the fracture strength.

7.5. Comparison of Observed and Predicted Low Temperature Performance

At the Manitoba test site crack detection circuits were used in an attempt to define initial times of fracture. Details of these circuits have been described by Deme and Fisher (1968). With the exception of SC-5 test sections and the asphaltic concrete pavement of Structure D which incorporated the high viscosity asphalt, crack detection circuits were included in all surfaces of the ten pavement sections under consideration. Unfortunately, the circuits did not perform entirely satisfactorily since, in some sections, visual crack surveys revealed cracking prior to the time of cracking indicated by the circuits. In the following comparisons initial cracking of the pavement surfaces was considered to have occurred when either the crack sensors indicated cracking or cracks were sighted visually, whichever came first.

During the first two winters that the Alberta test project was in service continuity circuits, consisting of a high conductivity silver base paint and placed in a longitudinal saw cut on the paved shoulder, enabled temperature conditions conducive to thermal fracture of the pavement sections to be defined. Details of these circuits have been described by Shields et al. (1969).

7.5.1. Manitoba Test Sections

A tabulation of the times in each day at which computed stresses intersect the fracture strengths of the asphaltic concretes included in the Manitoba test project is given in TABLES VII-2 and VII-3. A summary of the results obtained from the crack sensors and visual surveys, reported by Deme and Fisher (1968) and Young et al. (1969) is also included in TABLES VII-2 and VII-3. The following observations can be made on the comparison of predicted and observed behavior shown in these tables.

7.5.1.1. Structure D, Low Viscosity 150-200 Asphalt Pavement

Crack sensors indicated initial cracking at 2300 hours on the 30th day of December, 1967 (23/30/12). The pseudo-elastic slab and approximate viscoelastic slab analyses indicated initial cracking at the same time as that recorded in the field. The viscoelastic slab analysis predicted initial cracking 6 hours earlier while the pseudo-elastic beam analysis predicted fracture 8 hours later. The visco-elastic beam analysis did not predict cracking during this temperature cycle. The plot in FIGURE VII-5 compares the computed stress histories.

All analyses predicted cracking from 4 to 8 hours earlier than that indicated by the crack sensors on the night of January 3-4. Cracking predicted during the intervening time period by all analyses, with the exception of the viscoelastic beam analysis, was not recorded by the crack sensors or observed visually.

7.5.1.2. Structure B, Low Viscosity 300-400 Asphalt Pavement

Crack sensors indicated initial cracking at 2:50/4/1. Again the pseudo-elastic slab and the approximate viscoelastic slab analyses indicated initial cracking within an hour of the recorded initial fracture time. The viscoelastic slab analysis predicted cracking 4 hours earlier while the pseudo-elastic beam analysis effectively predicted cracking 5 hours later. The viscoelastic beam does not predict cracking in this temperature cycle. The computed stress histories for this pavement are shown in FIGURE VII-6. All analyses with the exception of the viscoelastic beam analysis also indicated cracking during the night of January 5, 1968. Such predicted fracture is consistent with the increase in cracking of this test section determined by the January 6, 1968 visual survey, reported by Young et al. (1969).

7.5.1.3. Structure B, Low Viscosity 150-200 Asphalt Pavement

Visual surveys indicated initial cracking had occurred on December 31, 1967. All analyses predicted cracking in the late afternoon and early evening of December 30, 1967. Therefore, there is no incompatibility between the times of predicted and observed initial cracking. As shown in FIGURE VII-7, the computed stresses continued to

exceed the fracture strength on the succeeding days when the majority of cracking was observed.

7.5.1.4. Structure C, Low Viscosity 150-200 Asphalt Pavement

Visual surveys indicated initial cracking occurred on January 1, 1968, while the majority of cracking occurred on the sixth and seventh days of the same month. All analyses, except the viscoelastic beam analysis, predicted initial cracking at sometime during the night of December 30, 1967, one day before cracking was observed. The stress predictions are shown in FIGURE VII-8 and, as observed from TABLE VII-2, all analyses predicted cracking over the time period during which the majority of cracking occurred.

7.5.1.5. Structure B, High Viscosity 150-200 Asphalt Pavement

No fracture was observed in this section of the test project. However, all stress analyses except the viscoelastic beam analysis predicted cracking at sometime during the period January 3 to January 6, 1968. The predicted stress histories are shown in FIGURE VII-9. As shown in this figure and TABLE VII-3, stresses computed using the elastic beam analysis slightly exceeded the average tensile strength of the asphaltic concrete only once during the 1967-68 winter when a near minimum 1/2 inch depth temperature of -36 F occurred.

7.5.1.6. Other Manitoba Test Sections

Results of stress analyses for the five remaining Manitoba pavement test sections under consideration are shown in FIGURES VII-10 to VII-14. In each of these five sections no fracture was predicted.

This result conforms to field observations summarized in TABLE VII-3.

7.5.2. Alberta Test Sections

Crack frequencies within the three pavement sections at the Alberta test site have been presented in TABLE VI-6 of CHAPTER VI. During the first two winters of service the majority of cracking occurred in the pavement section containing Asphalt Supply No. 1, and the temperature and continuity circuit systems revealed that initial cracking occurred at temperatures summarized in TABLE VII-4. During the third winter, such systems were not operative and, therefore, fracture times and temperatures of each pavement section were not recorded.

7.5.2.1. Results of Stress Analyses for First Winter of Service

The results of the stress analyses for the first winter of service indicated no fracture for each of the three test sections. The maximum computed stress, determined by the viscoelastic slab analysis, and associated with the test section containing Asphalt Supply No. 1 was 84 psi. This stress is considerably less than the corresponding measured tensile failure strength of the asphalt concrete shown in FIGURE VI-19 of CHAPTER VI. While this result is not consistent with the observed transverse cracking within this particular test section, the result conforms to field observations associated with the test sections incorporating asphalts obtained from Suppliers 2 and 3.

7.5.2.2. Results of Stress Analyses for Third Winter of Service

During January of the third winter, the winter of 1968-69, an extreme cold period of over 25 days was encountered. During this time

the predicted 1/2 inch depth temperatures at the test site never exceeded 0 F. Although the times of cracking were not recorded, the results of the stress analyses were compatible with observed low temperature performance, since all stress analyses predicted fracture of the test sections. Typical stress-time plots for the three test sections, obtained using the pseudo-elastic beam analysis, are shown in FIGURES VII-15, VII-16 and VII-17. The predicted temperatures of crack initiation of each section are summarized in TABLE VII-4.

7.6. Evaluation of Results

Considering the variability of the properties of asphaltic concrete mixtures and the approximations involved in the study of low temperature pavement behavior, a high degree of accuracy should not be expected of a predictive analyses. Before attempting to draw conclusions from the comparisons of observed and predicted performance the nature of the approximations and assumptions involved are briefly reviewed.

7.6.1. Approximations and Assumptions

(a) Material Characterization: It was assumed that the stiffness of the asphaltic concrete mixtures could be determined by indirect methods. The coefficient of thermal expansion was assumed to be independent of temperature and equal to 1.5×10^{-5} per degree Fahrenheit. For the approximate slab analyses Poisson's ratio was assumed to be 0.30. The fracture strengths of the pavements were assumed to be represented by the strength-temperature relationships

determined from the average of laboratory tests for pavement cores obtained from the test project.

(b) Nature of Loading: It was assumed that pavement cracking was a result of thermally induced stress and that all other loading mechanisms could be neglected. It was also assumed that interaction between the asphaltic concrete and the substructure did not influence thermally induced stresses.

(c) Fracture Criterion: The stress fracture criterion previously described was assumed valid.

In addition to the assumptions outlined above, each method of stress analyses assumes the validity of the corresponding constitutive equation and that the error of the numerical integration procedure is within acceptable limits.

7.6.2. Comparison of Stress Analyses

The suitability of any of the stress analysis procedures, for use with the proposed fracture criterion, may be assessed (a) by comparing times of predicted initial cracking with observed times of initial cracking, and (b) by correlating the time periods, during which subsequent cracking was observed with the time periods in which the predicted stress exceeded the fracture criterion employed. Strictly speaking, the stresses computed after initial cracking cannot be compared directly with the fracture criterion because the assumption that $\epsilon_x = 0$ is no longer valid.

Using the time period correlation method, method (b) above, it appears that the viscoelastic beam analysis underestimates stresses for the fracture criterion employed. (See Structure D, LV 150-200, TABLE VII-2 and FIGURE VII-5; Structure B, LV 300-400, TABLE VII-3 and FIGURE VII-6.)

It also appears that the viscoelastic slab analysis overestimates stresses for the fracture criterion employed. (See Structure B, HV 150-200, TABLE VII-3 and FIGURE VII-9.) The viscoelastic beam and slab analyses therefore appear to yield lower and upper bounds respectively, on computed stresses for the purpose of correlating with observed pavement behavior. The pseudo-elastic beam and approximate viscoelastic slab analyses appear to yield reasonable intermediate values of stresses for correlation purposes. The approximate pseudo-elastic slab analysis yields stresses similar to those of the approximate viscoelastic slab analysis. Since none of these analyses can be rigorously justified on a theoretical basis the author has selected the simplest, namely, the pseudo-elastic beam analysis for a comparison with observed results.

TABLE VII-5 shows a correlation of times of initial predicted fracture, using the pseudo-elastic beam analysis adopted for this study, with the observed cracking of the sixteen different combinations of structure, materials and temperature history incorporated in the study. In fourteen of these different combinations low temperature cracking was predicted at times approximating times of recorded and/or observed fracture. In the author's opinion this correlation is

sufficiently good to allow the low temperature fracture susceptibility of asphaltic concrete pavements to be assessed when subjected to thermal regimes similar to those experienced in Western Canada.

7.7. Summary

Five different methods of stress computation were employed to evaluate thermal stresses in a number of different test sections incorporated in two test projects in Western Canada. Stresses within the particular asphaltic concretes were evaluated using stiffness properties presented in CHAPTER VI. Fracture strength-temperature relationships of asphaltic concrete cores obtained from the test projects were used for predicting times and temperatures of fracture. Observed cracking in the test projects was compared to that predicted by the various stress analyses using a postulated fracture criterion.

To the author's knowledge, these test projects provide, for the first time, detailed records of field temperature data for which field observations of low temperature pavement cracking are also available. Such field data provides a basis on which to realistically assess various stress predictive methods. The correlation obtained between observed and predicted performance appears sufficiently good to indicate that reliable predictive analyses can be developed. The data currently available suggests that, for the present, a suitable pseudo-elastic beam analysis can yield reasonable results.

TABLE VII-1
PREDICTED THERMAL STRESSES IN LV 150/200 ASPHALTIC CONCRETE USING
VISCOELASTIC BEAM ANALYSIS AND VARIOUS TIME INCREMENTS

Time Increment (minutes)	Hour Day	Predicted Thermal Stress (lb per sq in)												Computer Time (seconds)
		2	4	6	8	10	12	14	16	18	20	22	24	
1	1	26.5	96.9	428.3	942.5	1376.2	1534.2	1202.2	622.0	130.5	-24.5	-32.9	-20.9	508
2	1	29.2	101.6	430.6	942.4	1375.4	1529.1	1198.6	618.2	127.3	-28.6	-35.2	-22.1	1100
	2	28.6	100.2	430.4	942.4	1373.8	1528.7	1197.9	612.9	126.5	-30.2	-36.1	-22.9	
15	1	38.0	115.1	439.5	942.1	1370.0	1521.6	1189.2	607.2	115.0	-58.4	-55.4	-33.4	47
	2	31.7	110.4	435.0	937.7	1365.5	1517.1	1184.8	603.0	110.6	-62.6	-58.8	-35.6	
	3	30.1	109.0	433.6	936.3	1364.2	1515.8	1183.5	601.6	109.2	-64.0	-59.9	-36.6	
	4	29.4	108.4	433.0	933.5	1363.5	1515.1	1182.8	601.0	108.5	-64.8	-60.5	-37.1	
120	1	147.0	313.3	648.2	968.5	1343.8	1478.2	1119.5	489.5	-113.1	-435.6	-277.1	-148.0	10
	2	139.1	307.6	642.9	963.2	1338.5	1472.9	1114.2	484.3	-118.3	-440.5	-281.0	-150.6	
	3	137.3	306.0	641.3	961.6	1336.9	1471.3	1112.7	482.7	-119.9	-442.9	-282.3	-151.7	
	4	136.4	305.2	640.6	960.8	1336.1	1470.5	1111.9	481.9	-120.7	-442.7	-283.0	-152.3	
120, 15, 5	1	38.0	115.1	439.5	942.1	1370.0	1521.6	1189.2	607.2	115.0	-58.4	-55.4	-33.4	12
	2	31.7	110.4	434.8	937.5	1365.3	1516.9	1184.6	602.0	110.4	-62.9	-59.1	-35.9	
	3	29.9	108.8	433.3	936.0	1363.8	1514.4	1183.1	601.3	108.9	-64.3	-60.4	-37.0	
	4	29.1	108.0	432.6	935.0	1363.1	1514.7	1182.4	600.6	108.1	-65.1	-61.0	-37.5	

TABLE VII-2
 PREDICTED AND OBSERVED TIMES AND TEMPERATURES OF
 THERMAL FRACTURE OF MANITOBA ASPHALTIC CONCRETE PAVEMENTS
 COMPOSED OF LV 150/200 ASPHALT CEMENT

Structure	Predicted Times and Temperatures of Thermal Fracture										Times and Temperatures of Observed Transverse Cracking (c)
	Pseudo-Elastic Beam		Approximate Pseudo-Elastic Slab		Viscoelastic Beam		Approximate Viscoelastic Slab		Viscoelastic Slab		
	Time (a)	Temp. (b)	Time	Temp.	Time	Temp.	Time	Temp.	Time	Temp.	
B	20/30/12	-23	18/30/12	-20	19/30/12	-22	18/30/12	-21	17/30/12	-18	Visual surveys indicated initial cracking December 31, 1967 and majority of cracking on this date and January 1, 3, 4, 5 and 7.
	19/31/12	-23	17/31/12	-20	19/31/12	-23	17/31/12	-20	17/31/12	-20	
	24/1/1	-23	19/1/1	-20	3/2/1	-25	18/1/1	-19	17/1/1	-17	
	20/2/1	-24	17/2/1	-19	20/2/1	-24	17/2/1	-19	17/2/1	-19	
	7/3/1	-23	19/3/1	-21	20/3/1	-23	8/3/1	-24	7/3/1	-22	
	20/3/1	-23	16/4/1	-20	18/4/1	-23	18/3/1	-19	17/3/1	-17	
	17/4/1	-22	15/5/1	-21	8/5/1	-26	17/4/1	-22	15/4/1	-19	
	6/5/1	-23	17/7/1	-20	17/5/1	-26	7/5/1	-24	5/5/1	-22	
	16/5/1	-23			19/6/1	-27	16/5/1	-23	15/5/1	-21	
	17/6/1	-24			19/7/1	-23	18/6/1	-25	17/6/1	-24	
18/7/1	-24					17/7/1	-20	16/7/1	-23		
C	5/31/12	-23	23/30/12	-20	22/3/1	-22	24/30/12	-21	18/30/12	-16	Visual surveys indicated initial cracking on January 1, 1968 and majority of cracking January 6 and 7.
	23/3/1	-24	4/2/1	-21	18/5/1	-24	4/2/1	-21	18/31/12	-17	
	18/5/1	-24	21/3/1	-21	18/7/1	-22	19/3/1	-19	2/2/1	-19	
	24/6/1	-24	8/5/1	-21			17/5/1	-22	21/2/1	-18	
	19/7/1	-24	17/5/1	-22			17/6/1	-19	19/3/1	-19	
			18/6/1	-21			17/7/1	-20	18/4/1	-20	
			17/7/1	-20					8/5/1	-21	
									16/5/1	-19	
									17/6/1	-19	
									17/7/1	-20	
D	7/31/12	-24	23/30/12	-20	23/3/1	-23	23/30/12	-20	17/30/12	-16	Crack sensors indicated initial cracking 23/30/12 @ -20F and subsequent cracking 2:45/31/12 @ -22F 1:30/4/1 @ -25F
	8/2/1	-23	5/2/1	-22			7/2/1	-24	18/31/12	-17	
	23/3/1	-23	21/3/1	-20			21/3/1	-20	1/2/1	-19	
									21/2/1	-19	
									19/3/1	-17	
									18/4/1	-19	

(a) hour/day/month. (b) degrees Fahrenheit. (c) after Dene and Fisher (1968).

TABLE VII-3
PREDICTED AND OBSERVED TIMES AND TEMPERATURES OF
THERMAL FRACTURE OF ASPHALTIC CONCRETE PAVEMENTS
COMPOSED OF LV 300/400, HV 150/200 AND SC-5 ASPHALTS

Asphalt Binder (Structure)	Predicted Times and Temperature of Thermal Fracture										Times and Temperatures of Observed Transverse Cracking (c)
	Pseudo-Elastic Beam		Approximate Pseudo-Elastic Slab		Viscoelastic Beam		Approximate Viscoelastic Slab		Viscoelastic Slab		
	Time (a)	Temp. (b)	Time	Temp.	Time	Temp.	Time	Temp.	Time	Temp.	
LV 300-400 (B)	8/4/1 5/6/1	-35 -35	2/4/1 19/5/1 6/7/1	-32 -30 -32	N.F.P. (d)		3/4/1 5/6/1	-32 -35	23/3/1 19/5/1	-30 -30	Crack sensors indi- cated initial cracking 2:50/4/1 @ -32F 6:40/4/1 @ -34F and majority of cracking occurred on this date.
LV 300-400 (C)	N.F.P.		N.F.P.		N.F.P.		N.F.P.		N.F.P.		No fracture
HV 150-200 (B)	6/6/1	-36	1/4/1 20/5/1 5/7/1	-30 -31 -31	N.F.P.		4/4/1 6/6/1	-33 -36	22/3/1 20/5/1	-29 -30	No fracture
HV 150-200 (C)	N.F.P.		N.F.P.		N.F.P.		N.F.P.		N.F.P.		No fracture
HV 150-200 (D)	N.F.P.		N.F.P.		N.F.P.		N.F.P.		N.F.P.		No fracture
SC-5 (B)	N.F.P.		N.F.P.		N.F.P.		N.F.P.		N.F.P.		No fracture
SC-5 (C)	N.F.P.		N.F.P.		N.F.P.		N.F.P.		N.F.P.		No fracture

(a) hour/day/month.
(b) degrees Fahrenheit.
(c) after Dene and Fisher (1968).
(d) No Fracture Predicted.

TABLE VII-4
TEMPERATURES DURING CRACK INITIATION
AT ALBERTA TEST PROJECT

Depth (inches)	First Winter (Recorded) (F)	Third Winter (Predicted) (F)		
1/2	-4.5	-19.0	-27.0	-19.0
2	-2.5	-15.0	-25.3	-15.0
6	+4.0	- 6.2	-17.0	- 6.2
Supplier	1	1	2	3

TABLE VII-5
CORRELATION OF PREDICTED AND OBSERVED INITIAL TIMES OF
FRACTURE USING THE PSEUDO-ELASTIC BEAM ANALYSIS

Structure	Asphalt	Correlation
D	LV 150/200	Predicted fracture 8 hours after that recorded by crack sensors.
B	LV 300/400	Predicted fracture 5 hours after that recorded by crack sensors.
B	LV 150/200	Predicted fracture the evening of December 30, 1967 - visual surveys indicated cracking the following day.
C	LV 150/200	Predicted fracture the morning of December 31, 1967 - visual surveys indicated cracking the following day.
A (at 34 months) A (at 34 months) A (at 34 months)	Asphalt Supply No. 1 Asphalt Supply No. 2 Asphalt Supply No. 3	Fracture predicted and observed, however time of fracture was not recorded.
C C C B D A (at construction) A (at construction)	HV 150/200 LV 300/400 SC-5 SC-5 HV 150/200 Asphalt Supply No. 2 Asphalt Supply No. 3	No fracture predicted or observed.
B	HV 150/200	Fracture predicted near seasonal minimum temperatures - no cracking observed.
A (at construction)	Asphalt Supply No. 1	No fracture predicted - cracking observed.

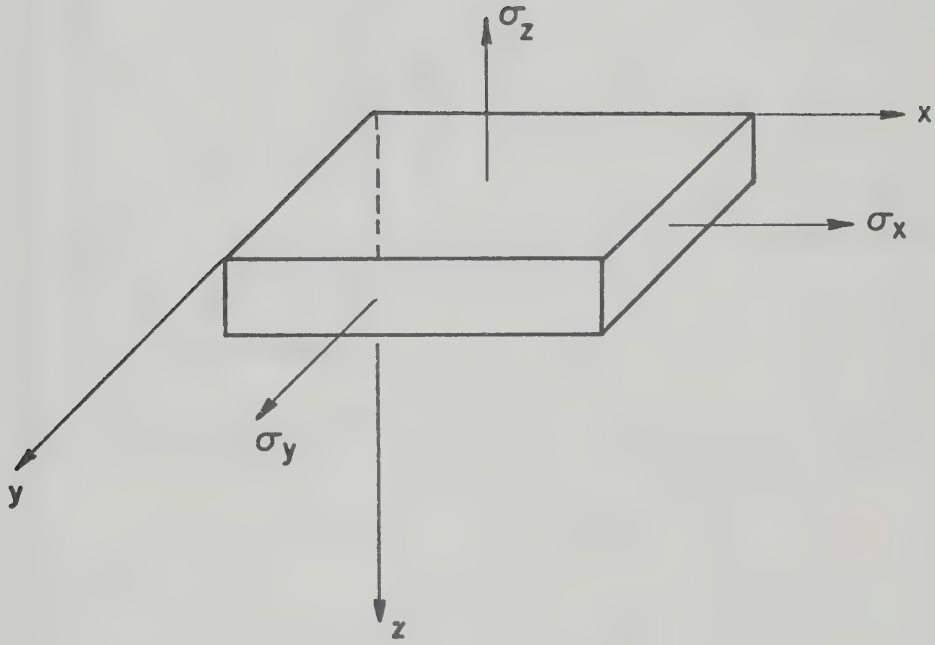


FIGURE VII-1 PAVEMENT ELEMENT.

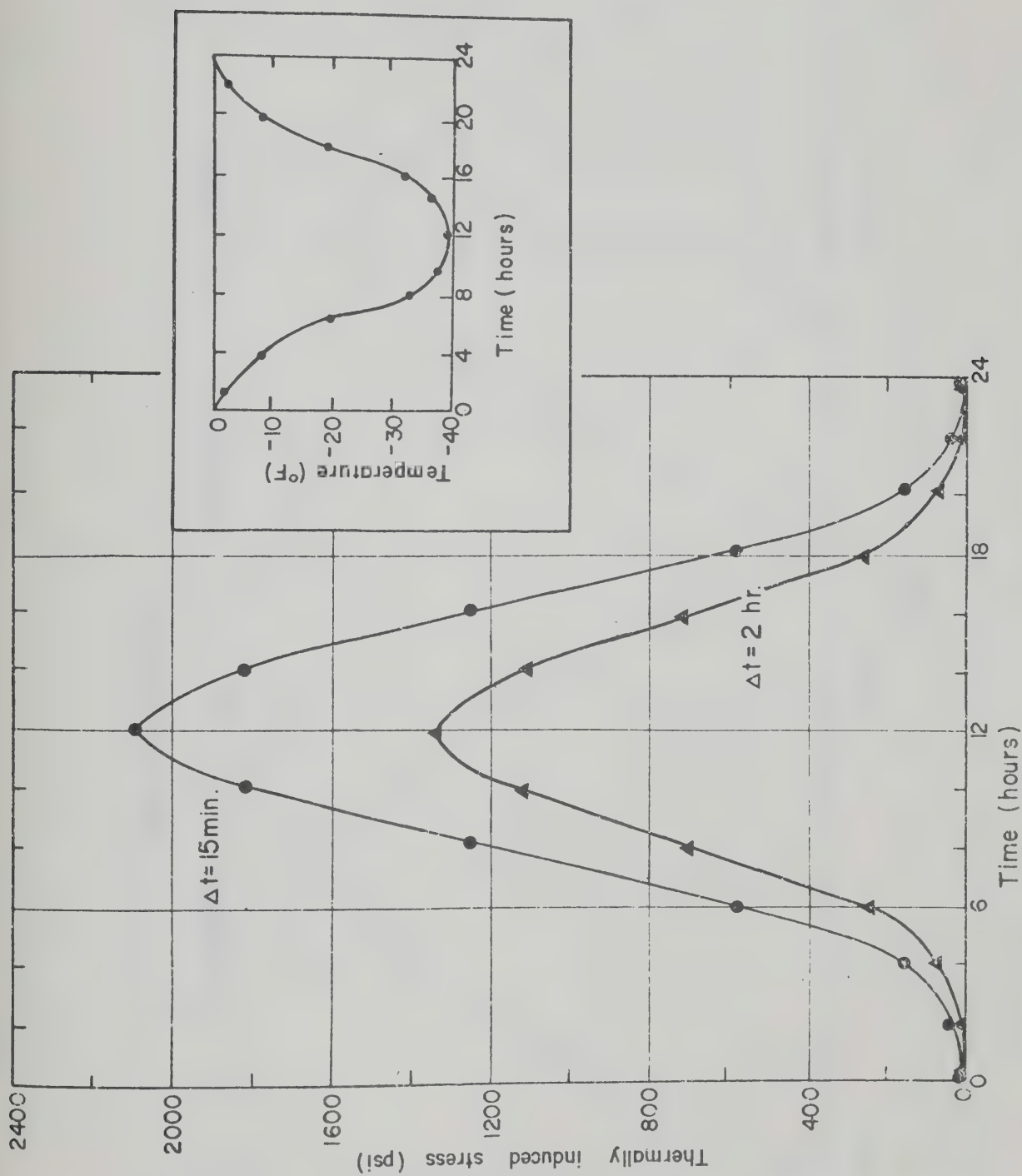


FIGURE VII-2 INFLUENCE OF TIME INCREMENT ON CALCULATED THERMALLY INDUCED STRESSES IN LV 150-200 ASPHALTIC CONCRETE USING ELASTIC BEAM ANALYSIS.

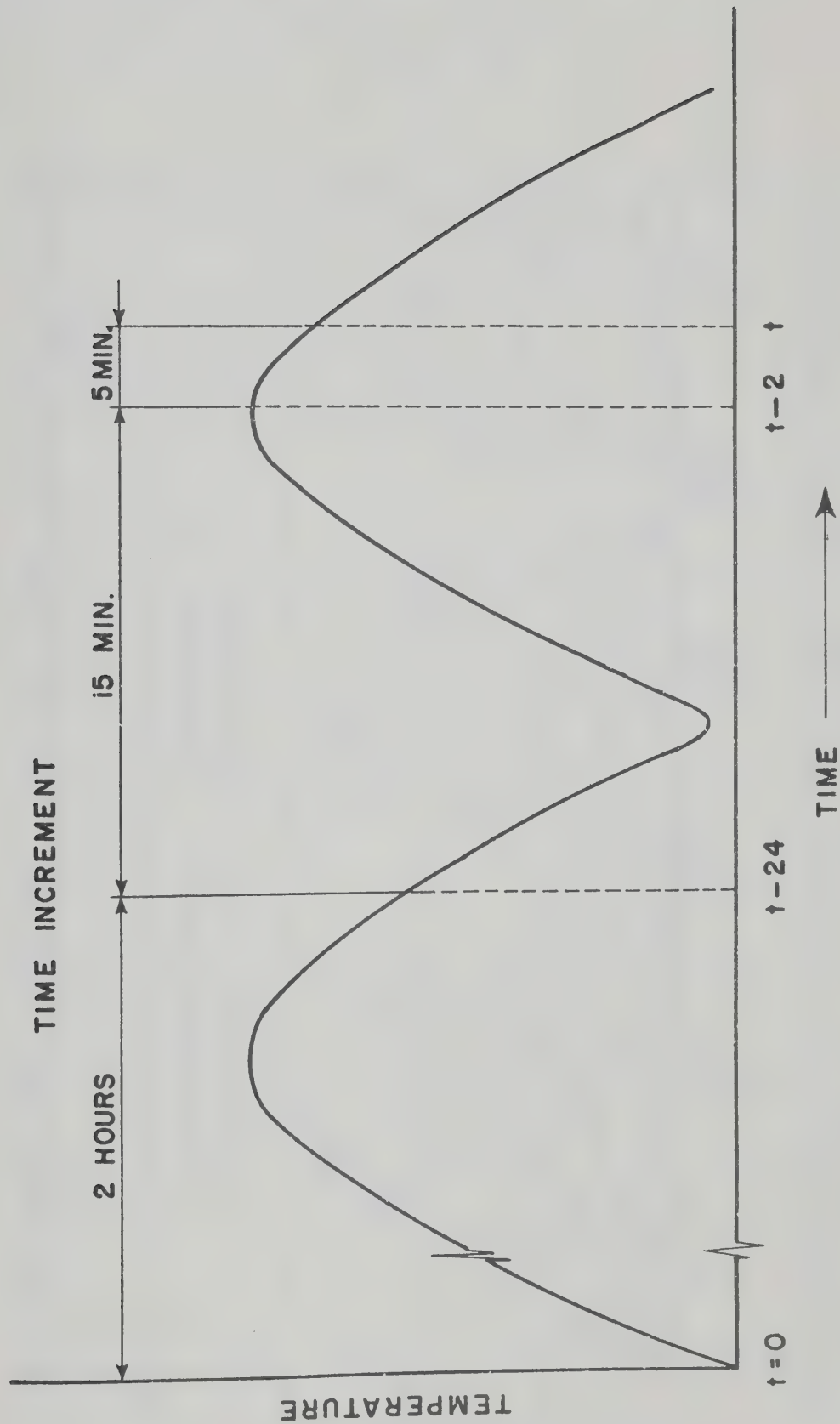


FIGURE. VII-3 . NUMERICAL INTEGRATION PROCEDURE FOR VISCOELASTIC ANALYSES.

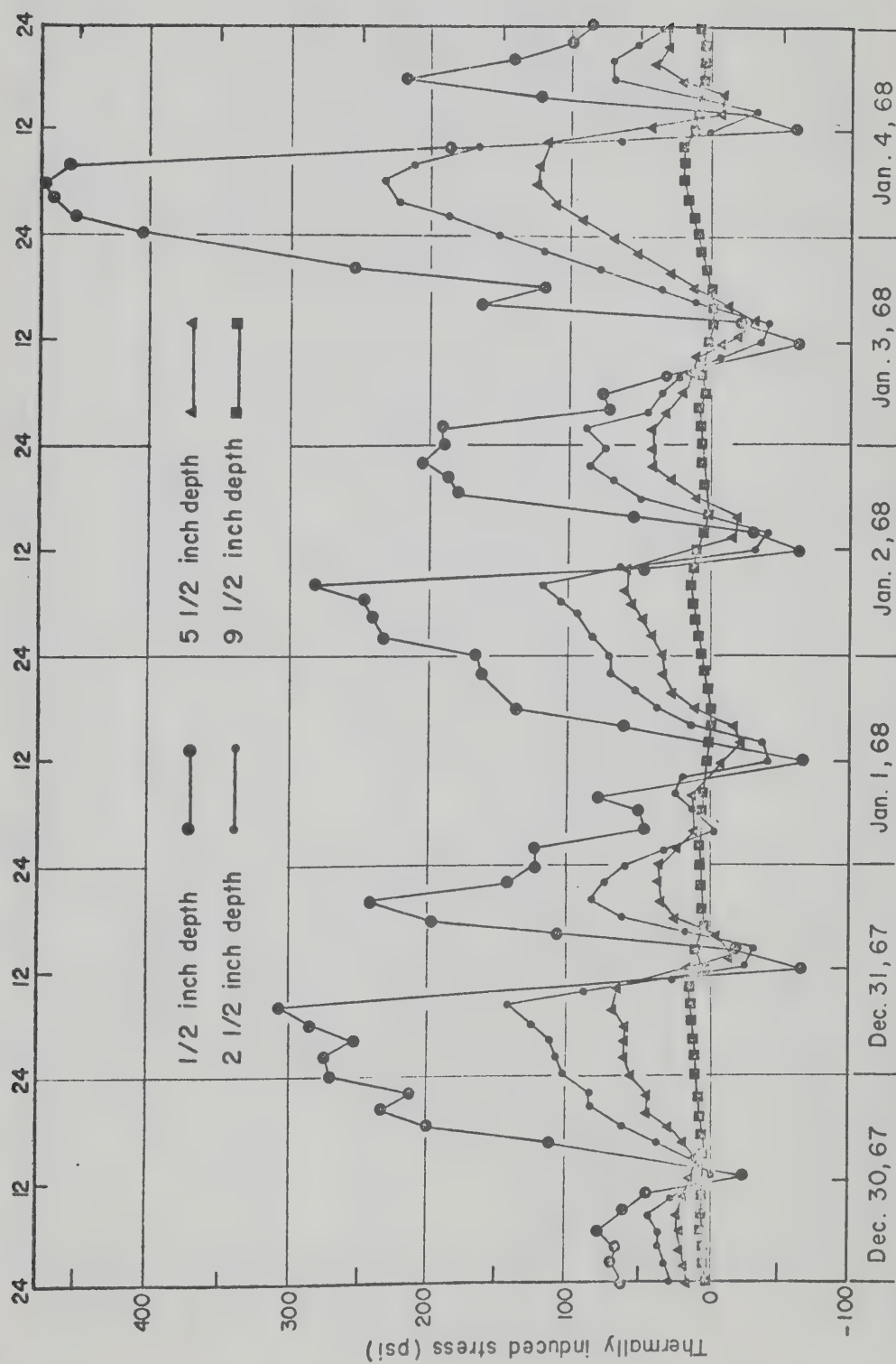


FIGURE VII-4 THERMALLY INDUCED STRESS AT VARIOUS DEPTHS IN THE LV 150-200 ASPHALTIC CONCRETE PAVEMENT SURFACE OF STRUCTURED USING VISCOELASTIC BEAM ANALYSIS.

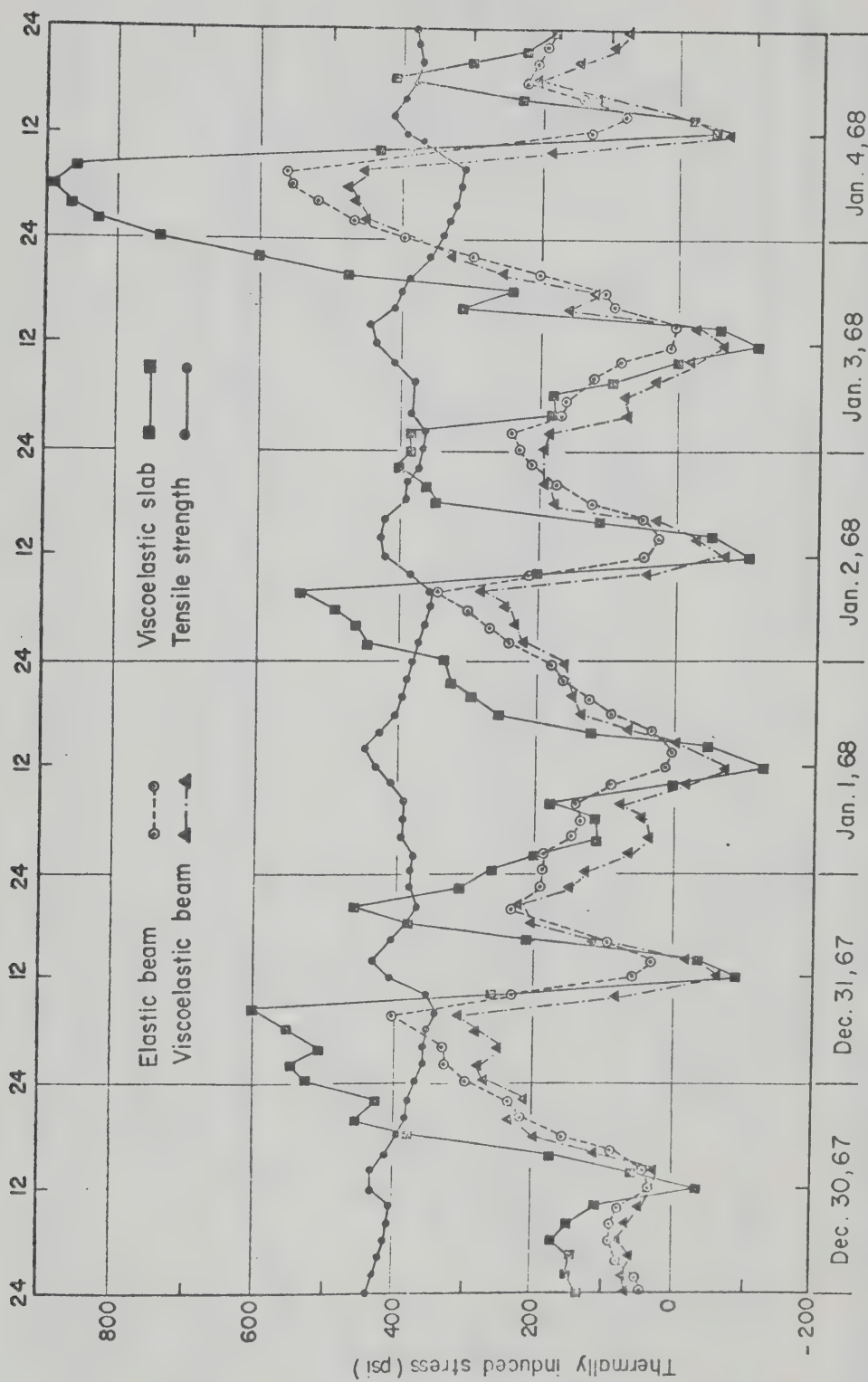


FIGURE VII-5 THERMALLY INDUCED STRESS AT 1/2 INCH DEPTH OF THE LV 150-200 ASPHALTIC CONCRETE PAVEMENT SURFACE OF STRUCTURE D.

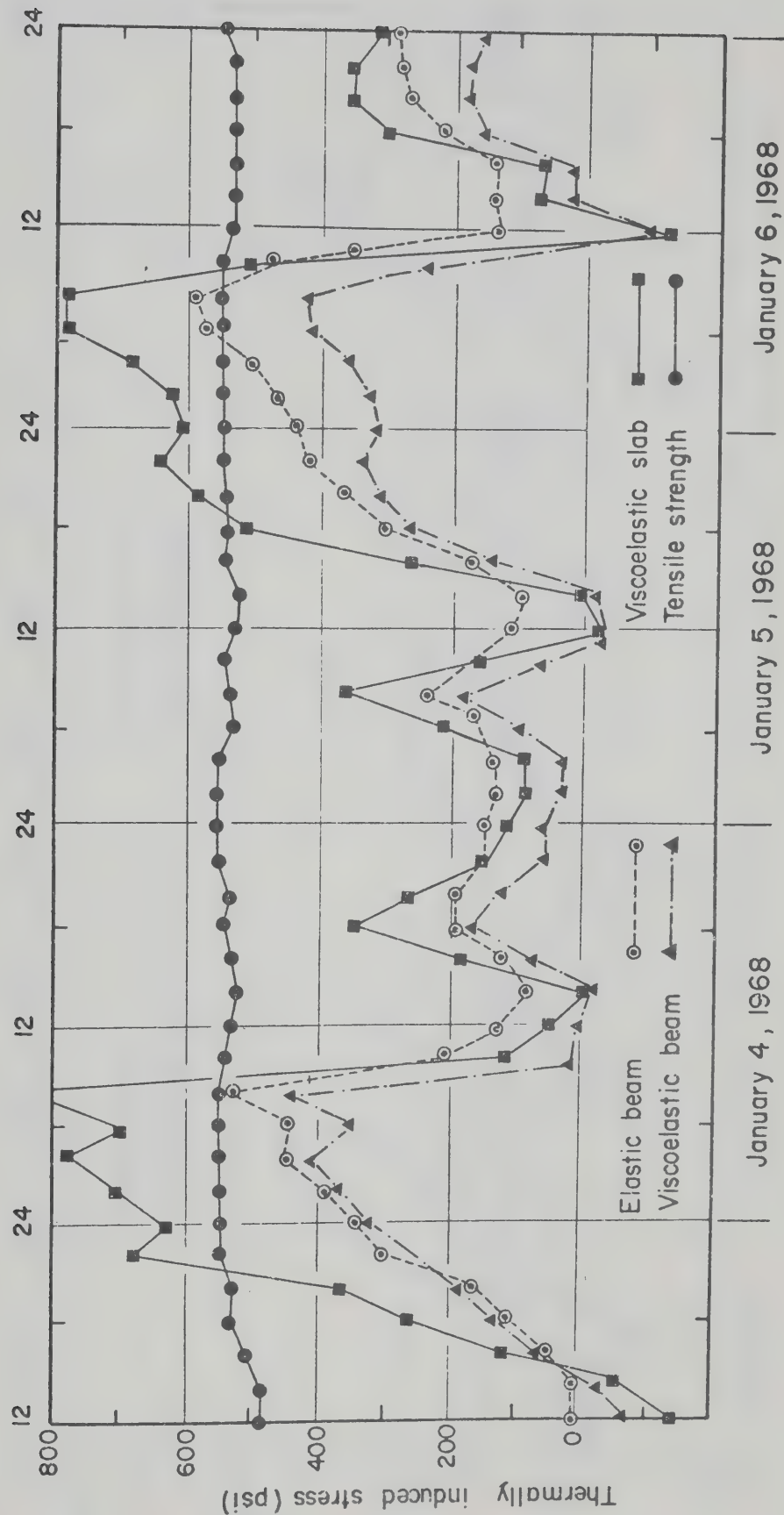


FIGURE VII-6 THERMALLY INDUCED STRESS AT 1/2 INCH DEPTH OF THE LV 300-400 ASPHALTIC CONCRETE PAVEMENT SURFACE OF STRUCTURE B.

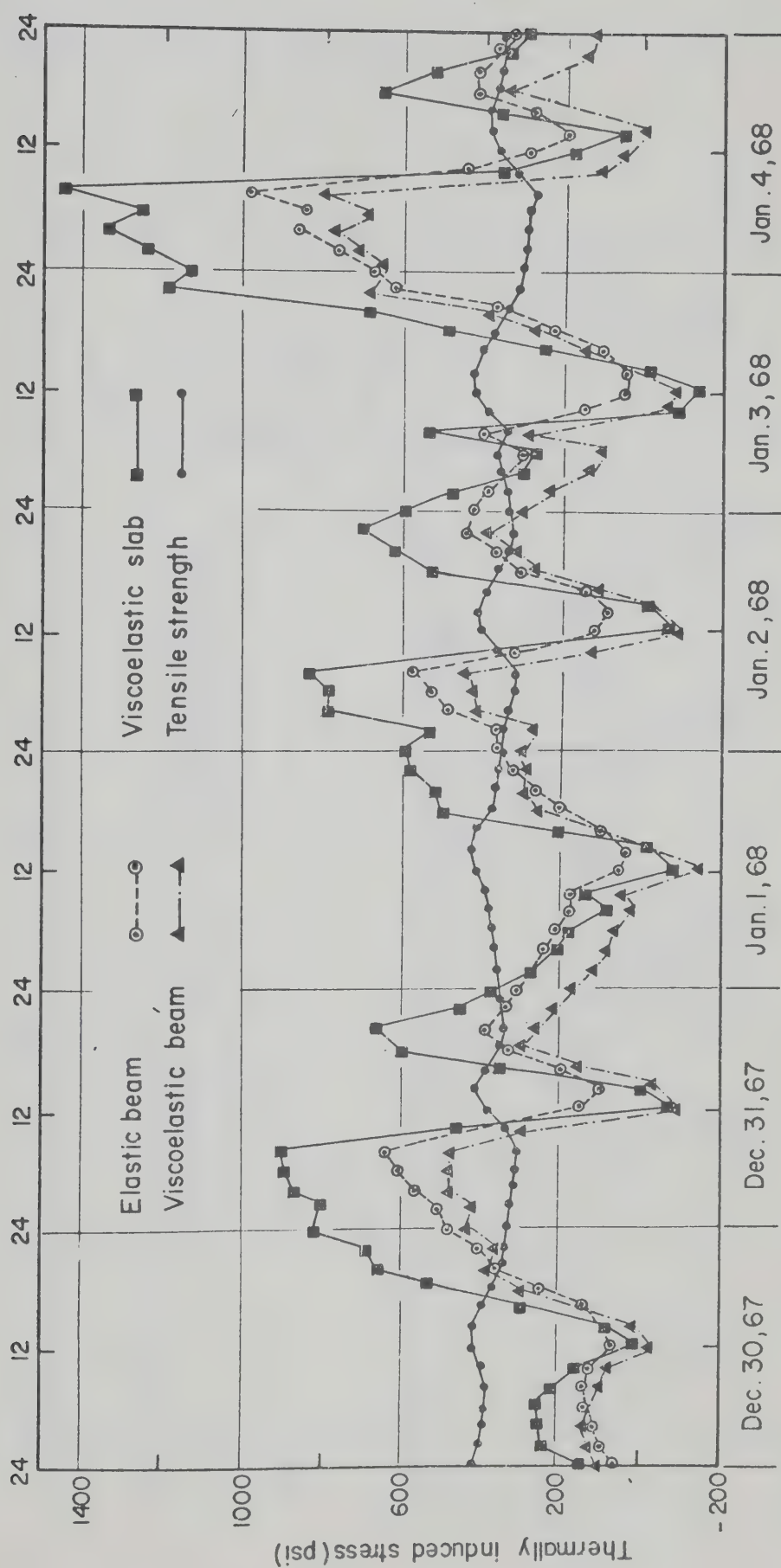


FIGURE VII-7 THERMALLY INDUCED STRESS AT 1/2 INCH DEPTH OF THE LV 150-200 ASPHALTIC CONCRETE PAVEMENT SURFACE OF STRUCTURE B .

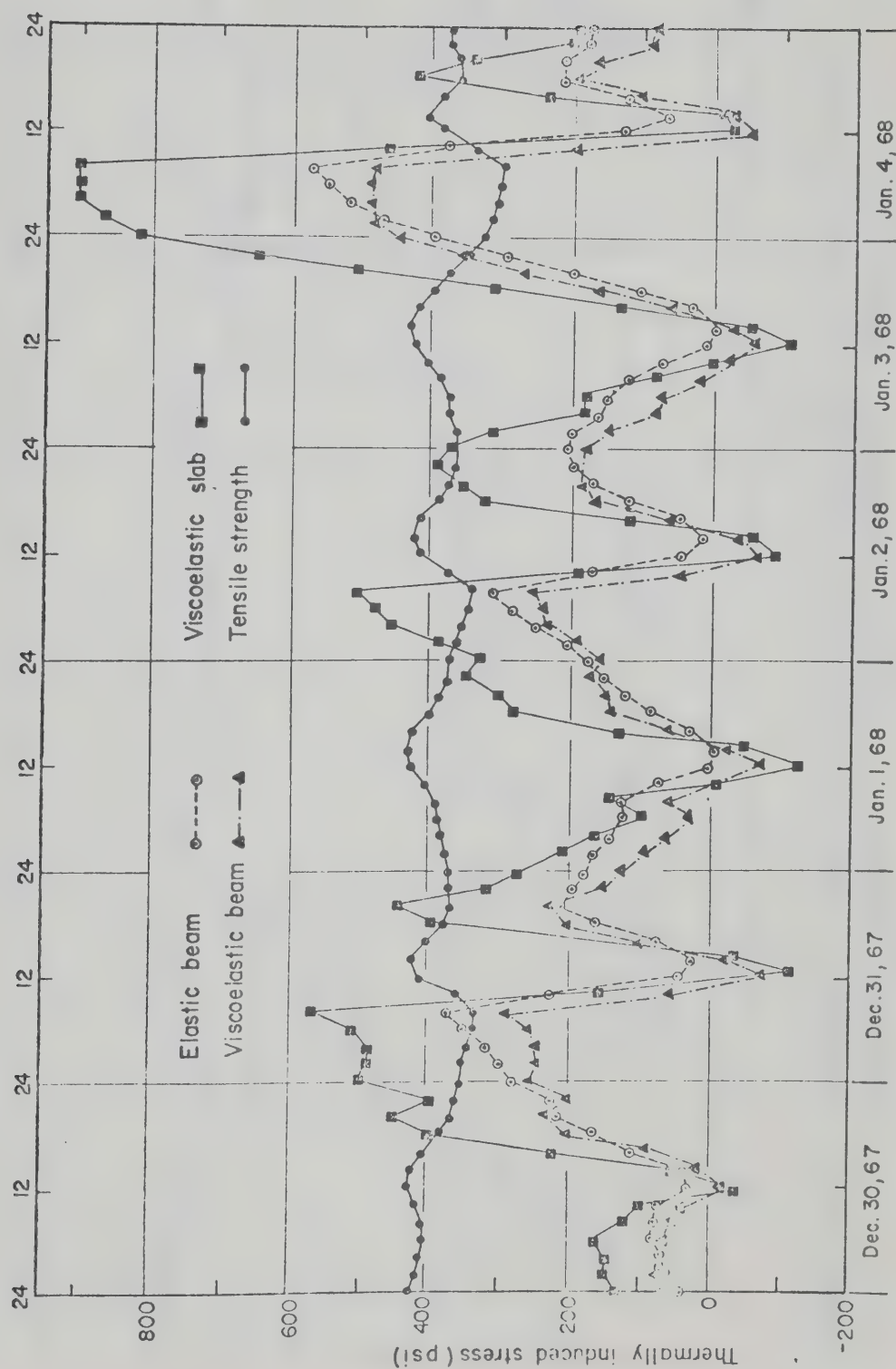


FIGURE VII-8 THERMALLY INDUCED STRESS AT 1/2 INCH DEPTH OF THE LV 150 - 200 ASPHALTIC CONCRETE PAVEMENT SURFACE OF STRUCTURE C.

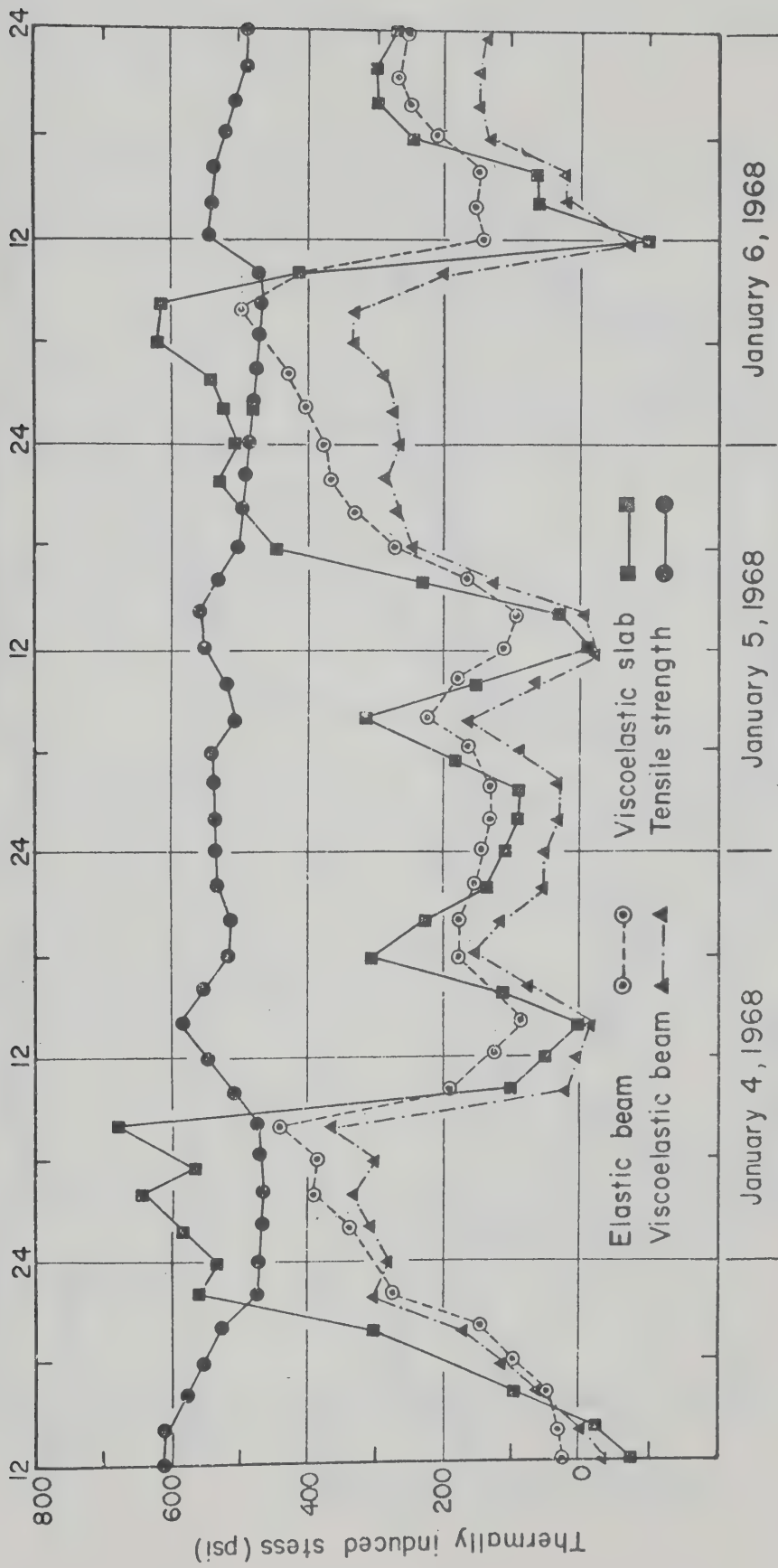


FIGURE VII-9 THERMALLY INDUCED STRESS AT 1/2 INCH DEPTH OF THE HV 150-200 ASPHALTIC CONCRETE PAVEMENT SURFACE OF STRUCTURE B .

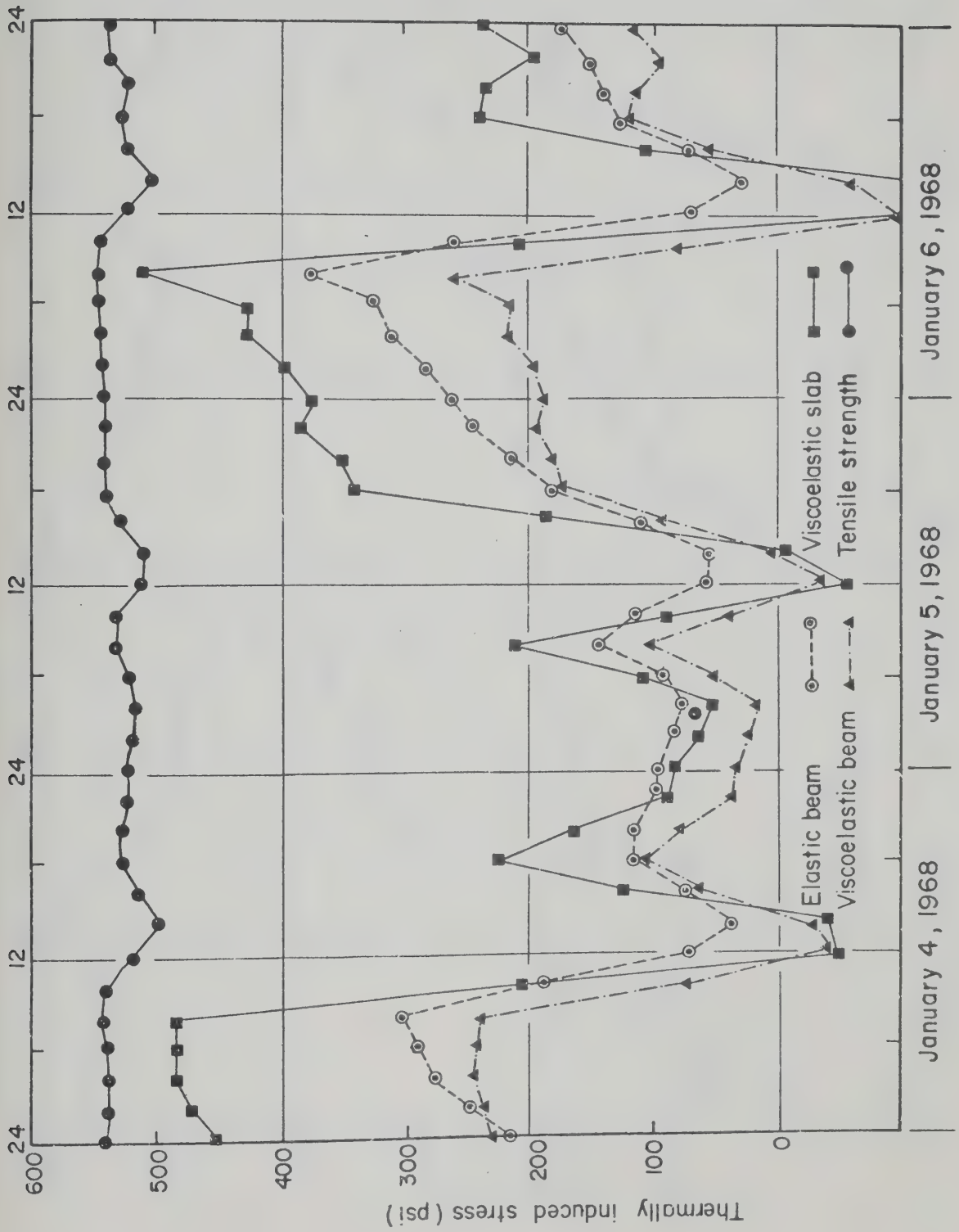


FIGURE VII-10 THERMALLY INDUCED STRESS AT 1/2 INCH DEPTH OF THE LV 300-400 ASPHALTIC CONCRETE PAVEMENT SURFACE OF STRUCTURE C.

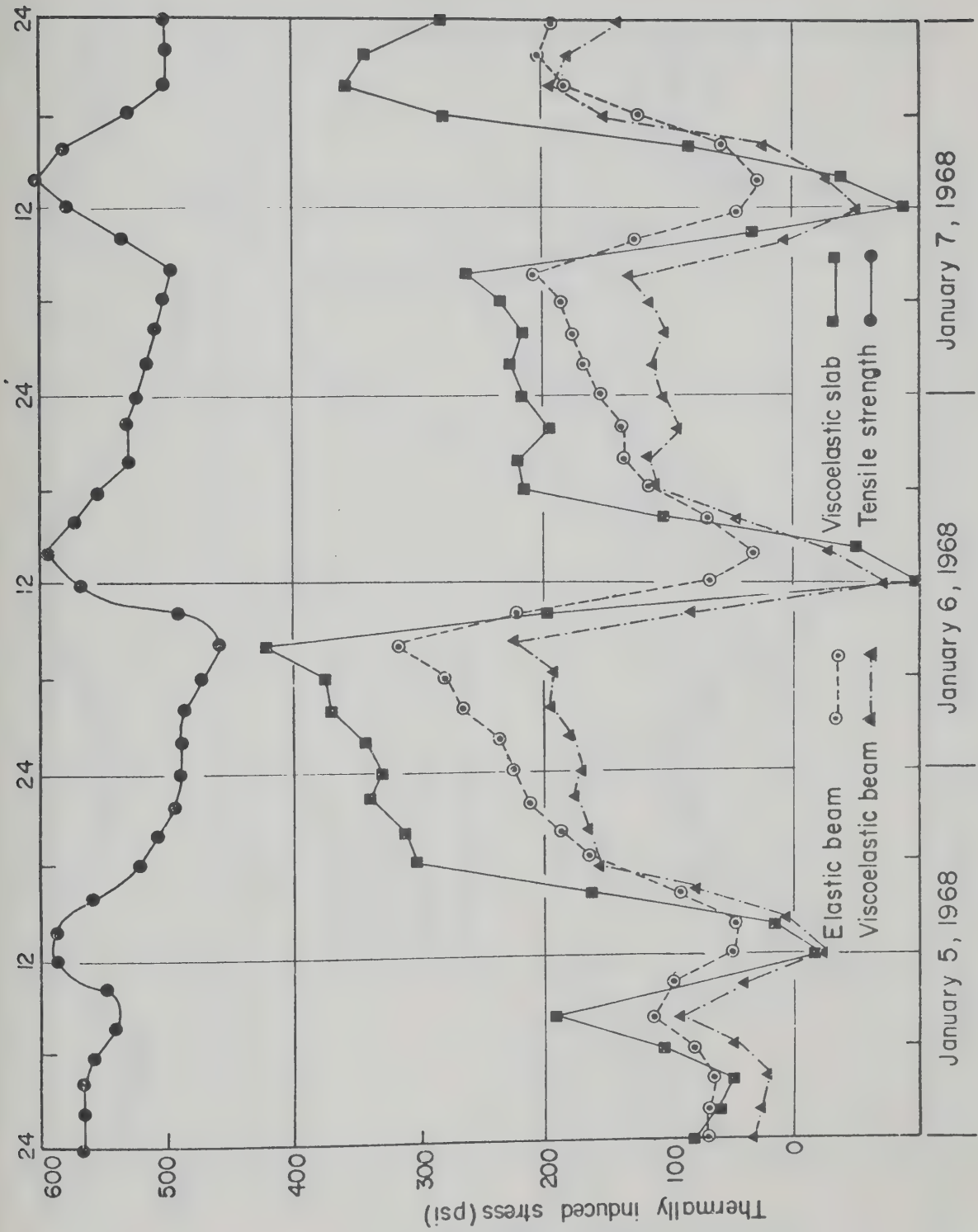


FIGURE VII-11 THERMALLY INDUCED STRESS AT THE 1/2 INCH DEPTH OF THE HV 150-200 ASPHALTIC CONCRETE PAVEMENT SURFACE OF STRUCTURE C.

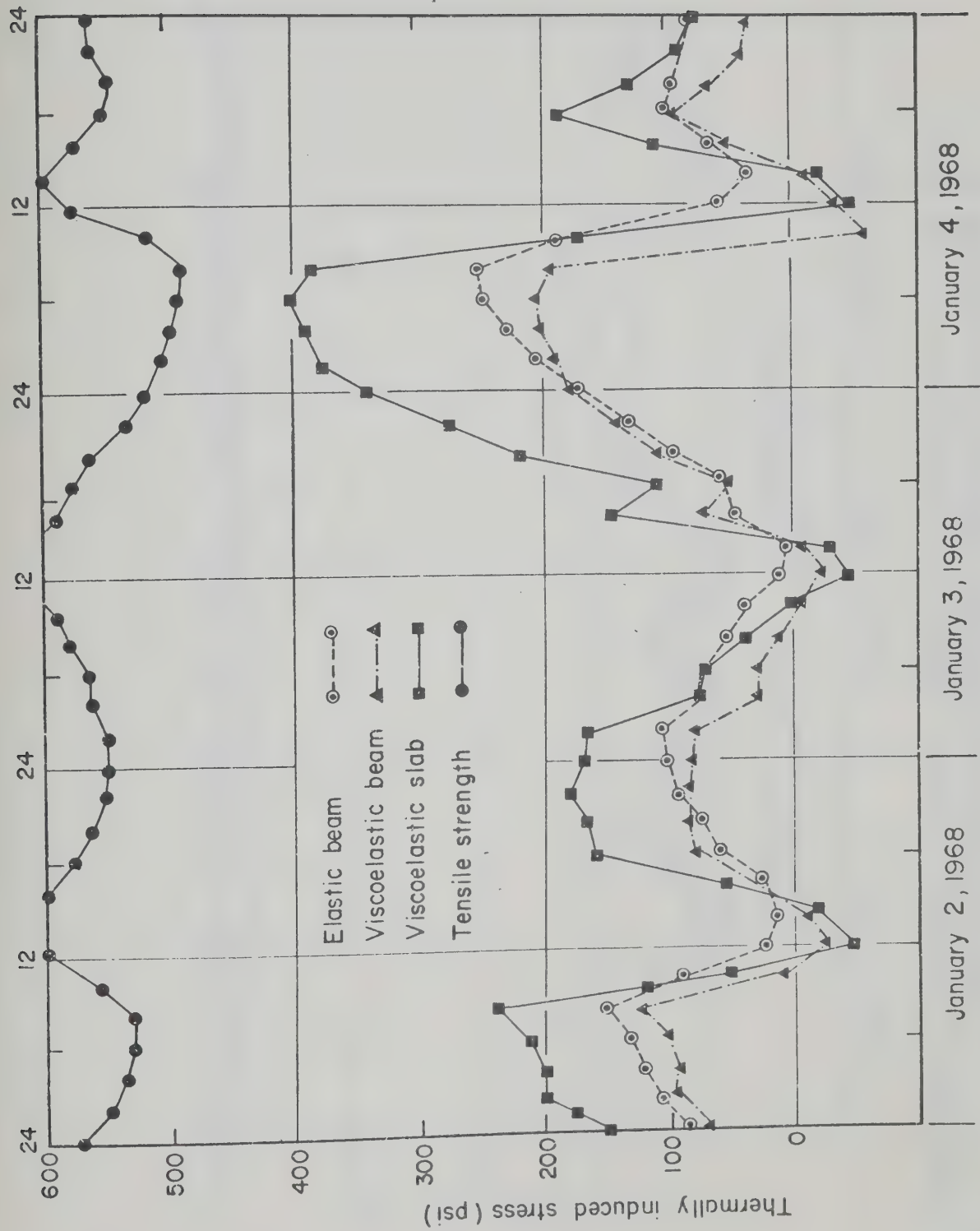


FIGURE VII-12 THERMALLY INDUCED STRESS AT THE 1/2 INCH DEPTH OF THE HV 150-200 ASPHALTIC CONCRETE PAVEMENT SURFACE OF STRUCTURE D.

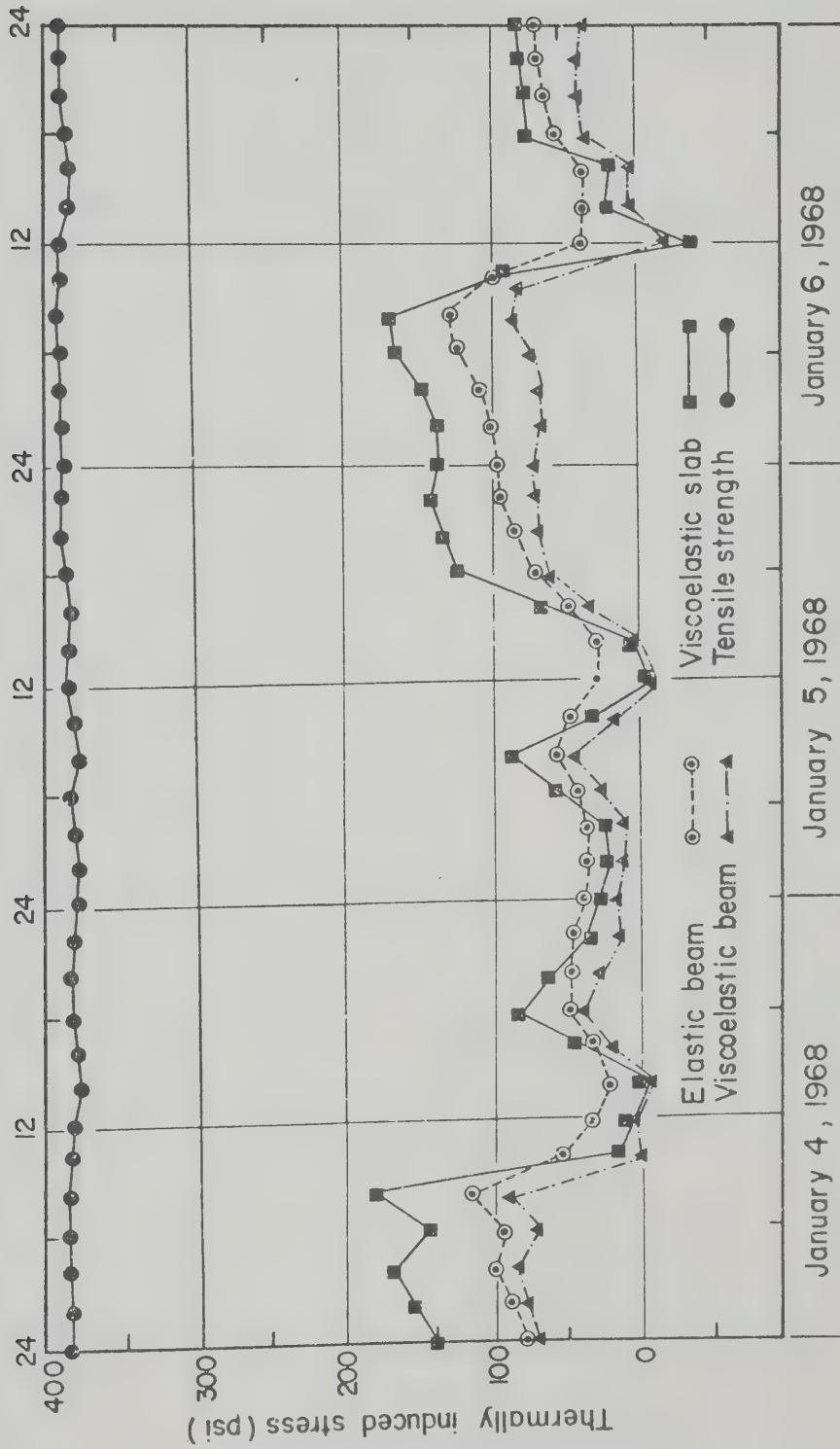


FIGURE VII-13 THERMALLY INDUCED STRESS AT 1/2 INCH DEPTH OF THE SC-5 ASPHALTIC CONCRETE PAVEMENT SURFACE OF STRUCTURE B.

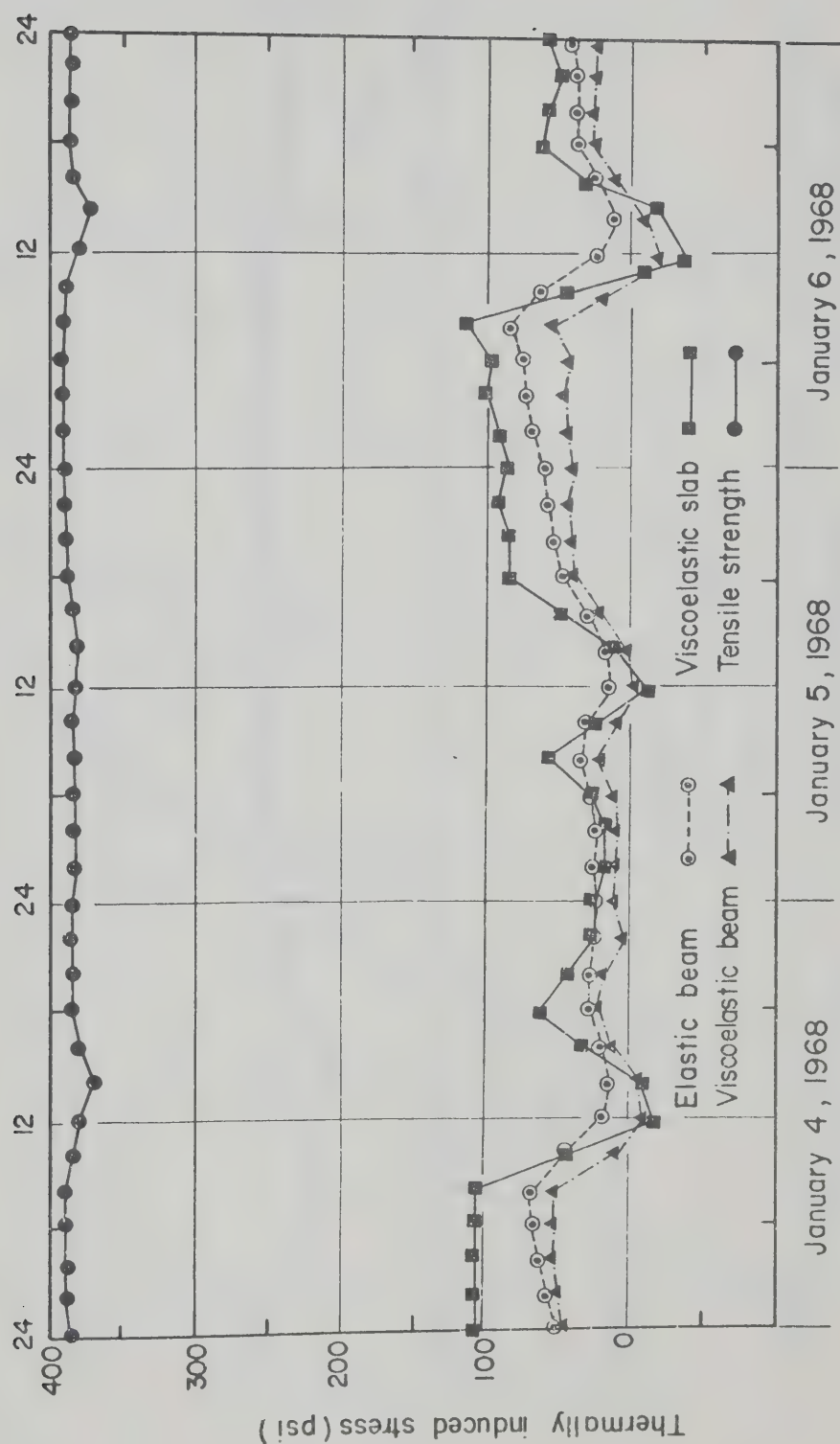


FIGURE VII-14 THERMALLY INDUCED STRESS AT 1/2 INCH DEPTH OF THE SC-5 ASPHALTIC CONCRETE PAVEMENT SURFACE OF STRUCTURE C.

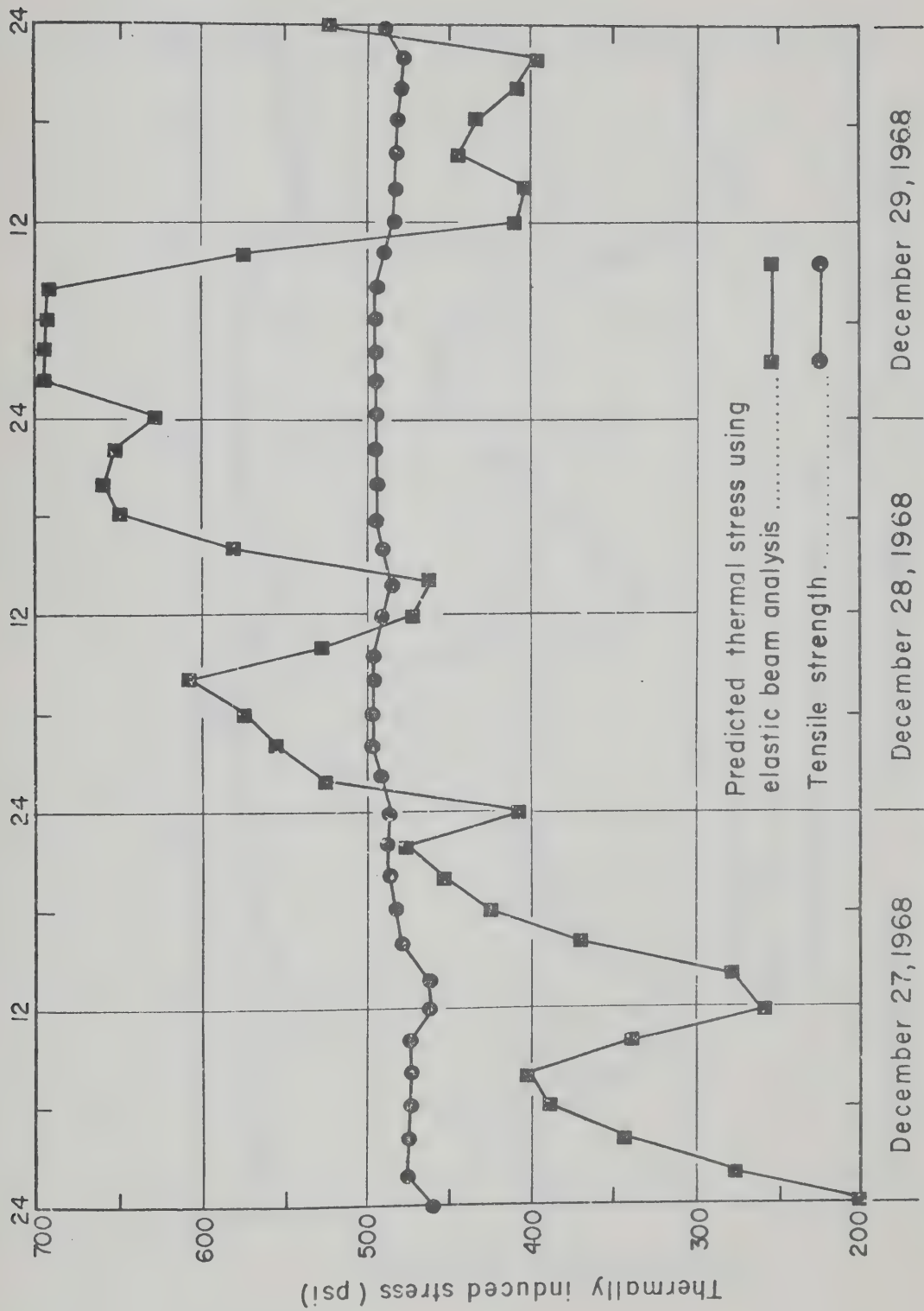


FIGURE VII - 15 THERMALLY INDUCED STRESS AT 1/2 INCH DEPTH OF ASPHALTIC CONCRETE PAVEMENT SURFACE COMPOSED OF SUPPLIER NO.1 ASPHALT CEMENT.

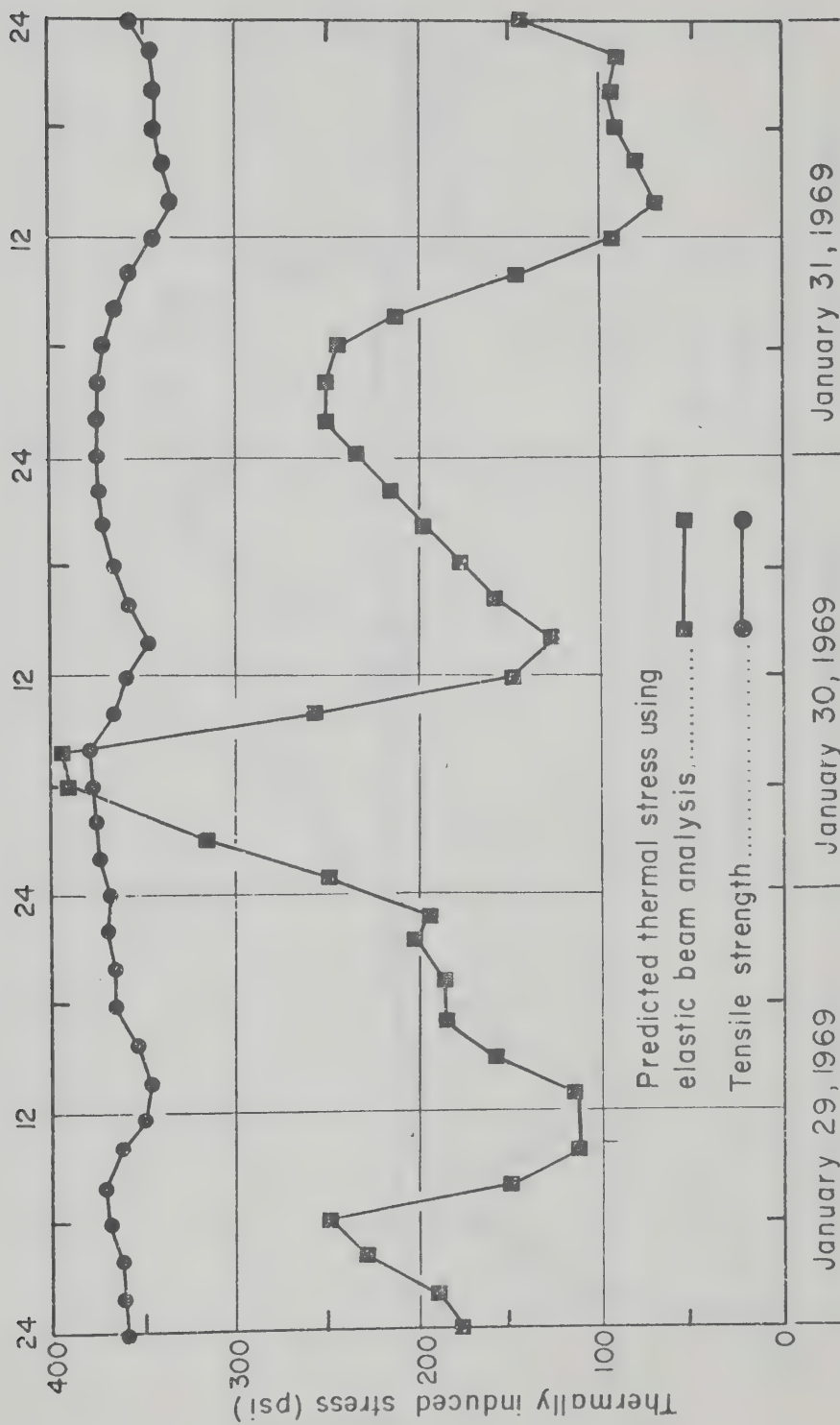


FIGURE VII - 16 THERMALLY INDUCED STRESS AT 1/2 INCH DEPTH OF ASPHALTIC CONCRETE PAVEMENT SURFACE COMPOSED OF SUPPLIER NO. 2 ASPHALT CEMENT.

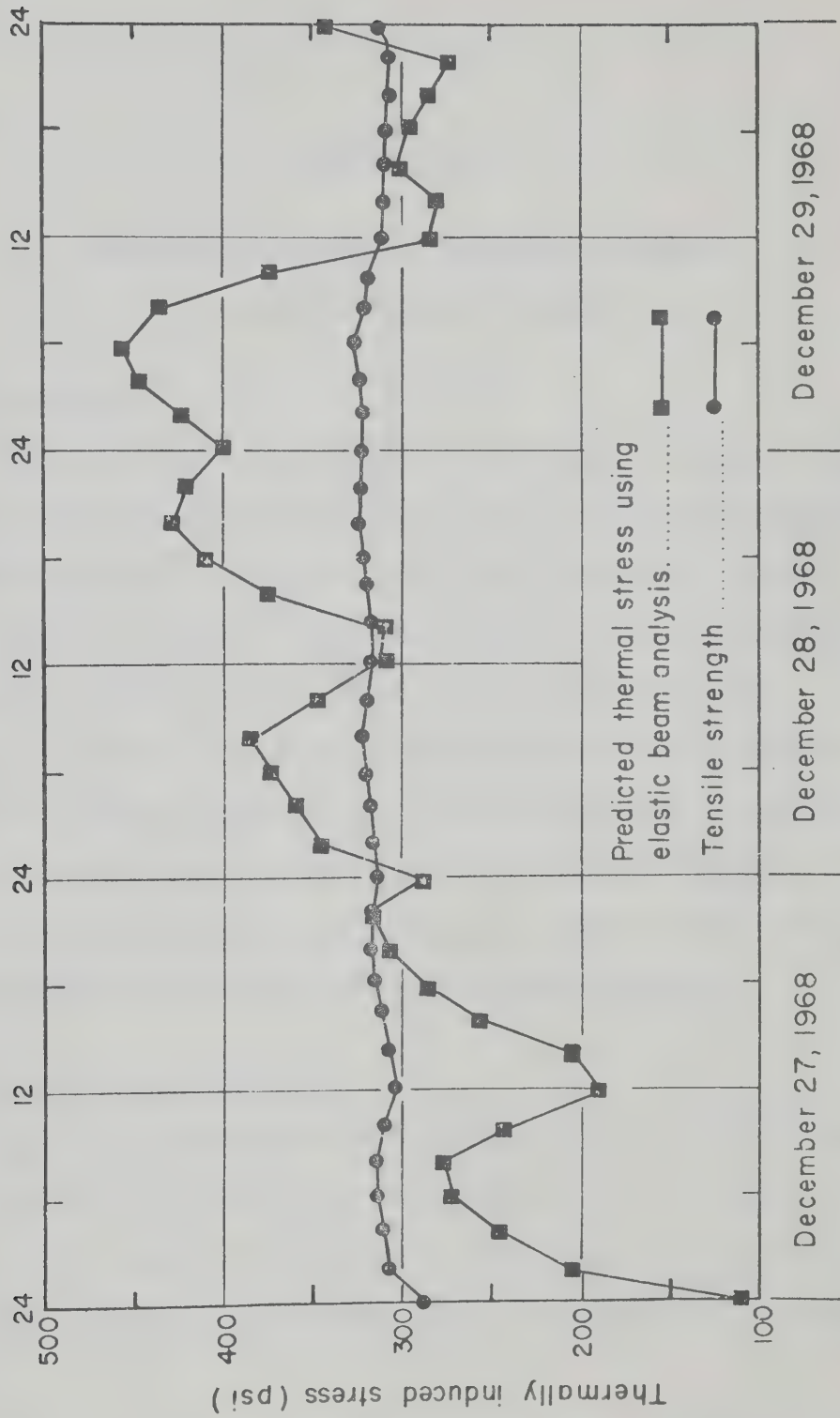


FIGURE VII-17 THERMALLY INDUCED STRESS AT 1/2 INCH DEPTH OF ASPHALTIC CONCRETE PAVEMENT SURFACE COMPOSED OF SUPPLIER NO.3 ASPHALT CEMENT.

CHAPTER VIII

GUIDELINES FOR REDUCING TRANSVERSE CRACKING OF ASPHALTIC CONCRETE PAVEMENTS

8.1. Introduction

During the past decade extensive data has been collected from field and laboratory studies related to the low temperature behavior of flexible pavements. From this data several approaches for minimizing transverse cracking within new pavements have been formulated. This chapter contains a brief review of these approaches and, employing the results of the stress prediction analyses contained in CHAPTER VII, a design guideline for reducing transverse cracking is developed. Comparisons are made between limiting low temperature design criteria specified by various agencies and individuals with similar criteria derived from the proposed design guideline.

8.2. Previous Design Approaches

Many of the developed design approaches associated with the low temperature cracking problem have been summarized by Haas et al. (1970). In view of this summary, the content of this section is limited to a brief review of suggested approaches which incorporate the following concepts.

- 1) setting limiting specifications on the asphalts,

- 2) setting limiting asphalt or asphaltic concrete mix stiffness values,
- 3) predicting fracture temperatures of asphaltic concrete mixes, and
- 4) predicting crack frequencies of asphaltic concrete pavements.

8.2.1. Setting Asphalt Specification Limits

From the results of field studies reviewed in CHAPTER II, the low temperature fracture susceptibility of an asphaltic concrete mixture appears primarily dependent on the asphalt used. Recognizing this dependency various highway departments modified their asphalt specifications in an attempt to reduce the occurrence of transverse cracking. These modifications included setting higher penetration values and/or implementing minimum viscosity requirements. Typical of such modifications were those introduced during the mid-1960's by the provinces of Saskatchewan and Alberta.

Prior to 1963, the Saskatchewan Department of Highways asphalt specification called for a 150-200 penetration grade asphalt. Subsequent modifications led to the present specification of minimum and maximum penetration and viscosity requirements at 77 F and 140 F, respectively. Until 1967, asphalt cements for use in highway construction in the Province of Alberta were graded according to penetration at 77 F. This grading resulted in asphalt cements of a given penetration grade exhibiting large differences in viscosity at 140 F. In 1967, the Alberta Department of Highways introduced their current asphalt specification which incorporates a minimum viscosity

requirement at 140 F. The grade most commonly used calls for a minimum penetration of 250 at 77 F and a minimum viscosity of 275 poises at 140 F. Anderson and Shields (1971) reported that this specification has resulted in a more uniform product from several distinct asphalt sources, the elimination of tender mixes and an apparent reduction in low temperature transverse cracking under normal winter conditions.

While highway agencies have reported a reduction in transverse cracking through the use of softer asphalts, the influence of these asphalts on traffic load associated distress, such as rutting and fatigue, has not been fully evaluated.

8.2.2. Limiting Asphalt or Mix Stiffness Values

From data collected from various field and laboratory investigations McLeod (1969) concluded that transverse cracking will occur if the stiffness of the asphaltic concrete paving mixture, at the minimum service temperature encountered, falls within the range of 1×10^6 to 2×10^6 psi. McLeod suggested that these values were applicable for a dense, well graded mix and asphalt stiffness values derived from McLeod's 1969 modification of Van der Poel's stiffness nomograph at a loading time of 20,000 seconds. TABLE VII-1 shows McLeod's tentative design guide for maximum mix stiffness values associated with various temperatures.

Using nomographic procedures for asphalt stiffness computations, Fromm and Phang (1971) determined the stiffness of asphalts comprising various mixtures known to exhibit different low temperature crack

frequencies. From these calculations the authors suggested a design approach that limits asphalt stiffness to 20,000 psi at a loading time of 10,000 seconds.

In the spring of 1972 the British Columbia Department of Highways introduced an asphalt specification which incorporates a limiting asphalt stiffness. The limiting stiffness, 30,000 psi at a specified temperature and at a loading time of 7,200 seconds, is computed from Van der Poel's nomograph, FIGURE VI-1, using asphalt properties evaluated in a manner proposed by Heukelom (1969).

8.2.3. Prediction of Asphaltic Concrete Fracture Temperature

Basically, this approach is a variation of the limiting stiffness approach. Using stiffness values, thermally induced stresses within an asphaltic concrete paving mixture subjected to a given temperature history are predicted. The predicted stresses are compared with the fracture strength-temperature relationship of the mix. Such a comparison provides a means of predicting the fracture temperature of the mix. This approach, initially proposed by Hills and Brien (1966), was used in CHAPTER VII to assess the results of various stress predictive methods.

8.2.4. Prediction of Crack Frequency

Recently, Hajek (1971) developed a mathematical model for predicting crack frequency of asphaltic concrete pavements as a function of several of the variables described in CHAPTER II. The model is based on field data from the provinces of Ontario and Manitoba

and is of the following form.

$$I = \text{function}(s, t, a, d, m) \pm E$$

where

I = cracking index (the sum of the full plus one-half of the half transverse cracks per 500 feet of two-lane roadway),

s = stiffness modulus of the original asphalt cement, kg per sq cm, according to McLeod (1969),

t = thickness of asphaltic concrete pavement layer, inches,

a = age of pavement, years,

d = subgrade soil type, classified as clay, loam or sand,

m = winter design temperature, C, and

E = standard error of estimate of I .

Hajek concluded that the model enables crack frequency to be predicted with a reasonable degree of confidence and has the capacity to provide an immediate engineering guide for preventing or controlling low temperature cracking in Canada.

8.3. Proposed Design Guideline

In CHAPTER VII comparisons have been made between predicted and observed fracture times and temperatures of various asphaltic concrete paving mixtures. For these comparisons results of different stress predictive methods were used. The correlation between predicted and observed fracture conditions, shown in TABLE VII-5 of CHAPTER VII and

obtained using the pseudo-elastic beam analysis, suggests that such an analysis provides a reliable means of assessing the low temperature fracture susceptibility of an asphaltic concrete paving mixture subjected to a particular temperature history. In view of this correlation, a design guideline for reducing the occurrence of transverse cracks, caused by thermally induced stresses exceeding the low temperature tensile strengths of asphaltic concrete paving mixtures, is proposed. The development of the guideline involved the following computations.

- 1) Using the pseudo-elastic beam analysis and a loading time of 7,200 seconds, thermal stresses within each of the asphaltic concrete paving mixtures, whose stiffness characteristics have been presented in CHAPTER VI, were computed when subjected to five different temperature histories. These temperature histories included, the three recorded at the Manitoba test project during the 1967-68 winter, the measured asphaltic concrete pavement temperatures at the Alberta test project during the winter of 1966-67 and the predicted third winter temperatures at this test site. For all stress predictions the coefficient of thermal expansion of each paving mixture was assumed constant and equal to a value of 1.5×10^{-5} per degree Fahrenheit.
- 2) At temperatures of 0 F and less, and using 5 F temperature increments, maximum thermally induced stresses within each

of the asphaltic concrete pavements were transcribed from the results of the stress analyses. At corresponding temperatures and employing a loading time of 7,200 seconds stiffness values of the paving mixtures were computed. For these computations the method adopted in CHAPTER VII to define the time and temperature dependence of the mixes was used. The maximum predicted thermally induced stress values were then plotted as a function of mix stiffness values. Individual stress and stiffness values of the low viscosity 150-200 asphalt pavement at the Manitoba test project are shown in FIGURE VIII-1, while, the bands in this figure represent the limits of the thermally induced stress-stiffness relationships of all asphaltic concrete mixtures considered.

- 3) The relationship between asphaltic concrete stiffness, asphalt stiffness and volume concentration of aggregate proposed by Heukelom and Klomp (1964), Equation (VI-3) of CHAPTER VI, is shown graphically in FIGURE VIII-2. Superimposed on this figure are the limits of the maximum predicted thermally induced stress-mix stiffness relationships shown in FIGURE VIII-1.

FIGURE VIII-2 provides a means of readily estimating thermally induced stresses within asphaltic concrete pavements subjected to low temperature climatic environments such as experienced in Western Canada. Such estimations assume that the unknown thermal stresses can be

approximated by use of the pseudo-elastic beam analysis and that the coefficient of thermal expansion of paving mixtures equals 1.5×10^{-5} per degree Fahrenheit and is temperature independent. With reference to Equation (VII-6), computed thermal stresses are directly proportional to a temperature independent expansion coefficient and therefore the position of the thermally induced stress limits may be shifted along the upper horizontal axis of FIGURE VIII-2 when a coefficient other than that assumed in the present study is used.

At a given temperature, the stress estimate requires a knowledge of asphalt stiffness at a loading time of 7,200 seconds, together with the appropriate volume concentration of aggregate value (C_v) for the paving mixture, or a knowledge of the asphaltic concrete stiffness at the same loading time. In the former case, the importance of defining the C_v value of the paving mixture is shown in FIGURE VIII-3. From this figure, relatively small variations in C_v can result in large differences between predicted thermally induced stresses in a paving mixture whose asphalt stiffness has been defined.

For design purposes, the correlations obtained between predicted and observed low temperature performance of the various pavements studied in CHAPTER VII suggest that comparisons between predicted thermally induced stresses obtained from FIGURE VIII-2 and measured tensile failure strengths of paving mixtures enable the low temperature fracture susceptibility of asphaltic concrete mixes to be readily assessed.

8.4. Comparisons Between Proposed and Previously Suggested Guidelines

In order to compare the proposed method of assessing the low temperature fracture susceptibility of paving mixtures with previously suggested methods a fracture strength-temperature relationship of an asphaltic concrete mix must be assumed. From the results of the tensile splitting test presented in CHAPTER VI and the results of direct tension tests on asphaltic concrete specimens reported by Haas (1968), the low temperature tensile fracture strength of asphaltic concrete paving mixtures composed of asphalts obtained from Western Canada crude sources have generally been found to be within the range of from 200 to 400 psi. For the following comparisons, a paving mixture having a fracture strength of 300 psi at temperatures less than 0 F has been assumed.

From FIGURE VIII-2 and considering the fracture strength of 300 psi, low temperature cracking could be expected if the stiffness of the asphaltic concrete paving mixture exceeded 1.7×10^6 psi. This value corresponds favourably with the stiffness limits of 1×10^6 to 2×10^6 psi suggested by McLeod (1969). If the volume concentration of the mix is 0.88 or 0.86 the maximum stiffness of the asphalt comprising the mix should be limited to 12,000 and 22,000 psi, respectively. These asphalt stiffness values approximate the limiting value of 20,000 psi at a loading time of 10,000 seconds suggested by Fromm and Phang (1971) and the limiting stiffness of 30,000 psi at a loading time of 7,200 seconds adopted by the British Columbia Department of Highways.

While previously suggested limiting asphalt and asphaltic concrete mix stiffness values for minimizing low temperature transverse cracking are in close agreement with values derived from FIGURE VIII-2, this figure enables the influences of variations in asphalt and mix stiffness and volume concentration of aggregate on computed thermal stresses which have been correlated with observed field behavior to be evaluated.

8.5. Summary

In this chapter suggested design approaches for reducing transverse cracking of asphaltic concrete pavements have been briefly reviewed and a guideline based on the correlation obtained between predicted and observed times and temperatures of fracture of various pavements studied in CHAPTER III has been developed. Using this developed guideline the influence of asphalt mix stiffness, asphalt stiffness and volume concentration of aggregate on maximum predicted thermally induced stress can be readily deduced.

TABLE VIII-1

MAXIMUM MIX STIFFNESS FOR SELECTING
ASPHALT GRADE (McLeod, 1969)

Minimum Temperature (F)	Stiffness Modulus (psi)	
	Cracking Expected	Cracking Eliminated
-40	1,000,000	500,000
-25	700,000	300,000
-10	400,000	200,000
+10	100,000	50,000

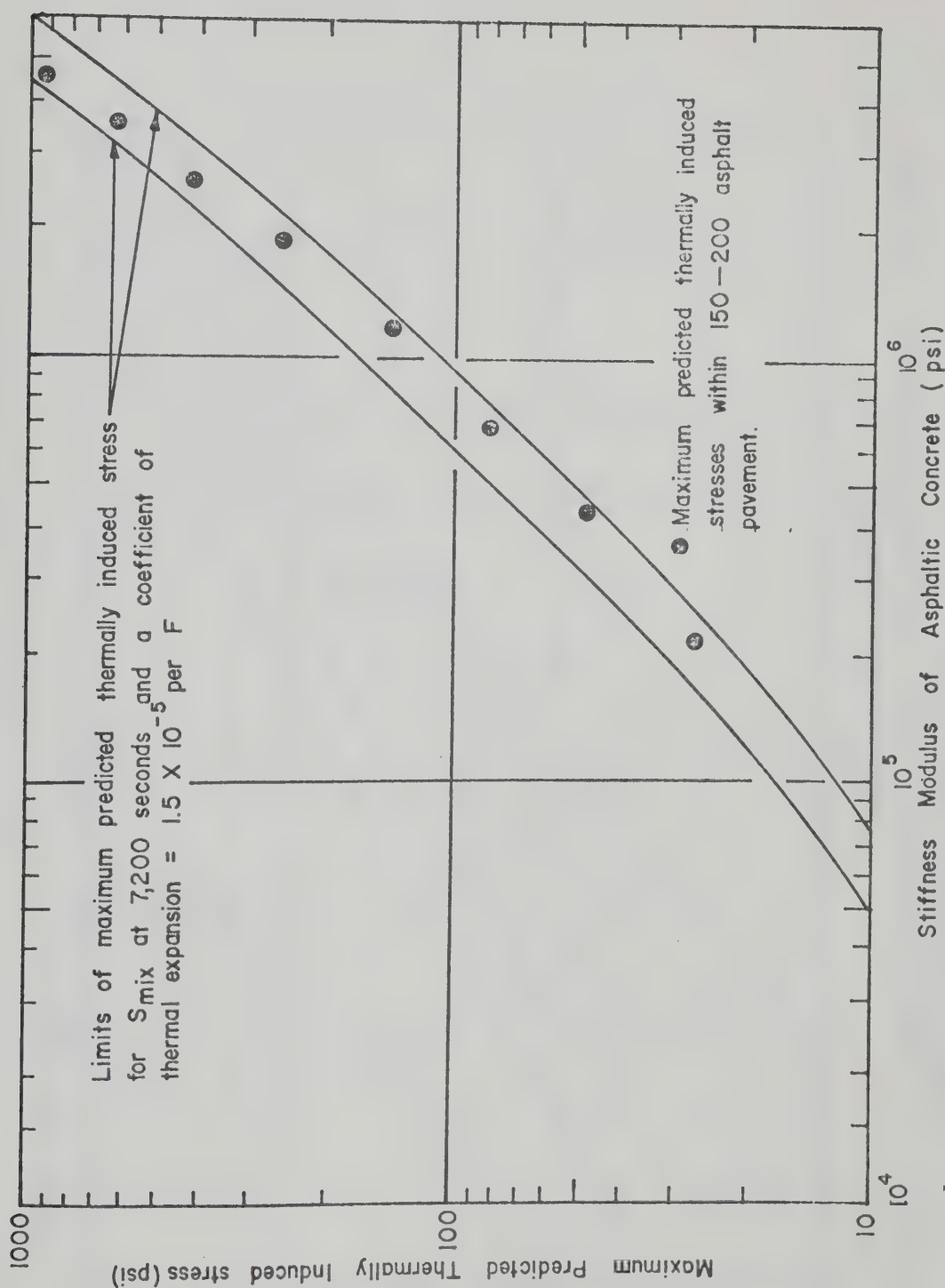


FIGURE VIII - 1 STIFFNESS MODULUS OF ASPHALTIC CONCRETE VERSUS MAXIMUM PREDICTED THERMALLY INDUCED STRESS

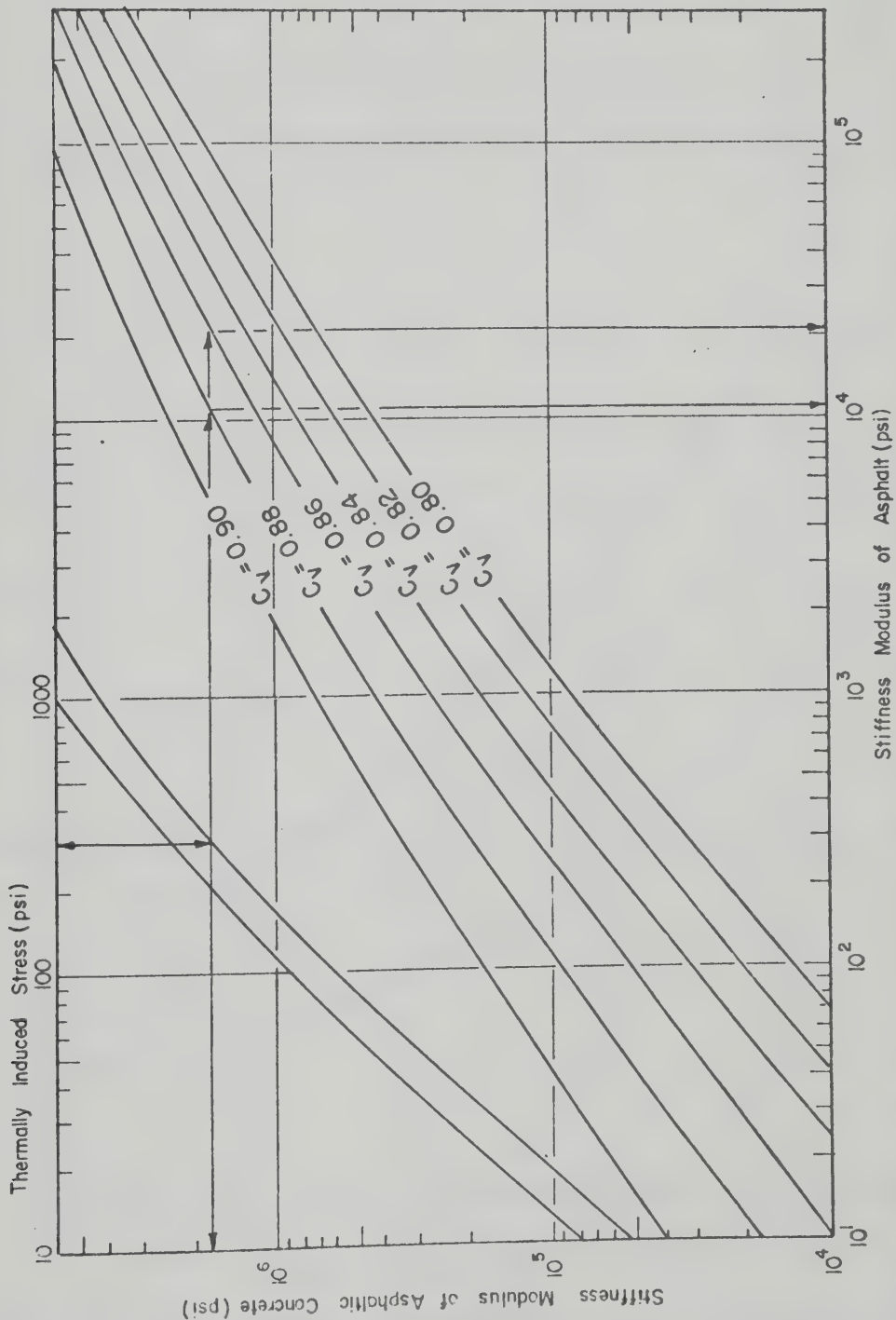


FIGURE VIII - 2 RELATIONSHIPS BETWEEN ASPHALT AND ASPHALTIC CONCRETE STIFFNESS MODULI (after Heukelom - Klomp; 1964)

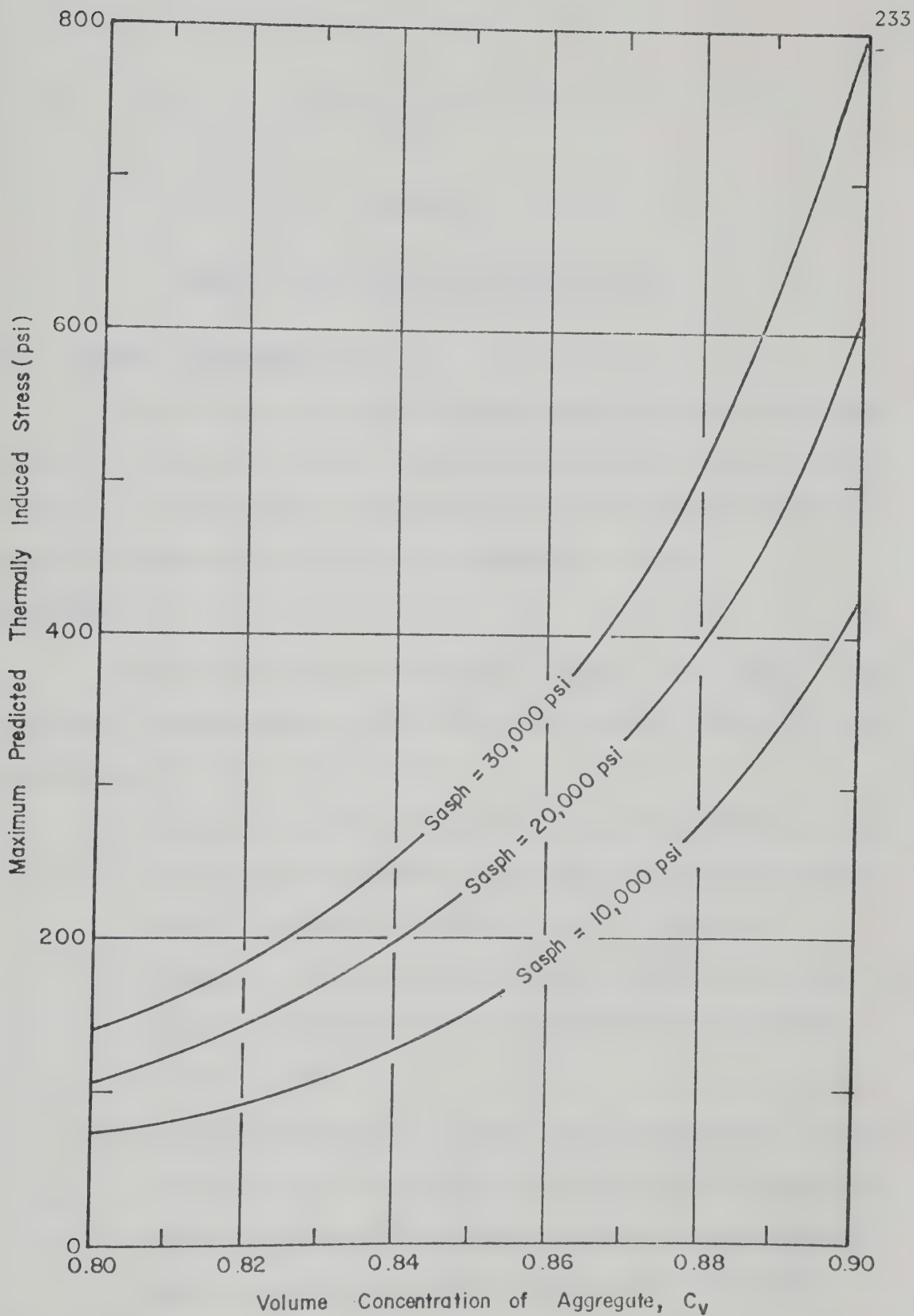


FIGURE VIII-3 VOLUME CONCENTRATION OF AGGREGATE VERSUS MAXIMUM PREDICTED THERMALLY INDUCED STRESS FOR VARIOUS ASPHALT STIFFNESS MODULI.

CHAPTER IX

SUMMARY, CONCLUSIONS AND RECOMMENDATIONS

9.1. Summary and Conclusions

This study has considered one manifestation of non-traffic load associated distress of flexible pavements, namely, transverse cracking caused by thermally induced stresses exceeding the tensile strength of paving mixtures when subjected to low temperature climatic environments.

Various factors found from previous studies to be related to the transverse cracking problem were reviewed. Principal findings of these studies are:

- 1) Transverse cracking of asphaltic concrete pavements can lead to significant performance losses and increased maintenance costs. In addition to being a source of maintenance expenditures, the reduction in pavement service life caused by transverse cracking may be of much more importance in an economic sense.
- 2) Documented results of detailed field test projects, located in Western Canada and designed to study the low temperature response of asphaltic concrete pavements, indicate that the majority of transverse cracks initiate at a time when

pavement surface temperatures are approaching or at seasonal minimum values.

- 3) The low temperature fracture susceptibility of an asphaltic concrete mix is primarily dependent on the asphalt used. This dependency is reflected by differences in crack frequencies of pavements composed of asphalts obtained from different crude sources, incorporating asphalts of various grades as specified in terms of viscosity and/or penetration and including asphalts which exhibit different low temperature stiffness properties.
- 4) The extent of cracking is not only dependent on the asphalt used but also on such variables as asphaltic concrete thickness, pavement age and subsurface materials. Generally, crack frequency is found to increase with decreasing asphaltic concrete thickness, increasing pavement age and is often found to be highest within pavement structures having sand subgrades.

The importance of temperature as related to the behavior of asphaltic concrete paving mixtures has long been recognized, however, it has only been in recent years that continuous temperature regimes within pavement structures subjected to low temperature climatic conditions and during periods of recorded transverse cracking have been collected. Analyses of such temperature data, obtained from field studies in Western Canada, has yielded specific information on time variations of temperature occurring in several pavement structures

subjected to climatic temperatures approaching -40 F. For the data analyzed, major findings are:

- 1) At equal depths within asphaltic concrete surfaces of different thicknesses, temperatures and temperature variations are nearly identical when the pavements are subjected to similar climatic environments.
- 2) Temperature gradients in asphaltic concrete surfacings increase with a decrease in daily minimum temperature, reflecting the existence of large stiffness and thermally induced stress gradients.
- 3) Rates of surface temperature change are generally less than 3 degrees Fahrenheit per hour during winter months and at depths of 10 inches rates of asphaltic concrete temperature change are reduced to approximately 0.5 degrees Fahrenheit per hour.
- 4) The thermal regime existing in a subgrade, subjected to prolonged subfreezing temperatures, is primarily dependent on the physical and thermal properties of the subgrade.

In the absence of recorded pavement temperatures a realistic assessment of the response of asphaltic concrete pavements to low temperature climatic environments is dependent on a method whereby pavement temperatures can be reliably predicted. The application of principles of heat transfer in which the influence of climatic factors and pavement material properties on pavement temperatures enabled such a predictive method to be developed. Prior to its development, heat

transfer concepts applied to pavement structures and thermal properties of pavement material properties were reviewed. Principal findings of this review may be stated as follows:

- 1) A rational approach to defining the influence of climatic variables on pavement surface temperature involves an energy balance procedure in which surface temperatures are related to various meteorological parameters. The accuracy of such a relationship is dependent on the method used to describe the influence of changing climatic conditions on surface temperatures, which will generally be governed by available meteorological data at a given locale.
- 2) Documented results of studies related to thermal properties of pavement component materials enable approximations of the thermal properties of specific component materials to be made.

Employing heat transfer concepts presented in the previously mentioned review, together with a finite difference approximation of the one-dimensional heat transfer equation, an analytical model for predicting temperatures in pavement structures was developed. Formulation of the finite difference equations was presented and input parameters for the model were described. The parameters include structural, physical and thermal properties of each component layer, meteorological data and a nonlinear relationship between unfrozen moisture content and temperature for each subsurface layer. Comparisons between predicted and recorded temperatures in various pavement structures were given.

The close agreement which was found to exist between predicted and recorded temperatures suggests:

- 1) The model can be used to obtain reliable predictions of thermal regimes in asphaltic concrete surfacings under actual climatic conditions.
- 2) The model enables thermal regimes existing in subgrades during periods of low temperature climatic environment to be approximated.

Using recorded and predicted asphaltic concrete temperatures, thermally induced stresses within pavement surfaces of field test projects located in Western Canada were computed by various stress prediction methods. Such computations require definition of the time and temperature dependent stiffness characteristics of the asphaltic concretes and in order to assess the low temperature fracture susceptibility of the paving mixtures, assuming a stress fracture criterion, the fracture strength-temperature relationships of the mixtures must be defined. Concepts used to characterize the time and temperature dependence of the asphaltic concrete mixtures were described and resulting stiffness modulus-reduced time relationships were presented. The low temperature tensile properties of pavement cores obtained from the test projects were determined by means of the tensile splitting test. All tests were conducted using a loading rate of 0.056 inches per minute at test temperatures ranging from +20 to -20 F. The results of these tests were summarized and briefly discussed in relation to observed differences in low temperature behavior of test control

sections within the projects. Principal findings associated with this summary and discussion are:

- 1) In terms of a relative comparison between different paving mixtures subjected to near identical low temperature histories, the paving mixture having the highest stiffness and lowest failure strain values exhibits the highest crack frequency.
- 2) The low temperature tensile failure strengths of asphaltic concrete mixtures composed of asphalts obtained from Western Canadian crude sources range from approximately 200 to 400 pounds per square inch and for a given mix an increase in density contributes to an increase in tensile failure strength.
- 3) Differences in asphalt grade, as expressed in terms of penetration and/or viscosity, reflect differences in low temperature behavior. For a particular penetration at 77 F, an increase in viscosity at 140 F, can be expected to produce a decrease in crack frequency and for a particular viscosity at 140 F, an increase in penetration at 77 F, can be expected to produce a decrease in crack frequency.

The stress prediction methods included in the study were pseudo-elastic and viscoelastic beam and slab analyses. Theoretical considerations for the formulation of the prediction methods were reviewed and numerical solutions of the stress equations were presented. Computed stresses were compared with fracture strength-temperature

relationships of the asphaltic concretes to predict times and temperatures of fracture. These predicted fracture conditions were then compared with times and temperatures of observed cracking of the corresponding pavements in the test projects. These comparisons permitted a realistic assessment of the various stress predictive methods from which the following conclusions are made:

- 1) Stress predictive methods coupled with the use of recorded or predicted temperature data and appropriate materials characterization provide a means of reliably assessing the low temperature fracture susceptibility of asphaltic concrete paving mixtures.
- 2) Maximum and minimum thermal stresses are computed using the viscoelastic slab and beam analyses, respectively, while the approximate viscoelastic slab analysis yields intermediate stress values.
- 3) Thermal stresses computed using the pseudo-elastic analyses are dependent upon the specified loading time used in the numerical integration of the stress equations. This dependency is primarily due to changes in asphaltic concrete stiffness with loading time.
- 4) Using a constant time increment for numerical integration of the viscoelastic stress equations necessitates long computer runs and large storage requirements if stresses are to be predicted over extended periods of times. These requirements can be reduced by employing a scheme of variable time increments.

- 5) The correlation between observed and predicted low temperature performance of the asphaltic concretes suggests that, for the data currently available, the low temperature fracture susceptibility of an asphaltic concrete paving mixture can be reliably assessed using stresses computed using the pseudo-elastic beam analysis together with the assumed fracture criterion.

In view of the correlation obtained between predicted and observed times and temperatures of fracture of the asphaltic concrete pavements included in the study, a simplified guideline for reducing the occurrence of transverse cracking caused by thermally induced stresses exceeding the low temperature tensile strengths of asphaltic concrete mixtures is proposed. Using this guideline the influence of variations in asphalt mix stiffness, asphalt stiffness and volume concentration of aggregate on thermal stresses computed by the pseudo-elastic beam analysis can be readily deduced.

9.2. Recommendations

Recommendations arising from this investigation and directed towards developing a solution to the low temperature cracking problem are listed as follows:

- 1) Before any of the stress predictive methods and fracture criterion presented in this study may be applied with full confidence, further comparisons between observed and predicted fracture times and temperatures of different pavement surfaces must be made. In the meantime the predictive

techniques should be implemented within the framework of present design, construction and material selection strategies so as to minimize the occurrence of low temperature cracking.

- 2) Future studies related to the low temperature cracking problem should be directed towards defining subgrade influences on crack initiation as well as crack frequency.
- 3) Efforts should be directed towards developing effective pavement maintenance and rehabilitation strategies for the many miles of existing cracked pavements in areas subjected to low temperature climatic conditions.

LIST OF REFERENCES

LIST OF REFERENCES

- Aldrich, H.P., Jr., 1956. "Frost Penetration Below Highway and Air-field Pavements", Highway Research Board Bulletin No. 135, pp. 124-144.
- Anderson, K.O., B.P. Shields and J.M. Dacyszyn, 1966. "Cracking of Asphalt Pavements Due to Thermal Effects", Proceedings of the Association of Asphalt Paving Technologists, Vol. 35, pp. 247-262.
- Anderson, K.O. and W.P. Hahn, 1968. "Design and Evaluation of Asphalt Concrete with Respect to Thermal Cracking", Proceedings of the Association of Asphalt Paving Technologists, Vol. 37, pp. 1-31.
- Anderson, K.O. and R.C.G. Haas, 1970. "Use of the Stiffness Concept to Characterize Bituminous Materials", Proceedings of the Canadian Technical Asphalt Association, Vol. XV
- Anderson, K.O. and B.P. Shields, 1971. "Some Alberta Experience with Penetration-Graded Asphalt Cements Having Differing Viscosities at 140 F", Highway Research Record No. 350, pp. 15-25.
- Barber, E.S., 1957. "Calculation of Maximum Pavement Temperatures from Weather Records", Highway Research Board Bulletin No. 168, pp. 1-8.
- Barry, R.G., 1968. "Atmosphere, Weather and Climate", Methuen and Company Limited, London.
- Bright, R., A. Justice and J. Steele, 1969. "Early Hardening of Asphaltic Binder in Bituminous Paving Mixtures", ASTM Journal of Materials, Vol. 4, No. 1, pp. 231-247.
- Burgess, R.A., O. Kopvillem and F.D. Young, 1971. "Relationships Between Predicted Fracture Temperatures and Low Temperature Field Performance", Proceedings of the Association of Asphalt Paving Technologists, Vol. 40, pp. 148-170.
- Carlson, H. and M.S. Kersten, 1953. "Calculation of Depth of Freezing and Thawing Under Pavements", Highway Research Board Bulletin No. 71, pp. 81-95.
- Carnahan, B., L.H. Luther and J.O. Wilkes, 1969. "Applied Numerical Methods", John Wiley and Sons Inc.

- Carroll, C., H. Schenck, Jr. and W. Williams, 1966. "Digital Simulation of Heat Flow in Soils", Journal of the Soil Mechanics and Foundations Division, Vol. 92, No. SM4, pp. 31-49.
- Christianson, R.H.A., 1970. "Analysis of the Tensile Splitting Test for Low Temperature Tensile Properties of Asphaltic Concrete", M.Sc. Thesis, The University of Alberta.
- Corlew, V.S. and P.F. Dickson, 1968. "Methods for Calculating Temperature Profiles of Hot-Mix Asphalt Concrete as Related to Construction of Asphalt Pavements", Proceedings of the Association of Asphalt Paving Technologists, Vol. 37, pp. 101-134.
- Culley, R.W., 1966. "Transverse Cracking of Flexible Pavements in Saskatchewan", Technical Report No. 3, Department of Highways, Regina, Saskatchewan.
- Culley, R.W., 1969. "Relationships Between Hardening of Asphalt Cements and Transverse Cracking of Pavements in Saskatchewan", Proceedings of the Association of Asphalt Paving Technologists, Vol. 38, pp. 629-645.
- Deme, I. and D. Fisher, 1968. "Ste. Anne Test Road - Instrumentation", Proceedings of the Canadian Technical Asphalt Association, Vol. XIII, pp. 305-350.
- Dempsey, B.J. and M.R. Thompson, 1970. Private Communication on unpublished paper presented at Conference Session 42, Highway Research Board.
- Dillon, H.B. and O.B. Andersland, 1966. "Predicting Unfrozen Water Contents in Frozen Soils", Canadian Geotechnical Journal, Vol. III, No. 2, pp. 53-60.
- Domaschuk, L., P.S. Skarsgard and R.H. Christianson, 1964. "Cracking of Asphalt Pavements Due to Thermal Contraction", Proceedings of the Canadian Good Roads Association, pp. 395-402.
- Farouki, O.T., 1966. "Physical Properties of Granular Materials with Reference to Thermal Resistivity", Highway Research Record No. 128, pp. 25-45.
- Fromm, H.J., 1966. "Prepared Discussion for Symposium on Non-Traffic Load Associated Cracking of Asphalt Pavements", Proceedings of the Association of Asphalt Paving Technologists, Vol. 35, pp. 324-329.

- Fromm, H.J. and W.A. Phang, 1971. "Temperature-Susceptibility Control in Asphalt Cement Specifications", Highway Research Record No. 350, pp. 30-38.
- Geiger, R., 1959. "The Climate Near the Ground", Harvard University Press, Cambridge, Massachusettes.
- Haas, R.C.G., 1968. "The Performance and Behavior of Flexible Pavements at Low Temperatures", Ph.D. Thesis, University of Waterloo.
- Haas, R.C.G. and K.O. Anderson, 1969. "A Design Subsystem for the Response of Flexible Pavements at Low Temperatures", Proceedings of the Association of Asphalt Paving Technologists, Vol. 38, pp. 179-213.
- Haas, R.C.G. and T.H. Topper, 1969. "Thermal Fracture Phenomena in Bituminous Surfaces", Highway Research Board, Special Report No. 101, pp. 136-152.
- Haas, R.C.G., et al., 1970. A paper prepared by a CGRA Ad Hoc Committee on Low Temperature Behavior of Flexible Pavements, "Low-Temperature Pavement Cracking in Canada: The Problem and its Treatment", Proceedings of the Canadian Good Roads Association, pp. 69-95.
- Hajek, J.J., 1971. "A Comprehensive System for Estimation of Low-Temperature Cracking Frequency of Flexible Pavements", A Technical Report Based on the author's M.A.Sc. Thesis, University of Waterloo.
- Hamilton, A.B., 1966. "Freezing Shrinkage in Compacted Clays", Canadian Geotechnical Journal, Vol. III, No. 1, pp. 1-17.
- Heukelom, W. and A.J.G. Klomp, 1964. "Road Design and Dynamic Loading", Proceedings of the Association of Asphalt Paving Technologists, Vol. 33, pp. 92-123.
- Heukelom, W., 1966. "Observations on the Rheology and Fracture of Bitumens and Asphalt Mixes", Proceedings of the Association of Asphalt Paving Technologists, Vol. 35, pp. 358-396.
- Heukelom, W., 1969. "A Bitumen Test Data Chart for Showing the Effect of Temperature on the Mechanical Behavior of Asphaltic Bitumens", Journal of the Institute of Petroleum, Vol. 55, No. 546, pp. 404-417.
- Hills, J.F. and D. Brien, 1966. "The Fracture of Bitumens and Asphalt Mixes by Temperature Induced Stresses", Proceedings of the Association of Asphalt Paving Technologists, Vol. 35, pp. 292-309.

- Ho, D.M., M.E. Harr and G.A. Leonards, 1970. "Transient Temperature Distributions in Insulated Pavements - Predictions vs. Observations", Canadian Geotechnical Journal, Vol. 7, pp. 275-284.
- Huculak, N.A., 1964. Discussion on "Cracking of Asphalt Pavements Due to Thermal Contraction", by Domaschuk, et al., Proceedings of the Canadian Good Roads Association, pp. 406-407.
- Hudson, W.R., et al., 1969. A paper prepared by the Committee on the Structural Design of Roadways authorized by the Highway Division of the ASCE, "The Problems of Designing Roadway Structures", Proceedings of the American Society of Civil Engineers, Transportation Engineering Journal, Vol. 95, No. TE2, pp. 289-315.
- Humphreys, J.S. and C.J. Martin, 1963. "Determination of Transient Thermal Stresses in a Slab with Temperature Dependent Viscoelastic Properties", Transactions of the Society of Rheology, Vol. VII, pp. 155-170.
- Hutchinson, B.G. and R.C.G. Haas, 1968. "A Systems Analysis of the Highway Pavement Design Process", Highway Research Record No. 239, pp. 1-24.
- Johnson, A.W., 1952. "Frost Action in Roads and Airfields", Highway Research Board Special Report No. 1.
- Kallas, B.F., 1966. "Asphalt Pavement Temperatures", Highway Research Record No. 150, pp. 1-11.
- Kasianchuk, D.A., 1968. "Fatigue Considerations in the Design of Asphalt Pavements", Ph.D. Dissertation, University of California, Berkeley.
- Kathol, B., 1968. "Transverse Cracking of Asphaltic Concrete Surfaces in Alberta", Paper presented at the annual meeting of the Western Association of Canadian Highway Officials.
- Kersten, M.S., 1949. "Thermal Properties of Soils", Bulletin No. 28, University of Minnesota, Engineering Experiment Station, Minneapolis, Minnesota.
- Kersten, M.S., 1959. "Frost Penetration: Relationship to Air Temperatures and other Factors", Highway Research Board Bulletin No. 225.
- Kersten, M.S. and R.U. Johnson, 1955. "Frost Penetration Under Bituminous Pavements", Highway Research Board Bulletin No. 111, pp. 37-62.

- Kingham, R.I., 1966. "Prepared Discussion for Symposium on Non-Traffic Load Associated Cracking of Asphalt Pavements", Proceedings of the Association of Asphalt Paving Technologists, Vol. 35, pp. 329-333.
- Kopvillem, O. and W. Heukelom, 1969. "The Effect of Temperature on the Mechanical Behavior of some Canadian Asphalts as shown by a Test Data Chart", Proceedings of the Canadian Technical Asphalt Association, Vol. XIV, pp. 262-286.
- Lachenbruch, A.L., 1961. "Depth and Spacing of Tension Cracks", Journal of Geophysical Research, Vol. 66, No. 12, pp. 4273-4292.
- Littlefield, G., 1967. "Thermal Expansion and Contraction Characteristics of Utah Asphaltic Concretes", Proceedings of the Association of Asphalt Paving Technologists, Vol. 36, pp. 673-697.
- Lovell, G.W., Jr., 1957. "Temperature Effects on Phase Composition and Strength of Partially-Frozen Soil", Highway Research Board Bulletin No. 168, pp. 79-96.
- McLeod, N.W., 1967. "Critical Appraisal of Proposal to Grade Paving Asphalts by Viscosity at 140 F", ASTM Special Technical Publication, No. 424, pp. 47-75.
- McLeod, N.W., 1968. "Transverse Pavement Cracking Related to Hardness of the Asphalt Cement", Proceedings of the Canadian Technical Asphalt Association, Vol. XIII, pp. 5-96.
- McLeod, N.W., 1969. Prepared Discussion on "Factors Influencing Dynamic Modulus of Asphalt Concrete", by Shook, J.F. and B.F. Kallas, Proceedings of the Association of Asphalt Paving Technologists, Vol. 38, pp. 166-175.
- McLeod, N.W., 1969. Prepared Discussion on "Ste. Anne Test Road: Construction Summary and Performance After Two Years Service", by Young, et al., Proceedings of the Canadian Asphalt Association, Vol. XIV, pp. 110-131.
- Monismith, C.L. and K.E. Secor, 1962. "Viscoelastic Behavior of Asphaltic Concrete Pavements", Proceedings of the First International Conference on the Structural Design of Asphalt Pavements, University of Michigan, pp. 476-498.
- Monismith, C.L., G.A. Secor and K.E. Secor, 1965. "Temperature Induced Stresses and Deformations in Asphalt Concrete", Proceedings of the Association of Asphalt Paving Technologists, Vol. 34, pp. 248-279.

- Monismith, C.L., R.L. Alexander and K.E. Secor, 1966. "Rheologic Behavior of Asphalt Concrete", Proceedings of the Association of Asphalt Paving Technologists, Vol. 35, pp. 400-441.
- Nerseova, Z.A. and N.A. Tsytoich, 1963. "Unfrozen Water in Frozen Soils", Proceedings of the International Conference on Permafrost, Lafayette, Indiana, pp. 230-234.
- Penner, E., M.D. Oosterbaan and R.W. Rodman, 1966. "Performance of City Pavement Structures Containing Foamed Plastic Insulation", Highway Research Record No. 128, pp. 1-17.
- Pfeiffer, J. Ph. and P.M. Van Doormaal, 1936. "The Rheological Properties of Asphaltic Bitumens", Journal of the Institute of Petroleum Technologists, No. 22.
- Puzinauskas, V.P., 1966. "Unprepared Discussion during Symposium on Non-Traffic Load Associated Cracking of Asphalt Pavements", Proceedings of the Association of Asphalt Paving Technologists, Vol. 35, pp. 342-343.
- Rader, L.F., 1935. "Investigations of the Physical Properties of Asphaltic Mixtures at Low Temperatures", Proceedings of the American Society for Testing Materials, Vol. 35, Part II, pp. 559-571.
- Rix, H.H., 1969. "Vertical Movements and Crack Width Changes on Highway Pavement Sections", Canadian Geotechnical Journal, Vol. VI, No. 3, pp. 253-270.
- Sanger, F.J., 1959. Discussion on "Frost Penetration: Relationship to Air Temperatures and Other Factors", by Kersten, M.S., Highway Research Board Bulletin No. 225.
- Sanger, F.J., 1963. "Degree Days and Heat Conduction in Soils", Proceedings of the International Conference on Permafrost, Lafayette, Indiana, pp. 253-262.
- Sayegh, G., 1967. "Viscoelastic Properties of Bituminous Mixtures", Proceedings of the Second International Conference on the Structural Design of Asphalt Pavements, University of Michigan, pp. 743-755.
- Scott, R.F., 1957. "Estimation of the Heat-Transfer Coefficient Between Air and the Ground Surface", Transactions, American Geophysical Union, Vol. 38, No. 1.
- Shields, B.P., 1964. "Current Studies on Transverse Cracking of Asphalt Pavements", Proceedings of the Conference on Recent Developments in the Design and Construction of Asphalt Pavements, The University of Alberta, pp. 127-147.

- Shields, B.P., 1966. "Unprepared Discussion during Symposium on Non-Traffic Load Associated Cracking of Asphalt Pavements", Proceedings of the Association of Asphalt Paving Technologists, Vol. 35, pp. 337-339.
- Shields, B.P. and K.O. Anderson, 1964. "Some Aspects of Transverse Cracking in Asphalt Pavements", Proceedings of the Canadian Technical Asphalt Association, Vol. IX, pp. 209-226.
- Shields, B.P., K.O. Anderson and J.M. Dacyszyn, 1969. "An Investigation of Low Temperature Cracking of Flexible Pavements", Proceedings of the Canadian Good Roads Association, pp. 273-307.
- Straub, A.L., H.N. Schenk, Jr. and F.E. Przybycien, 1968. "Bituminous Pavement Temperatures Related to Climate", Highway Research Record No. 256, pp. 53-77.
- Tons, E. and E.M. Krokosky, 1963. "Effect of Microaggregates on Tensile Strength of Bituminous Concrete", Proceedings of the Association of Asphalt Paving Technologists, Vol. 32, pp. 497-523.
- Van der Poel, C., 1954. "A General System Describing the Viscoelastic Properties of Bitumens and its Relation to Routine Test Data", Journal of Applied Chemistry, pp. 221-236.
- Vehrencamp, J.E., 1953. "Experimental Investigation of Heat Transfer at an Air-Earth Interface", Transactions, American Geophysical Union, Vol. 34, No. 1, pp. 22-29.
- Williams, P.J., 1968. "Properties and Behavior of Freezing Soils", Norwegian Geotechnical Institute Publication No. 72, Research Paper No. 359 of the Division of Building Research, National Research Council of Canada.
- Yong, R.N., 1965. "Soil Suction Effects on Partial Soil Freezing", Highway Research Record No. 68, pp. 31-42.
- Young, F.D., I. Deme, R.A. Burgess and O. Kopvillem, 1969. "Ste. Anne Test Road - Construction Summary and Performance After Two Years Service", Proceedings of the Canadian Good Roads Association, Vol. XIV, pp. 50-109.

APPENDIX A

COMPUTER PROGRAM FOR

PAVEMENT TEMPERATURE PREDICTIONS

APPENDIX A

COMPUTER PROGRAM FOR PAVEMENT TEMPERATURE PREDICTIONS

A.1. Introduction

This appendix contains details of a computer program developed for predicting temperatures in a one, two or three layered pavement structure. Temperature calculations are based on finite difference equations which have been formulated using an explicit procedure and assuming a one-dimensional heat transfer problem. These equations are as follows:

- 1) Temperatures within a component layer

$$T(x, t + \Delta t) = \frac{\alpha \Delta t}{\Delta x^2} [T(x - \Delta x, t) + T(x + \Delta x, t)] + \left[1 - \frac{2\alpha \Delta t}{\Delta x^2} \right] T(x, t) \quad (A-1)$$

- 2) Temperatures at the interface of component layers

$$T(x, t + \Delta t) = [2K_{i+1} \Delta t] T(x + \Delta x, t) + \left[1 - \frac{2K_i \Delta t}{I} - \frac{2K_{i+1} \Delta t}{I} \right] T(x, t) + \frac{2K_i \Delta t}{I} T(x - \Delta x, t) \quad (A-2)$$

- 3) Temperatures at an air-pavement surface boundary

$$T(x, t + \Delta t) = \frac{2\alpha \Delta t}{\Delta x^2} T(x + \Delta x, t) + \left(1 - \frac{2\alpha \Delta t}{\Delta x^2} \right) T(x, t) + \frac{2\alpha \Delta t}{K \Delta x} (Q_{\text{rad}} \pm Q_{\text{conv}}) \quad (A-3)$$

where

T	=	temperature,
x	=	depth,
t	=	time,
Δx and Δt	=	depth and time increments, respectively,
α	=	diffusivity,
K	=	thermal conductivity,
Q_{rad}	=	algebraic sum of short and long wave radiation heat fluxes,
Q_{conv}	=	heat flux resulting from convective heat transfer,
i	=	refers to the layer
I	=	$(\Delta x)^2 (\gamma_i C_i + \gamma_{i+1} C_{i+1})$, where γ and C are the dry density and mass heat capacity of the layers, respectively.

The program consists of a main program and nine subroutines. A listing of the program, compatible with the operations of an IBM-360 computer, is contained in this appendix. Within this listing many of the parameters used are defined and major program operations outlined. In the following section computations in the main program and each of the nine subroutines are described.

A.2. Program Operations

A generalized flow diagram for the entire program is shown in FIGURE A-1. From this figure, the operations of seven of the nine subroutines interact directly with those of the main program. Three of the subroutines, those titled Graphs, Graph1 and Graph2, have been

developed for Calcomp plotting of the calculated temperatures. When time-temperature plots are not required these three subroutines, together with those statements in the main program referring to Plot(s), Xlimit, and Graphs, should be deleted.

A.2.1. Main Program

The operations of the main program include specifying all input variables and the calling of subroutines for temperature calculations and plot displays. A flow diagram for the main program is shown in FIGURE A-2. With reference to this figure, operations within program involve the following sequence of events.

- 1) Input variables are specified.

These variables are defined in the program listing and are those used when calculating temperatures in two or three layered structures. For a one layered structure the number of layers (NL) must be specified as 2 and the fictitious uppermost layer, of an assumed thickness (TOL), is assigned identical thermal and physical properties as the layer under consideration.

- 2) Subroutines Boundary, Nodal and Depth are called.

Operations of these subroutines are given in subsections A.2.2, A.2.3 and A.2.4, respectively.

- 3) Initial temperature gradient is specified.

A temperature $TM(M,J)$ is assigned to each node point when time (J) is equal to 1. The number of nodes (KOA) equals (total thickness of the structure/depth increment, Δx) + 1.

The temperature of the deepest node ($M = KOA$) is assumed constant throughout the time period of temperature calculations.

4) Counters LLA, LLB and LLP are defined.

These counters, which are used throughout the entire program, direct program operations within subroutine Output where various commands for displaying the calculated temperatures are specified.

5) Climatic inputs are specified.

The date, air temperature and solar radiation values are read. The time of initial specified temperature and radiation values must correspond to the time at which the initial temperature gradient is defined. Solar radiation values are expressed in units of langley's per hour. However, radiation values in units such as Btu per hour may be specified provided that modifications are made within subroutine temperature as outlined in subsection A.2.7.

6) Subroutine Airsun, Temperature and Graphs are called.

Operations within these subroutines are described in subsections A.2.6, A.2.7 and A.2.8, respectively.

7) Temperature gradient is defined.

The last computed temperature gradient within a structure and for a given day's climatic input become equal to the first temperature gradient for the following day. Operations then return to set 5 where the date, air temperature and radiation values for the following day are read.

A.2.2. Subroutine Boundary

In subroutine Boundary multiplication constants of finite difference Equations (A-1), (A-2) and (A-3) are calculated. An outline of operations within this subroutine is shown in FIGURE A-3.

- 1) Diffusivity of each layer is calculated.

Using both unfrozen and frozen thermal properties the diffusivity of each layer is computed. These values are then multiplied by the mesh ratio ($\Delta t / \Delta x^2$) to obtain constants R_u and R_f for each component layer.

- 2) Latent heat released upon freezing of the lower layers is calculated.

Latent heat released upon freezing of the uppermost layer is assumed equal to zero. For each of the lower layers, latent heat released upon freezing (Btu per cubic foot) is evaluated by determining the product of, (1.44) (moisture content) (dry density) and the per cent of water frozen (PERWF) at temperature (F) which defines the limit of the "while" freezing condition.

- 3) Constants of the finite difference equations are computed.

Thermal conductivity, heat capacity, dry density values and time and depth increments specified in the main program are used to compute multiplication constants of the finite difference equations.

- 4) Temperature-apparent specific heat relationships of the lower layers are calculated.

Apparent specific heat values at the temperature limits defining the "while" freezing condition, temperatures B and F, are denoted as CWF and CF, respectively. During freezing, a linear relationship is assumed between the logarithm of these apparent specific heat values and temperatures B and F.

A.2.3. Subroutine Nodal

In this subroutine nodes at which temperatures are to be displayed in the output are determined. Temperatures at all nodes in the uppermost layer are displayed. For example, if the depth increment (DELX) equals 2 inches and the thickness of uppermost layer equals 6 inches then calculated temperatures at depths of 0,2,4 and 6 inches are shown in the output. The depth increment at which temperatures in the lower layers are displayed is controlled by the factor KMZ defined in the program listing of this subroutine.

A.2.4. Subroutine Depth

Subroutine depth calculates the depths of the nodes determined in subroutine nodal. These depths are shown in the output in the form of headings under which the calculated temperatures are printed. Using subroutines Graphs, Graph1 and Graph2 plots of these temperatures as a function of time can be obtained.

A.2.5. Subroutine Output

The operations in this subroutine, in which title headings, depths and temperatures are written, are described in the program listing. In addition to this output, commands are given for the last computed temperature gradient to be punched on cards. This temperature gradient, together with appropriate climatic variables, can be used as input to the main program when temperatures during the succeeding time period are to be calculated.

A.2.6. Subroutine Airsun

In this subroutine air temperature (TA) and solar radiation values (HS) are calculated at time increments of Δt (DELT). For these computations both air temperature and radiation values are assumed to vary linearly between the times in which they are specified in the main program.

A.2.7. Subroutine Temperature

This subroutine calculates temperatures in a pavement structure at time and depth increments of DELT and DELX, respectively. Program operations of this subroutine are outlined in the flow diagram shown in FIGURE A-4.

1) Surface temperature.

At time $J+1$ and depth M , $M=1$, the surface temperature T_M is calculated by means of Equation (A-1). Heat transfer by convection (CONV) is approximated by the product of convection coefficient, defined in the main program, and the difference

between air and pavement surface temperature at time (J). Heat transfer due to longwave radiation (RAD) is approximated by the product of emissivity (EM), Stefan-Boltzmann constant (SD) and difference between the fourth power of air and surface temperature. Shortwave radiation heat transfer is computed by multiplying the absorptivity of the surface (A) by the intensity of solar radiation (II) at time J. Since solar radiation values are specified in the main program in units of langleys per hour, a constant of 3.69 is used to obtain equivalent values in units of Btu per hour.

2) Temperature at depths.

At time J+1 the temperature at each node in the structure is determined. This computation is dependent on one of the three following conditions.

- a) whether the node is located at the interface of adjacent layers which are in an unfrozen or frozen state,
- b) whether the node is located within a layer which is in an unfrozen or frozen state, or
- c) whether the node is located within a layer(s) which is in a "while" freezing condition.

For each of these conditions the location of the node is defined by the magnitude of M with respect to the number of nodes in each layer. Unfrozen, frozen and freezing conditions

are defined by the magnitude of temperatures $TM(M-1,J)$, $TM(M,J)$ and $TM(M+1,J)$ with respect to the specified temperatures B and F defining the freezing zone.

3) Time interval for temperature display is specified.

In the program listing a time interval of 2 hours has been selected for temperature display. This time interval is defined by the summing factor SDEL which increases in magnitude by a factor of DELT with every increase in counter J.

4) Call Output.

If the factor SDEL, described in step 3, becomes equal to or greater than the selected time interval of temperature output subroutine Output is called. If this condition is not satisfied operations return to step 1, where temperature calculations for the following time step commence.

A.2.8. Subroutine Graphs

In this subroutine temperatures to be plotted are converted from array to vector notation. These temperatures are equivalent to those displayed in the output. This subroutine also calls for plot subroutines Graph1 and Graph2.

A.2.9. Subroutine Graph1

Subroutine Graph1 establishes a grid on which the temperatures are plotted. In the subroutine the scales selected for this grid are:

3 inches horz. = 24 hours

2 inches vert. = 10 degrees F.

A description of the structure is written in the upper lefthand corner of the grid and the ordinate is labeled.

A.2.10. Subroutine Graph2

In subroutine Graph2 calculated temperatures displayed in the output are plotted and for a given depth are shown as a continuous function of time. Having plotted one day's temperatures operations return to main program and step 5 described in subsection A.2.1.

THIS PROGRAM UTILIZES A FINITE DIFFERENCE TECHNIQUE TO
CALCULATE THE THERMAL REGIME IN A ONE, TWO OR THREE LAYERED
PAVEMENT STRUCTURE SUBJECTED TO VARIOUS CLIMATIC ENVIRONMENTS.
A ONE DIMENSIONAL HEAT CONDUCTION PROBLEM IS ASSUMED.

THE PROGRAM CONSISTS OF A MAIN PROGRAM AND NINE SUBROUTINES.
SIX OF THE NINE SUBROUTINES INTERACT TO CALCULATE AND WRITE OUT
THE GENERATED TEMPERATURES. THE FUNCTION OF THE THREE REMAINING
SUBROUTINES, THOSE ENTITLED GRAPHS, GRAPH1 AND GRAPH2, IS TO PLOT
THE GENERATED TEMPERATURES. WHEN PLOTS ARE NOT REQUIRED THESE THREE
SUBROUTINES COUPLED WITH THOSE STATEMENTS IN THE MAIN PROGRAM
REFERRING TO PLOT(S), XLIMIT AND GRAPHS SHOULD BE REMOVED.

MAIN PROGRAM *****

```
COMMON KU(3),KF(3),CU(3),CF(3),DDEN(3),WC(3),TOL(3),RU(3),RF(3),
1CWF(4),WDEN(3),NOP(3),HS(29),H(200),TA(30),TM(115,200),PERWF(2),
2TAT(200),TITLE1(20),TITLE2(20),IDEEP(30),SLOPE(3),BI(3),G(30),
3BUF(2048),DELX,KO,KMZ,NL,NOBC,NPB,LNPB,NPS,LNPS,KOA,TOTAL,
4LAST,LKL,KOLKL,KLK,KOLKLI,KOI,CA,CAF,CFF,CGF,CB,CBF,CC,CCF,CD,CDF,
5CE,CEF,CHF,CIF,B,F,DELT,JJJ,LLLL,RR,III,LLP,A,EM,UC,NOTI,X,
6TYME(30),M,ND,LLB,HR,LLA,J,INC
REAL KU,KF
INTEGER HR,X
CALL PLOTS(BUF,8192)
CALL XLIMIT(250.0)
```

THE FOLLOWING PARAMETERS ARE READ IN:

- ND - THE NUMBER OF DAYS FOR WHICH THE THERMAL REGIME IS
TO BE CALCULATED.
- NL - THE NUMBER OF LAYERS IN THE PAVEMENT STRUCTURE.
- INC - THE NODAL POINT NUMBER THAT DEFINES THE UPPERMOST DEPTH
IN THE LOWER LAYERS AT WHICH TEMPERATURES ARE TO
COMMENCE DISPLAY IN THE OUTPUT.
- X - THE NUMBER OF TEMPERATURES TO BE PLOTTED PER DAY
AT A GIVEN DEPTH IN THE STRUCTURE. (IF X=13 TEMPERATURES
ARE PLOTTED ON A BIHOURLY BASIS, MIDNIGHT TO MIDNIGHT.
IF X=25 TEMPERATURES ARE PLOTTED ON AN HOURLY BASIS.)
- JJJ - THE NUMBER OF AIR TEMPERATURES SPECIFIED PER DAY.
(IF JJJ=25 AIR TEMPERATURES ARE READ IN HOURLY,
MIDNIGHT TO MIDNIGHT.)
- LLLL- THE NUMBER OF SOLAR RADIATION READINGS SPECIFIED PER
DAY. (SIMILAR TO X AND JJJ ABOVE.)
- DELT- THE TIME INCREMENT IN HOURS AT WHICH THE TEMPERATURES
ARE TO BE CALCULATED.


```

C          DELX- THE DEPTH INCREMENT IN INCHES AT WHICH THE TEMPERATURES
C          ARE TO BE CALCULATED.
C          B   - THE TEMPERATURE AT WHICH FREEZING COMMENCES IN THE
C          SUBGRADE.
C
C          F   - THE TEMPERATURE AT WHICH A GIVEN PERCENTAGE OF WATER
C          IN THE SUBGRADE IS FROZEN.
C
C          READ(5,1)ND,NL,INC,X,JJJ,LLLL,DELT,DELX,B,F
C          1 FORMAT(6I5,4F10.3)
C
C          THE SURFACE COEFFICIENTS ARE READ IN;
C
C          A - ABSORPTIVITY
C          EM - EMISSIVITY
C          UC - CONVECTION COEFFICIENT (BTU/HR/DEGREE F/SQ FT)
C
C          READ(5,2)A,EM,UC
C          2 FORMAT(3F10.3)
C
C          THE FOLLOWING PARAMETERS ARE READ IN FOR EACH LAYER OF THE STRUCTURE;
C
C          KU - THE UNFROZEN THERMAL CONDUCTIVITY OF THE LAYER.
C          (BTU/HR/FT/DEGREE F)
C          KF - THE FROZEN THERMAL CONDUCTIVITY OF THE LAYER.
C          (BTU/HR/FT/DEGREE F)
C          CU - THE HEAT CAPACITY OF THE LAYER IN AN UNFROZEN
C          STATE.(BTU/LB/DEGREE F)
C          CF - THE HEAT CAPACITY OF THE LAYER IN A FROZEN
C          STATE.(BTU/LB/DEGREE F)
C          DDEN- THE DRY DENSITY OF THE LAYER.(LB/CUBIC FT)
C          WC - THE MOISTURE CONTENT OF THE LAYER.
C          (PERCENT OF DRY UNIT WEIGHT)
C          TOL - THE THICKNESS OF THE LAYER.(INCHES)
C
C          DO 4 JT=1,NL
C          READ(5,3)KU(JT),KF(JT),CU(JT),CF(JT),DDEN(JT),WC(JT),TOL(JT)
C          3 FORMAT(7F10.3)
C          4 CONTINUE
C
C          THE PERCENT OF WATER FROZEN AT TEMPERATURE F IS READ IN FOR
C          EACH LAYER WITH THE EXCEPTION OF LAYER ONE,THE PAVEMENT.(IF PERWF=0.0
C          TEMPERATURES ARE CALCULATED ON THE BASIS OF THE UNFROZEN
C          PROPERTIES OF THE LAYER.IF PERWF=100.0 TEMPERATURES ARE
C          CALCULATED ON THE BASIS OF THE FROZEN PROPERTIES OF THE LAYER.IF
C          PERWF>0.0 OR < 100.0 LATENT HEAT IS CONSIDERED IN A MOVING ZONE OF
C          FREEZING BETWEEN THE SPECIFIED TEMPERATURES B AND F.)
C
C          DO 6 NLF=2,NL
C          READ(5,5)PERWF(NLF)

```



```

5 FORMAT(1F10.3)
6 CONTINUE

C
C      TITLE1 APPEARS ON EACH PAGE OF OUTPUT AND AS A TITLE ON THE PLOTS.
C
      READ(5,7)(TITLE1(I),I=1,20)
7 FORMAT(20A4)
      CALL BRDY
      CALL NODAL
      CALL DEPTH

C
C      THE INITIAL TEMPERATURE GRADIENT IS SPECIFIED.THE GRADIENT
C      CONSISTS OF A TEMPERATURE FOR EACH NODAL POINT.THE TEMPERATURE OF THE
C      DEEPEST NODE IS ASSUMED CONSTANT THROUGHTOUT THE TIME PERIOD IN
C      WHICH THE TEMPERATURES ARE BEING CALCULATED.
C
      J=1
      READ(5,8)(TM(M,J),M=1,KOA)
8 FORMAT(8F10.1)
      LLA=0
      LLB=0
      LLP=1
      DO 150 III=1,ND
      HR=0

C
C      DAILY DATA IS READ IN.
C
C      TITLE2 - THE DATE
C      TA - AIR TEMPERATURES(DEGREES FAHRENHEIT)
C      HS - SOLAR RADIATION VALUES(LANGLEYS PER HOUR)
C
      READ(5,9)(TITLE2(I),I=1,20)
9 FORMAT(20A4)
      CALL OUTPUT
      READ(5,10)(TA(J),J=1,JJJ)
10 FORMAT(13F6.1)
      READ(5,11)(HS(J),J=1,LLLL)
11 FORMAT(13F6.1)
      CALL AIRSUN
      CALL TEMP
      CALL GRAPHS
      J=1
      DO 12 M=1,KOA
      TM(M,J)=TM(M,NOT I)
12 CONTINUE
150 CONTINUE
      LLB=1
      CALL OUTPUT
      CALL PLOT(0.0,0.0,999)
      STOP
      END

```


SUBROUTINE BRDY

SUBROUTINE BOUNDARY

SUBROUTINE BOUNDARY CALCULATES THE HEAT CONDUCTION PARAMETERS OF THE ENERGY BALANCE EQUATIONS AT THE AIR-SURFACE AND ADJACENT LAYER INTERFACES.

COMMON KU(3),KF(3),CU(3),CF(3),DDEN(3),WC(3),TOL(3),RU(3),RF(3),
1CWF(4),WDEN(3),NOP(3),HS(29),H(200),TA(30),TM(115,200),PERWF(2),
2TAT(200),TITLE1(20),TITLE2(20),IDEEP(30),SLOPE(3),BI(3),G(30),
3BUIF(2048),DELX,KO,KMZ,NL,NDBC,NPB,LNPB,NPS,LNPS,KOA,TOTAL,
4LAST,LKL,KOLKL,KLK,KOLKL1,KO1,CA,CAF,CFF,CGF,CB,CBF,CC,CCF,CD,CDF,
5CE,CEF,CHF,CIF,B,F,DELT,JJJ,LLLL,RR,III,LLP,A,EM,UC,NOTI,X,
6TYME(30),M,ND,LLB,HR,LLA,J,INC
REAL KU,KF,NOP
TOTAL=0.0

THE DIFFUSIVITY OF EACH LAYER IS CALCULATED.

DO 2 JT=1,NL
RU(JT)=(KU(JT)/(CU(JT)*DDEN(JT)))*DELT/((DELX/12.)**2)
RF(JT)=(KF(JT)/(CF(JT)*DDEN(JT)))*DELT/((DELX/12.)**2)
TOTAL=TOL(JT)+TOTAL
2 CONTINUE

THE LATENT HEAT IS CALCULATED IN ACCORDANCE WITH THE PERCENTAGE OF WATER FROZEN AT TEMPERATURE F SPECIFIED IN THE MAIN PROGRAM.

DO 4 NLF=2,NL
WDEN(NLF)=DDEN(NLF)*(1.+(WC(NLF)/100.))
CWF(NLF)=(1.44*WC(NLF)*(PERWF(NLF)/100.)*DDEN(NLF))/WDEN(NLF)
4 CONTINUE
NOP(1)=TOL(1)/DELX+1.
KO=NOP(1)
RR=(2.*(KU(1)/(CU(1)*DDEN(1)))*DELT)/(KU(1)*(DELX/12.))
TNP=TOTAL/DELX+1.
KOA=TNP

THE INTERFACE CONSTANTS OF THE FINITE DIFFERENCE EQUATIONS ARE DETERMINED.

IF(NL-2)10,8,6
6 CA=((DELX/12.)**2)*(DDEN(2)*CU(2)+DDEN(3)*CU(3))
CAF=((DELX/12.)**2)*(DDEN(2)*CF(2)+DDEN(3)*CF(3))
CFF=((DELX/12.)**2)*(DDEN(2)*CF(2)+DDEN(3)*CU(3))
CGF=((DELX/12.)**2)*(DDEN(2)*CU(2)+DDEN(3)*CF(3))
CB=2.*KU(3)*DELT


```

      CRF=2.*KF(3)*DELT
8  CC=2.*KU(1)*DELT
      CCF=2.*KF(1)*DELT
      CD=2.*KU(2)*DELT
      CDF=2.*KF(2)*DELT
      CE=((DELX/12.)**2)*(DDEN(1)*CU(1)+DDEN(2)*CU(2))
      CEF=((DELX/12.)**2)*(DDEN(1)*CF(1)+DDEN(2)*CF(2))
      CHF=((DELX/12.)**2)*(DDEN(1)*CF(1)+DDEN(2)*CU(2))
      CIF=((DELX/12.)**2)*(DDEN(1)*CU(1)+DDEN(2)*CF(2))
10  CONTINUE

```

```

C
C           THE RELATIONSHIP BETWEEN APPARENT SPECIFIC HEAT AND TEMPERATURE
C           IS DETERMINED FOR EACH OF THE LOWER LAYERS.
C

```

```

      DO 12 ID=2,NL
      SLOPE(ID)=(0.434*ALOG(CWF(ID))-0.434*ALOG(CF(ID)))/(0.434*ALOG(B)
1-0.434*ALOG(F))
      BI(ID)=0.434*ALOG(CWF(ID))-SLOPE(ID)*0.434*ALOG(B)
12  CONTINUE
      RETURN
      END

```


SUBROUTINE NODAL

SUBROUTINE NODAL

SUBROUTINE NODAL CALCULATES THE NODAL POINTS FOR WHICH THE
GENERATED TEMPERATURES ARE TO BE DISPLAYED IN THE OUTPUT.

```
COMMON KU(3),KF(3),CU(3),CF(3),DDEN(3),WC(3),TOL(3),RU(3),RF(3),
1CWF(4),WDEN(3),NOP(3),HS(29),H(200),TA(30),TM(115,200),PERWF(2),
2TAT(200),TITLE1(20),TITLE2(20),IDEEP(30),SLOPE(3),BI(3),G(30),
3BUF(2048),DELX,KO,KMZ,NL,NOBC,NPB,LNPB,NPS,LNPS,KOA,TOTAL,
4LAST,LKL,KOLKL,KLK,KOLKL1,KO1,CA,CAF,CFF,CGF,CB,CBF,CC,CCF,CD,CDF,
5SCE,CEF,CHF,CIF,B,F,DELT,JJJ,LLLL,RR,III,LLP,A,EM,UC,NOTI,X,
6TYME(30),M,ND,LLB,HR,LLA,J,INC
REAL NOP
```

TEMPERATURES AT ALL NODAL POINTS IN LAYER ONE ARE DISPLAYED
IN THE OUTPUT.

```
KO - THE NUMBER OF NODES IN LAYER ONE.
KMZ - THE NODAL INCREMENT IN THE LOWER LAYERS AT WHICH
      TEMPERATURES ARE TO BE WRITTEN. (IF KMZ=12 AND DELX=2.0
      INCHES, TEMPERATURES ARE WRITTEN AT 24 INCH INTERVALS.)
NOB - THE NUMBER OF NODES IN LAYER TWO.
NOBC - THE FIRST NODE IN LAYER TWO AT WHICH TEMPERATURES ARE
       WRITTEN.
LNPB - THE LAST NODE IN LAYER TWO AT WHICH TEMPERATURES ARE
       WRITTEN.
NPS - THE FIRST NODE IN LAYER THREE AT WHICH TEMPERATURES ARE
       WRITTEN.
```

```
SUM=-DELX
DO 1 NP=1,KO
SUM=DELX+SUM
1 CONTINUE
KMZ=12
NOP(2)=TOL(2)/DELX
NOB=NOP(2)
NOBC=KO+INC
NPB=NOB+KO
ABZ=KMZ
AB=ABZ*DELX
IF(NPB .LT. NOBC) GO TO 5
STOT=TOL(1)+TOL(2)
DO 3 NB=NOBC,NPB,KMZ
AC=STOT-SUM
IF(AC .LT. AB) GO TO 7
SUM=SUM+AB
```



```
LNPB=NB
NRE=NPB-NB
IF(NRE .LT. KMZ) GO TO 7
3 CONTINUE
5 NOBC=KO+1
LNPB=KO+1
SUM=SUM+DELX
7 CONTINUE
IF(NL .LT. 3) GO TO 11
NPS=LNPB+6
DO 9 NS=NPS,KOA,KMZ
AS=TOTAL-SUM
IF(AS .LT. AB) GO TO 11
SUM=SUM+AB
LNPS=NS
NER=KOA-NS
IF(NER .LT. KMZ) GO TO 11
9 CONTINUE
11 RETURN
END
```



```

C      SUBROUTINE DEPTH
C
C      SUBROUTINE DEPTH
C      *****
C
C      SUBROUTINE DEPTH CALCULATES THE DEPTHS WITHIN THE PAVEMENT
C      STRUCTURE OF THOSE NODAL POINTS DETERMINED IN SUBROUTINE NODAL.
C
C
C      COMMON KU(3),KF(3),CU(3),CF(3),DDEN(3),WC(3),TOL(3),RU(3),RF(3),
1 CWF(4),WDEN(3),NOP(3),HS(29),H(200),TA(30),TM(115,200),PERWF(2),
2 TAT(200),TITLE1(20),TITLE2(20),IDEEP(30),SLOPE(3),BI(3),G(30),
3 BUF(2048),DELX,KO,KMZ,NL,NOBC,NPB,LNPB,NPS,LNPS,KOA,TOTAL,
4 LAST,LKL,KOLKL,KLK,KOLKL1,KOI,CA,CAF,CFF,CGF,CB,CBF,CC,CCF,CD,CDF,
5 SCE,CEF,CHF,CIF,B,F,DELT,JJJ,LLLL,RR,III,LLP,A,EM,UC,NOTI,X,
6 TYME(30),M,ND,LLB,HR,LLA,J,INC
      I=1
      JUD=DELX
      DO 2 NP=1,KO
      IDEEP(I)=JUD*NP-JUD
      I=I+1
2 CONTINUE
      LAST=KO
      LKL=0
      DO 4 NB=NOBC,LNPB,KMZ
      IDEEP(I)=JUD*NB-JUD
      I=I+1
      LKL=LKL+1
4 CONTINUE
      KOI=KO+1
      KOLKL=KO+LKL
      LAST=KOLKL
      IF(NL .LT. 3) GO TO 8
      KLK=0
      DO 6 NS=NPS,LNPS,KMZ
      IDEEP(I)=JUD*NS-JUD
      I=I+1
      KLK=KLK+1
6 CONTINUE
      KOLKL1=KOLKL+1
      LAST=KO+LKL+KLK
8 RETURN
      END

```


SUBROUTINE OUTPUT

SUBROUTINE OUTPUT

SUBROUTINE OUTPUT WRITES OUT THE DEPTHS CALCULATED IN
SUBROUTINE DEPTH AND THE TEMPERATURES AT THESE DEPTHS .THIS
SUBROUTINE ALSO CALLS FOR THE PUNCHING OF THE LAST TEMPERATURE
GRADIENT WITHIN THE STRUCTURE.THIS TEMPERATURE GRADIENT BECOMES THE
INITIAL TEMPERATURE GRADIENT TO BE SPECIFIED IN THE MAIN PROGRAM
FOR THE SUCCEEDING TIME PERIOD IN WHICH THE THERMAL REGIME IS TO
BE CALCULATED.

```
COMMON KU(3),KF(3),CU(3),CF(3),DDEN(3),WC(3),TOL(3),RU(3),RF(3),
1CWF(4),WDEN(3),NUP(3),HS(29),H(200),TA(30),TM(115,200),PERWF(2),
2TAT(200),TITLE1(20),TITLE2(20),IDEEP(30),SLOPE(3),BI(3),G(30),
3BUF(2048),DELX,KO,KMZ,NL,NOBC,NPB,LNPB,NPS,LNPS,KOA,TOTAL,
4LAST,LKL,KOLKL,KLK,KOLKL1,KO1,CA,CAF,CFF,CGF,CB,CBF,CC,CCF,CD,CDF,
5SCE,CEF,CHF,CIF,B,F,DELT,JJJ,LLLL,RR,III,LLP,A,EM,UC,NOTI,X,
6TYME(30),M,ND,LLB,HR,LLA,J,INC
  INTEGER HR
  IF(LLA .EQ. 1) GO TO 27
  IF(LLB .EQ. 1) GO TO 35
  IF(III-LLP)23,1,23
1  LLP=LLP+3
```

HEADINGS FOR THE OUTPUT ARE WRITTEN.

```
WRITE(6,3)(TITLE1(I),I=1,20)
3  FORMAT(1H1,/25X,20A4/)
  WRITE(6,5)
5  FORMAT(50X,15HDEPTH IN INCHES//)
  IF(NL-2)11,11,7
7  WRITE(6,9)
9  FORMAT(2X,3HHR.,18X,7HLAYER 1,23X,7HLAYER 2,25X,7HLAYER 3//)
  GO TO 15
11 WRITE(6,13)
13 FORMAT(2X,3HHR.,18X,7HLAYER 1,35X,7HLAYER 2//)
```

THE DEPTHS WITHIN THE STRUCTURE ARE WRITTEN.

```
15 WRITE(6,17)(IDEEP(I),I=1,KO)
17 FORMAT(5X,7I5)
  WRITE(6,19)(IDEEP(I),I=KO1,KOLKL)
19 FORMAT(1H+,40X,9I5)
  IF(NL .LT. 3) GO TO 23
  WRITE(6,21)(IDEEP(I),I=KOLKL1,LAST)
21 FORMAT(1H+,60X,10I5)
```



```

C           THE DATE IS WRITTEN.
C
23 WRITE(6,25)(TITLE2(I),I=1,20)
25 FORMAT(/20X,20A4/)
   J=0
C
C           THE GENERATED TEMPERATURES ARE WRITTEN AT A TIME INTERVAL
C           SELECTED IN SUBROUTINE TEMPERATURE.
C
27 WRITE(6,29)HR,(TM(M,J+1),M=1,KC)
29 FORMAT(3X,I2,7F5.1)
   WRITE(6,31)(TM(M,J+1),M=NOBC,LNPB,KMZ)
31 FORMAT(1H+,40X,9F5.1)
   IF(NL .LT. 3) GO TO 43
   WRITE(6,33)(TM(M,J+1),M=NPS,LNPS,KMZ)
33 FORMAT(1H+,60X,10F5.1)
   GO TO 43
C
C           THE LAST TEMPERATURE GRADIENT IN THE STRUCTURE IS WRITTEN AND
C           PUNCHED ON CARDS.
C
35 WRITE(6,37)
37 FORMAT(1H1,5X,25HLAST TEMPERATURE GRADIENT)
   DO 39 M=1,KOA,8
   L=M+7
   IF(L .GT. KOA) L=KOA
   WRITE(6,41)(TM(N,1),N=M,L)
   WRITE(7,41)(TM(N,1),N=M,L)
39 CONTINUE
41 FORMAT(8(1X,F9.2))
43 RETURN
   END

```


SUBROUTINE TEMP

SUBROUTINE TEMPERATURE

SUBROUTINE TEMPERATURE CALCULATES THE TEMPERATURES WITHIN THE
PAVEMENT STRUCTURE AT EACH NODAL POINT AND AT EACH TIME INCREMENT
AS DEFINED BY DELX AND DELT RESPECTIVELY.

```
COMMON KU(3),KF(3),CU(3),CF(3),DDEN(3),WC(3),TOL(3),RU(3),RF(3),
1CWF(4),WDEN(3),NOP(3),HS(29),H(200),TA(30),TM(115,200),PERWF(2),
2TAT(200),TITLE1(20),TITLE2(20),IDEEP(30),SLOPE(3),BI(3),G(30),
3BUF(2048),DELX,KO,KMZ,NL,NOBC,NPB,LNPB,NPS,LNPS,KOA,TOTAL,
4LAST,LKL,KOLKL,KLK,KOLKL1,KO1,CA,CAF,CFF,CGF,CB,CBF,CC,CCF,CD,CDF,
5CE,CEF,CHF,CIF,B,F,DELT,JJJ,LLLL,RR,III,LLP,A,EM,UC,NOTI,X,
6TYME(30),M,ND,LLB,HR,LLA,J,INC
REAL KU,KF
INTEGER HR
DL=24./DELT
NOT=DL
NOTI=NOT+1
JFC=KOA-1
SDEL=0.0
SD=.1714E-08
```

THE TIME DURING THE DAY AT WHICH THE TEMPERATURES ARE BEING
CALCULATED IS DEFINED BY J.

```
DO 67 J=1,NOT
M=1
CONV=UC*(TAT(J)-TM(M,J))
RAD=EM*SD*(((TAT(J)+460.))**4)-(((TM(M,J)+460.))**4))
BC=(3.69*A*H(J))+CONV+RAD
TM(M,J+1)=(1.-2.*RU(1))*TM(M,J)+(2.*RU(1)*TM(M+1,J))+(RR*BC)
TM(KOA,J+1)=TM(KOA,J)
```

THE TEMPERATURE AT EACH NODAL POINT IN THE STRUCTURE IS
DETERMINED AT TIME J.

```
DO 61 M=2,JFC
IF(M-KO)29,1,3
1 IF(TM(M-1,J) .LT. B .AND. TM(M+1,J) .LT. B) GO TO 13
IF(TM(M-1,J) .LT. B .AND. TM(M+1,J) .GT. B) GO TO 15
IF(TM(M-1,J) .GT. B .AND. TM(M+1,J) .LT. B) GO TO 17
GO TO 19
3 IF(NL .LE. 2) GO TO 9
IF(M-NPB)7,11,5
5 IF(TM(M-1,J) .GT. F .AND. TM(M-1,J) .LT. B .AND. TM(M+1,J) .GT. F
1 .AND. TM(M+1,J) .LT. B) GO TO 51
```



```

      IF(M .GT. NPB .AND. TM(M,J) .GT. B) GO TO 31
      IF(M .GT. NPB .AND. TM(M,J) .LE. B) GO TO 37
7    IF(TM(M-1,J) .GT. F .AND. TM(M-1,J) .LT. B .AND. TM(M+1,J) .GT. F
      1 .AND. TM(M+1,J) .LT. B) GO TO 43
      IF(TM(M,J)-B)39,39,33
9    IF(M .GT. KO .AND. TM(M-1,J) .GT. F .AND. TM(M-1,J) .LT. B .AND.
      1 TM(M+1,J) .GT. F .AND. TM(M+1,J) .LT. B) GO TO 43
      IF(M .GT. KO .AND. TM(M,J) .GT. F) GO TO 33
      IF(M .GT. KO .AND. TM(M,J) .LE. F) GO TO 39
11   IF(TM(M-1,J) .LT. B .AND. TM(M+1,J) .LT. B) GO TO 21
      IF(TM(M-1,J) .LT. B .AND. TM(M+1,J) .GT. B) GO TO 23
      IF(TM(M-1,J) .GT. B .AND. TM(M+1,J) .LT. B) GO TO 25
      GO TO 27

```

C
C
C
C

TEMPERATURES AT NODAL POINTS AT INTERFACE BOUNDARIES ARE
CALCULATED.

```

13   TM(M,J+1)=TM(M,J)*(1.-CCF/CEF-CDF/CEF)+TM(M-1,J)*(CCF/CEF)+TM(M+1,
      1 J)*(CDF/CEF)
      GO TO 61
15   TM(M,J+1)=TM(M,J)*(1.-CCF/CHF-CD/CHF)+TM(M-1,J)*(CCF/CHF)+TM(M+1,J
      1)*(CD/CHF)
      GO TO 61
17   TM(M,J+1)=TM(M,J)*(1.-CC/CIF-CDF/CIF)+TM(M-1,J)*(CC/CIF)+TM(M+1,J)
      1*(CDF/CIF)
      GO TO 61
19   TM(M,J+1)=TM(M,J)*(1.-CC/CE-CD/CE)+TM(M-1,J)*(CC/CE)+TM(M+1,J)*(CD
      1/CE)
      GO TO 61
21   TM(M,J+1)=TM(M,J)*(1.-CDF/CAF-CBF/CAF)+TM(M-1,J)*(CDF/CAF)+TM(M+1,
      1 J)*(CBF/CAF)
      GO TO 61
23   TM(M,J+1)=TM(M,J)*(1.-CDF/CFF-CB/CFF)+TM(M-1,J)*(CDF/CFF)+TM(M+1,J
      1)*(CB/CFF)
      GO TO 61
25   TM(M,J+1)=TM(M,J)*(1.-CD/CGF-CBF/CGF)+TM(M-1,J)*(CD/CGF)+TM(M+1,J)
      1*(CBF/CGF)
      GO TO 61
27   TM(M,J+1)=TM(M,J)*(1.-CD/CA-CB/CA)+TM(M-1,J)*(CD/CA)+TM(M+1,J)*(CB
      1/CA)
      GO TO 61
29   NZ=1
      GO TO 35
31   NZ=3
      GO TO 35
33   NZ=2

```

C
C
C
C

TEMPERATURES AT NODAL POINTS IN A FROZEN OR UNFROZEN ZONE
WITHIN A LAYER ARE CALCULATED.


```

35 TM(M,J+1)=(RU(NZ)*TM(M-1,J))+(1.-2.*RU(NZ))*TM(M,J)+RU(NZ)*TM(M+1,
  1J)
  GO TO 61
37 NZ=3
  GO TO 41
39 NZ=2
41 TM(M,J+1)=(RF(NZ)*TM(M-1,J))+(1.-2.*RF(NZ))*TM(M,J)+RF(NZ)*TM(M+1,
  1J)
  GO TO 61
43 NZ=2

```

C
C
C
C

TEMPERATURES AT NODAL POINTS WITHIN A ZONE OF FREEZING ARE
CALCULATED.

```

  IF(PERWF(NZ) .EQ. 100.) GO TO 45
  IF(PERWF(NZ) .EQ. 0.0) GO TO 47
  GO TO 49
45 RWF=RF(NZ)
  GO TO 59
47 RWF=RU(NZ)
  GO TO 59
49 BF=(SLOPE(NZ)*.434*ALOG(TM(M,J))+BI(NZ))/(0.434)
  CBWF=EXP(BF)
  RWF=((KU(NZ)+KF(NZ))/2.)/(CBWF*DDEN(NZ))*DELT/((DELT/12.)**2)
  GO TO 59
51 NZ=4
  IF(PERWF(NZ-1) .EQ. 100.) GO TO 53
  IF(PERWF(NZ-1) .EQ. 0.0) GO TO 55
  GO TO 57
53 RWF=RF(NZ-1)
  GO TO 59
55 RWF=RU(NZ-1)
  GO TO 59
57 BF=(SLOPE(NZ-1)*.434*ALOG(TM(M,J))+BI(NZ-1))/(0.434)
  CBWF=EXP(BF)
  RWF=((KU(NZ-1)+KF(NZ-1))/2.)/(CBWF*DDEN(NZ-1))*DELT/((DELT/12.)*
  1**2)
59 TM(M,J+1)=RWF*TM(M-1,J)+(1.-2.*RWF)*TM(M,J)+RWF*TM(M+1,J)
61 CONTINUE
  SDEL=SDEL+DELT

```

C
C
C
C

THE TIME INTERVAL AT WHICH THE TEMPERATURES ARE TO BE
WRITTEN IS SELECTED.(THE TIME INTERVAL SELECTED IS 2 HOURS.)

```

  IF(SDEL .GE. 2.) GO TO 63
  GO TO 67
63 HR=HR+2
  LLA=1
  CALL OUTPUT
65 SDEL=0.0
  LLA=0
67 CONTINUE
  RETURN
  END

```


SUBROUTINE GRAPHS

C
C
C
C
C
C
C
C
C

SUBROUTINE GRAPHS

THIS SUBROUTINE CONVERTS THE TEMPERATURES TO BE PLOTTED FROM
ARRAY TO VECTOR NOTATION AND CALLS FOR THE PLOTTING OF THESE
TEMPERATURES.

```

COMMON KU(3),KF(3),CU(3),CF(3),DDEN(3),WC(3),TOL(3),RU(3),RF(3),
1CWF(4),WDEN(3),NOP(3),HS(29),H(200),TA(30),TM(115,200),PERWF(2),
2TAT(200),TITLE1(20),TITLE2(20),IDEEP(30),SLOPE(3),BI(3),G(30),
3BUF(2048),DELX,KO,KMZ,NL,NOBC,NPB,LNPB,NPS,LNPS,KOA,TOTAL,
4LAST,LKL,KOLKL,KLK,KOLKL1,KO1,CA,CAF,CFF,CGF,CB,CBF,CC,CCF,CD,CDF,
5CE,CEF,CHF,CIF,B,F,DELT,JJJ,LLLL,RR,III,LLP,A,EM,UC,NOTI,X,
6TYME(30),M,NO,LLB,HR,LLA,J,INC
  IF(III .GT. 1) GO TO 2
  CALL GRAPH1
2 CONTINUE
  JUDE=DELX
  DO 10 M=1, LAST
    IF(M .EQ. 1) GO TO 4
    I=(IDEEP(M)+JUDE)/JUDE
    GO TO 6
  4 I=1
  6 KK=1
    TU=1./DELT
    JU=TU
    DO 8 J=1, NOTI, JU
      G(KK)=TM(I,J)
      KK=KK+1
  8 CONTINUE
    KK=KK-1
    CALL GRAPH2
10 CONTINUE
  RETURN
  END

```


SUBROUTINE GRAPH1

SUBROUTINE GRAPH1

SUBROUTINE GRAPH1 ESTABLISHES A GRID ON WHICH THE TEMPERATURES
ARE PLOTTED.

COMMON KU(3),KF(3),CU(3),CF(3),DDEN(3),WC(3),TOL(3),RU(3),RF(3),
1CWF(4),WDEN(3),NOP(3),HS(29),H(200),TA(30),TM(115,200),PERWF(2),
2TAT(200),TITLE1(20),TITLE2(20),IDEEP(30),SLOPE(3),BI(3),G(30),
3BUF(2048),DELX,KO,KMZ,NL,NOBC,NPB,LNPH,NPS,LNPS,KOA,TOTAL,
4LAST,LKL,KOLKL,KLK,KOLKL1,KO1,CA,CAF,CFF,CGF,CB,CBF,CC,CCF,CD,CDF,
5CE,CEF,CHF,CIF,B,F,DELT,JJJ,LLLL,RR,III,LLP,A,EM,UC,NOTI,X,
6TYME(30),M,ND,LLB,HR,LLA,J,INC

ALEN - THE LENGTH OF THE PLOT. (SCALE:3 INCHES HORZ.=1 DAY)
THE MAXIMUM NUMBER OF DAYS THAT CAN BE PLOTTED IS
CONTROLLED BY XLIMIT IN THE MAIN PROGRAM.

ALEN=ND*3
CALL PLOT(4.00,0.21,-3)
CALL GRID(0.0,0.0,ALEN,2.0,1,13)

TITLE1 PLUS STRUCTURE DESCRIPTION IS WRITTEN.

CALL SYMBOL(1.0,25.0,0.5,TITLE1,0.0,80)
CALL SYMBOL(3.80,24.3,0.35,14H4 INCH SURFACE,0.0,14)
CALL SYMBOL(3.80,23.3,0.35,18H6 INCH BASE COURSE,0.0,18)
CALL SYMBOL(3.80,22.3,0.35,13HSAND SUBGRADE,0.0,13)

THE COORINATES OF THE GRID ARE LABELED FROM -50 DEG. F TO +80
DEG. F. (SCALE:2 INCHES VERT.=10 DEGREES F)

TEMP=-50.0
Y=-0.2
DO 14 I=1,5
CALL NUMBER(-1.40,Y,0.40,TEMP,0.0,-1)
Y=Y+2.0
TEMP=TEMP+10.
14 CONTINUE
CALL NUMBER(-0.60,Y,0.40,TEMP,0.0,-1)
DO 16 I=1,8
Y=Y+2.0
TEMP=TEMP+10.
CALL NUMBER(-1.00,Y,0.40,TEMP,0.0,-1)
16 CONTINUE
CALL SYMBOL(-2.0,7.70,0.60,21HTEMPERATURE (DEG. F.),90.0,21)
CALL PLOT(0.0,10.0,-3)
RETURN
END

SUBROUTINE GRAPH2

SUBROUTINE GRAPH2

SUBROUTINE GRAPH2 PLOTS THE CALCULATED TEMPERATURES AT
PREVIOUSLY DEFINED DEPTHS AS A CONTINUOUS FUNCTION OF TIME.

```
COMMON KU(3),KF(3),CU(3),CF(3),DDEN(3),WC(3),TOL(3),RU(3),RF(3),
1CWF(4),WDEN(3),NOP(3),HS(29),H(200),TA(30),TM(115,200),PERWF(2),
2TAT(200),TITLE1(20),TITLE2(20),IDEEP(30),SLOPE(3),BI(3),G(30),
3BUF(2048),DELX,KO,KMZ,NL,NOBC,NPB,LNPB,NPS,LNPS,KOA,TOTAL,
4LAST,LKL,KOLKL,KLK,KOLKL1,KO1,CA,CAF,CFF,CGF,CH,CBF,CC,CCF,CD,CDF,
5CE,CEF,CHF,CIF,B,F,DELT,JJJ,LLLL,RR,III,LLP,A,EM,UC,NOTI,X,
6TYME(30),M,ND,LLB,HR,LLA,J,INC
  INTEGER X
  IF(M.EQ. 1)GO TO 18
  GO TO 20
```

THE DATE AND TIME OF DAY ARE WRITTEN.

```
18 CALL SYMBOL(0.65,-7.90,0.15,TITLE2,0.0,80)
  CALL SYMBOL(-0.10,-8.20,0.16,2H24,0.0,2)
  CALL SYMBOL(0.95,-8.20,0.16,1H8,0.0,1)
  CALL SYMBOL(1.90,-8.20,0.16,2H16,0.0,2)
  CALL SYMBOL(2.90,-8.20,0.16,2H24,0.0,2)
  CALL SYMBOL(1.3,-8.35,0.12,4HRS.,0.0,4)
20 CONTINUE
  TYME(1)=0.0
  DO 26 I=2,X
  IF (X.EQ. 13) GO TO 22
  TYME(I)=I-1
  GO TO 24
22 TYME(I)=(I-1)*2
24 CONTINUE
26 CONTINUE
  TYME(X+1)=0.0
  TYME(X+2)=8.0
  G(X+1)=0.0
  G(X+2)=5.0
```

TEMPERATURES AT A GIVEN DEPTH ARE PLOTTED.

```
CALL LINE(TYME,G,X,1,0,0)
IF(M.EQ. LAST) GO TO 28
GO TO 30
28 CALL PLOT(3.0,0.0,-3)
30 RETURN
END
```

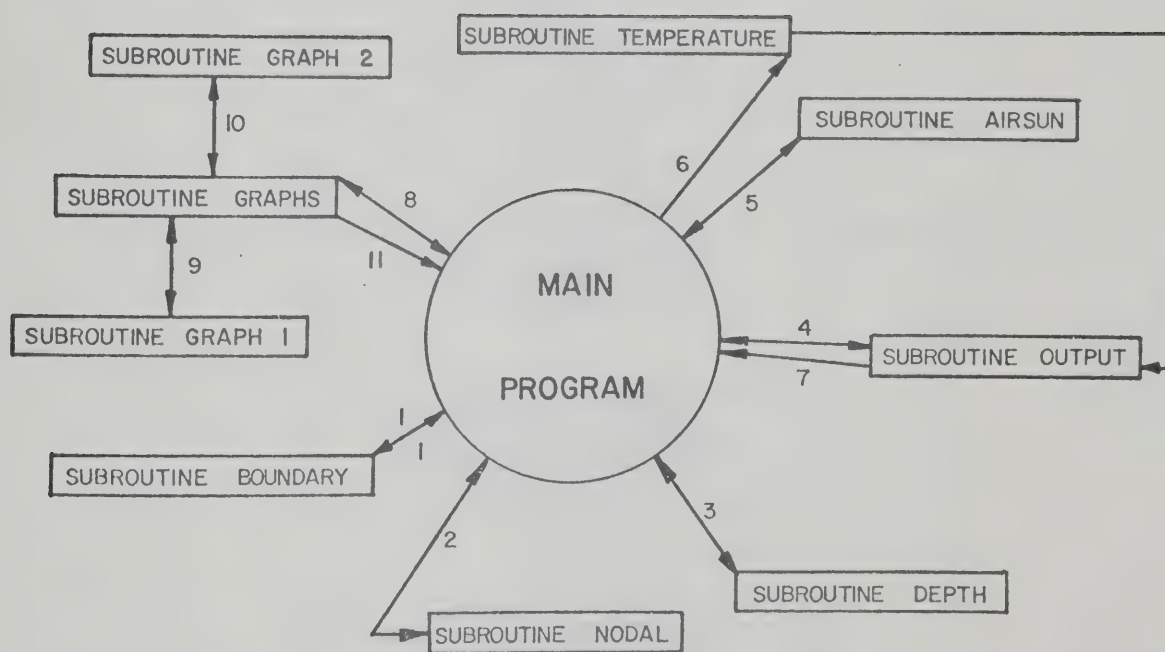



FIGURE A-1 GENERALIZED FLOW DIAGRAM OF TEMPERATURE PREDICTION PROGRAM.

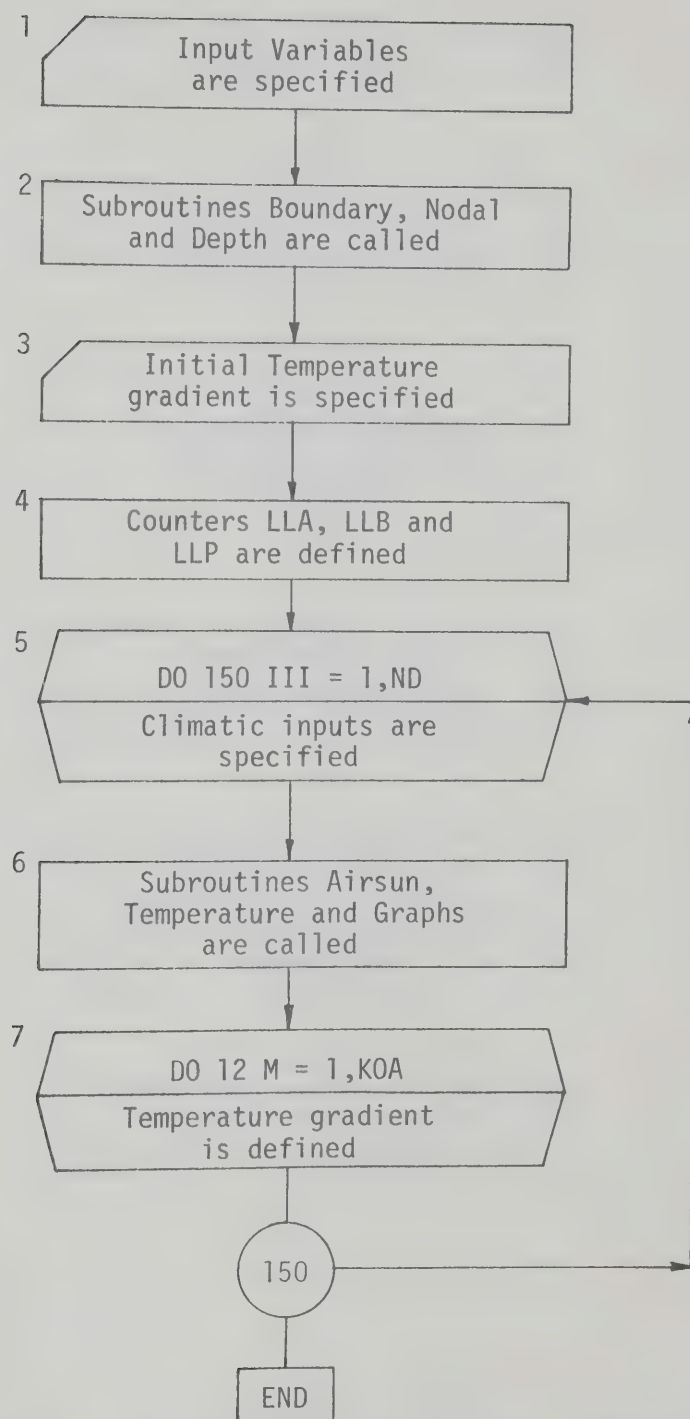


FIGURE. A-2 FLOW DIAGRAM FOR MAIN PROGRAM.

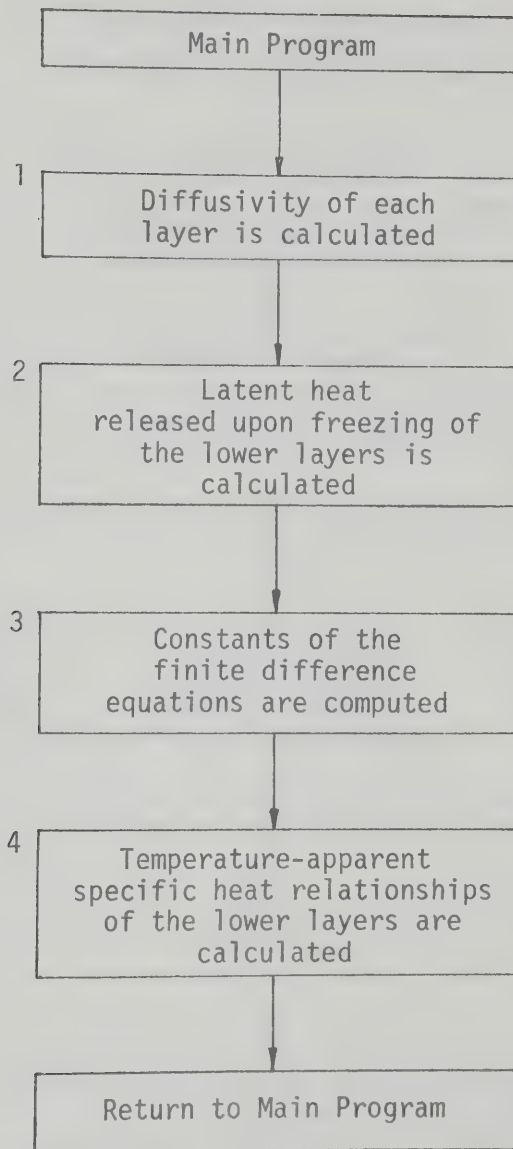


FIGURE. A-3 FLOW DIAGRAM FOR SUBROUTINE BOUNDARY.

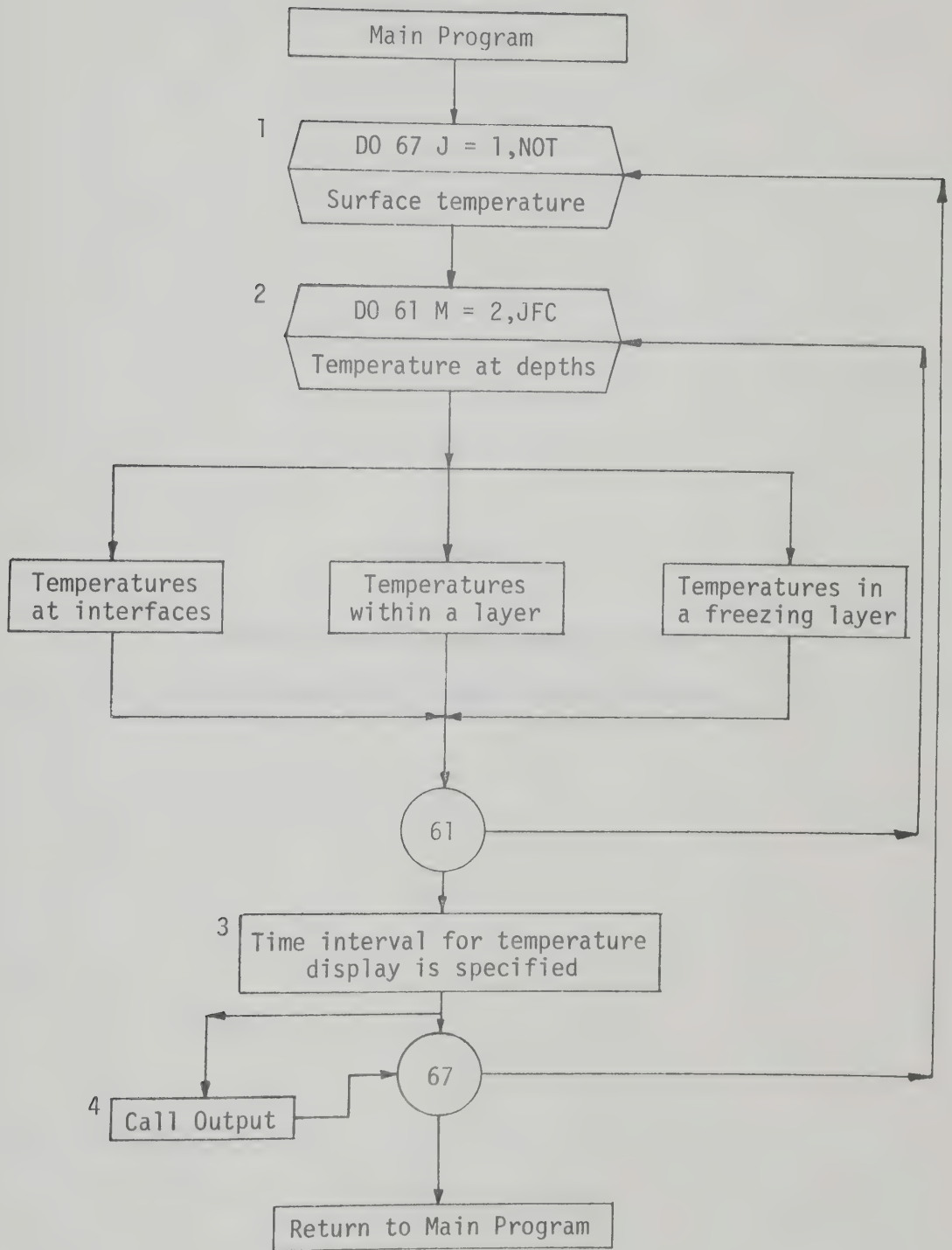


FIGURE. A-4 FLOW DIAGRAM FOR SUBROUTINE TEMPERATURE.

APPENDIX B

COMPUTER PROGRAM FOR THERMAL STRESS PREDICTIONS USING PSEUDO-ELASTIC ANALYSES

APPENDIX B

COMPUTER PROGRAM FOR THERMAL STRESS PREDICTIONS
USING PSEUDO-ELASTIC ANALYSESB.1. Introduction

This appendix contains details of a computer program for calculating thermal stresses in an asphaltic concrete subjected to a known temperature change. For these stress computations pseudo-elastic beam and slab analyses are used.

The stress equation for the pseudo-elastic beam analysis is

$$\sigma_x(t) = - \int_{t_0}^t S(\Delta t, T) \alpha_0(T) dT(t) \quad (B-1)$$

where $S(\Delta t, T)$ is the time and temperature dependent stiffness modulus and $\alpha_0(T)$ the coefficient of thermal expansion. To evaluate stress numerically Equation (B-1) is written as

$$\sigma_x(t_i) = \sigma_x(t_{i-1}) + (\Delta \sigma_x)_i \quad (B-2)$$

where

$$(\Delta \sigma_x)_i = - \int_{t_{i-1}}^{t_i} S(\Delta t, T) \alpha_0(T) dT(t) \quad (B-3)$$

Using the trapezoidal rule, with stiffnesses evaluated at times t_i and t_{i-1} and a loading time equal to the time step $t_i - t_{i-1}$, and assuming α_0 temperature independent, the stress increments in Equation (B-3) are computed by the expression

$$(\Delta\sigma_x)_i = \frac{\alpha_0}{2} (S_i + S_{i-1}) (T_i - T_{i-1}) \quad (B-4)$$

Approximate pseudo-elastic slab stresses are obtained by multiplying Equation (B-2) by the factor of $1/(1-\nu)$, where Poisson's ratio, ν , is assumed time and temperature independent.

B.2. Program Operations

The computer program consists of a main program and three subroutines, titled Readin, Linear and Stress. Operations within each of these four components are given in the following subsections.

B.2.1. Main Program

A flow diagram for the main program is shown in FIGURE B-1. Within this program all subroutines are called and all output commands are introduced.

B.2.2. Subroutine Readin

In this subroutine all parameters necessary for the numerical solution of Equation (B-2) are specified. These parameters are defined in the program listing.

B.2.3. Subroutine Linear

Linear relationships are assumed between the logarithms of stiffness and the logarithms of reduced time values, and between the logarithms of shift factor values and temperatures, specified in subroutine Readin. In subroutine Linear the coefficients of these relationships are computed. Such relationships enable the stiffness of the asphaltic concrete to be readily evaluated.

Temperatures (TT) at time increments of $t_i - t_{i-1}$ (DELT) are computed. For these computations, a linear temperature-time relationship is assumed over the time period INCTIM defined in the main program.

B.2.4. Subroutine Stress

In this subroutine thermal stresses (ST) are calculated at time increments of DELT. Using a loading time equal to DELT and knowing the temperature TT at each time step stiffness values are computed. Upon substituting these values into Equation (B-4), or the corresponding pseudo-elastic slab equation, the stress increment $(\Delta\sigma_x)_i$ (STR2) is calculated. In the program listing the initial stress $\sigma_x(t_0)$ (ST) is equated to zero.

Program operations return to the main program where temperatures and thermal stresses are written in time increments of NT defined in subroutine Linear as $(INCTIM)(60)/DELT$.

THIS PROGRAM USES A MODIFIED ELASTIC APPROACH TO
CALCULATE THE THERMAL STRESSES IN AN ASPHALTIC CONCRETE
SUBJECTED TO A KNOWN TEMPERATURE FIELD.

STRESSES ARE CALCULATED AT EQUAL TIME INTERVALS
OVER THE TOTAL TIME PERIOD IN WHICH THE TEMPERATURE FIELD
IS DEFINED.

THE PROGRAM CAN BE USED TO DETERMINE THE THERMAL STRESSES
ASSUMING ONE OF THE FOLLOWING CONDITIONS:

- 1) RESTRAINED BEAM, $E = \text{FUNCTION}(\text{REDUCED TIME})$
- 2) RESTRAINED SLAB, $E = \text{FUNCTION}(\text{REDUCED TIME})$

MAIN PROGRAM

```
COMMON TITLE1(20),T(15),AT(15),E(15),XI(15),A1(15),A2(15),B1(15),
1B2(15),TEMP(1300),TT(3000),E1(3000),ST(3000),NUMDAY,NUMEXI,NUMATT,
2DELT,ALPHA,U,CODE,NEXI1,NATT1,NN,NT,MT,STRI,NUMINC,INCTIM
CALL READIN
CALL LINEAR
DO 1 MT=1,NN
CALL STRESS
1 CONTINUE
WRITE(6,3)(TITLE1(I),I=1,20)
3 FORMAT(6X,20A4)
```

TEMPERATURES AND STRESSES ARE WRITTEN AT TIME INCREMENTS
CORRESPONDING TO THOSE AT WHICH THE TEMPERATURES WERE SPECIFIED.

```
DO 7 J=1,NN,NT
WRITE(6,5)TT(J),ST(J)
5 FORMAT(12X,2F10.1)
7 CONTINUE
STOP
END
```


SUBROUTINE READIN

SUBROUTINE READIN

THIS SUBROUTINE READS IN ALL DATA NECESSARY FOR THE
GENERATION OF THERMAL STRESSES. THIS DATA CAN BE DIVIDED INTO
THE FOLLOWING THREE CATEGORIES;

- 1) THE ASSUMPTION OF A RESTRAINED BEAM OR SLAB,
CONDITIONS 1 OR 2 MENTIONED PREVIOUSLY.
- 2) MATERIAL PROPERTIES.
- 3) TEMPERATURE AT A GIVEN DEPTH IN THE ASPHALTIC
CONCRETE AS A FUNCTION OF TIME.

COMMON TITLE1(20),T(15),AT(15),E(15),XI(15),A1(15),A2(15),B1(15),
1B2(15),TEMP(1300),TT(3000),E1(3000),ST(3000),NUMDAY,NUMEXI,NUMATT,
2DELTA,ALPHA,U,CODE,NEXI1,NATT1,NN,NT,MT,STRI,NUMINC,INCTIM

THE INPUT PARAMETERS ARE DEFINED AS FOLLOWS:

CODE - CODE=1.0 DENOTES CONDITION 1.

CODE=2.0 DENOTES CONDITION 2.

U - POISSONS RATIO. ONLY IF CONDITION 2 IS SPECIFIED

A VALUE OF POISSONS RATIO MUST BE READ IN.

NUMDAY - THE NUMBER OF DAYS IN WHICH THE TEMPERATURE
REGIME IS READ IN.

NUMEXI - THE NUMBER OF VALUES SPECIFIED FROM THE STIFFNESS MODULUS-
REDUCED TIME RELATIONSHIP.

NUMATT - THE NUMBER OF VALUES SPECIFIED FROM THE SHIFT FACTOR-
TEMPERATURE RELATIONSHIP.

INCTIM - THE TIME INCREMENT IN WHICH THE TEMPERATURE
REGIME IS SPECIFIED.(HRS)

DELTA - THE TIME INCREMENT IN WHICH THE THERMAL STRESSES
ARE TO BE CALCULATED.(MINS.)

ALPHA - THE COEFFICIENT OF THERMAL EXPANSION AND CONTRACTION
OF THE ASPHALTIC CONCRETE.(IN/IN/DEG F)

E - THE STIFFNESS MODULUS OF THE ASPHALTIC CONCRETE.(PSI)
THESE VALUES ARE TO BE READ IN IN DESCENDING ORDER
OF MAGNITUDE.

XI - REDUCED TIME.(SECS) THESE VALUES ARE SPECIFIED IN
ASCENDING ORDER OF MAGNITUDE AND MUST BE COMPATIBLE
WITH THE E VALUES.

AT - SHIFT FACTORS.

T - TEMPERATURES COMPATIBLE WITH THE SHIFT FACTORS.(DEG F)

TEMP - THE TEMPERATURES AT A GIVEN DEPTH WITHIN THE
ASPHALTIC CONCRETE.(DEG F)

READ(5,1)(TITLE1(I),I=1,20)

1 FORMAT(20A4)

READ(5,2)CODE

2 FORMAT(1F5.0)


```
      IF(CODE-2.0)8,4,8
4  READ(5,6)U
6  FORMAT(1F5.2)
   GO TO 10
8  U=0.0
10 READ(5,12)NUMDAY,NUMEXI,NUMATT,INCTIM,DELT,ALPHA
12 FORMAT(4I10,1F10.2,1E8.1)
   READ(5,14)(E(I),I=1,NUMEXI)
14 FORMAT(11E7.2)
   READ(5,16)(XI(I),I=1,NUMEXI)
16 FORMAT(11E7.1)
   READ(5,18)(AT(I),I=1,NUMATT)
18 FORMAT(9E7.2)
   READ(5,20)(T(I),I=1,NUMATT)
20 FORMAT(9F8.0)
   NUMINC=24/INCTIM
   NUMTEM=NUMINC*NUMDAY+1
   DO 24 L=1,NUMTEM
   READ(5,22)TEMP(L)
22 FORMAT(1F10.0)
24 CONTINUE
   RETURN
   END
```


SUBROUTINE LINEAR

```

C
C
C      SUBROUTINE LINEAR
C      *****
C
C      A LINEAR RELATIONSHIP IS ASSUMED BETWEEN LOG(E) AND
C      LOG(XI), AND LOG(AT) AND T VALUES. THIS SUBROUTINE CALCULATES
C      THE A AND B COEFFICIENTS OF THE RESULTING LINEAR EQUATIONS.
C      ALSO, TEMPERATURES OF THE ASPHALTIC CONCRETE AT TIME
C      INTERVALS OF DELT ARE CALCULATED.
C
C      COMMON TITLE1(20),T(15),AT(15),E(15),XI(15),A1(15),A2(15),B1(15),
C      1B2(15),TEMP(1300),TT(3000),E1(3000),ST(3000),NUMDAY,NUMEXI,NUMATT,
C      2DELT,ALPHA,U,CODE,NEXI1,NATT1,NN,NT,MT,STR1,NUMINC,INCTIM
C      NEXI1=NUMEXI-1
C      NATT1=NUMATT-1
C
C      THE A AND B COEFFICIENTS FOR THE LOG(E)-LOG(XI)
C      EQUATIONS ARE EVALUATED.
C
C      DO 1 J=1,NEXI1
C      A1(J)=-1.0*ALOG10(E(J)/E(J+1))
C      B1(J)=ALOG10(E(J))-A1(J)*ALOG10(XI(J))
C 1 CONTINUE
C
C      THE A AND B COEFFICIENTS FOR THE LOG(AT)-T EQUATIONS
C      ARE EVALUTED.
C
C      DO 3 J=1,NATT1
C      A2(J)=(ALOG10(AT(J))-ALOG10(AT(J+1)))/(T(J)-T(J+1))
C      B2(J)=ALOG10(AT(J))-A2(J)*T(J)
C 3 CONTINUE
C      STR1=0.0
C      TIME=INCTIM
C      NT=(TIME*60.)/DELT
C      NT1=NT+1
C      N=NUMDAY*NUMINC
C      NN=N*NT+1
C
C      TEMPERATURES (TT) AT INTERVALS OF DELT ARE CALCULATED.
C
C      TT(1)=TEMP(1)
C      L=2
C      DO 7 M=1,N
C      DO 5 LM=2,NT1
C      TT(L)=TEMP(M)+((TEMP(M+1)-TEMP(M))/NT)*(LM-1)
C      L=L+1
C 5 CONTINUE
C 7 CONTINUE
C      RETURN
C      END

```



```

C      SUBROUTINE STRESS
C
C          SUBROUTINE STRESS
C          *****
C
C          SUBROUTINE STRESS CALCULATES THERMAL STRESSES AT TIME
C          INTERVALS OF DELT.
C
C          COMMON TITLE1(20),T(15),AT(15),E(15),XI(15),A1(15),A2(15),B1(15),
1      B2(15),TEMP(1300),TT(3000),EI(3000),ST(3000),NUMDAY,NUMEXI,NUMATT,
2      DELT,ALPHA,U,CODE,NEXI1,NATT1,NN,NT,MT,STR1,NUMINC,INCTIM
C          DO 1 L=1,NATT1
C              IF(TT(MT) .LT. T(L) .AND. TT(MT) .GE. T(L+1)) GO TO 3
1      CONTINUE
C          A=AT(1)
C          GO TO 5
3      A=EXP((A2(L)*TT(MT)+B2(L))/0.434)
C
C          THE REDUCED TIME (XI1) AS A FUNCTION OF DELT AND
C          TEMPERATURE IS CALCULATED.
C
5      XI1=(DELT*60.)/A
C          IF(XI1 .LT. XI(1)) GO TO 9
C          IF(XI1 .GT. XI(NUMEXI)) GO TO 11
C          DO 7 L=1,NEXI1
C              IF(XI1 .GE. XI(L) .AND. XI1 .LE. XI(L+1)) GO TO 13
7      CONTINUE
9      EI(MT)=E(1)
C          GO TO 15
11     EI(MT)=E(NUMEXI)
C          GO TO 15
13     EI(MT)=EXP((B1(L)+A1(L)*ALOG10(XI1))/0.434)
15     IF(MT .EQ. 1) GO TO 17
C
C          THE THERMAL STRESS INCREMENT (STR2),TOGETHER WITH THE
C          TOTAL STRESS (ST) ARE CALCULATED.
C
C          STR2=(1.0/(1.0-U))*(ALPHA/2.0)*(EI(MT)+EI(MT-1))*(TT(MT-1)-TT(MT))
C          STR1=STR2+STR1
C          ST(MT)=STR1
C          GO TO 19
17     ST(MT)=0.0
19     RETURN
C          END

```

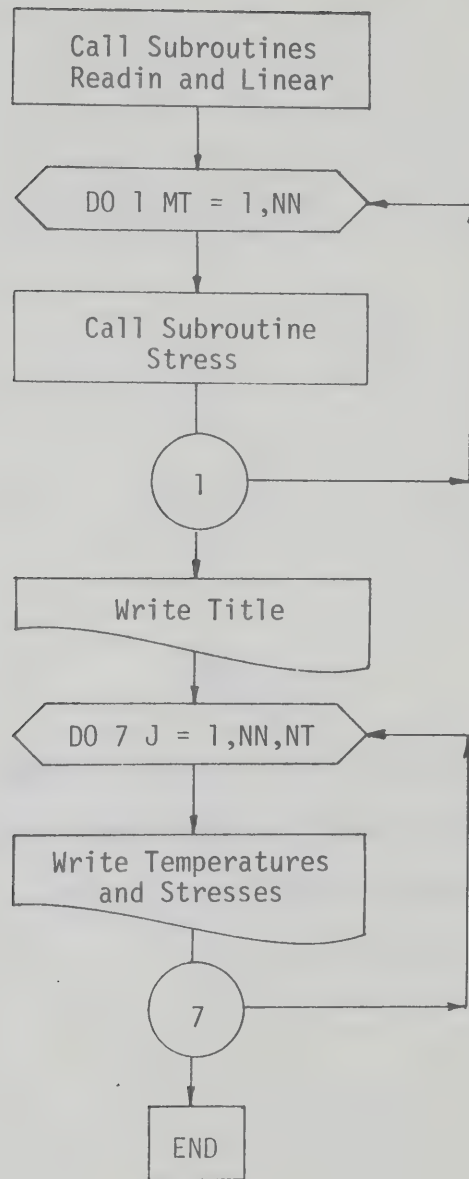



FIGURE. B-1 FLOW DIAGRAM FOR MAIN PROGRAM.

APPENDIX C

COMPUTER PROGRAM FOR THERMAL STRESS
PREDICTIONS USING VISCOELASTIC ANALYSES
WITH VARIABLE TIME INCREMENTS

APPENDIX C

COMPUTER PROGRAM FOR THERMAL STRESS PREDICTIONS USING
VISCOELASTIC ANALYSES WITH VARIABLE TIME INCREMENTSC.1. Introduction

This appendix contains details of a computer program developed for calculating thermal stresses in an asphaltic concrete with temperature dependent viscoelastic properties. The program can be used for stress computations involving three different analyses. These analyses are designated as:

- 1) Viscoelastic slab,
- 2) Viscoelastic beam, and
- 3) Approximate viscoelastic slab.

Assuming the coefficient of thermal expansion of an asphaltic concrete to be a constant value, stress equations for the viscoelastic slab and beam analysis are

$$\sigma_x(t) = - 3 \alpha_0 \int_{t_0}^t R[\xi - \xi'] dT(t') \quad (C-1)$$

and

$$\sigma_x(t) = - \alpha_0 \int_{t_0}^t S[\xi - \xi'] dT(t'), \quad (C-2)$$

respectively

where

- α_0 = coefficient of thermal expansion
- $R(\xi)$ = a modulus function
- $S(\xi)$ = stiffness modulus
- T = temperature
- t = time

Evaluating Equations (C-1) and (C-2) by the trapezoidal rule, results in

$$\sigma_x(t) = - \frac{3\alpha_0}{2} \sum_{i=1}^N [R(\xi - \xi_i) + R(\xi - \xi_{i-1})] (T_i - T_{i-1}) \quad (C-3)$$

and

$$\sigma_x(t) = - \frac{\sigma_0}{2} \sum_{i=1}^N [S(\xi - \xi_i) + S(\xi - \xi_{i-1})] (T_i - T_{i-1}) \quad (C-4)$$

where N is the number of time steps from 0 to t .

Approximate viscoelastic slab stresses are obtained by multiplying Equation (C-4) by the factor $1/(1-\nu)$, where Poisson's ratio, ν , is assumed constant.

For stress computations at a time t the viscoelastic stress equations require numerical integration over the entire previous temperature history to which the asphaltic concrete was subjected. Therefore, when stresses are to be predicted over extended periods of time long computer runs and large storage requirements are involved. Since the most recent temperature history is the most significant for stress evaluation, the following scheme of variable time increments is included in the program.

- 1) For times up to $(t-24)$ hours a time increment of 2 hours is employed.
- 2) For the following 22 hours a time increment of 15 minutes is employed.
- 3) For the 2 hours immediately prior to t , a time increment of 5 minutes is employed.

C.2. Program Operations

The program consists of a main program and seven subroutines. Computations within each of these components are outlined in the following subsections.

C.2.1. Main Program

A flow diagram for the main program is shown in FIGURE C-1. Within this program all subroutines are called and all output statements are given. In the listing, output display consists of temperatures (TT) and computed stresses (ST) at 2 hour time intervals.

C.2.2. Subroutine Readin

In this subroutine all parameters necessary for the numerical solution of the viscoelastic stress equations are specified. These parameters are defined in the program listing.

C.2.3. Subroutine Linear

For the stress computations, stiffness values at times J and temperatures TT are evaluated by assuming linear relationships between logarithm of stiffness and logarithm of reduced time values, and

between logarithm of shift factor values and temperatures specified in subroutine Readin. In subroutine Linear the coefficients of these relationships, designated as A1, B1, A2 and B2, are calculated.

C.2.4. Subroutine XI15M

In this subroutine the reduced time vector ξ (XI15M) associated with the input temperatures (TEMPS) is calculated at time steps of 15 minutes. For this computation a linear temperature-time relationship is assumed over the time period INCTIM. Temperatures at 15 minute intervals are computed and used to evaluate the corresponding shift factors AT15. Then, using the trapezoidal rule, the reduced time vector XI15M is calculated.

C.2.5. Subroutine Str2

In this subroutine thermal stresses are computed for times up to (t-24) hours using time increments of 2 hours. The limit of this time period is defined by the parameter LM2, while, the limits of the time periods over which 15 and 5 minute time increments are used are defined by the parameters LM15 and LMXI, respectively. Stiffness values $E1(J)$ are determined at reduced time values of $(\xi - \xi')$ [XI15(LMXI)] - [XI15(J)], where J increases in increments of 2 hours, and the thermal stress ST1 at the time limit LM2 is computed.

C.2.6. Subroutine Str15

In subroutine Str15 thermal stresses are calculated over the time period LM2 to LM15. During this period, a time increment of 15 minutes is employed for stress evaluation and operations proceed in a manner similar to that described for subroutine Str2.

C.2.7. Subroutine XI5M

The reduced time vector ξ (XI5M), for temperatures over the 2 hour time period immediately prior to the time of stress prediction, is computed. For this computation a linear temperature-time relationship is assumed and temperatures at 5 minute intervals together with the corresponding shift factors (AT5) are determined. The reduced time vector XI5M is then computed.

C.2.8. Subroutine Str5

Using the reduced time vector XI5M and temperatures computed in subroutine XI5M, thermal stresses during the 2 hour time period are calculated. The predicted thermal stress ST at time LMXI represents the sum of stress increments computed in each of the three stress sub-routines. Operations return to the main program where calculations commence for stresses at subsequent times and temperatures.

IN THIS PROGRAM VISCOELASTIC ANALYSES ARE USED TO
CALCULATE THERMAL STRESS IN AN ASPHALTIC CONCRETE SUBJECTED
TO A KNOWN TEMPERATURE FIELD.

STRESSES ARE CALCULATED USING A NUMERICAL
INTEGRATION PROCEDURE WHICH INCORPORATES TIME STEPS
OF 2 HOURS, 15 MINUTES AND 5 MINUTES.

THE PROGRAM CAN BE USED TO DETERMINE THE THERMAL STRESSES
ASSUMING ONE OF THE FOLLOWING CONDITIONS;

- 1) RESTRAINED BEAM, E=FUNCTION(REduced TIME)
- 2) RESTRAINED SLAB, E=FUNCTION(REduced TIME)
- 3) RESTRAINED SLAB, R=FUNCTION(REduced TIME)

MAIN PROGRAM

```
COMMON TITLE1(20),T(15),AT(15),E(15),XI(15),A1(15),A2(15),B1(15),
1B2(15),TEMP(1300),TT(3000),AT15(3000),XI15(3000),E1(3000),ST(3000)
2,TA(50),AT5(50),XI5(50),NUMDAY,NUMEXI,NUMATT,NUMINC,INCTIM,ALPHA,
3NATT1,NEXI1,CODE,U,ST1,LM,MT,LM2,LM15,LMXI
DOUBLE PRECISION DXI,XI15,XI5
CALL READIN
CALL LINEAR
CALL XI15M
DO 1 MT=14,LM
CALL STR2
CALL STR15
CALL XI5M
CALL STR5
1 CONTINUE
WRITE(5,3)(TITLE1(I),I=1,20)
3 FORMAT(6X,20A4)
L=105
```

TEMPERATURES AND STRESSES ARE WRITTEN.

```
DO 7 MZ=14,LM
WRITE(6,5)TT(L),ST(MZ)
5 FORMAT(6X,2F10.1)
L=L+8
7 CONTINUE
STOP
END
```


SUBROUTINE READIN

SUBROUTINE READIN

THIS SUBROUTINE READS IN ALL DATA NECESSARY FOR THE
THERMAL STRESS PREDICTIONS. THIS DATA CAN BE DIVIDED INTO
THE FOLLOWING THREE CATEGORIES;

- 1) THE ASSUMPTION OF A RESTRAINED BEAM OR SLAB,
CONDITIONS 1,2 OR 3 MENTIONED PREVIOUSLY.
- 2) MATERIAL PROPERTIES.
- 3) TEMPERATURE AT A GIVEN DEPTH IN THE ASPHALTIC
CONCRETE AS A FUNCTION OF TIME.

COMMON TITLE1(20),T(15),AT(15),E(15),XI(15),A1(15),A2(15),B1(15),
1B2(15),TEMP(1300),TT(3000),AT15(3000),XI15(3000),E1(3000),ST(3000)
2,TA(50),AT5(50),XI5(50),NUMDAY,NUMEXI,NUMATT,NUMINC,INCTIM,ALPHA,
3NATT1,NEXI1,CODE,U,ST1,LM,MT,LM2,LM15,LMX1
DOUBLE PRECISION DXI,XI15,XI5

THE INPUT PARAMETERS ARE DEFINED AS FOLLOWS:

CODE - CODE=1.0 DENOTES CONDITION 1.

CODE=2.0 DENOTES CONDITION 2.

CODE=3.0 DENOTES CONDITION 3.

U - POISSONS RATIO. ONLY IF CONDITION 2 IS SPECIFIED
A VALUE OF POISSONS RATIO MUST BE READ IN.

NUMDAY - THE NUMBER OF DAYS IN WHICH THE TEMPERATURE
REGIME IS SPECIFIED.

NUMEXI - THE NUMBER OF VALUES SPECIFIED FROM THE STIFFNESS MODULUS-
REDUCED TIME RELATIONSHIP.

NUMATT - THE NUMBER OF VALUES SPECIFIED FROM THE SHIFT FACTOR-
TEMPERATURE RELATIONSHIP.

INCTIM - THE TIME INCREMENT IN WHICH THE TEMPERATURE
REGIME IS SPECIFIED.(HRS)

ALPHA - THE COEFFICIENT OF THERMAL EXPANSION AND CONTRACTION
OF THE ASPHALTIC CONCRETE.(IN/IN/DEG F)

E - THE STIFFNESS MODULUS OF THE ASPHALTIC CONCRETE.(PSI)
THESE VALUES ARE SPECIFIED IN DESCENDING ORDER
OF MAGNITUDE.

XI - REDUCED TIME.(SECS) THESE VALUES ARE SPECIFIED IN
ASCENDING ORDER OF MAGNITUDE AND MUST BE COMPATIBLE
WITH THE E VALUES.

AT - SHIFT FACTORS.

T - TEMPERATURES COMPATIBLE WITH THE SHIFT FACTORS.(DEG F)

TEMP - THE TEMPERATURES AT A GIVEN DEPTH WITHIN THE
ASPHALTIC CONCRETE.(DEG F)

READ(5,1)(TITLE1(I),I=1,20)

1 FORMAT(20A4)

READ(5,2)CODE

2 FORMAT(1F5.0)

SUBROUTINE LINEAR

C
C
C
C
C
C
C

SUBROUTINE LINEAR

A LINEAR RELATIONSHIP IS ASSUMED BETWEEN LOG(E) AND LOG(XI), AND LOG(AT) AND T VALUES. THIS SUBROUTINE CALCULATES THE A AND B COEFFICIENTS OF THE RESULTING LINEAR EQUATIONS.

COMMON TITLE1(20),T(15),AT(15),E(15),XI(15),A1(15),A2(15),B1(15),
B2(15),TEMP(1300),TT(3000),AT15(3000),XI15(3000),E1(3000),ST(3000)
2,TA(50),AT5(50),XI5(50),NUMDAY,NUMEXI,NUMATT,NUMINC,INCTIM,ALPHA,
3NATT1,NEXI1,CODE,U,ST1,LM,MT,LM2,LM15,LMX1
DOUBLE PRECISION DXI,XI15,XI5
NEXI1=NUMEXI-1
NATT1=NUMATT-1

C
C
C
C

THE A AND B COEFFICIENTS FOR THE LOG(E)-LOG(XI)
EQUATIONS ARE EVALUATED.

DO 1 J=1,NEXI1
A1(J)=-1.0*ALOG10(E(J)/E(J+1))
B1(J)=ALOG10(E(J))-A1(J)*ALOG10(XI(J))
1 CONTINUE

C
C
C
C

THE A AND B COEFFICIENTS FOR THE LOG(AT)-T EQUATIONS
ARE EVALUTED.

DO 3 J=1,NATT1
A2(J)=(ALOG10(AT(J))-ALOG10(AT(J+1)))/(T(J)-T(J+1))
B2(J)=ALOG10(AT(J))-A2(J)*T(J)
3 CONTINUE
RETURN
END


```

C      SUBROUTINE XI15M
C
C          SUBROUTINE XI15M
C          *****
C
C          THIS SUBROUTINE CALCULATES THE REDUCED TIME VECTOR(XI15M)
C          ASSOCIATED WITH THE INPUT TEMPERATURE FIELD. THIS VECTOR IS
C          DETERMINED AT TIME INTERVALS OF 15 MINUTES OVER THE
C          COMPLETE TIME PERIOD IN WHICH THE TEMPERATURE FIELD IS
C          DEFINED.
C
C          COMMON TITLE1(20),T(15),AT(15),E(15),XI(15),A1(15),A2(15),B1(15),
C          B2(15),TEMP(1300),TT(3000),AT15(3000),XI15(3000),E1(3000),ST(3000)
C          2,TA(50),AT5(50),XI5(50),NUMDAY,NUMEXI,NUMATT,NUMINC,INCTIM,ALPHA,
C          3NATT1,NEXI1,CODE,U,ST1,LM,MT,LM2,LM15,LMX1
C          DOUBLE PRECISION DXI,XI15,XI5
C          ST1=0.0
C          LM=NUMDAY*12+1
C          TIME=INCTIM
C          NT=TIME*60./15.
C          NT1=NT+1
C          N=NUMDAY*NUMINC
C          TT(1)=TEMP(1)
C
C          TEMPERATURES (TT) AT 15 MIN. INTERVALS ARE CALCULATED.
C
C          L=2
C          DO 3 M=1,N
C          DO 1 MM=2,NT1
C          TT(L)=TEMP(M)+((TEMP(M+1)-TEMP(M))/NT)*(MM-1)
C          L=L+1
C          1 CONTINUE
C          3 CONTINUE
C          NN=N*NT+1
C
C          SHIFT FACTORS (AT15) AT 15 MIN. INTERVALS ARE CALCULATED.
C
C          DO 9 L=1,NN
C          DO 5 J=1,NATT1
C          IF(TT(L) .LT. T(J) .AND. TT(L) .GE. T(J+1)) GO TO 7
C          5 CONTINUE
C          AT15(L)=AT(1)
C          GO TO 9
C          7 AT15(L)=EXP((A2(J)+TT(L)+B2(J))/0.434)
C          9 CONTINUE
C
C          THE REDUCED TIME VECTOR (XI15) IS CALCULATED.
C
C          XI15(1)=0.0

```



```
DO 11 L=2,NN  
XI15(L)=(900./2.0)*{(1.0/AT15(L)+1.0/AT15(L-1))}+XI15(L-1)  
11 CONTINUE  
RETURN  
END
```


SUBROUTINE STR2

C
C
C
C
C
C
C
C
C

SUBROUTINE STR2

SUBROUTINE STR2 CALCULATES THERMAL STRESSES DURING THE
TIME PERIOD PRIOR TO (T-24HRS.). THESE STRESSES ARE CALCULATED
USING A 2 HOUR INTERVAL.

COMMON TITLE1(20),T(15),AT(15),E(15),XI(15),A1(15),A2(15),B1(15),
B2(15),TEMP(1300),TT(3000),AT15(3000),XI15(3000),E1(3000),ST(3000)
2,TA(50),AT5(50),XI5(50),NUMDAY,NUMEXI,NUMATT,NUMINC,INCTIM,ALPHA,
3NATT1,NEXI1,CODE,U,ST1,LM,MT,LM2,LM15,LMXI
DOUBLE PRECISION DXI,XI15,XI5
LM2=(MT-13)*8+1
LM15=(MT-2)*8+1
LMXI=(MT-1)*8+1

C
C
C
C

THE CHANGE IN REDUCED TIME (DXI) AS A FUNCTION OF TIME
AND TEMPERATURE IS EVALUATED.

DO 10 J=1,LM2,8
DXI=XI15(LMXI)-XI15(J)
IF(DXI .LE. XI(1))GO TO 4
DO 2 L=1,NEXI1
IF(DXI .GE. XI(L) .AND. DXI .LE. XI(L+1)) GO TO 6
2 CONTINUE
E1(J)=E(NUMEXI)
GO TO 8
4 E1(J)=E(1)
GO TO 8
6 E1(J)=DEXP((B1(L)+A1(L)*DLOG10(DXI))/0.434)
8 IF(J .EQ. 1) GO TO 10

C
C
C
C

THE THERMAL STRESS INCREMENT (STR2) ,TOGETHER WITH THE
TOTAL STRESS (ST1),IS CALCULATED.

ST2=(CODE/(1.-U))*ALPHA*(E1(J-8)+E1(J))*((TT(J-8)-TT(J))/2.0)
ST1=ST2+ST1
10 CONTINUE
RETURN
END

SUBROUTINE STR15

SUBROUTINE STR15

SUBROUTINE STR25 CALCULATES THERMAL STRESSES DURING THE
TIME PERIOD (T-24HRS.) TO (T-2HRS.). THESE STRESSES ARE
CALCULATED USING A 15 MINUTE TIME INTERVAL.

COMMON TITLE1(20),T(15),AT(15),E(15),XI(15),A1(15),A2(15),B1(15),
1B2(15),TEMP(1300),TT(3000),AT15(3000),XI15(3000),E1(3000),ST(3000)
2,TA(50),AT5(50),XI5(50),NUMDAY,NUMEXI,NUMATT,NUMINC,INCTIM,ALPHA,
3NATT1,NEXI1,CODE,U,ST1,LM,NT,LM2,LM15,LMXI
DOUBLE PRECISION DXI,XI15,XI5

THE CHANGE IN REDUCED TIME (DXI) AS A FUNCTION OF TIME
AND TEMPERATURE IS EVALUATED.

DO 11 J=LM2,LM15
DXI=XI15(LMXI)-XI15(J)
IF(DXI .LE. XI(1)) GO TO 5
DO 3 L=1,NEXI1
IF(DXI .GE. XI(L) .AND. DXI .LE. XI(L+1)) GO TO 7
3 CONTINUE
E1(J)=E(NUMEXI)
GO TO 9
5 E1(J)=E(1)
GO TO 9
7 E1(J)=DEXP((B1(L)+A1(L)*DLOG10(DXI))/0.434)
9 IF(J .EQ. LM2) GO TO 11

THE THERMAL STRESS INCREMENT (STR2) ,TOGETHER WITH THE
TOTAL STRESS (ST1), IS CALCULATED.

ST2=(CODE/(1.-U))*ALPHA*(E1(J-1)+E1(J))*((TT(J-1)-TT(J))/2.0)
ST1=ST2+ST1
11 CONTINUE
RETURN
END


```

C      SUBROUTINE XISM
C
C          SUBROUTINE XISM
C          *****
C
C          THIS SUBROUTINE CALCULATES THE REDUCED TIME VECTOR(XISM)
C          ASSOCIATED WITH TEMPERATURES 2 HOURS IMMEDIATELY PRIOR TO
C          THE TIME AT WHICH STRESSES ARE TO BE DETERMINED.
C
C          COMMON TITLE1(20),T(15),AT(15),E(15),XI(15),A1(15),A2(15),B1(15),
C          B2(15),TEMP(1300),TT(3000),AT15(3000),XI15(3000),E1(3000),ST(3000)
C          2,TA(50),AT5(50),XIS(50),NUMDAY,NUMEXI,NUMATT,NUMINC,INCTIM,ALPHA,
C          3NATT1,NEXI1,CODE,U,ST1,LM,MT,LM2,LM15,LMXI
C          DOUBLE PRECISION DXI,XI15,XIS
C          TA(1)=TT(LM15)
C
C          TEMPERATURES (TA) AT INTERVALS OF 5 MIN. ARE CALCULATED.
C
C          DO 2 L=2,25
C          TA(L)=TT(LM15)+((TT(LM15+8)-TT(LM15))/24.)*(L-1)
C          2 CONTINUE
C
C          SHIFT FACTORS (AT5) AT INTERVALS OF 5 MIN. ARE CALCULATED.
C
C          AT5(1)=AT15(LM15)
C          DO 10 L=2,25
C          DO 6 J=1,NATT1
C          IF(TA(L) .LT. T(J) .AND. TA(L) .GE. T(J+1)) GO TO 8
C          6 CONTINUE
C          AT5(L)=AT(1)
C          GO TO 10
C          8 AT5(L)=EXP((A2(J)*TA(L)+B2(J))/0.434)
C          10 CONTINUE
C
C          THE REDUCED TIME VECTOR (XIS) IS CALCULATED.
C
C          XIS(1)=XI15(LM15)
C          DO 12 L=2,25
C          XIS(L)=(300./2.0)*((1.0/AT5(L)+1.0/AT5(L-1)))+XIS(L-1)
C          12 CONTINUE
C          RETURN
C          END

```



```

C      SUBROUTINE STR5
C
C              SUBROUTINE STR5
C              *****
C
C              SUBROUTINE STR5 CALCULATES THERMAL STRESSES FOR THE TIME
C              PERIOD(T-2HRS.) TO THE TIME AT WHICH STRESSES ARE TO BE
C              DETERMINED.
C
C              COMMON TITLE1(20),T(15),AT(15),E(15),XI(15),A1(15),A2(15),B1(15),
C              1B2(15),TEMP(1300),TT(3000),AT15(3000),XI15(3000),E1(3000),ST(3000)
C              2,TA(50),AT5(50),XI5(50),NUMDAY,NUMEXI,NUMATT,NUMINC,INCTIM,ALPHA,
C              3NATT1,NEXI1,CODE,U,ST1,LM,MT,LM2,LM15,LMXI
C              DOUBLE PRECISION DXI,XI15,XI5
C              DO 10 J=1,25
C
C              THE CHANGE IN REDUCED TIME (DXI) AS A FUNCTION OF TIME
C              , AND TEMPERATURE IS EVALUATED.
C
C              DXI=XI15(LMXI)-XI5(J)
C              IF(DXI .LE. XI(1)) GO TO 4
C              DO 2 L=1,NEXI1
C              IF(DXI .GE. XI(L) .AND. DXI .LE. XI(L+1)) GO TO 6
C              2 CONTINUE
C              E1(J)=E(NUMEXI)
C              GO TO 8
C              4 E1(J)=E(1)
C              GO TO 8
C              6 E1(J)=DEXP((B1(L)+A1(L)*DLOG10(DXI))/0.434)
C              8 IF( J .EQ. 1) GO TO 10
C
C              THE THERMAL STRESS INCREMENT (STR2) ,TOGETHER WITH THE
C              TOTAL STRESS (ST1),IS CALCULATED.
C
C              ST2=(CODE/(1.-U))*ALPHA*(E1(J-1)+E1(J))*((TA(J-1)-TA(J))/2.0)
C              ST1=ST2+ST1
C              10 CONTINUE
C              ST(MT)=ST1
C              ST1=0.0
C              RETURN
C              END

```


APPENDIX D

COMPUTER PROGRAM FOR CALCULATING THE MODULUS FUNCTION $R(\xi)$

APPENDIX D

COMPUTER PROGRAM FOR CALCULATING
THE MODULUS FUNCTION $R(\xi)$

D.1. Introduction

Humphreys and Martin (1963)* proposed a method of determining thermal stresses in an infinite rigidly constrained slab with temperature viscoelastic properties. Assuming the coefficient of thermal expansion, α_0 , of the slab to be a constant value the stress equation suggested by the authors may be expressed as

$$\sigma_x = - 3\alpha_0 \int_0^t R[\xi - \xi'] dT(t') \quad (D-1)$$

where R is a time and temperature dependent modulus of the slab. The authors presented a numerical method for evaluating the modulus function $R(\xi)$ from known stiffness-reduced time relationships. In this appendix, equations used for this numerical evaluation are presented and a listing of a computer program developed for the solution of these equations is given.

D.2. Numerical Method for Evaluating $R(\xi)$

Assuming the material is elastic in dilatation, Humphreys and Martin presented the following expressions for the numerical evaluation of $R(\xi)$.

* Humphreys, J.S. and C.J. Martin, 1963. "Determination of Transient Thermal Stresses in a Slab with Temperature Dependent Viscoelastic Properties", Transactions of the Society of Rheology, Vol. VII.

$$\begin{aligned}
 y(\xi_{n+1}) = & \frac{f(\xi_{n+1}) + \frac{\mu}{2} y(\xi_n) [f(o) - f(\xi_{n+1} - \xi_n)]}{1 - \frac{\mu}{2} [f(o) - f(\xi_{n+1} - \xi_n)]} \\
 & + \frac{\frac{\mu}{2} \sum_{i=1}^{n-1} [y(\xi_{i+1}) + y(\xi_i)] [f(\xi_{n+1} - \xi_{i+1}) - f(\xi_{n+1} - \xi_i)]}{1 - \frac{\mu}{2} [f(o) - f(\xi_{n+1} - \xi_n)]}
 \end{aligned} \tag{D-2}$$

which is made dimensionless by the substitutions

$$y(\xi) = 2(1-\nu)(R(\xi)/E_0)$$

$$f(\xi) = 2E(\xi)/3E_0$$

$$\mu = 3(1-\nu_0)/4(1-\nu_0)$$

where

$$R(\xi) = \text{a modulus function,}$$

$$\nu_0 = \text{Poisson's ratio,}$$

$$E_0 = \text{initial elastic Young's modulus,}$$

$$E(\xi) = \text{time dependent Young's modulus.}$$

Using these relationships $R(\xi)$ can be evaluated provided that the latter three listed parameters are defined.

D.3. Program Operations

The listing of the computer program developed for calculating $R(\xi)$ contains a description of the necessary input parameters. In the program a linear relationship is assumed between logarithm of the stiffness (E) and the logarithm of reduced time (XI). Therefore, in order to obtain accurate moduli, E and XI values should be specified using small increments of reduced time.

Operations within the program are outlined in the listing. The output consists of stiffness and reduced time values, together with corresponding modulus function values. From this output modulus function-reduced time plots can be readily established.


```

C
C      THIS PROGRAM SOLVES FOR THE MODULUS FUNCTION (R) USING
C      A NUMERICAL PROCEDURE PROPOSED BY HUMPHREYS AND MARTIN;1963.
C
C      DIMENSION TITLE1(20),XI(40),E(40),F(40),R(40),Y(40),A1(40),B1(40),
C      IC(40),SUMY(40)
C      DOUBLE PRECISION F,R,Y,C,SUMY,DXI,EI
C
C      THE FOLLOWING VALUES ARE SPECIFIED.
C
C      NUMMAT - THE NUMBER OF SETS OF DATA SPECIFIED.
C      NUMEXI - THE NUMBER OF STIFFNESS AND REDUCED TIME VALUES
C               IN EACH SET OF DATA.
C      TITLE1 - A TITLE DESCRIBING THE MATERIAL.
C      U - INITIAL POISSON'S RATIO.
C      EO - INITIAL STIFFNESS MODULUS.
C      XI - REDUCED TIME VALUES FROM STIFFNESS-REDUCED TIME
C           PLOT.
C      E - CORRESPONDING STIFFNESS VALUES FROM STIFFNESS-
C          REDUCED TIME PLOT.
C
C      READ(5,2)NUMMAT,NUMEXI
C      2 FORMAT(2I5)
C      DO 36 II=1,NUMMAT
C      READ(5,4)(TITLE1(I),I=1,20)
C      4 FORMAT(20A4)
C      READ(5,6)V,EO
C      6 FORMAT(1F5.2,1E6.2)
C      DO 10 L=2,NUMEXI
C      READ(5,8)XI(L),E(L)
C      8 FORMAT(1E6.1,1E6.2)
C      10 CONTINUE
C
C      INITIAL VALUES OF Y AND F IN EQUATION(D-2) ARE CALCULATED.
C
C      E(1)=EO
C      XI(1)=0.0
C      U=(3.0*(1.0-2.0*V))/(4.0*(1.0-V))
C      F(1)=2.0/3.0
C      R(1)=E(1)/(3.0*(1.0-V))
C      Y(1)=2.0*(1.0-V)*(R(1)/E(1))
C      NEXI1=NUMEXI-1
C      NEXI2=NUMEXI-2
C      DO 12 J=2,NEXI1
C      A1(J)=-1.0*ALOG10(E(J)/E(J+1))
C      B1(J)=ALOG10(E(J))-A1(J)*ALOG10(XI(J))
C      12 CONTINUE
C
C      THE MODULUS FUNCTION R IS CALCULATED.

```



```

DO 28 KK=1,NEXI2
C
C      THE CHANGE IN REDUCED TIME IS CALCULATED AND THE PARAMETER
C      F IS DETERMINED.
C
DO 18 KL=1, KK
DXI=XI(KK+1)-XI(KL)
DO 14 L=2,NEXI1
IF(DXI .GE. XI(L) .AND. DXI .LE. XI(L+1)) GO TO 16
14 CONTINUE
16 E1=DEXP((B1(L)+A1(L)*DLOG10(DXI))/0.434)
F(KL+1)=(2.0/3.0)*(E1/E(1))
18 CONTINUE
C
C      THE DENOMINATOR OF EQUATION(D-2) IS CALCULATED.
C
C(1)=(U/2.0)*(F(1)-F(KK+1))
IF(KK .EQ. 1) GO TO 22
IL=KK+1
DO 20 KM=2, KK
C(KM)=(U/2.0)*(F(IL)-F(IL-1))
IL=IL-1
20 CONTINUE
22 IF(KK .GT. 1) GO TO 24
Y(KK+1)=((2.0/3.0)*(E(KK+1)/E(KK)))+(C(1)*Y(1))/(1.0-C(1))
R(KK+1)=(Y(KK+1)*E(1))/(2.0-(1.0-V))
SUMY(1)=Y(KK+1)+Y(1)
GO TO 28
24 LA=KK-1
LB=KK
SUMYF=0.0
C
C      THE NUMERATOR OF THE SECOND TERM OF EQUATION(D-2) IS CALCULATED.
C
DO 26 MW=1, LA
PRODYF=C(LB)*SUMY(MW)
SUMYF=SUMYF+PRODYF
LB=LB-1
26 CONTINUE
Y(KK+1)=((2.0/3.0)*(E(KK+1)/E(1))+SUMYF+(C(1)*Y(KK)))/(1.0-C(1))
R(KK+1)=(Y(KK+1)*E(1))/(2.0*(1.0-V))
SUMY(KK)=Y(KK+1)+Y(KK)
28 CONTINUE
C
C      TITLE1, REDUCED TIME, STIFFNESS AND THE MODULUS FUNCTION
C      (R) ARE WRITTEN.
C
WRITE(6,30)(TITLE1(I), I=1,20)
30 FORMAT(6X,20A4)
DO 34 I=1,NEXI1

```



```
      WRITE(6,32)XI(I),E(I),R(I)
32  FORMAT(5X,1E7.2,5X,1E9.4,5X,1E9.4)
34  CONTINUE

C
C      OPERATIONS RETURN TO BEGINNING OF PROGRAM WHERE A SECOND
C      SET OF DATA MAY BE SPECIFIED.
C
36  CONTINUE
    STOP
    END
```


APPENDIX E

LISTING OF A COMPUTER PROGRAM FOR
THERMAL STRESS PREDICTIONS USING VISCOELASTIC
ANALYSES WITH CONSTANT TIME INCREMENTS

APPENDIX E

LISTING OF A COMPUTER PROGRAM FOR
THERMAL STRESS PREDICTIONS USING VISCOELASTIC
ANALYSES WITH CONSTANT TIME INCREMENTSE.1. Introductory Remarks

This appendix contains the listing of a computer program used to perform thermal stress calculations in which viscoelastic analyses are employed. Stress equations for the analyses are those given in APPENDIX C. Thermal stresses are computed using a numerical integration scheme which incorporates a constant time increment. In the listing this time increment is defined by the term DELT. With the exception of differences in numerical integration schemes, operations within the program parallel those described in APPENDIX C.


```

C
C
C      THIS PROGRAM USES VISCOELASTIC ANALYSES TO CALCULATE
C      THERMAL STRESSES IN AN ASPHALTIC CONCRETE SUBJECTED TO A
C      KNOWN TEMPERATURE FIELD.
C
C      STRESSES ARE CALCULATED AT EQUAL TIME INTERVALS
C      OVER THE TOTAL TIME PERIOD IN WHICH THE TEMPERATURE FIELD
C      IS DEFINED.
C
C      THE PROGRAM CAN BE USED TO DETERMINE THE THERMAL STRESSES
C      ASSUMING ONE OF THE FOLLOWING CONDITIONS;
C      1) RESTRAINED BEAM,E=FUNCTION(REduced TIME)
C      2) RESTRAINED SLAB,E=FUNCTION(REduced TIME)
C      3) RESTRAINED SLAB,R=FUNCTION(REduced TIME)
C
C
C      .
C      MAIN PROGRAM
C      *****
C
C      COMMON TITLE1(20),T(15),AT(15),E(15),XI(15),A1(15),A2(15),B1(15),
C      1B2(15),TEMP(1300),TT(3000),A(3000),XI1(3000),E1(3000),ST(3000),
C      2NUMDAY,NUMEXI,NUMATT,NUMINC,INCTIM,DELT,ALPHA,NN,NATT1,NEXI1,NT,
C      3CODE,U
C      DOUBLE PRECISION DXI,XI1
C      CALL READIN
C      CALL LINEAR
C      CALL XIS
C      CALL STRESS
C      WRITE(6,1)(TITLE1(I),I=1,20)
C 1  FORMAT(5X,20A4/)
C
C      TEMPERATURES AND STRESSES ARE WRITTEN AT TIME INCREMENTS
C      CORRESPONDING TO THOSE AT WHICH TEMPERATURES ARE SPECIFIED.
C
C      DO 3 LT=1,NN,NT
C      WRITE(6,2)TT(LT),ST(LT)
C 2  FORMAT(12X,2F10.1)
C 3  CONTINUE
C      STOP
C      END

```


SUBROUTINE READIN

SUBROUTINE READIN

THIS SUBROUTINE READS IN ALL DATA NECESSARY FOR THE
GENERATION OF THERMAL STRESSES. THIS DATA CAN BE DIVIDED INTO
THE FOLLOWING THREE CATEGORIES;

- 1) THE ASSUMPTION OF A RESTRAINED BEAM OR SLAB,
CONDITIONS 1,2 OR 3 MENTIONED PREVIOUSLY.
- 2) MATERIAL PROPERTIES.
- 3) TEMPERATURE AT A GIVEN DEPTH IN THE ASPHALTIC
CONCRETE AS A FUNCTION OF TIME.

COMMON TITLE1(20),T(15),AT(15),E(15),XI(15),A1(15),A2(15),B1(15),
B2(15),TEMP(1300),TT(3000),A(3000),XI1(3000),E1(3000),ST(3000),
2NUMDAY,NUMEXI,NUMATT,NUMINC,INCTIM,DELT,ALPHA,NN,NATT1,NEXI1,NT,
3CODE,U
DOUBLE PRECISION DXI,XI1

THE INPUT PARAMETERS ARE DEFINED AS FOLLOWS:

CODE - CODE=1.0 DENOTES CONDITION 1.

CODE=2.0 DENOTES CONDITION 2.

CODE=3.0 DENOTES CONDITION 3.

U - POISSONS RATIO. ONLY IF CONDITION 2 IS SPECIFIED
A VALUE OF POISSONS RATIO MUST BE READ IN.

NUMDAY - THE NUMBER OF DAYS IN WHICH THE TEMPERATURE
REGIME IS SPECIFIED.

NUMEXI - THE NUMBER OF VALUES SPECIFIED FROM THE STIFFNESS MODULUS-
REDUCED TIME RELATIONSHIP.

NUMATT - THE NUMBER OF VALUES SPECIFIED FROM THE SHIFT FACTOR-
TEMPERATURE RELATIONSHIP.

INCTIM - THE TIME INCREMENT IN WHICH THE TEMPERATURE
REGIME IS SPECIFIED.(HRS)

DELT - THE TIME INCREMENT IN WHICH THE THERMAL STRESSES
ARE TO BE CALCULATED.(MINS.)

ALPHA - THE COEFFICIENT OF THERMAL EXPANSION AND CONTRACTION
OF THE ASPHALTIC CONCRETE.(IN/IN/DEG F)

E - THE STIFFNESS MODULUS OF THE ASPHALTIC CONCRETE.(PSI)
THESE VALUES ARE SPECIFIED IN DESCENDING ORDER
OF MAGNITUDE.

XI - REDUCED TIME.(SECS) THESE VALUES ARE SPECIFIED IN
ASCENDING ORDER OF MAGNITUDE AND MUST BE COMPATIBLE
WITH THE E VALUES.

AT - SHIFT FACTORS.

T - TEMPERATURES COMPATIBLE WITH THE SHIFT FACTORS.(DEG F)

TEMP - THE TEMPERATURES AT A GIVEN DEPTH WITHIN THE
ASPHALTIC CONCRETE.(DEG F)

READ(5,1)(TITLE1(I),I=1,20)


```
1  FORMAT(20A4)
   READ(5,2)CODE
2  FORMAT(1F5.0)
   IF(CODE-2.)8,4,8
4  READ(5,6)U
6  FORMAT(1F5.2)
   GO TO 10
8  U=0.0
10 READ(5,12)(NUMDAY,NUMEXI,NUMATT,INCTIM,DELT,ALPHA)
12 FORMAT(4I10,1F10.2,1E8.1)
   READ(5,14)(E(I),I=1,NUMEXI)
14 FORMAT(11E7.2)
   READ(5,16)(XI(I),I=1,NUMEXI)
16 FORMAT(11E7.1)
   READ(5,18)(AT(I),I=1,NUMATT)
18 FORMAT(9E7.2)
   READ(5,20)(T(I),I=1,NUMATT)
20 FORMAT(9F8.0)
   NUMINC=24/INCTIM
   NUMTEM=NUMINC*NUMDAY+1
   DO 24 L=1,NUMTEM
   READ(5,22)TEMP(L)
22 FORMAT(1F10.0)
24 CONTINUE
   RETURN
   END
```


SUBROUTINE LINEAR

SUBROUTINE LINEAR

A LINEAR RELATIONSHIP IS ASSUMED BETWEEN LOG(E) AND
LOG(XI), AND LOG(AT) AND T VALUES. THIS SUBROUTINE CALCULATES
THE A AND B COEFFICIENTS OF THE RESULTING LINEAR EQUATIONS.

COMMON TITLE1(20),T(15),AT(15),E(15),XI(15),A1(15),A2(15),B1(15),
B2(15),TEMP(1300),TT(3000),A(3000),XI1(3000),E1(3000),ST(3000),
2NUMDAY,NUMEXI,NUMATT,NUMINC,INCTIM,DELT,ALPHA,NN,NATT1,NEXI1,NT,
3CODE,U
DOUBLE PRECISION OXI,XI1
NEXI1=NUMEXI-1
NATT1=NUMATT-1

THE A AND B COEFFICIENTS FOR THE LOG(E)-LOG(XI)
EQUATIONS ARE EVALUATED.

DO 1 J=1,NEXI1
A1(J)=-1.0*ALOG10(E(J)/E(J+1))
B1(J)=ALOG10(E(J))-A1(J)*ALOG10(XI(J))
1 CONTINUE

THE A AND B COEFFICIENTS FOR THE LOG(AT)-T EQUATIONS
ARE EVALUATED.

DO 3 J=1,NATT1
A2(J)=(ALOG10(AT(J))-ALOG10(AT(J+1)))/(T(J)-T(J+1))
B2(J)=ALOG10(AT(J))-A2(J)*T(J)
3 CONTINUE
RETURN
END

SUBROUTINE XIS

C
C
C
C
C
C
C
C

SUBROUTINE XIS

THIS SUBROUTINE CALCULATES THE REDUCED TIME VECTOR(XI1)
ASSOCIATED WITH THE INPUT TEMPERATURE FIELD. THIS VECTOR IS
DETERMINED AT TIME INTERVALS OF DELT OVER THE COMPLETE
TIME PERIOD IN WHICH THE TEMPERATURE FIELD IS DEFINED.

COMMON TITLE1(20),T(15),AT(15),E(15),XI(15),A1(15),A2(15),B1(15),
B2(15),TEMP(1300),TT(3000),A(3000),XI1(3000),E1(3000),ST(3000),
2NUMDAY,NUMEXI,NUMATT,NUMINC,INCTIM,DELT,ALPHA,NN,NATT1,NEXI1,NT,
3CODE,U
DOUBLE PRECISION DXI,XI1
TIME=INCTIM
NT=(TIME*60.)/DELT
NT1=NT+1
N=NUMDAY*NUMINC

C
C
C

TEMPERATURES (TT) AT INTERVALS OF DELT ARE CALCULATED.

TT(1)=TEMP(1)
L=2
DO 3 M=1,N
DO 1 LM=2,NT1
TT(L)=TEMP(M)+((TEMP(M+1)-TEMP(M))/NT)*(LM-1)
L=L+1
1 CONTINUE
3 CONTINUE

C
C
C

SHIFT FACTORS (A) AT INTERVALS OF DELT ARE CALCULATED.

NN=N*NT+1
DO 9 L=1,NN
DO 5 J=1,NATT1
IF(TT(L) .LT. T(J) .AND. TT(L) .GE. T(J+1)) GO TO 7
5 CONTINUE
A(L)=AT(1)
GO TO 9
7 A(L)=EXP((A2(J)*TT(L)+B2(J))/0.434)
9 CONTINUE

C
C
C

THE REDUCED TIME VECTOR (XI1) IS CALCULATED.

XI1(1)=0.0
DO 11 L=2,NN
XI1(L)=(DELT*60./2.)*{1./A(L)+1./A(L-1)}+XI1(L-1)
11 CONTINUE
RETURN
END

SUBROUTINE STRESS

SUBROUTINE STRESS

SUBROUTINE STRESS CALCULATES THERMAL STRESSES AT TIME
INTERVALS OF DELT.

COMMON TITLE1(20),T(15),AT(15),E(15),XI(15),A1(15),A2(15),B1(15),
1B2(15),TEMP(1300),TT(3000),A(3000),X11(3000),E1(3000),ST(3000),
2NUMDAY,NUMEXI,NUMATT,NUMINC,INCTIM,DELT,ALPHA,NN,NATT1,NEXI1,NT,
3CODE,U
DOUBLE PRECISION DXI,XI1
STR1=0.0
DO 11 KK=1,NN
KT=KK-1

THE CHANGE IN REDUCED TIME (DXI) AS A FUNCTION OF TIME
AND TEMPERATURE IS EVALUATED.

DO 5 I=1,KT
DXI=XI1(KK)-XI1(I)
IF(DXI .LE. XI(1)) GO TO 3
DO 1 L=1,NEXI1
IF(DXI .GE. XI(L) .AND. DXI .LE. XI(L+1)) GO TO 4
1 CONTINUE
E1(I)=E(NUMEXI)
GO TO 5
3 E1(I)=E(1)
GO TO 5
4 E1(I)=DEXP((B1(L)+A1(L)*DLOG10(DXI))/0.434)
5 CONTINUE
IF(KK .EQ. 1) GO TO 9

THE THERMAL STRESS INCREMENT (STR2),TOGETHER WITH THE
TOTAL STRESS (ST),IS COMPUTED.

DO 7 KL=1,KT
STR2=(CODE/(1.-U))*ALPHA*(E1(KL)+E1(KL+1))*((TT(KL)-TT(KL+1))/2.0)
7 STR1=STR2+STR1
ST(KK)=STR1
GO TO 10
9 ST(KK)=0.0
10 STR1=0.0
11 CONTINUE
RETURN
END

B30038